Blood-Brain Barrier Permeability and Inflammation in Cerebral Small Vessel Disease

Jessica Walsh

Darwin College

Department of Clinical Neurosciences

University of Cambridge

This dissertation is submitted for the degree of Doctor of Philosophy

October 2019

Declaration

This dissertation is the result of my own work and includes nothing which is the outcome of work done in collaboration except as declared in the Preface and specified in the text.

It is not substantially the same as any that I have submitted, or, is being concurrently submitted for a degree or diploma or other qualification at the University of Cambridge or any other University or similar institution except as declared in the Preface and specified in the text. I further state that no substantial part of my dissertation has already been submitted, or, is being concurrently submitted for any such degree, diploma or other qualification at the University of Cambridge or any other University or similar institution except as declared in the Preface and specified in the text.

It does not exceed the prescribed word limit for the Clinical Medicine and Clinical Veterinary Medicine Degree Committee (60,000 words).

The work described in this thesis has been conducted primarily in the Department of Clinical Neurosciences at the University of Cambridge; patients were recruited and seen in the outpatient clinic in R3 at Addenbrooke's Hospital and all scans were carried at the Wolfson Brain Imaging Centre at the University of Cambridge.

I was personally involved in leading the ethics application of the BBB permeability and Neuroinflammation in SVD study through Research and Development, ARSAC and Research Ethics Committee approvals. I have actively screened and recruited all participants into the study, been present for all imaging sessions undertaken, performed all cognitive tests on of the participants and processed the blood samples for analysis. I have completed all of the marking of white matter lesions, image analysis of DTI data and processing of cognitive tests. I have performed all statistical analysis of the data.

Summary

Name: Jessica Walsh

Thesis Title: Blood-Brain Barrier Permeability and Inflammation in Cerebral Small Vessel Disease

Introduction: Cerebral small vessel disease (SVD) is responsible for a third of strokes and is the most common cause of vascular dementia. It is characterised by white matter lesions and more diffuse damage outside of the lesions. Despite its importance, the mechanisms causing white matter damage are incompletely understood. Both increased blood-brain barrier (BBB) permeability and inflammation have been suggested to play a role. We hypothesised that BBB permeability and microglia activation would be increased in SVD and explored the relationship between these processes and other imaging, cognitive and blood markers.

Methods: A PET/MR system was used to acquire simultaneous dynamic contrast enhanced MRI with Patlak modelling to measure BBB leakage, and $[C^{11}]$PK-11195 PET to assess microglia activation. We recruited 20 sporadic SVD patients, 20 monogenic SVD patients (CADASIL) and 20 healthy controls to this study.

Results: BBB permeability in the white matter of the sporadic SVD group was significantly higher than control (p=0.001), with a significantly higher volume of focal hotspots (p=0.010). The focal hotspots of activated microglia also had a significantly higher mean in the white matter (p<0.001). The role of BBB permeability and PK binding in CADASIL was less clear, with no difference in permeability but a significantly higher mean of focal hotspot of activated microglia in the CADASIL white matter, compared to control (p=0.015). In the sporadic SVD and CADASIL groups, the number of voxels containing both significant permeability and microglia activation was significantly lower than expected (p<0.001).

Conclusion: Areas of focal increase in both BBB permeability and microglia activation occur in SVD and therefore may have a role in the pathophysiology of white matter damage. In this cross-sectional dataset, the two processes were spatially independent of one-another. However, we cannot exclude a temporal relationship, where one process may precede another, without follow-up data. Further research is needed to see if these markers predict white matter damage in longitudinal studies, and whether they can be altered therapeutically.

Dedication

Completing this PhD has been an incredible experience and I'm so grateful to everyone who has helped me along the way. This work has been a collaborative project that would not have been possible without the support of many individuals. Additionally to those already named above, this project has been assisted by the WBIC staff, doctors, research nurses, secretaries and many others; thank you all for your help over the past three years.

The other people who have made this project possible are the research participants. I am continually in awe of all the lovely people who were happy to give up their time to take part. Their selflessness and will to help others is so inspiring and I can't thank them enough.

The British Heart Foundation has been an incredible charity to work with during this PhD, providing me with so many opportunities aside from the studentship. I would also like to thank the MRC for their generous funding of the BBB and Neuroinflammation in SVD project, without which this work would not have been possible.

I'd like to thank my supervisors Hugh and Dan for all of their support and encouragement. I'm incredibly grateful for the trust they put in me to manage this project and for everything they taught me along the way.

The student's room in R3 has been my second home for the past three years and I have been so lucky to work with so many brilliant people. Jonathan and I have been on this journey together since our first day, and I couldn't have done it without him. Jenny, Anna and Hayley are three of the most incredible girls I've ever met; thank you for the laughs, the wine and the doughnuts.

Darwin College Boat Club has played a huge role in my life over the past three years. I never expected to be so involved in a society during my PhD, but I can honestly say it was a privilege to be vice-captain and then captain. The people I've met here will be

lifelong friends and the experiences will stay with me forever. I'd particularly like to thank Magda for being my absolute rock throughout my time at Cambridge and always being there for me whenever I've needed her.

I am incredibly lucky to have such an amazing family and I know I would never have been able to achieve this without their unconditional love and support. Mum and Dad have always encouraged me to do what I love and take every opportunity. My Nana, who has always been my number one fan, has made me believe I can do anything I set my mind to. And Bob, my incredible granddad, who continually inspires me with his passion for his own work, has engaged in countless discussions with me over my project and also proofread my entire thesis. Thank you all.

And finally I'd like to thank Shaun; for listening to my endless presentations, calming me down when I was stressed and forever telling me that I could do it. This PhD will be as much yours as it is mine - thank you.

Table of Contents

Glossary of Terms

3.0T	3.0 Tesla
AC-PC	Anterior comissure-posterior commissure
AIF	Arterial input function
ALCAM	Activated leukocyte cell adhesion molecule
ANCOVA	Analysis of covariance
ApoE	Apolipoprotein E
ASL	Arterial spin labelling
BBB	Blood-brain barrier
BMIPB	BIRT Memory and Information Processing Battery
BP_{ND}	Non-displaceable compartment
CADASIL	Cerebral autosomal dominant arteriopathy with subcortical infarcts and leukoencephalopathy
CARASIL	Cerebral autosomal recessive arteriopathy with subcortical infarcts and leukoencephalopathy
CBF	Cerebral blood flow
CDH5	Cadherin-5
CHI3L1	Chitinase-3-like protein 1
CMB	Cerebral microbleed
CNS	Central nervous system
COX-2	Cyclooxygenase-2
CRP	C-reactive protein
CSF	Cerebrospinal fluid
CT	Computerised tomography
CVD	Cardiovascular disease
DCE	Dynamic contrast enhanced
DTI	Diffusion tensor imaging
DWI	Diffusion-weighted imaging
EF	Executive function
eGFR	Estimated glomerular filtration rate
ELISA	Enzyme-linked immunosorbent assay

FA	Fractional anisotropy
FDR	False discovery rate
FLAIR	Fluid attenuated inversion recovery
FOV	Field of view
FW	Freewater
GC	Global cognition
GM	Grey matter
GRE	Gradient recalled echo
GWAS	Genome-wide association studies
HIF-1α	Hypoxia inducible factor-1α
IBA1	Ionised calcium-binding adapter molecule-1
ICAM-1	Intracellular adhesion molecule-1
ICV	Intracranial volume
IL	Interleukin
IL-1α	Interleukin-1α
IL-1β	Interleukin-1β
IL-1R1	Interleukin-1 receptor type 1
IL-6	Interleukin-1
IL-6	Interleukin-6
IL-6Rα	Interleukin-6 receptor subunit α
IL-10	Interleukin-10
IL-18	Interleukin-18
IL-18BP	Interleukin-18 binding protein
ITGB2	Integrin β2
JAK	Janus kinases
JAM-A	Junctional adhesion molecule A
LTM	Long-term memory
MAO-B	Monoamine oxidase B
MD	Mean diffusivity
MMP	Matrix metalloproteinase
MMP-2	Matrix metalloproteinase-2
MMP-3	Matrix metalloproteinase-3

MMP-8	Matrix metalloproteinase-8
MMP-9	Matrix metalloproteinase-9
MMP-13	Matrix metalloproteinase-13
MMSE	Mini mental state exam
MoCA	Montreal cognitive assessment
MRI	Magnetic resonance imaging
MS	Multiple Sclerosis
mWCST	Modified Wisconsin card sort test
NAWM	Normal appearing white matter
NF-κB	Nuclear factor kappa-light-chain-enhancer of activated B cells
OEF	Oxygen extraction factor
PBR	Peripheral benzodiazepine receptor
PCR	Polymerase chain reaction
PECAM-1	Platelet endothelial cell adhesion molecule-1
PET	Positron emission tomography
PK	$[C^{11}]PK11195$
PS	Processing speed
PSGL-1	P-selectin glycoprotein ligand-1
RF	Radiofrequency
ROI	Region of interest
ROS	Reactive oxygen species
RVCL	Retinal vasculopathy with cerebral leukodystrophy
SBR	Signal-to-background ratio
SD	Standard deviation
SHR	Spontaneously hypertensive rats
SHRSP	Stroke prone spontaneously hypertensive rats
SRTM	Simplified reference tissue model
STAT	Signal transducer and activator of transcription
SVD	Small vessel disease
TAC	Time-activity curve
TIA	Transient ischaemic attack
TIMP	Tissue inhibitor of metalloproteinase

TIMP-2	Metalloproteinase inhibitor-2
TIMP-4	Metalloproteinase inhibitor-4
TNF-R1	Tumour necrosis factor receptor 1
TNF-R2	Tumour necrosis factor receptor 2
TNF-α	Tumour necrosis factor-α
TSPO	Translocator protein-18
TRAF2	Tumour necrosis factor associated factor 2
TRADD	Tumour necrosis factor receptor associated death domain protein
TACE	Tumour necrosis factor-α converting enyme
VCAM-1	Vascular cellular adhesion molecule-1
vWF	von Willebrand factor
WM	White matter
WML	White matter lesion
WMS-III	Weschler Memory Scale 3rd edition
WoM	Working memory

Chapter 1: Introduction to the Pathogenesis of Cerebral Small Vessel Disease

1.1 Imaging Features of Cerebral Small Vessel Disease

1.1.1 Cerebral Small Vessel Disease

Cerebral small vessel disease (SVD) refers to a group of pathological processes which affect the small vessels in the brain (Pantoni, 2010). SVD spans the fields of stroke, dementia and ageing, and is a highly diverse and heterogeneous disease. Our knowledge of SVD is still very limited and there are no treatments that target the underlying mechanism. This is largely due to a lack of understanding of the basic pathophysiology.

SVD accounts for approximately one-third of symptomatic strokes including lacunar stroke (Fisher, 1982) and parenchymal brain haemorrhage (Greenberg, 2006). SVD is the leading cause of vascular dementia, which make up around 15% of all dementia cases (O'Brien and Thomas, 2015). Together, vascular dementia and Alzheimer's disease make up 70-75% of total dementia cases (Gorelick et al., 2011). Many of the dementia patients actually have both dementias to a certain degree, with vascular comorbidity present in 30-60% of Alzheimer's disease patients and Alzheimer's disease pathology present in 40-80% of vascular dementia patients (Attems and Jellinger, 2014, Wallin et al., 2018). SVD is also thought to contribute towards age related cognitive decline. SVD is frequently seen on the magnetic resonance imaging (MRI) scans of brains of cognitively healthy elderly individuals (van der Flier et al., 2005). Therefore, the reality is that the prevalence of SVD is actually much higher than our current statistics would suggest (Hachinski, 2008).

Like many countries, the UK has an ageing population, meaning that the prevalence of SVD will only continue to rise over the coming years (Kuller and Lopez, 2016). The disease is not only life-changing for patients affected and their families, but also has large economic implications for health service providers (Poggesi et al., 2011), making research into this area even more important.

MRI is a versatile tool used throughout the field of neurology for imaging of the brain. MRI utilises the differing water composition of tissues to create contrast in images. In the brain, this is mainly used to discriminate between grey matter (GM), white matter (WM) and cerebrospinal fluid (CSF); plus showing up any pathology.

Since imaging the small vessels themselves in the brain is not possible with current techniques, other imaging markers are used for diagnosis, tracking disease progression and research end-points. Features of SVD on neuroimaging include recent subcortical infarcts, lacunes, white matter lesions (WMLs), perivascular spaces, cerebral microbleeds (CMBs) and brain atrophy (Wardlaw et al., 2013c). These features are summarised in Figure 1.1.

	Recent small subcortical infarct	White matter hyperintensity	Lacune	Perivascular space	Cerebral microbleed
Example image					
Schematic	DWI	FLAIR	FLAIR	T1/FLAIR	T2*/SWI
Usual diameter	≤20 mm	Variable	3-15 mm	≤2 mm	≤10 mm
Comment	Best identified on DWI	Located in white matter	Usually have hyperintense rim	Most linear without hyperintense rim	Detected on GRE seq., round or ovoid, blooming
DWI	↑	↔	↔/(↓)	↔	↔
FLAIR	↑	↑	↓	↓	↔
T2	↑	↑	↑	↑	↔
T1	↓	↔/(↓)	↓	↓	↔
T2*-weighted GRE	↔	↑	↔ (↓ if haemorrhage)	↔	↓↓

↑ Increased signal   ↓ Decreased signal   ↔ Iso-intense signal

Figure 1.1: Characteristic MRI markers of SVD. Example images (upper), schematic representations (middle) and MRI features (lower) for the individual markers. DWI= diffusion-weighted imaging, FLAIR=fluid-attenuated inversion recovery, GRE = gradient-recalled echo. Reproduced with permission from (Wardlaw et al., 2013c).

1.1.3 Lacunar Infarcts

Lacunar infarcts (or lacunar strokes) are key feature of SVD. Lacunar infarcts are small strokes (3-15mm in diameter) in the deep cerebral WM, deep GM nuclei and brainstem, which are thought to result from the occlusion of a single small perforating artery (Wardlaw, 2005). Acute lacunar infarcts are easily detected on diffusion-weighted imaging (DWI) if imaged within a few weeks of the acute event, where they appear as a region of hyperintensity.

After the initial acute phase of the infarct, most lacunar infarcts will then cavitate to become a fluid filled cavity known as a lacune. Lacunes can be imaged as a hypointense region on both T1 and T2-fluid attenuated inversion recovery (FLAIR) scans. However, lacunar infarcts do not always cavitate into lacunes. Recent studies have shown that $1/3^{rd}$ of recent infarcts do not lead to cavity formation within a 2-year period and will either disappear completely or become part of a WML (Okazaki et al., 2015). These studies have led to the suggestion that counting lacunes probably substantially underestimates the real burden of lacunar infarcts (Loos et al., 2012).

Lacunar infarcts have various clinical symptoms depending on lesion location, but around 30% of patients with lacunar stroke are left dependent (Bamford et al., 1991). Lacunar infarcts are associated with cognitive decline and dementia onset during follow-up (Samuelsson et al., 1996). Lacunes are also found in the brains of around 20-50% of the healthy elderly population (Vermeer et al., 2007). They are often termed 'silent' brain infarcts, but they have been shown to correlate with subtle deficits in physical and cognitive function, suggesting they are clinically relevant (Schneider et al., 2007, Choi et al., 2012, Vermeer et al., 2007).

Lacunar strokes have a 22.4% recurrence rate and 25% mortality rate at five years (Norrving, 2003). This suggests our current preventative treatments are not good enough to prevent recurrences.

1.1.4 WMLs

WMLs are another key characteristic of SVD seen on MRI. They are thought to represent a reduction in tissue, gliosis and a loss of myelin and axons due to chronic diffuse injury (Gouw et al., 2011). WMLs appear as a region of hyperintensity on T2 and T2-FLAIR scans. WMLs tend to be bilateral and symmetrical and are found mainly in the periventricular and deep WM regions (Wardlaw et al., 2013c). They can also be found in the subcortical GM structures and brainstem.

WML burden has been correlated with cognitive function, mood, mobility, depression and urinary problems in cross-sectional studies (Pantoni, 2008). They have been associated with both cognitive decline and dementia in longitudinal studies (Pantoni et al., 2007). Studies have also investigated the effect of WMLs on recurrent stroke risk and have found that presence of WML during first stroke increases the risk of having a second stroke (Miyao et al., 1992).

WMLs are commonly seen as an incidental finding on MRI scans of the cognitively healthy elderly (Ylikoski et al., 1995). Up to 90% of patients over 65 years present with some degree of WMLs on MRI (Schmidt et al., 2011). As with silent lacunes, when these healthy elderly individuals are tested for cognitive impairment, there is a correlation between extent of WML and cognition (Nylander et al., 2018). This cognitive impairment, which can be associated with WML, is often at a sub-clinical level but can still impact the daily lives of these individuals.

There is evidence that WMLs in the periventricular or deep WM should be differentiated in studies (Griffanti et al., 2018). Studies have reported that there is a greater association between perivascular WMLs and cognitive performance (Bolandzadeh et al., 2012), whereas deep WMLs are more associated with mood disorders (Krishnan et al., 2006, de Groot et al., 2000). Postmortem studies have also shown there seems to be an anatomical difference in the lesions. Smooth perivascular WMLs predominantly show demyelination and gliosis; whereas deep WMLs and irregular periventricular WMLs show increased axonal and tissue loss suggesting infarction, in addition to demyelination and gliosis (Fazekas et al., 1998, Kim et al., 2008). It has also been suggested that the two types may have different underlying

pathologies; smooth periventricular WMLs could be attributed to increased blood-brain barrier (BBB) permeability whereas deep WMLs and irregular periventricular WMLs are a result of hypoperfusion. However, this is likely an oversimplified model. Additionally, in severe SVD it can be difficult to differentiate between deep and periventricular WML, as the extent of the damage means that the WMLs extend all the way from the ventricles out into the deep WM. Therefore, despite this differentiation, most studies still measure WML volume in its entirety.

It is generally accepted that WMLs increase over time (Schmidt et al., 2016); however, the growth rates vary widely between studies. In the normal aging person with confluent WMLs, the mean rate of progression ranges from 0.23-1.33cm^3/year (Sachdev et al., 2007). This WML growth does not seem to be random; a recent study estimated that around 80% of incident WMLs occurring over four years represented extensions of pre-existing lesions (Maillard et al., 2012). WMLs have also been shown to expand from the periventricular WM, where they tended to be most prevalent, toward the subcortical WM (Duering et al., 2013). They grew along the trajectories of small perforating arteries, suggesting WMLs are prone to growing in the vascular end zone.

The progression of WMLs has been associated with cognitive decline, dementia, incident stroke, gait dysfunction and depression (Schmidt et al., 2016). WMLs have been associated with both general cognitive decline and a decline in information processing speed (PS) (van Dijk et al., 2008). Greater WML load at baseline has also been shown to predict both conversion from normal ageing to mild cognitive impairment (Smith et al., 2008) and functional decline and disability (Inzitari et al., 2009).

Some studies have demonstrated that WML burden appears stable or even decreases over time. Early reports of this were put down to a measurement error (Schmidt et al., 2003, Sachdev et al., 2007). However, multiple case reports then emerged, suggesting there can be regression of WMLs after ischaemic stroke (Moriya et al., 2009, Durand-Birchenall et al., 2012), hepatic encephalopathy treatment (Minguez et al., 2007, Rovira et al., 2007) and carotid artery stenting (Yamada et al., 2010).

Following this, more recent studies have revalidated this finding in larger sample sizes of SVD patients, showing there does indeed seem to be regression of WMLs in some patients, suggesting these WMLs are far more dynamic than originally thought (Cho et al., 2015, Ramirez et al., 2016, van Leijsen et al., 2017). Interestingly, the retraction of WML was found to be associated with no change in cognition, but rather it is associated with stable SVD (van Leijsen et al., 2019).

The progression of WMLs, and their relationship to cognition and clinical endpoints, means that WML volume is commonly used as a trial end-point. Studies using blood pressure lowering medication and statins have shown this to reduce WML growth compared to placebo (Dufouil et al., 2005, Mok et al., 2009), suggesting that the process is both modifiable and influenced by cardiovascular risk factors. This dynamic nature of the WMLs has led researchers to wonder about whether WML reversal with therapeutics is potentially possible, whereas previously the best outcome was thought to be slowing WML progression. New therapeutics will look to both slow down progression and reverse these WMLs, in the hope to slow down the progression of clinical symptoms.

1.1.5 WM Microstructural Changes

In addition to the WMLs seen in SVD, there is more widespread tissue damage to WM microstructure that cannot be detected through T2-weighted or FLAIR imaging.

Diffusion tensor imaging (DTI) allows assessment of the microstructural integrity of whole WM by measuring the direction and magnitude of water diffusion in the intracellular compartment of the axons (Pierpaoli et al., 1996). It provides two main scalar parameters: mean diffusivity (MD), which is a measure of the magnitude of diffusion of water averaged in all spatial directions, and fractional anisotropy (FA), which provides information about the directionality of water diffusion. DTI measures correlate with markers of myelin integrity, and axonal damage and density (Shereen et al., 2011, Gouw et al., 2008). A reduction in FA and increase in MD are believed to represent reduced microstructural integrity in SVD (Jones et al., 1999).

DTI has been shown to significantly correlate with cognitive performance in SVD patients (van Norden et al., 2012, D'Souza et al., 2018). Studies have also correlated it with the risk factor hypertension in SVD patients (Gons et al., 2010). Looking longitudinally, DTI has been shown to predict faster cognitive decline (Jokinen et al., 2013) and a decrease in the Rankin score (Holtmannspotter et al., 2005).

Longitudinal studies have suggested that DTI is the most sensitive measure to ongoing changes in SVD patients; Nitkunan et al. reported a 2.96% increase in MD and 2.13% decrease in FA in SVD patients over one year, despite an unchanged lesion load and brain volume (Nitkunan et al., 2008). Further, thalamic FA was found to predict WML accrual four years on, suggesting that these underlying WM microstructural changes are pathological (Cavallari et al., 2014).

The strong evidence for the clinical relevance of DTI to SVD has led to the incorporation of DTI into clinical trials with MD and FA used as primary end-points (Holtmannspotter et al., 2005).

1.1.6 CMBs

CMBs are small hypointense regions present on T2* weighted or susceptibility-weighted sequences (Wardlaw et al., 2013c). They are small (usually 2-5mm in diameter) and generally cannot be seen on FLAIR, T1-weighted or T2-weighted sequences. CMBs are seen in 5 to 15% of the elderly population (Cavalieri et al., 2012) and in 85% of patients with vascular dementia (Seo et al., 2007).

CMBs have been associated with lacunar infarcts and WMLs (Vernooij et al., 2008, Gao et al., 2014, Cordonnier et al., 2007, Wardlaw et al., 2006). In longitudinal studies, subjects with CMBs at baseline showed more than five times higher risk for newly occurring CMBs compared to those without (Poels et al., 2011).

The clinical relevance of CMBs is still poorly understood. Meta-analyses of the studies showed that patients with CMBs had a higher incidence of cognitive impairment, lower scores of cognitive functions from the Mini Mental State

Examination (MMSE) and Montreal Cognitive Assessment (MoCA) and conversion to dementia (Li et al., 2017b, Charidimou et al., 2018). Follow-up studies have associated an increasing number of CMBs with a decline in global cognition (GC) (Liem et al., 2009, Akoudad et al., 2016) and executive function (EF) (Meier et al., 2014, Gregoire et al., 2012). However, not all studies have shown a relationship between CMB and cognitive decline (Jimenez-Balado et al., 2019). Therefore, more studies are required to confirm the pathological association with CMBs before they are used as common practice clinically and as research end-points.

1.1.7 Enlarged Perivascular Spaces

The human brain contains a lymphatic drainage system for interstitial fluid from the brain along perivascular spaces around the arteries, arterioles, veins and venules. Perivascular spaces are microscopic in the healthy brain; however, larger spaces can be seen using MRI (Groeschel et al., 2006). Enlarged perivascular spaces have similar signal intensity to CSF on all sequences; they follow the blood vessels so they will appear linear if imaged parallel to the vessel and circular if imaged perpendicular to the vessel (Wardlaw et al., 2013c). It can be difficult to discriminate between enlarged perivascular spaces and lacunes as they both appear hypointense on T2-weighted or FLAIR imaging; so the general rule is that if it is <3mm and does not have a rim or area of high signal intensity around it, then it is an enlarged perivascular space. T2* can also be used to check there is no evidence of hemosiderin in its wall to distinguish it from a CMB (Ding et al., 2017).

Enlarged perivascular spaces are commonly found in SVD, particularly in the basal ganglia, centrum semiovale and midbrain (Wardlaw et al., 2013a). They have been associated with WMLs and lacunar infarcts (Doubal et al., 2010, Loos et al., 2015). Some studies have shown there to be a relationship between cognitive decline and the number of perivascular spaces in the basal ganglia (Huijts et al., 2014, Arba et al., 2018, Maclullich et al., 2004) and total number (Passiak et al., 2019, Ding et al., 2017). However, not all studies have shown this association (Benjamin et al., 2018, Riba-Llena et al., 2016, Yao et al., 2014). Therefore, the clinical significance of perivascular spaces remains controversial.

1.1.8 Brain Atrophy

Brain atrophy is common in diseases that affect the brain and in normal ageing (Fjell et al., 2009). Brain volume is calculated from T1 MRI scans, which can be used to determine the volume of the GM, WM and CSF. Normalising these measures for intracranial volume (ICV) accounts for head size and reduces interindividual variation (Whitwell et al., 2001). Brain volume can be tracked over time and brain atrophy can be calculated.

Within vascular disease, brain atrophy is thought to include neuronal loss, cortical thinning and WM reduction (Wardlaw et al., 2013c). Cross-sectionally, brain volume is lower in SVD compared to controls and is associated with reduced EF (Nitkunan et al., 2011). Longitudinally, brain atrophy has been shown to occur in SVD and correlate with cognitive decline (Nitkunan et al., 2011, Jokinen et al., 2012).

Many studies have shown an association between brain volume and WMLs (Appelman et al., 2009, Aribisala et al., 2013, Godin et al., 2009, Lambert et al., 2015), but until recently it was unclear as to whether these processes had a common pathogenesis or just shared risk factors. More recent work has suggested that WML progression is associated with accelerated brain atrophy, suggesting that atrophy is a secondary mechanism in WML degeneration (Lambert et al., 2016). Aribisala et al. also showed a focal thinning in GM regions connected to subcortical infarcts (Aribisala et al., 2013). Therefore, brain atrophy is thought to be a pathological and clinically relevant process in SVD, resulting from the underlying changes occurring in the WM. If treatments could reduce the progression of WMLs and appearance of lacunar infarcts then this would hopefully also slow down brain atrophy and reduce the cognitive decline seen.

1.2 SVD Subtypes

1.2.1 Sporadic SVD

Sporadic SVD is prevalent within our population, associated with a variety of genetic, cardiovascular and environmental risk factors, which all increase the risk of it developing. The single biggest risk factor for SVD is age, which has led some to conclude that SVD may be a natural consequence of living beyond our physiological means (Thompson and Hakim, 2009).

Hypertension is the major modifiable risk factor associated with SVD. Longitudinal studies have consistently shown that blood pressure correlates with the likelihood of WMLs being present, and also the severity of them, in both SVD patients and in the elderly population (Guo et al., 2009, van Dijk et al., 2004, Liao et al., 1996, Godin et al., 2011). Long-term hypertension has been shown to result in lipohyalinosis of the media and thickening of the vessel walls, which leads to narrowing of the lumen of the arterioles and small perforating arteries (Pantoni and Garcia, 1995). Further it has been shown to increase blood vessel fibrosis and alter the distribution of collagen and other extracellular matrices to result in stiffness of the vessel walls and reduced cerebral blood flow (CBF) (Faraco and Iadecola, 2013). Other cardiovascular risk factors have also been associated with SVD: female sex, smoking, and high baseline WML load were all significantly associated with SVD progression and a decline in cognitive function (van Dijk et al., 2008).

Both twin and family history studies suggest that SVD has a heritable element (Carmelli et al., 1998). Twin studies have shown there is a WML concordance rate of 61% in monozygotic pairs and 38% in dizygotic pairs (Carmelli et al., 1998). Candidate gene and genome-wide association studies (GWAS) have attempted to uncover which genes may be mediating this effect. Rannikmae et al. found that genetic variations in *COL4A2* and *HTRA1* are associated with lacunar stroke (Rannikmae et al., 2017), whilst Traylor et al. found that variations in *PLEKHG1* are associated with WMLs (Traylor et al., 2019). Further, genetic variants in the *VCAN* gene have been associated with FA and MD, suggesting they may have a role in the WM microstructural alterations that occur in SVD (Rutten-Jacobs et al., 2018).

22

Treatment of risk factors is still the primary treatment used for SVD, predominantly with anti-hypertensives and statins; there are currently no therapeutics that target the underlying mechanism of SVD.

1.2.2 Monogenic SVD (CADASIL)

There are several single-gene disorders known to cause SVD. Cerebral autosomal dominant arteriopathy with subcortical infarcts and leukoencephalopathy (CADASIL), cerebral autosomal recessive arteriopathy with subcortical infarcts and leukoencephalopathy (CARASIL), COL4A1-related SVD, retinal vasculopathy with cerebral leukodystrophy (RVCL) and Fabrys disease are all examples (Choi, 2015).

CADASIL is the most common form of hereditary stroke disorder. The disorder is thought to have a prevalence of between 2 and 5 in 100,000 but may vary between populations (Di Donato et al., 2017). It is caused by mutations in the *Notch3* gene on chromosome 19q12 (Joutel et al., 1996). The Notch3 receptor protein is predominantly expressed in adults by vascular smooth muscle cells and pericytes. The initial symptom of CADASIL tends to be migraine, with onset at around 20-30 years old (Tan and Markus, 2016). Transient ischaemic attacks (TIAs) and strokes are reported in around 85% of symptomatic patients (Dichgans et al., 1998), with mean age at onset being 45-50 years old (Opherk et al., 2004).

CADASIL patients show extensive WMLs and lacunes on T2-weighted and FLAIR scans. WM changes can often involve the anterior temporal lobe, external capsule and superior frontal gyrus (Auer et al., 2001); this differs from the pattern seen in sporadic SVD. These WM changes can be seen in presymptomatic CADASIL patients, from the age of 20-30 onwards (Singhal et al., 2005). Life expectancy is also reduced to 64.6 years in men and 70.7 years in women (Opherk et al., 2004).

In CADASIL, arterioles and venules accumulate granular osmiophilic material within the vascular smooth muscle cell membrane (Yamamoto et al., 2013). The vascular smooth muscle cells gradually undergo degeneration with mural fibrosis which results

in stenosis of the arteries and a loss of the ability to autoregulate (Stojanov et al., 2015). Recent evidence has shown that the accumulation of Notch3 protein also affects the capillary pericytes, affecting CBF and BBB permeability (Dziewulska and Lewandowska, 2012).

In CADASIL, cardiovascular or environmental risk factors are not required for manifestation of the disease. However, the same risk factors as sporadic SVD are still known to accelerate the disease pathogenesis (Adib-Samii et al., 2010). Hypertension and smoking have been associated with earlier onset of stroke (Singhal et al., 2004) and an increased likelihood of progression to dementia (Chabriat et al., 2016).

Similarly to sporadic SVD, current treatments for CADASIL include treatment of the risk factors, such as anti-hypertensives and statins, and treatment of the symptoms, such as migraine medication. There are no treatments that target the underlying pathogenesis of the disease.

1.3 Clinical Features of SVD

The vessel pathology in SVD leads to many changes in the brain, which manifest as clinical symptoms. SVD is fairly unique in the sense that the symptoms seen will progress in both a slow and a sudden way; the gradual build up of brain pathology due to chronic damage leads to a gradual symptom increase, which will then be mixed with acute damage from strokes, leading to a more sudden increase in symptoms specific to the stroke.

1.3.1 Cognitive Symptoms

SVD is the most common cause of vascular cognitive impairment and vascular dementia (Pantoni, 2010, Wardlaw et al., 2013a). It has also been shown to worsen the symptoms of other dementia disorders, such as Alzheimer's disease.

Cross-sectional studies have characterised the profile of the cognitive impairment seen in SVD. SVD patients show early impairments in PS and EF, with long-term memory (LTM) mostly spared (Lawrence et al., 2013). Similarly, CADASIL patients show a deficit in PS and EF, although they also seem to have a deficit in both working memory (WoM) and LTM (Charlton et al., 2006b).

Studies have then looked at cognition longitudinally over a three-year period; Lawrence et al. found that average cognitive change declined most for the domains that were most impaired at baseline but noted that in most individuals, the declines were slow and were only statistically significant for EF (Lawrence et al., 2015). Comparably, the rate of cognitive decline seen in SVD is higher than seen for healthy aging (Charlton et al., 2006a). However, the rate of cognitive decline is less than reported for Alzheimer's disease and mild cognitive impairment, but with more variability in disease progression (Bennett et al., 1994, Wallin et al., 2018).

SVD can exist alone or in combination with other dementias. Studies have investigated the severity of dementia in community-dwelling elderly cohorts, exploring the presence of Alzheimer's disease, SVD and Parkinson's disease/Lewy

body dementia (Eggink et al., 2019). Schneider et al. found that in persons with dementia, over 50% had multiple diagnoses, whereas, in persons without dementia, over 80% had either one or no diagnosis; suggesting that these diseases working in combination had the largest contribution to dementia (Schneider et al., 2007). The presence of lacunar infarcts was also found to increase the prevalence of dementia and worsened cognitive function in Alzheimer's disease patients, suggesting SVD lowers the threshold for dementia in these patients (Snowdon et al., 1997, Toledo et al., 2013).

Alzheimer's disease and SVD share various risk factors, including age, hypertension, diabetes, smoking, hypercholesterolemia, hyperhomocysteinemia and *APOE4* isoforms (Santos et al., 2017). Chronic hypertension in an animal model of Alzheimer's disease shows accelerated amyloid deposition, BBB dysfunction, microglial activation and subsequent neuronal loss and cognitive impairment (Kruyer et al., 2015). There are also other underlying biological mechanisms shared by Alzheimer's disease and SVD including oxidative stress, inflammation, mitochondrial disruption and metabolic dysfunction (Liu et al., 2018b).

Amyloid peptides are generated by amyloid precursor protein cleavage and can aggregate into fibrillar deposits in brain tissue and in vessel walls (Hardy and Higgins, 1992). An association of amyloid-β1-40, but not amyloid-β1-42, with WMLs and lacunar infarcts was described in a mixed population of Alzheimer's disease, mild cognitive impairment and CAA patients (Gurol et al., 2006) and in SVD patients (Gomis et al., 2009). It is thought that amyloid-β1-40 has a toxic effect on the vessel wall.

CMBs were significantly associated with amyloid-β pathology in Alzheimer's disease patients (Liu et al., 2018b). Amyloid-β pathology was also significantly associated with WMLs in Alzheimer's patients but not in normal age-matched controls, suggesting there is a negative interaction between the diseases.

However, how Alzheimer's disease and SVD pathology combine to increase dementia is not well understood and the relationship between these diseases remains

controversial. A limiting factor is that there are limited animal models for both diseases and so it is difficult to study the mechanisms *in vivo*. The link between Alzheimer's disease and SVD could potentially be explained through the BBB, as it explains the protein infiltration, perivascular oedema and secondary axonal and neuronal damage seen in SVD; plus it could provide a route of entry of amyloid-β and inflammatory cells into the brain in Alzheimer's disease (Biron et al., 2011). However, the evidence for this is limited so this is currently just speculative.

1.3.2 Psychiatric Symptoms

The psychiatric symptoms associated with SVD include apathy and depression (Staekenborg et al., 2010). Studies have a history of grouping the two together, but more recently research has attempted to separate out these two distinct symptoms. In sporadic SVD, around 15% have been seen to have apathy, 12% have both apathy and depression and 1% have only depression (Lohner et al., 2017). Studies investigating apathy and depression have found that apathy, but not depression, is associated with impaired EF and with WM network disruption (Tay et al., 2019, Hollocks et al., 2015). Depression has, however, been associated with WML volume (de Groot et al., 2000).

In CADASIL, psychiatric disturbances are present in 20-41% of patients, with apathy and depression being the main psychiatric symptoms seen (Valenti et al., 2008).

1.3.3 Motor Symptoms

Gait and balance disturbances and related falls are a major symptom of patients with SVD, and are an important cause of morbidity and mortality in the elderly (Issac et al., 2015). SVD motor deficits can present in many different ways, including unsteadiness of gait and impaired balance on walking, all leading to increased fall risk. Studies have shown WMLs correlate with walking speed, balance and physical activity in an SVD cohort (Baezner et al., 2008). Lacunar infarcts in the frontal lobe and the thalamus are also associated with a lower walking speed (de Laat et al., 2010).

1.3.4 CADASIL-specific Symptoms

Migraine is often the earliest feature of CADASIL, present in about 55-75% of Caucasian cases (Tan and Markus, 2016). The migraine experienced by CADASIL patients is predominantly with aura. Encephalopathy is a rarer symptom of CADASIL, described in around 10% of patients (Drazyk et al., 2019). Encephalopathy is also known as 'CADASIL coma' and is an acute event of altered state of consciousness in a CADASIL patient, manifesting as signs of brain dysfunction. History of migraine increases the risk of encephalopathy, suggesting a common pathology between the two.

1.4 Pathogenesis of SVD

1.4.1 Anatomy

Most often, SVD is thought of as a disease of the small arteries and arterioles, however, it technically encompasses all of the small vessels including the capillaries and small veins (Pantoni, 2010).

Anatomically, small arterial vessels stem from two origins. Superficially, they stem from medium sized arteries, which have originated as larger arteries (Pantoni, 2010). Deeper in the brain, they stem directly from the large arteries as arterial perforators. These penetrating arteries run through the cortical layers perpendicular to the brain surface and enter the WM along the myelinated fibres (Pantoni and Garcia, 1997). These two types of small arterial vessels converge in the deepest areas of the subcortical WM. The vessels measure 20-50mm in length and have a diameter of around 40-200μm, but have been shown to become more tortuous and longer with ageing (Spangler et al., 1994). These vessels are the terminal end of the blood supply, known as the watershed area (Pantoni and Garcia, 1997). If there is impaired circulation within the brain, it is the watershed areas that suffer first and foremost.

Early pathological descriptions of these vessels came from C. Miller Fisher in the 1950s and 1960s; he carried out various experiments on post-mortem brains. He observed that occlusion of the small penetrating arteries occurred by two main pathologies: either a diffuse arteriopathy with hyaline deposition (termed lipohyalinosis) or atherosclerosis (Fisher, 1968). He reported that the lipohyalinosis affected smaller arteries (200-800μm) and atherosclerosis affected the larger perforating arteries near their origins (Lammie, 2000). Later studies have suggested that the lipohyalinosis of the smaller arteries leads to multiple small infarcts with WMLs, whereas atherosclerosis of the larger perforating arteries leads to isolated larger lacunar infarcts, and that differing risk factors may affect these subtypes (Khan et al., 2007). Examples of this pathology can be seen in Figure 1.2.

Our understanding of the anatomical vessel pathology has not progressed greatly since Fisher's experiments and the cause of these changes in the vessels at early

29

stages of the disease is largely unknown. The main limitation in furthering our understanding of the vessel pathology is the difficulty imaging them *in vivo* due to their size. However, even if we could image the vessels *in vivo*, features of SVD often develop slowly and silently until the damage reaches clinical levels, making it difficult to research into the early stages. Post-mortem studies are possible, but lacunar stroke has a low mortality rate compared to other stroke causes (Lund, 2014), meaning that there are few post-mortem studies available from patients in early stages of the disease.
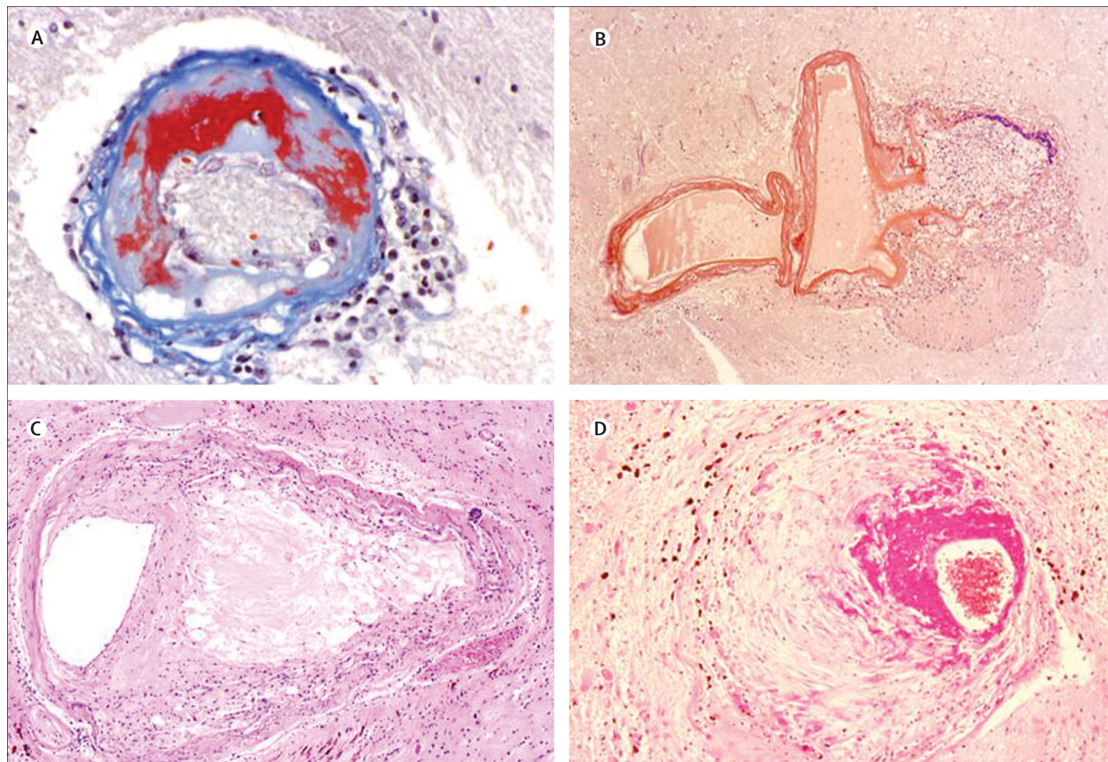
Figure 1.2: Pathological features of SVD. A) Lipohyalinosis in the basal ganglia (x100). B) Microaneurysm in the right thalamus (x25). C) Microatheroma in the basal ganglia (x20). D) Atheroma in the basal ganglia (x20). D) Fibrinoid necrosis in the pons (x20). Reproduced with permission from (Pantoni, 2010).

1.4.2 Hypoperfusion

There is evidence for a reduction in CBF in SVD (Marstrand et al., 2002, O'Sullivan et al., 2002). A meta-analysis of the literature found that CBF does seem to be lower in subjects with higher WML volume, when measured globally and in the GM and

WM regions separately (Shi et al., 2016). WMLs also commonly occur in the watershed regions of the brain, which provides further evidence for a role of CBF and oxygen delivery in the pathology.

Longitudinal studies have had conflicting results about whether this reduction in CBF is causative or consequential of the underlying problems in the microvasculature. Studies have shown an increase in WML growth in patients with higher CBF at baseline, suggesting that CBF has a role in the pathogenesis of WML formation (Bernbaum et al., 2015, ten Dam et al., 2007). However, the largest longitudinal study in the literature suggested that high WML volume at baseline was associated with falling CBF over time, suggesting CBF is a result of underlying WM damage (van der Veen et al., 2015). This research would suggest that potentially there is a role for CBF in both the initiation of SVD, and later down the line as a secondary effect, although it is unclear.

A potential explanation for the discrepancies within the literature comes from more recent work investigating capillary dynamics and their relationship with oxygen extraction factor (OEF) (Jespersen and Østergaard, 2012). The theory behind this body of work is that heterogeneity in the transit time of red blood cells through the capillaries leads to variation in how much oxygen can be extracted, which means CBF cannot be simply measured to determine the amount of oxygenation in the brain. In SVD, capillary dysfunction can mean that, even when high amounts of CBF occur, the extraction of oxygen may still not be sufficient to supply the tissues (Østergaard et al., 2016). Capillary dysfunction has been associated with increased clinical symptoms in an Alzheimer's disease population (Eskildsen et al., 2017) and strongly hypothesised to show a similar pattern in a SVD population (Østergaard et al., 2016), although this has not yet been directly tested.

Whether a reduction in CBF or OEF is important in the pathogenesis SVD, they would both result in a reduction of oxygen and triggering of a hypoxic response in both the vessels and the brain. The hypoxia experienced by the vessels is thought to lead them to become stiff, impairing cerebrovascular autoregulation (Birns et al., 2009). The hypoxic response in the brain leads to many downstream mechanisms,

including an inflammatory response and increased permeability of the BBB (Martinez Sosa and Smith, 2017).

1.4.3 BBB permeability and Inflammation

There is a growing body of evidence suggesting that the BBB increases in permeability in SVD and that this is an important component of SVD pathogenesis (Farrall and Wardlaw, 2009). Neuropathological studies, CSF studies and MRI studies have all shown an increased permeability of the BBB (Wardlaw, 2010) and have linked this directly to a decrease in CBF (Wong et al., 2019). There is also evidence of endothelial cell dysfunction and damage (Hassan et al., 2003), which is a key component of the BBB. Increased permeability of the BBB would allow blood-borne substances to enter the brain parenchyma and lead to damage (Farrall, 2009).

Using animal models, a proposed pathway which links the various mechanisms together has been hypothesised. The pathway proposes a link between an initial hypoxia of the brain tissue leading to production of hypoxia inducible factor-1α (HIF-1α) and an inflammatory response (Rosenberg, 2018). This inflammatory response is thought to lead to activation of matrix metalloproteinases (MMPs), which disrupt the tight junctions and extracellular matrix of the vascular endothelial cells and increase the permeability of the BBB. This would therefore allow various blood-borne, and potentially toxic, substances through into the brain, which would result in damage to the brain tissue and further damage to the small vessel wall itself (Wardlaw, 2010). The combination of all of this damage could then lead to pathological hallmarks of SVD seen on MRI. The hypothesised cascade can be seen in Figure 1.3.

Evidence supporting and opposing this hypothesised pathology will be discussed further on, including where there are gaps in the knowledge. Uncovering this underlying pathophysiology is vital for our understanding of how SVD progresses and whether we can reduce the progression by targeting the pathway with therapeutics.
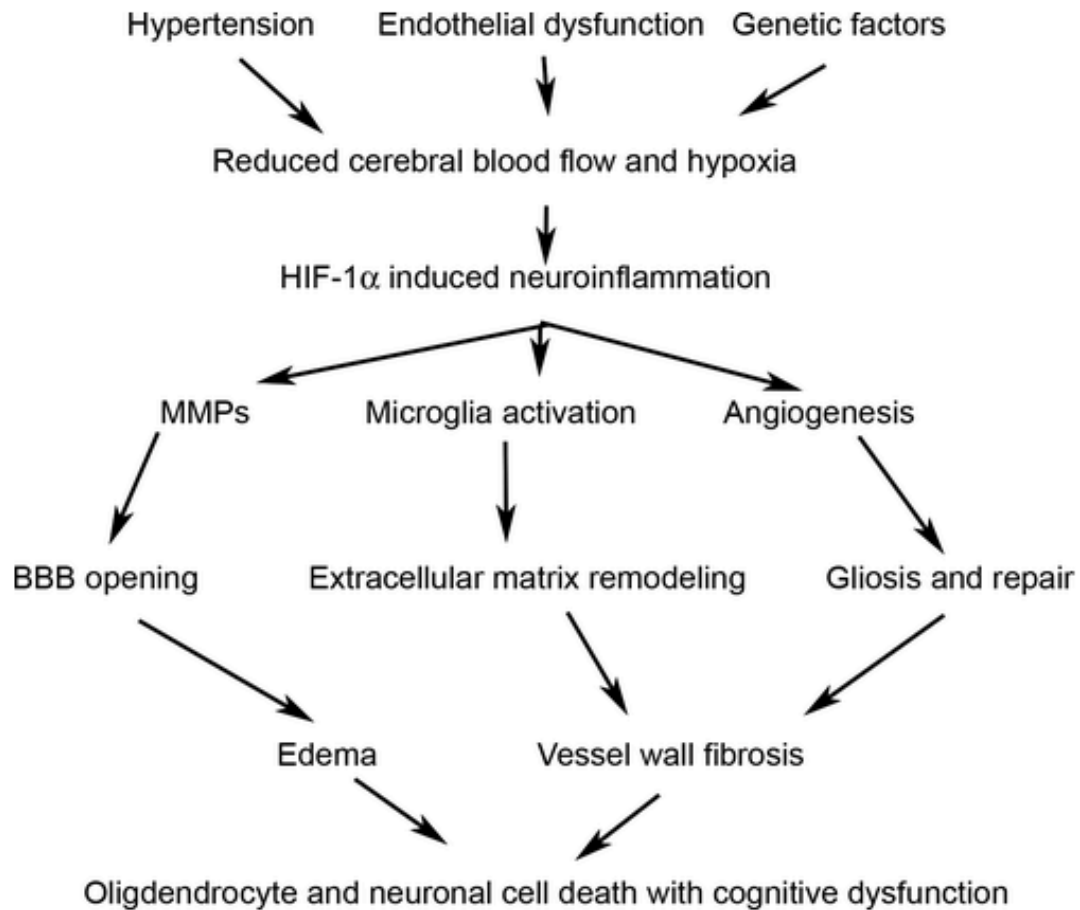
Figure 1.3: Schematic of the hypothetical injury cascade in SVD, involving the initial insult of hypertension, endothelial dysfunction and genetic factors leading to hypoxia, which triggers HIF-1α production. HIF-1α then activates a variety of inflammatory mechanisms leading to an opening of the BBB and vasogenic oedema, as well as vessel wall fibrosis leading to cell death and the clinical symptoms seen. Reproduced with permission from (Rosenberg, 2018).

1.5 BBB

1.5.1 Anatomy and Function of the BBB

The BBB is a complex structure that forms the walls of the capillaries within the central nervous system (CNS). A schematic is shown in Figure 1.4.

The main physical barrier comes from the endothelial cells, which form tight junctions that seal the paracellular diffusional pathway between cells (Luissint et al., 2012). Surrounding the endothelial cell surface is a basal lamina containing type IV collagen, fibronectin, heparin sulphate and laminin, which interacts with integrins to act as a molecular weight filter (Rosenberg, 2012). Accompanying the endothelial cells in its structure are many other cell types, including pericytes and astrocytes (Abbott et al., 2010). Pericytes wrap around the endothelial cells, forming a perivascular extracellular matrix. Pericytes are macrophage-like cells with smooth muscle properties; they are important as they can regulate blood flow and permeability through release of vasoactive substances (Rosenberg, 2012). Foot processes from the astrocytes then form around this matrix, which contain proteases, neurotransmitters and other essential molecules.

The function of the BBB is to regulate molecules passing into the brain and provide neurons with a stable environment for optimal synaptic signalling (Abbott et al., 2010). The permeability of specific substances through the BBB are regulated by transport systems. Only small solutes are able to pass through by diffusion, with solute carriers, transcytosis and mononuclear cell migration used for larger molecules.

The CNS does not have a large regenerative capacity, so any amount of cell death can have significant consequences. Leakage of blood-borne substances into the brain parenchyma can upset neuronal signalling, lead to problems with cellular communication and ultimately cause excitotoxic cell death. Further, reactive oxygen species (ROS) generation can occur, due to red blood cells depositing iron from haemoglobin (Zhong et al., 2008) and fibrinogen activating various intracellular pathways (Iadecola, 2013). Blood clots can also occur through the interaction of blood with collagen on the damaged endothelial cells; leading to ischaemia of the

small vessels, whilst also causing activation of fibrin, thrombin and plasmin, all of which have neurotoxic effects (Armao et al., 1997, Mhatre et al., 2004, Paul et al., 2007).
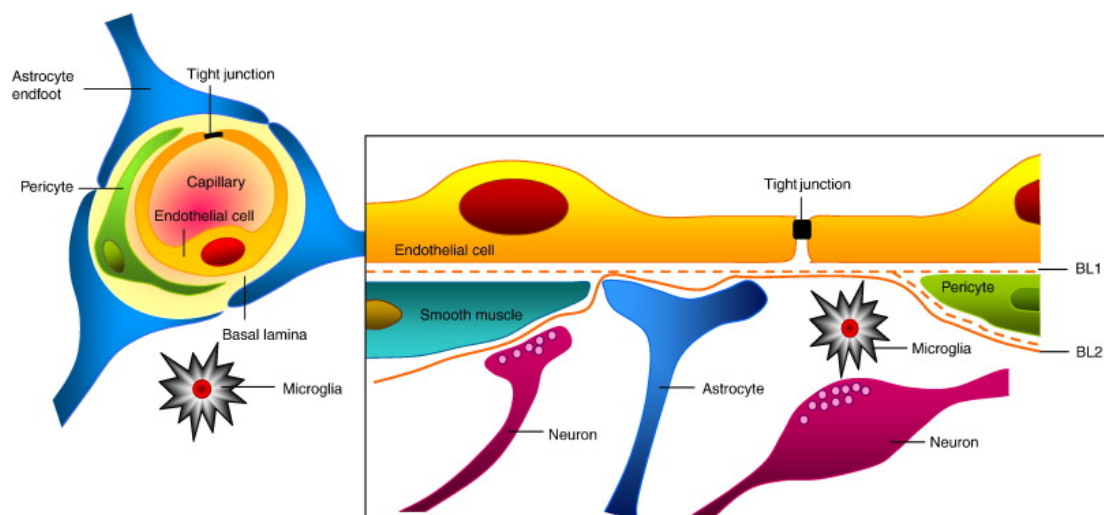
Figure 1.4: A schematic of the components of the BBB. The endothelial cells form tight junctions with pericytes distributed around them, enclosed by the basal lamina. Foot processes from astrocytes form a complex network around them. Reproduced with permission from (Abbott et al., 2010).

1.5.2 Role in Ageing

Many diseases increase in frequency with age: including heart disease, cancer, Alzheimer's, Parkinson's and all types of stroke (Erdő et al., 2017). The single biggest risk factor for SVD is age (Thompson and Hakim, 2009), leading researchers to question what is occurring in the ageing brain that makes it so susceptible to SVD.

Studies spanning from *in vitro* cell work to *in vivo* human populations have shown that there is an increased permeability of the BBB with ageing (Mooradian and McCuskey, 1992, Farrall, 2009, Goodall et al., 2018). Studies investigating endothelial cells have found that they undergo both oxidative stress and inflammation in healthy older adults, leading to a dysfunction and reduction in the cells (Donato et al., 2015). Further, there is decreased expression of tight junctions (Elahy et al., 2015, Goodall et al., 2018) and increased thickness of basement membrane (Candiello et al., 2010). These changes all likely have an impact on the permeability of the BBB with

35

ageing. Therefore, it is important to use age-matched controls in research studies to ensure that the BBB permeability changes that occur with normal ageing can be differentiated from the increased permeability in disease.

In the healthy ageing brain, BBB breakdown has been shown to start in the hippocampus, which has implications for Alzheimer's disease and cognitive impairment (Montagne et al., 2015). It has been suggested that in Alzheimer's disease, the accumulation of amyloid plaques in the brain is due to a lack of amyloid clearance across the BBB rather than a lower rate of production (Bateman et al., 2009).

Although increased BBB permeability is found in ageing and throughout age-associated disorders, it is difficult to know if it is pathogenic or simply resultant of other initiating pathologies. In some situations, extrinsic system factors such as infections and autoimmune processes effect blood vessels and initiate damage, whilst in others the blood vessels are damaged secondary to the injury through neuroinflammatory responses (Rosenberg, 2012).

1.5.3 BBB permeability in SVD

Early indications about an increase in BBB permeability in SVD came from studies investigating the CSF/serum albumin ratio. The more permeable the BBB, the more albumin will be present in CSF compared to serum and therefore the higher the ratio (Blennow et al., 1993, Tibbling et al., 1977). The ratio has been shown to be increased in both sporadic SVD (Alafuzoff et al., 1983, Wada, 1998) and CADASIL (Dichgans et al., 1999).

Further evidence came from post-mortem studies that can investigate levels of plasmas proteins in the CNS. Post-mortem examinations have found increased levels of the blood-borne proteins immunoglobulin and fibrinogen in the brains of diagnosed SVD patients (Tomimoto et al., 1996) and elderly patients with WMLs (Akiguchi et al., 1998). This indicates a disruption of the BBB, allowing these proteins to leak through the vessels into the brain.

MRI has been used to both quantify and map BBB permeability in the brain. Dynamic contrast enhanced (DCE)-MRI involves gadolinium contrast agent injection followed by periodic imaging of the gadolinium-induced signal change in the brain parenchyma, to measure permeability (Armitage et al., 2011). Many studies have applied this technique to an SVD population, and there is a fairly consistent finding that BBB permeability is higher in SVD patients compared to controls (Hanyu et al., 2002, Topakian et al., 2010, Taheri et al., 2011a, Huisa et al., 2015). Full details on the progression and application of DCE-MRI techniques will be discussed in Chapter Four.

BBB permeability can be measured in the whole brain or in specific brain regions using DCE-MRI. Studies have mainly focused on the WM, as this is thought to contain most of the SVD pathology. BBB leakage has been shown to be higher in the WM of SVD patients compared to controls (Taheri et al., 2011a, Huisa et al., 2015) and compared to cortical stroke patients (Wardlaw et al., 2009). The amount of BBB permeability was not increased in the GM in SVD compared to controls (Zhang et al., 2019, Zhang et al., 2017) and cortical stroke patients (Wardlaw et al., 2008), although an increased leakage volume in the GM was seen in SVD compared to control (Zhang et al., 2019, Zhang et al., 2017). In the CSF, increased permeability was seen in SVD compared to controls (Topakian et al., 2010) and cortical stroke patients (Wardlaw et al., 2008, Wardlaw et al., 2009).

Taking this further, studies have segmented the WM into normal-appearing white matter (NAWM) and WML and measured BBB permeability. This can help establish whether it is the already damaged WML tissue that has the increased permeability, or the seemingly healthy tissue of the NAWM. Studies have shown that there is an increase in BBB permeability in the NAWM compared to controls (Topakian et al., 2010). Leakage volume, but not leakage rate, was also found to be higher in NAWM compared to controls (Zhang et al., 2017).

Whether there is increased permeability in the WML of SVD compared to the WML of asymptomatic healthy elderly is controversial. Some studies showing that there is

increased WML permeability in SVD patients compared to healthy controls (Hanyu et al., 2002) whilst others show that the WMLs have the same amount of permeability (Topakian et al., 2010, Bronge and Wahlund, 2000). A recent study showed that there was higher leakage volume, but not leakage rate, in WMLs of SVD patients compared to WMLs of controls (Zhang et al., 2017). The discrepancies here could be explained through differences in methodology for quantifying permeability. Further studies are required to come to a consensus.

Studies have investigated the associations between BBB permeability and WML volume. Associations between BBB permeability in the NAWM and WML volume have been seen (Topakian et al., 2010, Wardlaw et al., 2017, Munoz Maniega et al., 2017, Li et al., 2017c). Other studies have also found that increased BBB permeability in the WML is associated with WML volume (Munoz Maniega et al., 2017, Wardlaw et al., 2017). However, this is controversial within the literature, with other studies showing different results: Zhang et al. showed that larger leakage volume but lower leakage rate in the WML was associated with larger WML in SVD (Zhang et al., 2019), whilst Huisa et al. found no correlation between WML BBB permeability and WML volume (Huisa et al., 2015). Huisa et al. then looked longitudinally at BBB permeability and WML lesion load; this found that only around 11% of new WML voxels had prior abnormal permeability over the previous 1-2 years (Huisa et al., 2015).

Studies then investigated the relationship beween BBB permeability and cognition. Scores on MMSE and MoCA decreased with increasing leakage rate in WML and GM (Li et al., 2017c). Higher leakage rate in NAWM was associated with lower scores in EF and PS in healthy controls, but not in SVD patients (Zhang et al., 2019). Looking longitudinally, poorer cognitive outcome at three year follow-up was associated with increased basal ganglia BBB permeability at baseline (Wardlaw et al., 2013b).

Overall, studies do suggest a role for BBB permeability in SVD, but how it fits in with the overall disease pathology in terms of imaging markers and clinical outcomes is unclear. Studies have not yet managed to reach a consensus about whether BBB

permeability is an initiating mechanism in the pathophysiology of SVD, or whether it is just a consequence of the other pathologies occurring. Additional studies are required to investigate this further.

1.5.4 Endothelial Cell Activation

Endothelial cells line all of the blood vessels throughout the body. Endothelial cells in the brain are unique in terms of their role in the BBB, regulation of CBF and interactions with other members of the neurovascular unit. In SVD, endothelial cells are seen to survive in histological studies, even in late stages of sporadic SVD (Lammie, 2002) and in CADASIL (Craggs et al., 2013). However, despite their survival, many functional studies have shown that the endothelial cells are activated and are therefore thought to be in a state of inflammation, growth and thrombosis (Hainsworth et al., 2015).

Endothelial cell activation results in a change of the expression of surface markers on the endothelium. Blood biomarkers of endothelial cell activation have been widely studied in SVD and recently reviewed (Poggesi et al., 2016). These circulating markers include, but are not limited to, intracellular adhesion molecule-1 (ICAM-1), vascular cellular adhesion molecule-1 (VCAM-1), E-selectin and P-selectin. ICAM-1 and VCAM-1 levels are elevated in patients with lacunar infarcts compared to controls (Rouhl et al., 2012). ICAM-1 is also found to be higher in a healthy population with silent brain infarcts (Sarchielli et al., 2013). WMLs have been associated with higher levels of ICAM-1, VCAM-1, E-selectin and P-selectin (Fassbender et al., 1999, Hassan et al., 2003, Han et al., 2009, Markus et al., 2005, de Leeuw et al., 2002). Looking longitudinally, ICAM-1 levels at baseline can predict future WML progression seen on MRI at 3 and 6 years in SVD patients (Markus et al., 2005), and future silent brain infarcts in a type 2 diabetes population (Umemura et al., 2008).

Markers of coagulation and fibrolysis have been investigated in SVD. Thrombomodulin is an integral membrane protein found in the vascular endothelium of systemic blood vessels; its function is to modulate the prothrombotic molecule

thrombin, so that thrombin becomes incapable of generating a fibrin clot from fibrinogen, protecting the brain from thrombosis (Fisher, 2012). Once bound to thrombin, the complex activates protein C and initiates an anticoagulant pathway. High levels of thrombomodulin found in the blood are believed to reflect endothelial injury, which would be consistent with a breakdown of the BBB (Hassan et al., 2003). One study did show a positive association of thrombomodulin with lacunar infarcts (Hassan et al., 2003) whereas two further studies did not see this association (Gottesman et al., 2009, Knottnerus et al., 2010). Von Willebrand factor (vWF) is a glycoprotein expressed by endothelial cells after tissue damage, leading to thrombus formation and blood coagulation (Hassan et al., 2012). It was found to be associated with the presence and number of silent brain infarcts (Gottesman et al., 2009) and WML volume (Kearney-Schwartz et al., 2009).

Animal models of SVD have also been used to try to uncover SVD pathology (Hainsworth et al., 2012). Animal models are particularly important for discovering early stage pathology in SVD and whether endothelial cell dysfunction could be an initiating mechanism. The most common animal models used are the stroke prone spontaneously hypertensive rats (SHRSP) and the spontaneously hypertensive rats (SHR), derived from selective breeding. These rats show similar degrees of hypertension, SVD-like vessel pathology, focal infarcts, cognitive impairment and WM damage, although this varies between the models (Lin et al., 2001). It is important to note that no current animal models of SVD completely replicate the pathology we see in human SVD, and therefore results should always be treated with caution (Hainsworth and Markus, 2008).

SHRSP and SHR rats show endothelial dysfunction, manifesting as BBB impairment, histopathologically (Sadoshima and Heistad, 1982, Hazama et al., 1979, Lee et al., 2007, Braun et al., 2012, Kaiser et al., 2014) and on imaging (Sironi et al., 2004, Guerrini et al., 2002). Studies have suggested that endothelial tight junctions occur in these rats at the earliest ages, preceding other damage (Bailey et al., 2011) and treatment with endothelial cell stabilising drugs can prevent SVD from manifesting (Rajani et al., 2018). Further, studies have shown that endothelial function deteriorates with an increasing hypertension (Lee et al., 2007, Knox et al., 1980). This

evidence, and other evidence from human studies, has lead to debate on the systemic vs. localised nature of SVD (Thompson and Hakim, 2009). Is SVD a systemic disease or a disease confined to the CNS?

The dysregulation of CBF is an important factor in the pathology of SVD, which has been suggested to come from endothelial cell dysfunction. CBF relies on endothelial nitric oxide signalling, so a dysfunction of endothelial cells may lead to impaired regulation globally. Functional studies have shown that lacunar infarct patients are less able to respond to vasodilatory stimuli (Deplanque et al., 2013). Further, SVD patients have been seen to have a reduced response to L-arginine and flow-mediated dilatation experiments, with the amount of systemic endothelial dysfunction paralleled with the WML volume (Zupan et al., 2015, Pretnar‑Oblak et al., 2017). These experiments suggest a systemic change in vasodilatation, which may be mediated by an underlying endothelial cell dysfunction.

Additionally, there are diseases of other blood vessels that seem to associate with SVD. Retinopathy has been correlated with poorer cognitive function and greater risk of lacunar stroke (Wong et al., 2002). Additionally, patients with chronic kidney disease were found to have a greater prevalence of WMLs (Khatri et al., 2007), suggesting that there could be a widespread small arteriopathy or endotheliopathy.

Various proteins produced in other organs are associated with SVD pathology. Homocysteine is produced in the liver and kidney as a product of metabolism of methionine; elevated levels of homocysteine can result from folate deficiency or in patients with kidney disease (Cianciolo et al., 2017). Homocysteine is elevated in SVD (Hassan et al., 2004) and has been shown to correlate with lower brain volume and increased risk of silent brain infarcts (Seshadri et al., 2008). It is also associated with WML volume (Rosenberg et al., 2014, Kloppenborg et al., 2014, Nam et al., 2019). Homocysteine levels have also been found to correlate with cognitive function, suggesting a relation with clinical status (Pavlovic et al., 2011). The evidence for an involvement of homocysteine in SVD was so strong that clinical trials were carried out, to see if lowering homocysteine with vitamins could improve cognition; unfortunately the trials were all negative (Clarke et al., 2014).

Microalbuminuria is a ratio of urinary albumin to creatinine ratio and is thought to reflect early kidney damage or systemic endothelial dysfunction (Abdelhafiz et al., 2011). It was seen to be a risk factor for silent brain infarcts and WMLs in a healthy elderly population (Wada et al., 2007) and hypertensive populations (Delgado et al., 2014, Knopman et al., 2008).

All of these diseases share common cardiovascular risk factors, so it could be that the prevalence is simply due to the shared risk. Further, it is possible that SVD in one organ could accelerate the involvement of other organs through the release of certain factors; this is something that has been seen in studies but the extent of this effect in SVD is unknown (Touyz, 2004). However, evidence suggests that SVD is a heterogeneous and multi-factorial disease, which likely impacts other organs with widespread effects throughout the body.

1.5.5 Pericytes

Pericytes are known to be an important component of the BBB. Cerebral pericytes are contractile and regulate capillary diameter during functional activation (Peppiatt et al., 2006). Animal models have shown that a loss of pericytes leads to brain vascular damage through a reduction in CBF and breakdown of BBB (Bell et al., 2010). Under ischaemic conditions, pericytes have been shown to die and remain in a rigor mortis state, which restricts the vessels and limits blood flow to those areas (Hall et al., 2014). Pericyte deficient mice have increased BBB permeability (Armulik et al., 2010, Reske-Nielsen et al., 1966), which leads to WM changes (Montagne et al., 2018).

Pericyte loss and basement membrane thickening have been seen in conditions that represent major risk factors for SVD, such as ageing (Kalaria, 1996, Bell et al., 2010), hypertension (Tagami et al., 1990) and diabetes (Johnson et al., 1982). Post-mortem analysis has shown a reduction in pericyte number in aged brains compared to young brains (Stewart et al., 1987) and in Alzheimer's disease compared to age matched

controls (Miners et al., 2018). However, this has not been reported in post-mortem SVD brains.

The majority of the SVD pericyte research has occurred in the CADASIL mouse model of *Notch3* mutation. The CADASIL mouse shows Notch3 aggregation in the pericytes leads to a reduction in pericyte coverage of vessels over time (Ghosh et al., 2015). These vessels are then shown to have increased leakage of albumin, suggesting they have a BBB disturbance. This work has been shown in human CADASIL patients, with degeneration and loss of pericytes from capillary vessels leading to increased permeability of the vessels and disturbances in cerebral microcirculation (Dziewulska and Lewandowska, 2012)

1.5.6 Astrocytes

The contribution of astrocytes to maintaining BBB function is not fully understood (Erdő et al., 2017). Astrocytes show a number of different morphologies depending on their location. There is now strong evidence that astrocytes may upregulate many BBB features, including increasing the tightness of the tight junctions, which would regulate permeability (Abbott et al., 2006).

Astrocyte end-feet cover over 99% of cerebral capillaries, leading to cell-cell interactions that modulate and regulate the BBB (Abbott et al., 2006). Loss of astroglial function and astroglial reactivity contributes to aging of the brain and neurodegeneration, but it is highly heterogeneous (Rodriguez-Arellano et al., 2016). Astrocytes are involved in the production of lipoproteins including Apolipoprotein E (ApoE), which has an important role in Alzheimer's pathology and BBB injury (Erdő et al., 2017). However, astrocytic involvement in BBB permeability of SVD has not been specifically investigated.

1.6 Inflammation

1.6.1 Neuroinflammation

Microglia are the resident macrophages of the brain, and are rapidly activated in response to brain injury (Aloisi, 2001). Microglia activation induces the release of pro-inflammatory mediators, such as cytokines, chemokines, ROS and interleukins (ILs), which increase the permeability of the BBB. This then allows for subsequent infiltration of peripheral leukocytes into the CNS, including T cells and macrophages. Therefore, this increased BBB permeability means that peripheral macrophages can have a role in neuroinflammatory outcomes, leading to neuronal cell death, releasing further neurotoxins and causing further microglial activation as a negative feedback loop.

Activated microglia have been described as a double-edged sword, where they can have both toxic and beneficial roles. Research now suggests that microglia activate in a similar way to macrophages, with both an M1 and an M2 phenotype (Hu et al., 2015). The M1 phenotype represents a proinflammatory phenotype releasing inflammatory mediators such as prostaglandins, tumour necrosis factor-α (TNF-α), interleukin-6 (IL-6), interleukin-1β (IL-1β), ROS and glutamate. However, the M2 phenotype attempts to resolve the inflammation, with release of anti-inflammatory mediators such as interleukin-10 (IL-10), insulin-like growth factor 1 and neurotrophic factors (Reus et al., 2015).

1.6.2 Inflammation in SVD

Inflammation has been recognised as a key component of cerebrovascular and neurological diseases. Inflammatory cell infiltrations in the arteriolar wall and perivascular tissue have been noted in the elderly since 1902 (Ferrand, 1902).

In SVD, there is a combination of both acute and chronic inflammation. Acute inflammation occurs with the formation of lacunar infarcts due to acute vessel blockage, leading to activation of inflammation in response to hypoxia/ischaemia (Fu and Yan, 2018). The chronic inflammation is thought to be related to the underlying

hypoperfusion and BBB changes and is likely more similar in pathophysiology to chronic neurodegenerative diseases such as Alzheimer's disease. Studies looking at both systemic and central inflammatory markers can help discover more about the underlying pathogenesis of the disease and potentially uncover biomarkers that can be used to track disease severity and treatment effect.

Immunohistochemical techniques can be used to detect specific molecular markers that can identify activated microglia. Constitutive expression of ionized calcium-binding adapter molecule-1 (IBA1) is specific for microglia, irrespective of activation state. A marker of M1 microglia phenotype is CD68, mannose receptor CD206 can be used as a marker of M2 phenotype. Post-mortem studies have shown there is an increase in CD68 positive microglia in the WML in the aged brain compared to control WM (Simpson et al., 2007a, Waller et al., 2019). Studies into Alzheimer's disease patients showed a similar pattern of increased CD68 activated microglia in the patient brain compared to control (Hopperton et al., 2018). This suggests that in these neurodegenerative states there is an increase in activated pro-inflammatory M1 microglia, but not in the anti-inflammatory M2 microglia.

In recent years, several radioligands have been developed to image the activation of microglia in experimental models. The majority of these ligands bind to the 18kDa translocator protein (TSPO). Under normal conditions, TSPO levels are low in the CNS (Lavisse et al., 2012). However, during neuroinflammation, TSPO is over-expressed in microglia, representing an activated microglia state (Liu et al., 2014b, Venneti et al., 2006, Rupprecht et al., 2010).

By far the most validated PET tracer for TSPO human studies, and therefore most commonly used, is $[C^{11}]$PK11195 (PK) (Chauveau et al., 2008). This method has been used previously for detection of microglia activation in ischaemic stroke and has showed increased activation around the infarct site (Gerhard et al., 2005). This has also been linked to cognition, with a high correlation seen between microglial activation in the stroke-affected hemisphere WM and cognitive impairment (Thiel et al., 2014). However, to the best of my knowledge, it has not been investigated in SVD. The application of PK for SVD will be thoroughly discussed in Chapter Five.

45

Inflammation can also be quantified through the measurement of various inflammatory biomarkers. Most of them can be detected in serum/plasma samples or in the CSF and quantified using various assay techniques. The CSF provides a more accurate representation of their concentration within the CNS, but is far more difficult to obtain due to the requirement of a lumbar puncture. An 'index' can also be calculated to distinguish between endogenous and exogenous proteins, through measurement of the biomarker in both the CSF and blood to form a ratio (Candelario-Jalil et al., 2011). Alternatively, levels of these biomarkers can be measured post-mortem, which allows for the anatomical mapping of their location.

Circulating inflammatory biomarkers in SVD have recently been reviewed in detail (Low et al., 2019) and will be discussed in more detail in Chapter Seven. Briefly, the most commonly studied systemic inflammatory biomarkers in this field are C-reactive protein (CRP) and IL-6 (Vilar-Bergua et al., 2016). C-reactive protein is an acute-phase reactant synthesised in the liver in response to IL-6, and has been widely used as a vascular inflammatory marker. IL-6 is secreted by T cells and macrophages to stimulate immune response and by smooth muscle cells of blood vessels as a proinflammatory cytokine. CRP and IL-6 have been associated with a variety of cardiovascular risk factors including diabetes (Pradhan et al., 2001) and hypertension (Sesso et al., 2003). CRP and IL-6 have also been associated with infarcts (Hoshi et al., 2005, Yoshida et al., 2009), enlarged perivascular spaces (Aribisala et al., 2014) WMLs and brain atrophy (Satizabal et al., 2012).

MMP-2, MMP-3 and MMP-9 are produced by microglia, astrocytes and endothelial cells as part of the inflammatory response (Gottschall and Deb, 1996, Asahi et al., 2001, Rosenberg et al., 2001a). Early stages of hypoxia are thought to activate matrix metalloproteinase-2 (MMP-2), which initiates reversible disruption of the basal lamina proteins and opening of the tight junction proteins (Yang et al., 2007); this is thought to be short lived. However, increasing hypoxia levels activate inducible matrix metalloproteinase-3 (MMP-3) and matrix metalloproteinase-9 (MMP-9), which causes irreversible degradation to the basal lamina and tight junction proteins (Rosenberg, 2016). One study found that MMP-9 levels were elevated in CSF of

vascular dementia patients, with no changes in MMP-2 effect (Adair et al., 2004). A further study then went on to use the 'index' method and found that MMP-9 was elevated in both the CSF and blood, meaning no change in the index, whereas MMP-2 index was reduced, suggesting possible endogenous consumption (Candelario-Jalil et al., 2011). This study also showed MMP-3 to be elevated in the CSF of SVD patients. An investigation into the differences between SVD and Alzheimer's disease found that MMP-9 and MMP-2 were two of the markers that contributed most to SVD, but little to Alzheimer's disease (Bjerke et al., 2011). Autopsy results showed that vascular dementia patients were found to have MMP-2 in macrophages and astrocytes near blood vessels and MMP-3 in microglia/macrophage cells around infarctions (Rosenberg et al., 2001b).

1.7 Conclusion

SVD is a highly prevalent disease within our population, leading to vascular dementia and stroke. SVD is heterogeneous, with a complex pathophysiology. Our lack of understanding of the underlying pathogenesis has limited the discovery of new treatments.

Studies have indicated that there does seem to be an increase in BBB permeability in SVD patients. There also seems to be a role for neuroinflammation in SVD. However, whether these pathologies are causal or consequential of the other damage occurring is unclear and requires further investigation.

The emergence of new imaging techniques means that BBB permeability and neuroinflammation can now be accurately quantified and mapped in SVD patients. Utilising these techniques would allow the role of BBB permeability and neuroinflammation to be fully explored to determine if the processes are pathological in SVD.

Furthering our understanding of the pathophysiology of SVD would allow for new treatments to be tested, which target the underlying mechanisms directly, to reduce disease progression and the prevalence of vascular dementia and stroke.

1.8 Objectives of the Research

The availability of PET/MR imaging allows for simultaneous DCE-MRI for mapping of BBB permeability and PK PET imaging of activated microglia, in the same patients. The imaging modalities can be overlayed into the same space to determine the spatial association between the two. Using sporadic SVD patients, monogenic SVD (CADASIL) patients and controls, we can explore the relationship between BBB permeability and inflammation in both disease and healthy ageing.

This thesis aims to address the following research questions:

- Are conventional MRI and DTI markers associated with cognitive decline? (Chapter Three)
- Is there increased BBB permeability in sporadic SVD and CADASIL patients compared to controls? Does BBB permeability associate with conventional MRI, DTI and cognition? (Chapter Four)
- Is there increased PK binding in sporadic SVD and CADASIL patients compared to controls? Does PK binding associate with conventional MRI, DTI and cognition? (Chapter Five)
- Is there a spatiotemporal relationship between BBB permeability and PK binding hotspots? (Chapter Six)
- Are serum markers of inflammation, MMPs and endothelial cell activation increased in SVD? Are they associated with BBB permeability and PK binding? (Chapter Seven)

The primary hypothesis of the thesis is:
BBB permeability and PK binding are increased in sporadic SVD and CADASIL compared to control.

The secondary hypotheses of the thesis are:

- BBB permeability and PK binding are associated with conventional MRI and DTI
- BBB permeability and PK binding are associated with cognition
- BBB permeability and PK binding are spatially related to each other

- BBB permeability is associated with circulating MMPs and markers of endothelial cell activation
- PK binding is associated with circulating inflammatory markers

Chapter 2: Methods

2.1 Study Set-up

2.1.1 Study Approvals and Support

The BBB permeability and Neuroinflammation in SVD study ran from January 2017 and is currently ongoing. It was approved by the East of England – Cambridge South Ethics Committee (REC no: 16/EE/0468, IRAS project ID: 212632). Approval was also granted by the Administration of Radioactive Substances Advisory Committee (ARSAC ref: 999/9000/35589). The study was supported by the National Institute for Health Research through inclusion in its Clinical Research Network Portfolio.

2.1.2 Power Calculations

Power calculations from preliminary data were used to estimate the sample sizes required for this study to allow us to detect a difference in BBB permeability and PK binding. For prediction of the DCE-MRI data (n=6), using a similar technique to this study, we found a mean BBB permeability in WM of SVD patients of 9×10^{-4} (SD 2×10^{-4}) L/g min. Therefore, we could detect a 20% change in permeability in the control group with power 0.8 and p=0.05, using a two-sided test, with 20 participants per group. Similarly for the PET data, our pilot data (n=3) found WM binding of 0.174 (SD 0.04). With a power of 0.8 and p=0.05, a two-sided test can detect a 20% change in binding with a sample size of 21 per group. These calculations suggested that 20 participants per group would be realistic for detecting a difference in these parameters.

2.2 Participants

2.2.1 Groups

Three groups of 20 participants (60 participants in total) were recruited for this study into the following groups: sporadic SVD, CADASIL and healthy control. Patients were recruited from the Addenbrooke's Stroke Service, and from Professor Hugh Markus' national CADASIL clinic. All participants gave written informed consent. Participant age ranged from 31 to 90 years old, with a mixture of male and female.

2.2.2 Inclusion/Exclusion Criteria

Sporadic SVD participants were defined as patients who had clinical evidence of lacunar stroke syndrome (e.g. pure motor stroke, pure sensory stroke, sensorimotor stroke or ataxic hemiparesis, or clumsy hand dyarthria syndrome) with a corresponding lacunar infarct on DWI, for cases imaged within 3 weeks of stroke, or an anatomically compatible lacunar infarct on FLAIR/T1 MRI, for cases imaged later after stroke (<=1.5cm diameter). They also had to have confluent WMLs on T2 weighted MRI (Fazekas et al., 1987). Participants were not recruited until at least 3 months since their last acute infarct, to avoid changes secondary to acute injury. These patients had no stroke cause other than SVD and no evidence of cortical stroke.

CADASIL participants were subjects with a confirmed genetic diagnosis as defined by a recognised *Notch3* mutation. They also had to be at least 3 months from their last stroke to avoid changes secondary to acute injury.

Healthy controls were participants with no history of stroke or evidence of other major neurological disorder. These were of similar age to the sporadic SVD patients.

The MMSE of all participants had to be >21 for consent purposes. All subjects had to have no contraindications for taking part in an MRI study (e.g. pacemaker). Women of childbearing age were not allowed to take part due to ethical reasons concerning the radioactive ligand injection. The participants also had to have an eGFR >=59ml/min/1.73m^2 from the past 3 months to ensure gadolinium was safe to administer.

2.3 Demographics and Clinical Assessments

Participant demographics were collected during the baseline appointment. Date of birth, sex, occupation, years in education and ethnicity were all recorded. Height, weight and blood pressure were also all measured and recorded. Age and sex were required so that analyses could be controlled for any age or sex related differences (Mooradian, 1988, Sohrabji, 2007).

The cardiovascular risk factors of hypertension, hyperlipidaemia, type 2 diabetes and smoking were also recorded, as they were required to provide additional controls for analyses (Becker et al., 2019). Participants were marked as a smoker if they indicated that they had ever been a smoker, even if they had since stopped. Additionally, the neurological risk factors of history of depression and migraine were noted.

All current medications were listed, with dates the participants began taking them, so that these could be controlled for if they were found to have any effect on the primary end-points.

For participants who had experienced a stroke, the date of the stroke was documented, the age at the stroke, as well as whether they were thrombolysed and a description of the clinical symptoms experienced. If the participant had experienced multiple strokes/TIAs then these were also documented with the date, age at stroke and the clinical symptoms.

2.4 Scanning

2.4.1 Baseline PET/MRI scan

All participants underwent a PET/MR scan on the GE SIGNA PET/MR scanner (GE Healthcare, Waukesha, USA) at the Wolfson Brain Imaging Centre in Cambridge, UK. The scanner had a 3.0T MR, which scans simultaneously with PET. The scan was carried out using a 32-channel NOVA coil (Nova Medical, Wilmington, USA). All subjects were placed in the head coil in a neutral position; minimal head movement was ensured during the scan through the use of foam pads.

Total imaging time was 80 minutes. Patients were injected with PK radioligand for the PET scan at the beginning of the session; 80 minutes of PET recording then occurred. 5 minutes after injection, 45 minutes of non-contrast MRI sequences begun, followed by 25 minutes of DCE-MRI.

The DCE-MRI was acquired in a sub-section of the brain, manually chosen by the radiographer to include the regions of characteristic SVD damage. All other sequences were acquired across the whole brain.

2.4.2 Non-Contrast MRI

Non-contrast MRI was run within the PET bed. These sequences were as follows:

1. 3D T1 weighted images taken with a fast spoiled gradient echo sequence. Flip angle = 12°, TI = 450, field of view (FOV) =28mm, slice thickness = 1 mm, number of slices – 192, reconstructed matrix size = 512x512. This sequence allows for accurate brain volume measurements and for general structural knowledge.

2. Axial susceptibility weighted imaging. Flip angle = 17°, TR = 40.6ms, TE = 24.2ms, FOV = 22mm, slice thickness = 2 mm, number of slices = 70, reconstructed matrix size = 256x256. This sequence can be used to detect CMBs.

3. Axial T2 FLAIR sequence, angled anterior commissure-posterior commissure (AC-PC). Flip angle = 160°, TR = 8800ms, TE = 120ms, TI = 2445ms, FOV =

22mm, slice thickness = 5 mm, number of slices = 28, reconstructed matrix size = 256x256. This sequence is for identification of WMLs and lacunes.

4. Axial diffusion tensor imaging (DTI) in 63 directions. TE = minimum, TR = 15763ms, FOV = 19.2mm, slice thickness = 2 mm, number of slices = 665-670 depending on slice angulation, reconstructed matrix size = 256x256. This sequence can be used to extract MD and FA values that represent WM microstructure integrity.

5. Axial T2 fast spoiled gradient echo sequence in AC-PC angle. Flip angle = 111°, TE = 85ms, TR = 6000ms, FOV = 22mm, slice thickness = 5mm, number of slices = 31, reconstructed matrix size = 1024x1024. This sequence is used for identification and counting of CMBs.

2.4.3 Contrast MRI

Following this, gadoterate meglumine (Dotarem) was used to visualise BBB permeability. The gadolinium dose was 0.025mmol/kg, a quarter of the dose used clinically (Taheri et al., 2011b). The injection flow rate was 6m/s followed by a saline flush. T1 was mapped prior to injection, followed by the gadolinium, followed by 25 minutes of T1 mapping.

The sequence uses a 3D radiofrequency (RF)-spoiled gradient echo imaging sequence to obtain T1 relaxation times. 6 flip angles were used (2°, 5°, 12°, 17°, 22°, 27°) to calculate each map. 8 post injection maps with temporal resolution of about 2.5 minutes were collected. TR=6.3ms, TE=1.784ms, resolution = 2x2x3mm (reconstructed to 0.94x0.94x3mm) number of slices = 16 and reconstructed matrix size = 256x256. There is a B0 mapping sequence for flip angle correction; flip angle = 15°, number of echoes = 1, receiver bandwidth = 15.63, FOV = 35mm, slice thickness = 5 mm.

2.4.4 PET

An MR localiser was used so that the scanner bed could be translated to locate the brain in the centre of the axial PET FOV (25cm). Prior to PET tracer injection, an

MR attenuated correction (MRAC) sequence (2-point Dixon, LAVA-Flex) was acquired to provide information utilised for attenuation correction of the PET data.

Following the MRAC sequence, the tracer PK (produced at the Wolfson Brain Imaging Centre Radiopharmaceutical Unit) was injected over approximately 30s and list-mode PET data were acquired for 75 minutes. The effective/target tissue dose per administration was 2.6mSv with proposed activity of 500MBq. The median injected activities were 438 (IQR 400-482) MBq with corresponding injected mass values of 4.2 (IQR 2.8-6.3) μg.

2.5 Non-Contrast MRI Analysis

2.5.1 WMLs

WML were quantified as the presence of signal abnormalities or hyperintensities from the WM of the periventricular and subcortical regions on the axial FLAIR T2 sequence. Both hemispheres were marked for WML volume by a single trained rater (JW) using the semi-automatic contouring technique Jim analysis software version 7.0.5 (Xinapse Systems Limited, http://www.xinapse.com/j-im-7-software/). Whole brain WML maps were generated.

To assess inter-rater reliability, ten of the FLAIR scans were remarked in a randomised, blinded setting. They were marked for the second time by JW and once by a second experienced rater (DT). The inter-rater and intra-rater reliability coefficients were 0.988 and 0.993 respectively. An example WML marked T2-FLAIR scan is shown in Figure 2.1.
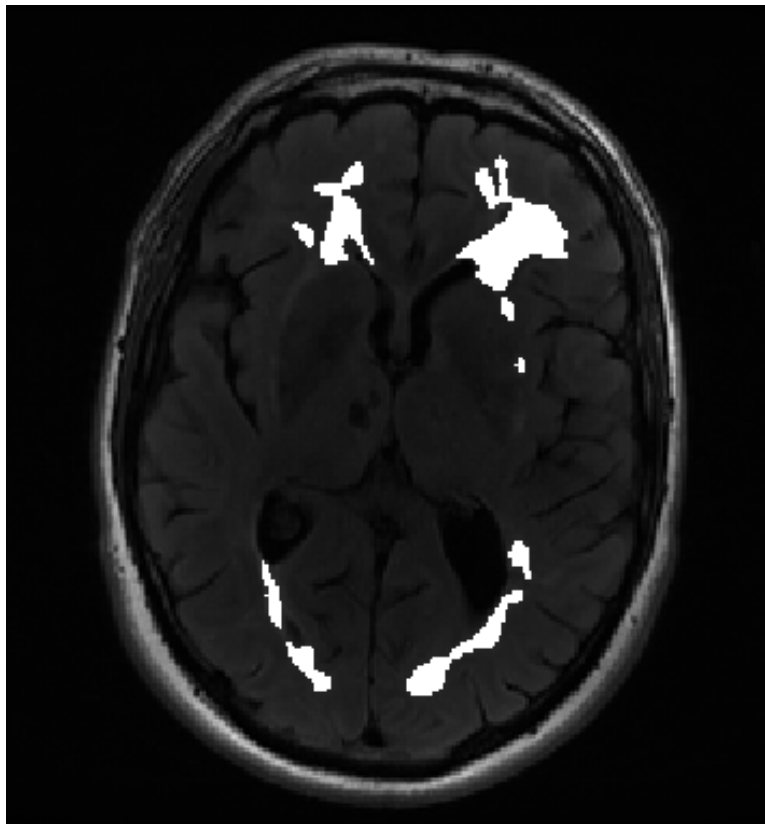
Figure 2.1: Example image of a T2-FLAIR scan marked for WMLs (white).

All areas of hyperintensity on the FLAIR scan were included unless they were:

- Surrounding an established infarct unless this infarct is with an area of confluent white matter hyperintensity
- A narrow band around the ventricles that you would consider normal clinically
- Midline high signal streaks as these are likely to be artifact
- Small punctuate of only moderate intensity
- Infratentorial
- Established lacunes i.e. seen as dark on T1
- Acute infarcts i.e. seen as bright on DWI

2.5.2 Lacunar Infarcts

Lacunes were defined as CSF filled cavities at least 3mm in diameter. They were marked on FLAIR images manually by a single neurologist (AD). T1, T2 and FLAIR scans were all used to identify and confirm the lacunes. The neurologist had training in distinguishing them from perivascular spaces. The lacunes were defined as a lesion occurring in the subcortical and deep white matter regions of the brain, likely supplied by a single small vessel. Location, size, shape (round or oval shape) were all considered in order to distinguish lacunes from other mimics such as perivascular spaces or CMBs.

The lacunes were both counted and drawn around using semi-automatic contouring with Jim analysis software version 7.0.5, in a similar way to the WMLs. The neurologist was blinded to the clinical status of the subject.

2.5.3 CMBs

CMBs were defined as focal areas of very low signal intensity on the T2* weighted images. They were manually counted by a neurologist (AD) and the neurologist recorded the number of CMBs for each participant. The neurologist was blinded to the clinical data.

2.5.4 Brain Volume

T1 images were used to calculate the brain volumes. The FLAIR image was registered to the T1 image using a rigid body transformation in Advanced Normalization Tools (ANTs, http://stnava.github.io/ANTs/). The resulting transformation was used to resample the WML mask from the FLAIR image to the T1 image using nearest-neighbour interpolation.

T1 images were processed using the 'segment' routine in SPM12 (https://www.fil.ion.ucl.ac.uk/spm/software/spm12/). This segmentation alternates between image registration, bias correction and tissue classification. Image registration aligns the two images together. Bias correction corrects the bias field signal caused by magnetic field inhomogeneities. Tissue classification assigns a probability value for GM, WM and CSF for every voxel in the brain. This is conditional based on a previously-defined population template (Ashburner and Friston, 2005). The process alternates between these steps to create the best segmentation possible.

Segmentation provides tissue probability maps for every subject, where every voxel has an assigned probability of belonging to a certain tissue class. Volumes for each tissue class were calculated as the sum of all voxels that have a probability of >0.5 of belonging to that class, after having WML voxels removed. Total brain volume is the sum of the GM and WM volumes, and ICV is the sum of the total brain volume and CSF volumes.

All segmentations and registrations were visually inspected for errors.

2.5.5 WM Microstructure

DWI is a variant of conventional MRI based on the tissue water diffusion rate. DWI refers to the contrast of the acquired images, whilst DTI is a specific type of modelling using the DWI datasets, which allows for modelling of WM microstructure (Soares et al., 2013). DW images are made sensitive to the movement of water molecules within a tissue by the application of gradients, which 'measure' how far the

water molecules have moved in a certain time. This movement will differ amongst directions depending on the tissue type, integrity, architecture and presence of barriers. Applying the diffusion gradients in a specific direction sensitises your images to diffusion in that direction so by acquiring multiple images you can obtain information on the ease and directionality of diffusion in the tissue. There are two key parameters that are taken from DTI imaging: MD is the molecular diffusion rate, or a measure of the ease of diffusion, and FA is a measure of the directional dependence of diffusion. Within WM, diffusion tends to be easier along the axons than across it, so is anisotropic; in GM it is less anisotropic and in CSF it is unrestricted in all directions, so is isotropic.

DTI analysis was carried out in the same way it has been described previously (Croall et al., 2017). Briefly, FSL software ("FDT"; FMRIB's Diffusion Toolbox, http://fsl.fmrib.ox.ac.uk/fsl/fslwiki/FDT) was used for DTI preprocessing. Scans were corrected for eddy current and a binary brain mask in DTI space was calculated. FA and MD maps were then calculated from this data. Voxels with MD values above 2.6×10^{-4} mm^2s^{-1} were removed from analyses as these likely contain CSF. Likewise, voxels with FA>1 were also removed. For each participant, FMRIB Linear Image Registration Tool was used to register the T1 weighted image to the B0 image, which could then be used to create a transformation of FLAIR to DTI. These were all manually checked. Tissue probability maps and WML masks were then transformed into DTI space. The tissue and WML masks were then used to create tissue specific diffusion parameter maps.

Histogram analysis was performed on the FA and MD maps in WM, NAWM and WML. Normalised histograms with 1000bins (FA range: 0-1, bin width: 0.001; MD range: $0-4 \times 10^{-3}$ mm^2s^{-1}, bin width: 0.004×10^{-3} mm^2s^{-2}) were computed and median, peak height, peak location, skew and kurtosis were extracted. These metrics were chosen as summary measures as FA and MD are non-normally distributed in WM.

2.5.6 Freewater

Freewater (FW) maps and FW adjusted FA and MD maps were estimated using a non-linear regularised minimisation process implemented in Matlab (Pasternak et al., 2009) and were carried out in a similar way to previously described (Duering et al., 2018). Briefly, each voxel was fitted to a two-compartment model, which included a FW compartment (isotropic tensor with fixed diffusion constant of water at 37°C) and a tissue compartment (FW corrected tensor). The estimated parameters were the fractional volume of the FW compartment and the tensor of the tissue compartment. The FW measure ranges from 0 to 1 and expresses the relative contribution of FW in each voxel. The tensor of the tissue compartment reflects the tissue microstructure with the signal from FW removed. Following this, MD and FA were recalculated using the histogram analysis described above.

2.6 Contrast MRI analysis

2.6.1 Data Processing

Permeability maps were created as detailed in the previous literature (Taheri et al., 2011b). The T1 maps from the contrast MRI can be used to calculate estimations of gadolinium concentration in the tissue, assuming a linear relationship.

As described above, T1 values are calculated using a variable flip angle technique with 6 flip angles (2°, 5°, 12°, 17°, 22°, 27°). We obtained one map prior to injection then 8 post contrast injection maps with at temporal resolution of about 2.5 minutes. The T1 values can be calculated from the multiple flip angles (α) by fitting the data to the equation below to the data.

$$S = M_0 \sin(\alpha) \left(\frac{1 - e^{-\frac{TR}{T_1}}}{1 - \cos(\alpha) \cdot e^{-\frac{TR}{T_1}}} \right)$$

The relationship between the pre- and post-contrast longitudinal relaxation rate difference at any point in time ($\Delta(1/T_1(t))$) and the concentration of contrast agent at that time point ($C(t)$) is assumed to be linear, with k as the constant of proportionality.

$$\Delta(1/T_1(t)) \cdot k = C(t)$$

The concentration of gadolinium over time can then be used to calculate the level of permeability, using the Patlak modelling technique (Patlak and Blasberg, 1985). The Patlak technique uses the following equation:

$$C_{tiss}(t) = Ki \int_0^t C_{pa}(\tau)d\tau + C_{pa}(t)V_p$$

$C_{tiss}(t)$ is the concentration of the tracer in the tissue at time t (L/g of tissue), $C_{pa}(t)$ is the concentration of the tracer in the plasma (L/g of plasma), V_p is the fraction of total volume occupied by the blood volume (L/g) and K_i is the blood to tissue transfer constant of gadolinium per gram of tissue per minute (L/g min). The same equation can be used to calculate K_i directly from the T1 values, by replacing the concentrations with T1 relaxation rates, scaled by the proportionality constant *k*.

Dividing both sides of the equation with $C_{pa}(t)$ allows K_i to be determined by linear regression. $C_{pa}(t)$ is the arterial input function (AIF), designed to represent the concentration of gadolinium measured in arterial plasma. Ideally, this would be an artery as the model requires an AIF, but there is no artery in the FOV. Therefore, the sagittal sinus is used, corrected by the factor (1-haematocrit) as this is assumed to be representative of the arterial concentration of contrast agent (Taheri et al., 2011b). The sagittal sinus is obtained through semiautomatic segmentation using ITK-snap to get the mean activity in the sagittal sinus. K_i can then be determined for every voxel in the image across the time of the experiment.

2.6.2 Global BBB permeability

The T1 weighted images were then registered using ANTS to the FLAIR images and the tissue segments and WML mask used to create the WM and NAWM masks. We then eroded the masks by 3mm using fslmaths (https://fsl.fmrib.ox.ac.uk/fsl/fslwiki), to ensure there was no ventricular or GM contamination.

Global values of BBB permeability in the WM (sum of NAWM and WML), NAWM and WML were calculated as mean K_i values for every voxel in that region.

2.6.3 Hotspot BBB permeability

Hotspots were classified as voxels with a value greater than the 95th centile of the permeability distribution from the NAWM of the control population. The tissue segments and the parameter maps were then used along with this threshold to generate the hotspot maps using the fslmaths threshold and mask features. The mean value and

volume of these hotspots present in the whole WM, NAWM and WML could then be determined.

2.6.4 Penumbra BBB permeability

The penumbra was defined by taking the lesion mask and dilating this by 3mm in all directions using fslmaths. The lesion mask was then subtracted from the dilated image to give the penumbra. This was further masked using the CSF and GM segments to leave only WM. Again, global penumbra and hotspot penumbra values were obtained.

2.7 PET analysis

2.7.1 Image Reconstruction

List-mode PET data were histogrammed into 55 time frames and then reconstructed
into images (128 x 128 x 89 matrix; 2.0 x 2.0 x 2.8 mm voxel size) using time-of-
flight ordered subsets expectation maximisation (Hudson and Larkin, 1994) with 16
subsets, 6 iterations and no smoothing. Attenuation correction was applied using an
attenuation coefficient map produced offline from the combination of non-patient
object templates and a pseudo-CT generated from the T1-weighted MR image
acquired during PET data acquisition. The multi-subject atlas method was used to
generate the pseudo-CT (Burgos et al., 2014), which was converted to linear
attenuation coefficient at 511 keV using a transformation (Carney et al., 2006). Image
reconstruction also included corrections for random coincidences, dead time,
normalisation, scattered coincidences, radioactive decay and sensitivity.

2.7.2 Global PK binding

SPM12 was used to realign each dynamic image series and hence reduce the impact
of head motion. A mean realigned PET image was then used to co-register each
realigned dynamic PET image series to the BBB MR image from the same scan via
the T1 image mentioned above and the FLAIR images.

To estimate specific tracer binding, PK PET data were analysed with the simplified
reference tissue model (SRTM) to quantify binding potential relative to a non-
displaceable compartment (BP_{ND}) (Lammertsma and Hume, 1996). The WM
reference region was estimated with supervised cluster analysis for PK (Yaqub et al.,
2012) with the library data determined from control scans of another PK project on
the GE SIGNA PET/MR with the same acquisition and processing protocol
(BIODEP; PI Prof ET Bullmore). Correction for vascular binding was also applied to
the PK data (Yaqub et al., 2012).

For regional analysis, NAWM and WML regions of interest (ROIs) were delineated
on the FLAIR MR image and subsequently transformed to PET space via the BBB
MR image. To reduce the impact of differential atrophy and ventricle size, the time-

activity curve (TAC) of each ROI was corrected for CSF contamination through division with the mean sum of GM and WM probabilities in the ROI, with both SPM12 probability maps smoothed to PET spatial resolution. SRTM was then applied to the CSF-corrected ROI TACs. A basis function implementation of SRTM was used for parametric mapping due to its robustness at the higher noise levels found at the voxel level (Gunn et al., 1997). A 4mm full width at half maximum Gaussian was applied to the dynamic images prior to parametric mapping.

For comparison with the BBB permeability data, only PET data from the tissue that corresponds to the BBB data was analysed.

2.7.3 Hotspot PK binding

PK binding was calculated for every voxel in the brain, which could then be segmented into NAWM and WML using the methods specified previously. Further, hotspots were classified in the same way as for BBB permeability, using the control population to define a value of 'significant' binding.

2.7.4 Penumbra PK binding

Penumbra values were calculated in the same way as documented above for BBB permeability.

2.8 Cognitive tests

2.8.1 Cognitive Test Battery

A battery of cognitive tests that had been previously established for an SVD cohort was used to provide an assessment of cognitive function (Lawrence et al., 2013). Premorbid IQ was estimated using the restandardised National Adult Reading Test (NART, 2nd Edition) (Nelson and Willison, 1991). Assessment was usually on the same day but always within 2 weeks of the PET/MRI scan. The tests took around 1 hour in total.

The tasks were divided into EF, PS, WoM and LTM. The specific tasks used to calculate each of these cognitive indices can be found in Table 2.1. Further, a GC was produced which summarised performance on all the tasks.

To construct each index, task measures were transformed into z-scores using psychometric standardisation using the best available age-scaled normative data. The exception to this was the modified Wisconsin Card Sort Test (mWCST), where a published study was used to select normative data with comparable age and gender distribution (Nagahama et al., 2003). Task z-scores were then averaged to create the cognitive index scores.

All participants were able to take part in the cognitive testing, but in some cases participants were not able to finish individual tests. In these cases, the minimum scaled score attainable for that task was substituted.

Cognitive Index	Task & Normative Data reference	Task Measure(s) Used & Additional Details
EF		
	Trail making test (Mitrushina et al., 2005)	Time to complete Part B (number-letter switching)
	Verbal Fluency (Delis et al., 2001)	Total number of Correct Words generated
	Modified Wisconsin Card Sort Test (Nagahama et al., 2003)	Categories Achieved & Perseverative Errors*
PS		
	BMIPB Speed of Information Processing (Coughlan et al., 2007)	Total correct, adjusted for motor score & errors (%)*
	Digit Symbol Substitution (Wechsler, 1997a)	Total Correct
	Grooved Pegboard Task (Dawson et al., 2010)	Time to complete (average of 2 hands)
WoM		
	Digit Span Task (Wechsler, 1997a)	Total Score
LTM		
	WMS-III Logical Memory (Wechsler, 1997b)	Total Score: Immediate Recall & Delayed Recall*
	WMS-III Visual Reproduction (Wechsler, 1997b)	Total Score: Immediate Recall & Delayed Recall*

*Composite scores used for multiple task measures

Table 2.1: Summary of tasks making up the various cognitive indices and references used to calculate z-scores.

2.8.2 Trail Making Test

The Trail Making Test contained two parts: Part A required the participant to draw lines that sequentially connected numbers 1-25 on a sheet of paper. For Part B, the task was similar, but the participant had to alternate between numbers and letters (e.g. 1, A, 2, B, 3, C). If the participant made a mistake, they were stopped and told to return to the previous correct point. The time taken to complete the task was recorded. To calculate our cognitive indices, we were only interested in the time taken to complete part B.

2.8.3 Verbal Fluency

The verbal fluency assessment used in this study was letter fluency. Participants were given 60 seconds to produce as many words as possible for a letter. They were instructed that none of the words could be names of people, names of places or numbers. Letters used were F A and S.

2.8.4 mWCST

The mWCST is a simplification of the Wisconsin Card Sorting Test, which consists of only two sets of 24 cards (Nagahama et al., 2003). In this test, six consecutive correct responses were required to complete a category. In the mWCST, the "categories completed" and "perseverative errors" are the parameters thought to categorise ability most accurately (Cianchetti et al., 2005), so a composite score was created from these parameters.

2.8.5 BIRT Memory and Information Processing Battery

The BIRT Memory and Information Processing Battery (BMIPB) is a collection of seven psychological tests that measure various aspects of cognitive function. The Speed of Information Processing required the participant to recognise and draw a line through the second highest number in a row of numbers. They did this for 4 minutes, and the amount they managed to complete was recorded. They were then also tested for their speed and were given a page of figures; they had to cross through these

figures as quickly as possible and the number completed in the given 25 seconds was recorded. A composite score was then created combining both parts of the task.

2.8.6 Digit Symbol Substitution

Digit symbol substitution is a test of psychomotor performance; participants were given a key grid of numbers and corresponding symbols and a test sheet with numbers and empty boxes. The participant had to fill in as many of the boxes with the matching symbol as possible within two minutes (Rosano et al., 2016).

2.8.7 Grooved Pegboard Task

The Grooved Pegboard Task involved a board with pegs and grooves. The grooves were at random rotations across the board, requiring the participant to rotate the pegs around in their hand in order to fit them in. The task was done firstly with the dominant hand and then with the non-dominant hand. We took the best score from either hand to minimise the effect of post-stroke disability on the score.

2.8.8 Digit Span Task

The Digit Span Task involved reading out a series of numbers that the participant had to repeat; they started short but got longer throughout the task. The task finished when the participant got two of the same length wrong. The second part of the task involved the tester reading another line of the numbers, which the participant then had to repeat backwards. Again, this started short and got longer with time and stopped when the participant got two of the same length wrong.

2.8.9 Logical Memory

Logical memory was taken from the Weschler Memory Scale 3rd edition (WMS-III), which involved reading a story to the participant and then asking them to immediately recall everything they could remember about the story. A further story was then read to the participants and they were again asked to tell everything they could remember.

This same story was then read again and the task was repeated. 25-35 minutes later, they were then further asked to remember everything they could from the stories.

2.8.10 Visual Reproduction

Visual reproduction was also taken from WMS-III. This involved showing the participant designs. They got 10 seconds to look at the design before the design was covered and they were asked to draw it in the booklet. There were a total of five designs. 25-35 minutes later the participants were asked to draw any of the designs that they could still remember.

2.9 Blood Biomarkers

2.9.1 Blood Sampling and Storage

Blood samples were taken from all participants at baseline. 10ml of whole blood was collected in serum separator tubes. The blood was left to clot for 30 minutes at room temperature before being centrifuged for 15 minutes at 1000g. ~4ml of serum was then pipette and aliquot into 50μl eppendorfs. These were stored in a -70°C freezer until they were sent for analysis.

2.9.2 Sample Analysis

Olink Proteomics (https://www.olink.com/) is an analysis service for targeted protein biomarker discovery. The panel chosen was the Cardiovascular Disease III panel measuring 92 cardiovascular disease related human protein biomarkers simultaneously (https://www.olink.com/products/cvd-iii-panel/).

Olink uses Proximity Extension Assay technology, where 92 oligonucleotide labelled antibody probe pairs bind to their respective target protein present in the sample (Assarsson et al., 2014, Lundberg et al., 2011). Full details of the methodology is available on their website (https://www.olink.com/content/uploads/2018/03/Olink-CVD-III-Validation-Data-v2.0.pdf). However, briefly, a polymerase chain reaction (PCR) reporter sequence was formed by a proximity dependent DNA polymerisation event and was subsequently detected and quantified using real-time PCR. The analysis was performed in a homogeneous 96-well format without any need for washing steps.

Internal and external controls were used for data normalisation and quality control purposes. Internal controls were added to each sample and included two immunoassay controls, one extension control and one detection control. The controls were then used to normalise the data. The extension control was used to normalise for technical variations within one run, whilst the interplate control normalised for between runs. In the final step of pre-processing the values were set relative to a correction factor which generates a Normalised Protein Expression unit on a log2 scale, where a larger

number represents a higher protein level in the sample, with background level around zero.

In addition to the Olink analysis, we were interested in C reactive protein (CRP). CRP was analysed using an enzyme-linked immunosorbent assay (ELISA) at the Core Biochemical Assay Laboratory at Addenbrooke's hospital using the Siemens Dimension high sensitivity CRP Assay (https://www.siemens-healthineers.com/point-of-care/poc-cardiac-topics/cardiac-assays/high-sensitivity-reactive-protein-hscrp-assay).

The specific proteins used in our analysis were chosen based on hypothesis-driven methods from the literature. The proteins of interest to us are as follows:

- **Inflammation:** Tumour necrosis factor receptor 1 (TNF-R1), Tumour necrosis factor receptor 2 (TNF-R2), FAS, Interleukin-1 receptor type 1 (IL-1RT1), Interleukin-6 receptor subunit α (IL-6Rα), Interleukin-18 binding protein (IL-18BP), C-reactive protein (CRP) and Chitinase-3-like protein 1 (CHI3L1)
- **MMPs:** MMP-2, MMP-3, MMP-9 and Metalloproteinase inhibitor 4 (TIMP-4)
- **Endothelial Cell Activation:** E-selectin, P-selectin, Integrin β2 (ITGB2), vWF Cadherin-5 (CDH5), Junctional adhesion molecule A (JAM-A), Platelet endothelial cell adhesion molecule (PECAM-1) and CD166 antigen (ALCAM)

2.10 Statistical analysis

All statistical analysis was carried out using R (version 3.3.1 2016, R Foundation for Statistical Computing, Vienna, Austria). The statistical tests used for each analysis are detailed in the methods section of the individual chapters.

Chapter 3: Demographics, Conventional MRI, DTI and Cognition

3.1 Subject Numbers

There were a total of 60 participants recruited to this study, which formed three groups (20 sporadic SVD, 20 CADASIL and 20 control).

However, all patients did not complete every aspect of the study (Figure 3.1). Cognitive data and serum samples were collected for every participant. Non-contrast structural MRI was collected for all but one participant for whom there was a technical scanner problem that meant no images could be acquired.

DCE-MRI permeability data was collected for all but two participants, with a third subsequently excluded. One participant was the same as above where technical problems with the scanner prevented images being collected. A second subject encountered a radiographer error where the gadolinium line was not attached to the participant's cannula. A third subject exhibited significant motion meaning that the permeability data could not be analysed. PET yielded the lowest n numbers, with a total of twelve patients who did not receive PET. This was due to problems with producing the ligand or failure to meet quality control after production, meaning injection could not go ahead.

Total recruited n=60		
Control n=20	**Sporadic SVD n=20**	**CADASIL n=20**
Non-contrast MRI n=19	Non-contrast MRI n=20	Non-contrast MRI n=20
DCE-MRI n=19	DCE-MRI n=19	DCE-MRI n=19
PK PET n=17	PK PET n=17	PK PET n=14
Cognition n=20	Cognition n=20	Cognition n=20
Serum n=20	Serum n=20	Serum n=20

Figure 3.1: Final subject numbers for the end-points collected.

3.2 Patient Demographics and Medical History

3.2.1 Statistical Analysis

The demographic data consisted of frequency and continuous data. For frequency data, chi-squared tests with the false discovery rate (FDR) correction for multiple comparison were used to compare between sporadic SVD and control and CADASIL and control. For continuous data, a Dunnett's test was used to compare between SVD and control and CADASIL and control.

3.2.2 Group Differences

Demographics and medical history were collected from all patients during their baseline visit (Table 3.1).

Age was not statistically significant between the sporadic SVD and control group, but it was significantly lower in the CADASIL group compared to control ($p<0.001$). There was no significant difference in the sex ratio between sporadic SVD and control or CADASIL and control. Similarly, there was no difference in the years in education. The cohort was predominantly White British in all the groups, with no significant difference between sporadic SVD and control or CADASIL and control. The groups were also of a similar height, weight and BMI.

Systolic blood pressure was no different in sporadic SVD compared to control, but was significantly lower in CADASIL compared to control ($p=0.037$). Diastolic blood pressure was similar between the groups. There was an increased prevalence of hypertension in the sporadic SVD group compared to control ($p<0.001$), but not in the CADASIL group compared to control.

Hyperlipidaemia, diabetes, depression and smoking status were all similar between the groups. Migraine prevalence was significantly higher in CADASIL compared to control ($p=0.002$), but no different between sporadic SVD compared and control.

	Group			P value	P value
	Control	**Sporadic SVD**	**CADASIL**	**SVD vs. control**	**CADA SIL vs. control**
	N=20	**N=20**	**N=20**		
Age (years) *	66.35 (6.74)	70.90 (9.01)	51.85 (9.46)	0.167	**<0.001**
Sex (total male) **	13 (65.0)	10 (50.0)	13 (65.0)	0.784	1.000
Education (years) *	13.40 (3.79)	12.95 (2.93)	14.10 (3.28)	0.878	0.734
Ethnicity **				0.394	0.407
White British	9 (95.0)	14 (70.0)	16 (80.0)	-	-
White Irish	0 (0.0)	3 (15.0)	0 (0.0)	-	-
Pakistani	0 (0.0)	0 (0.0)	1 (5.0)	-	-
Any other black background	0 (0.0)	0 (0.0)	1 (5.0)	-	-
Any other white background	1 (5.0)	3 (15.0)	2 (10.0)	-	-
Height (cm) *	175.00 (10.63)	169.33 (10.70)	171.35 (8.68)	0.171	0.463
Weight (kg) *	80.61 (11.76)	80.72 (20.98)	84.71 (15.72)	1.000	0.689
BMI (kg/m^2)*	26.34 (3.33)	27.88 (5.86)	28.80 (4.45)	0.516	0.217
Systolic blood pressure (mmHg) *	142.05 (17.70)	153.21 (26.59)	126.05 (17.22)	0.183	**0.037**
Diastolic blood pressure (mmHg) *	81.21 (9.03)	76.89 (13.99)	74.40 (11.22)	0.414	0.128
Hypertension **	6 (30.0)	18 (90.0)	8 (40.0)	**<0.001**	0.741
Hyperlipidaemia **	7 (35.0)	11 (55.0)	3 (15.0)	0.341	0.341
Diabetes **	1 (5.0)	4 (20.0)	0 (0.0)	0.513	1.000
Smoking **	12 (60.0)	11 (55.0)	7 (35.0)	1.000	0.512
Depression**	7 (35.0)	5 (25.0)	8 (40.0)	1.000	1.000
Migraine **	5 (25.0)	5 (25.0)	16 (80.0)	1.000	**0.002**

*(mean(SD) displayed with p value from Dunnetts test, **(total (%)) displayed with fisher-exact with FDR correction

Table 3.1: Demographics and medical history were collected from patients. P values are shown for comparisons between sporadic SVD and control groups, and between CADASIL and control groups. Significant p-values are shown in bold.

3.3 Conventional MRI markers

3.3.1 Statistical Analysis

All of the conventional MRI markers had a non-normal distribution. To allow them to be analysed with parametric statistics, they were transformed. Brain volume and GM volume were both squared. CSF volume, NAWM volume, WML volume, lacune volume, lacune count and CMB count were all cube rooted. WM volume was logged (base:10).

Analysis of covariance (ANCOVA) tests controlling for age and sex were performed between the sporadic SVD and control groups and the CADASIL and control groups. ICV was used as an additional control for all volumetric measures. Bonferroni adjustment was used between the pairs of p-values to correct for multiple comparisons.

3.3.2 Group Differences

MRI markers were quantified from the various non-contrast MRI scans and mean values were calculated for each of the groups (Table 3.2).

There was no significant difference in brain volume between SVD and control, but CADASIL had a significantly higher brain volume compared to control (p<0.001). Brain volume was then segmented into GM, WM and CSF and compared. GM volume was not significantly different between the groups. WM volume was significantly higher in sporadic SVD compared to control (p=0.023) and in CADASIL compared to control (p<0.001). CSF volume was significantly higher in sporadic SVD compared to control (p=0.002), was no different between CADASIL and control.

We then split the WM into NAWM and WML and compared these volumes. NAWM volume was no different between sporadic SVD and control, but was significantly lower in CADASIL compared to control (p=0.009). WML volume was significantly higher in the sporadic SVD group compared to control (p<0.001) and in the CADASIL group compared to control (p<0.001).

78

Lacunes were measured as volume and also as a total count. Lacune volume was significantly higher in sporadic SVD compared to control (p<0.001) and in CADASIL compared to control (p<0.001). Similarly, lacune count was significantly higher in sporadic SVD compared to control (p<0.001) and in CADASIL compared to control (p<0.001).

Finally, CMBs were counted. The CMB count was significantly higher in sporadic SVD compared to control (p=0.002) and in CADASIL compared to control (p=0.008).

MRI characteristic		Group (Median[Q1, Q3])			P value	P value
		Control	Sporadic SVD	CADASIL	SVD vs. control	CADASIL vs. control
		N=19	N=20	N=20		
Brain Volume	Raw (cm^3)	1104 [1042, 1145]	1121 [958, 1177]	1210 [1148, 1319]		
	% ICV (%)	70.83 [69.87, 75.19]	66.62 [63.64, 73.46]	75.40 [70.06, 80.31]	0.745	**<0.001**
GM Volume	Raw (cm^3)	652.7 [626.4, 679.4]	640.2 [549.7, 688.8]	697.9 [621.4, 778.6]		
	% ICV (%)	42.57 [40.86, 46.49]	38.09 [32.59, 43.73]	40.77 [38.49, 45.83]	0.668	0.376
CSF Volume	Raw (cm^3)	461.6 [332.3, 508.1]	532.8 [424.3, 585.9]	399.3 [298.5, 510.9]		
	% ICV (%)	29.17 [24.81, 30.13]	33.38 [26.54, 36.36]	24.60 [19.69, 29.94]	**0.002**	0.761
WM Volume	Raw (cm^3)	450.7 [411.2 463.6]	471.7 [436.3, 513.5]	527.5 [488.6, 609.9]		
	% ICV (%)	28.95 [28.06, 30.00]	29.26 [27.88, 31.80]	31.72 [28.10, 34.75]	**0.023**	**<0.001**
NAWM Volume	Raw (cm^3)	449.1 [407.7, 463.3]	444.3 [415.2, 490.7]	473.3 [443.3, 530.0]		
	% ICV (%)	28.77 [27.50, 29.91]	27.64 [26.64, 31.22]	28.95 [25.23, 32.34]	0.450	**0.009**
WML Volume	Raw (cm^3)	0.980 [0.372, 2.596]	15.51 [11.17, 33.69]	50.65 [40.40, 87.26]		
	% ICV (%)	0.05 [0.02, 0.19]	0.97 [0.66, 2.01]	3.06 [2.26, 4.85]	**<0.001**	**<0.001**
Lacune Volume	Raw (cm^3)	0.00 [0.00, 0.00]	0.140 [0.04, 2.30]	0.210 [0.00, 1.66]		
	% ICV (%)	0.00 [0.00, 0.00]	0.01 [0.00, 0.01]	0.01 [0.00, 0.10]	**<0.001**	**<0.001**
Lacune count	Count	0.00 [0.00, 0.00]	1.00 [0.75, 2.25]	2.00 [0.00, 8.50]	**<0.001**	**<0.001**

CMB count	Count	0.00 [0.00, 0.00]	1.00 [0.00, 2.50]	0.00 [0.00, 5.50]	**0.002**	**0.008**

Table 3.2: Median values for MRI markers in the control, sporadic SVD and CADASIL groups are shown. P values are shown comparing sporadic SVD and control groups, and CADASIL and control groups. Analyses were controlled for age and sex, with volumetric measures also controlled for ICV. Significant p values are shown in bold.

3.4 DTI markers

3.4.1 Statistical Analysis

Some of the DTI variables were normally distributed whilst others were not. Non-normal variables were transformed so that parametric statistics could be used. FA NAWM median and FA NAWM peak location were squared. FA WML median, FA WML peak height, MD WML peak height and MD WML peak location were logged (base:10). FA WML peak location and MD WML median were square rooted.

ANCOVA tests controlling for age and sex were performed between the sporadic SVD and control groups and the CADASIL and control groups. Bonferonni adjustment was used between the pairs of p-values to correct for multiple comparisons.

3.4.2 Group Differences

Differences in the DTI parameters between sporadic SVD and control and CADASIL and control are shown in Table 3.3.

FA median in the NAWM was significantly lower compared to control in the sporadic SVD group (p<0.001) and the CADASIL group (p<0.001). FA peak height in the NAWM was similar in the sporadic SVD and control groups but was significantly higher in the CADASIL group compared to control (p=0.001). FA peak location in the NAWM was lower compared to control in the sporadic SVD group (p<0.001) and in the CADASIL group (p<0.001).

FA median in the WML was not significantly different between sporadic SVD and control or CADASIL and control. However, FA peak height in the WML was significantly lower in the sporadic SVD group compared to control (p<0.001) and in the CADASIL group compared to control (p<0.001). FA peak location in the WML was not significantly different between the groups.

MD median in the NAWM was significantly higher compared to control in the sporadic SVD group (p<0.001) and in the CADASIL group (p<0.001). MD peak height in the NAWM was significantly lower in the sporadic SVD group compared to control (p<0.001) and in CADASIL compared to control (p<0.001). Similarly, MD peak location in the NAWM was significantly higher compared to control in the sporadic SVD group (p<0.001) and CADASIL group (p<0.001).

MD median in the WML was significantly higher in the CADASIL group compared to control (p=0.009). However, it was not significantly different between the sporadic SVD group and control. MD peak height was significantly lower in the sporadic SVD group compared to control (p<0.001) and in CADASIL compared to control (p<0.001). MD peak location in the WML was significantly higher in the CADASIL group compared to control (p=0.017). However, it was not significantly different between the sporadic SVD group and control.

Histogram parameter			Group (Median [Q1, Q3])			P value SVD vs. control	P value CADA SIL vs. control
			Control N=19	Sporadic SVD N=20	CADASIL N=20		
FA	NAWM	Median	0.41 [0.38, 0.42]	0.35 [0.34, 0.36]	0.32 [0.28, 0.35]	**<0.001**	**<0.001**
FA	NAWM	Peak height*	2.63 [2.44, 2.67]	2.69 [2.47, 2.80]	2.84 [2.60, 3.08]	0.482	**0.001**
FA	NAWM	Peak location	0.40 [0.37, 0.40]	0.32 [0.30, 0.35]	0.30 [0.26, 0.35]	**<0.001**	**<0.001**
FA	WML	Median	0.20 [0.17, 0.26]	0.24 [0.22, 0.26]	0.20 [0.18, 0.23]	0.492	0.808
FA	WML	Peak height*	9.62 [8.16, 16.85]	4.77 [4.38, 5.15]	4.68 [4.23, 5.34]	**<0.001**	**<0.001**
FA	WML	Peak location	0.12 [0.11, 0.24]	0.20 [0.15, 0.22]	0.14 [0.10, 0.18]	0.702	0.790
MD	NAWM	Median*	0.78 [0.76, 0.79]	0.85 [0.82, 0.87]	0.89 [0.83, 0.91]	**<0.001**	**<0.001**
MD	NAWM	Peak height*	14.59 [13.44,15.21]	10.77 [10.00,11.64]	11.11 [9.75,13.08]	**<0.001**	**<0.001**
MD	NAWM	Peak location*	0.76 [0.75, 0.77]	0.82 [0.79, 0.84]	0.83 [0.81, 0.87]	**<0.001**	**<0.001**
MD	WML	Median*	0.94 [0.86, 1.15]	1.16 [1.13, 1.18]	1.19 [1.14, 1.30]	0.060	**0.009**
MD	WML	Peak height*	16.63 [10.90,25.23]	7.61 [7.09, 8.80]	6.76 [6.05, 7.38]	**<0.001**	**<0.001**
MD	WML	Peak location*	0.85 [0.80, 0.97]	1.07 [1.00, 1.18]	1.19 [0.94, 1.33]	0.067	**0.017**

*($x10^{-3}$)

Table 3.3: Median values for the various DTI histogram parameters are shown for control, sporadic SVD and CADASIL groups. P values are shown comparing sporadic SVD and control groups, and CADASIL and control groups. Analyses were controlled for age and sex. Significant p values are shown in bold.

3.5 FW corrected DTI

3.5.1 Statistical Analysis

Some of the FW and FW corrected DTI variables were normally distributed whilst others were not. Non-normal variables were also transformed so that parametric statistics could be used. FW NAWM peak height, FW NAWM peak location, FW WML peak height, FW corrected FA NAWM peak height, FW corrected FA NAWM peak location, FW corrected FA WML peak height and FW corrected MD WML peak height were logged (base:10). FW corrected MD NAWM peak height was squared.

ANCOVA tests controlling for age and sex were performed between the sporadic SVD and control groups and the CADASIL and control groups. Bonferroni adjustment was used between the pairs of p-values to correct for multiple comparisons.

3.5.2 Group Differences

FW and FW corrected FA and MD values are shown, with differences between sporadic SVD and control and CADASIL and control analysed in Table 3.4.

FW median in the NAWM was significantly higher in the sporadic SVD group compared to control (p<0.001) and in the CADASIL group compared to control (p<0.001). FW peak height in the NAWM was similar in sporadic SVD and control, but was significantly lower in the CADASIL group compared to control (p<0.001). Similarly, FW peak location in the NAWM was similar in the sporadic SVD and control groups, but was significantly higher in the CADASIL group compared to control (p=0.016).

FW median in the WML was significantly higher compared to control in the sporadic SVD group (p=0.033) and CADASIL group (p=0.003). FW peak height in the WML was significantly lower than control for both sporadic SVD (p<0.001) and CADASIL (p<0.001). FW peak location in the WML was significantly higher than control for sporadic SVD (p=0.039) and CADASIL (p<0.001).

FW adjusted FA median values in the NAWM were significantly lower compared to control for both sporadic SVD (p<0.001) and CADASIL (p<0.001). FW adjusted FA peak height in the NAWM was similar between sporadic SVD and control groups, but was significantly lower in the CADASIL group compared to control (p<0.001). Similarly, FW adjusted FA peak location in the NAWM was similar between sporadic SVD and control groups, but was significantly lower in the CADASIL group compared to control (p<0.001).

FW adjusted FA median values in the WML were significantly higher in sporadic SVD compared to control (p=0.032) but were similar between CADASIL and control. FW adjusted FA peak height values in the WML were significantly lower than control for both sporadic SVD (p<0.001) and CADASIL (p<0.001). FW adjusted FA peak location values in the WML were significantly higher than control for both sporadic SVD (p<0.001) and CADASIL (p=0.027).

FW adjusted MD median values in the NAWM were significantly lower in the sporadic SVD group compared to control (p<0.001) and in the CADASIL group compared to control (p<0.001). However, FW adjusted MD peak height values in the NAWM were no different between sporadic SVD and control or CADASIL and control. Similarly, FW adjusted MD peak location values in the NAWM were no different between the groups.

FW adjusted MD median values in the WML were significantly lower than control for both sporadic SVD (p<0.001) and CADASIL (p<0.001). FW adjusted MD peak height values in the WML were also significantly lower than control for both sporadic SVD (p<0.001) and CADASIL (p<0.001). FW adjusted MD peak location values in the WML were significantly lower than control for both sporadic SVD (p=0.001) and CADASIL (p=0.011).

Histogram parameter			Group (Median [Q1, Q3])			P value	P value
			Control	Sporadic SVD	CADASIL	SVD vs. control	CADA SIL vs. control
			N=19	N=20	N=20		
FW	NAWM	Median	0.25 [0.24, 0.26]	0.31 [0.29, 0.33]	0.34 [0.30, 0.36]	**<0.001**	**<0.001**
FW	NAWM	Peak height*	4.44 [4.29, 4.83]	4.04 [3.68, 5.78]	3.63 [3.16, 4.12]	1.000	**<0.001**
FW	NAWM	Peak location	0.00 [0.00, 0.24]	0.00 [0.00, 0.28]	0.31 [0.26, 0.32]	1.000	**0.016**
FW	WML	Median	0.40 [0.33, 0.54]	0.53 [0.51, 0.54]	0.56 [0.53, 0.63]	**0.033**	**0.003**
FW	WML	Peak height*	8.01 [4.44, 19.22]	3.76 [3.48, 4.04]	3.49 [3.03, 4.14]	**<0.001**	**<0.001**
FW	WML	Peak location	0.34 [0.27, 0.51]	0.53 [0.46, 0.61]	0.64 [0.55, 0.70]	**0.039**	**<0.001**
FA	NAWM	Median	0.29 [0.27, 0.30]	0.26 [0.24, 0.26]	0.23 [0.21, 0.25]	**<0.001**	**<0.001**
FA	NAWM	Peak height*	5.77 [4.18, 7.57]	4.94 [4.06, 7.07]	3.54 [3.33, 4.06]	1.000	**0.001**
FA	NAWM	Peak location	1.00 [1.00, 1.00]	1.00 [0.81, 1.00]	0.20 [0.18, 0.42]	0.675	**<0.001**
FA	WML	Median	0.18 [0.14, 0.20]	0.21 [0.19, 0.22]	0.19 [0.18, 0.21]	**0.032**	0.400
FA	WML	Peak height*	12.76 [10.23,23.02]	6.61 [5.92, 6.96]	6.07 [5.53, 6.52]	**<0.001**	**<0.001**
FA	WML	Peak location	0.12 [0.10, 0.16]	0.18 [0.17, 0.20]	0.18 [0.17, 0.19]	**<0.001**	**0.027**
MD	NAWM	Median	0.49 [0.49, 0.50]	0.49 [0.49, 0.49]	0.49 [0.48, 0.49]	**<0.001**	**<0.001**
MD	NAWM	Peak height*	2.31 [2.15, 2.47]	2.15 [2.03, 2.41]	2.51 [2.21, 2.67]	1.000	0.071
MD	NAWM	Peak location	0.50 [0.50, 0.50]	0.50 [0.50, 0.50]	0.50 [0.50, 0.50]	0.643	0.144

MD	WML	Median	0.47 [0.46, 0.49]	0.46 [0.45, 0.46]	0.45 [0.44, 0.46]	**<0.001**	**<0.001**
MD	WML	Peak height*	6.41 [4.45, 16.32]	2.79 [2.57, 3.12]	2.67 [2.19, 2.91]	**<0.001**	**<0.001**
MD	WML	Peak location	0.48 [0.45, 0.49]	0.44 [0.43, 0.45]	0.43 [0.43, 0.46]	**0.001**	**0.011**

*(x10^{-3})

Table 3.4: Median values for the various DTI histogram parameters with FW correction are shown for control, sporadic SVD and CADASIL groups. P values are shown comparing sporadic SVD and control groups, and CADASIL and control groups. Analyses were controlled for age and sex. Significant p values are shown in bold.

3.6 Cognition

3.6.1 Statistical Analysis

Cognitive scores were normally distributed. ANCOVA tests controlling for age, sex and premorbid IQ were performed between the sporadic SVD and control groups and the CADASIL and control groups. Bonferroni adjustment was used between the pairs of p-values to correct for multiple comparisons.

3.6.2 Group Differences

Mean cognitive scores for each group and comparisons between sporadic SVD and control and CADASIL and control can be seen in Table 3.5. GC was significantly lower in the sporadic SVD compared to control (p=0.021) and in CADASIL compared to control (p=0.011). EF was similar between the groups. PS was significantly reduced compared to control in sporadic SVD (p<0.001) and CADASIL (p=0.027). WoM was similar between the groups. LTM was similar between sporadic SVD and control but was significantly reduced in CADASIL compared to control (p=0.007).

	Group (Mean (SD))			P value	P value
Cognitive index	Control N=20	Sporadic SVD N=20	CADASIL N=20	SVD vs. control	CADASIL vs. control
GC	0.22 (0.52)	-0.16 (0.80)	-0.37 (0.96)	**0.021**	**0.011**
EF	0.15 (0.87)	-0.28 (1.09)	-0.20 (1.44)	0.128	0.649
PS	0.42 (0.43)	-0.58 (1.12)	-0.61 (1.85)	**<0.001**	**0.027**
WoM	-0.01 (0.76)	-0.09 (0.95)	-0.36 (0.61)	1.000	0.099
LTM	0.30 (0.75)	0.30 (0.71)	-0.32 (0.78)	1.000	**0.007**

Table 3.5: Z scores for the various cognitive domains for control, sporadic SVD and CADASIL groups. P values for comparisons between the sporadic SVD and control groups, and the CADASIL and control groups are shown. Analyses were controlled for age, sex and premorbid IQ. Significant p values are shown in bold.

3.7 Associations between MRI markings and Cognition

3.7.1 Statistical Analysis

Multivariate linear regressions were performed to determine if any of the imaging markers were significantly associated with cognition. Some of the imaging markers were not normally distributed and therefore transformations were performed. Brain volume, GM volume, FA NAWM median, FW MD NAWM peak height were all squared. CSF volume, NAWM volume, WML volume, lacune volume, lacune count and CMB count were all cube rooted. WM volume, FA WML median, MD WML peak height and FW MD WML peak height were logged (base:10).

Linear regression models were controlled for age, sex and premorbid IQ. Models containing volumetric measure were also controlled for ICV. FDR correction was used to correct the p values for multiple comparisons.

3.7.2 Group Differences

The associations between the various MRI markers and cognition are shown in Tables 3.6-3.10.

Associations with GC are shown in Table 3.6. In the sporadic SVD group, GC was significantly associated with GM volume (β=0.557, p=0.003), FA median in the NAWM (β=0.485, p=0.025) and FW median in the NAWM (β=-0.464, p=0.022). In the CADASIL group, GC was also significantly associated with GM volume (β =0.874, p=0.006) and FA median in the NAWM (β =1.015, p=0.003). CADASIL GC was also significantly associated with FW adjusted FA median in the NAWM (β =1.054, p<0.001). There were no associations in the control group between any of the imaging markers and GC.

Associations with EF are shown in Table 3.7. A higher GM volume was significantly associated with higher EF in the CADASIL group (β=1.083, p=0.001) (Table 3.7). FA median in the NAWM was also significantly associated with EF in the CADASIL group (β=1.087, p=0.005). This association was still present using the FW corrected

FA values in the NAWM (β=1.077, p=0.004). There was no association between any of the imaging markers and EF in the control or sporadic SVD groups.

Associations with PS are shown in Table 3.8. In the sporadic SVD group, there was a significant association between PS and FW median in the NAWM (β=-0.689, p=0.016). In the CADASIL group, FA median in the NAWM significantly associated with PS, both uncorrected (β=0.960, p=0.010) and FW corrected (β=0.997, p=0.003). There was no association between any of the imaging markers and PS in the control group.

There was no association between any of the imaging markers and WoM or LTM for any of the groups (Table 3.9 and 3.10).

Brain region	Control		Sporadic SVD		CADASIL	
	β	P value	β	P value	β	P value
WML volume	-0.176	0.561	0.070	0.808	-0.240	0.664
Lacunar volume	-0.459	0.761	-0.230	0.127	-0.483	0.210
GM volume	-0.370	0.210	**0.557**	**0.003**	**0.874**	**0.006**
Lacune count	0.011	0.998	-0.358	0.127	-0.531	0.127
CMB count	-0.126	0.680	-0.210	0.439	-0.334	0.483
FA median in NAWM	-0.017	0.998	**0.485**	**0.025**	**1.015**	**0.003**
FA median in WML	0.276	0.439	0.078	0.808	0.133	0.790
MD peak height in NAWM	0.429	0.263	0.312	0.229	0.606	0.134
MD peak height in WML	0.205	0.483	0.127	0.708	0.126	0.790
FW median in NAWM	-0.078	0.870	**-0.464**	**0.022**	-0.563	0.210
FW median in WML	0.054	0.892	-0.204	0.472	-0.527	0.189
FW FA median in NAWM	-0.052	0.894	0.422	0.177	**1.054**	**<0.001**
FW FA median in WML	0.416	0.127	-0.086	0.808	-0.064	0.892
FW MD peak height in NAWM	-0.226	0.664	0.390	0.088	-0.274	0.509
FW MD peak height in WML	0.174	0.561	-0.005	0.998	0.000	0.998

Table 3.6: Linear models of associations between various MRI markers and GC, controlled for sex, age, and premorbid IQ. All volumetric measures were also controlled for ICV. Table shows standardised β coefficients and p values. Significant p values are shown in bold.

Brain region	Control		Sporadic SVD		CADASIL	
	β	P value	β	P value	β	P value
WML volume	-0.231	0.630	0.117	0.668	-0.204	0.669
Lacunar volume	-1.179	0.505	-0.100	0.668	-0.404	0.505
GM volume	-0.432	0.426	0.311	0.492	**1.083**	**0.001**
Lacune count	-0.632	0.668	-0.217	0.528	-0.502	0.374
CMB count	-0.267	0.505	-0.097	0.686	-0.320	0.635
FA median in NAWM	0.062	0.798	0.388	0.210	**1.087**	**0.005**
FA median in WML	0.229	0.635	0.140	0.660	0.124	0.707
MD peak height in NAWM	0.298	0.635	0.088	0.707	0.713	0.210
MD peak height in WML	0.327	0.429	0.102	0.687	0.169	0.668
FW median in NAWM	-0.213	0.660	-0.343	0.255	-0.669	0.338
FW median in WML	0.059	0.798	-0.115	0.668	-0.440	0.505
FW FA median in NAWM	0.087	0.765	0.582	0.070	**1.077**	**0.004**
FW FA median in WML	0.250	0.630	0.097	0.706	-0.188	0.668
FW MD peak height in NAWM	-0.442	0.505	0.157	0.635	-0.299	0.630
FW MD peak height in WML	0.188	0.635	0.121	0.668	0.122	0.707

Table 3.7: Linear models of associations between various MRI markers and EF, controlled for sex, age, and premorbid IQ. All volumetric measures were also controlled for ICV. Table shows standardised β coefficients and p values. Significant p values are shown in bold.

Brain region	Control		Sporadic SVD		CADASIL	
	β	P value	β	P value	β	P value
WML volume	-0.048	0.902	0.347	0.445	-0.216	0.803
Lacunar volume	0.275	0.902	-0.166	0.728	-0.554	0.155
GM volume	0.105	0.902	0.598	0.157	0.690	0.083
Lacune count	1.115	0.677	-0.333	0.443	-0.557	0.111
CMB count	-0.034	0.917	-0.347	0.357	-0.223	0.803
FA median in NAWM	0.032	0.918	0.613	0.083	**0.960**	**0.010**
FA median in WML	0.408	0.468	0.107	0.902	0.198	0.803
MD peak height in NAWM	0.678	0.267	0.612	0.083	0.573	0.170
MD peak height in WML	0.063	0.902	0.045	0.902	0.135	0.856
FW median in NAWM	-0.066	0.902	**-0.689**	**0.016**	-0.631	0.170
FW median in WML	0.120	0.902	-0.236	0.677	-0.490	0.261
FW FA median in NAWM	-0.080	0.902	0.404	0.468	**0.997**	**0.003**
FW FA median in WML	0.664	0.083	-0.050	0.902	0.072	0.902
FW MD peak height in NAWM	-0.276	0.832	0.580	0.083	-0.177	0.822
FW MD peak height in WML	-0.049	0.902	-0.104	0.902	-0.065	0.902

Table 3.8: Linear models of associations between various MRI markers and PS, controlled for sex, age, and premorbid IQ. All volumetric measures were also controlled for ICV. Table shows standardised β coefficients and p values. Significant p values are shown in bold.

Brain region	Control		Sporadic SVD		CADASIL	
	β	P value	β	P value	β	P value
WML volume	-0.182	0.757	0.162	0.720	-0.323	0.720
Lacunar volume	-0.002	0.998	-0.120	0.720	0.138	0.757
GM volume	-0.301	0.720	0.505	0.203	0.539	0.550
Lacune count	0.051	0.977	-0.187	0.704	0.077	0.909
CMB count	-0.183	0.720	-0.102	0.720	-0.263	0.720
FA median in NAWM	-0.064	0.913	0.157	0.720	0.482	0.655
FA median in WML	-0.186	0.757	-0.116	0.720	-0.121	0.757
MD peak height in NAWM	-0.080	0.913	0.065	0.809	0.228	0.720
MD peak height in WML	0.046	0.916	-0.072	0.757	-0.026	0.940
FW median in NAWM	0.180	0.757	-0.134	0.720	-0.164	0.757
FW median in WML	0.241	0.720	-0.015	0.940	-0.358	0.704
FW FA median in NAWM	-0.085	0.909	0.243	0.704	0.519	0.619
FW FA median in WML	0.307	0.720	-0.233	0.655	-0.309	0.704
FW MD peak height in NAWM	-0.284	0.724	0.034	0.913	-0.219	0.720
FW MD peak height in WML	0.230	0.720	-0.071	0.757	0.125	0.757

Table 3.9: Linear models of associations between various MRI markers and WoM, controlled for sex, age, and premorbid IQ. All volumetric measures were also controlled for ICV. Table shows standardised β coefficients and p values. Significant p values are shown in bold.

Brain region	Control		Sporadic SVD		CADASIL	
	β	P value	β	P value	β	P value
WML volume	-0.003	0.988	-0.632	0.204	-0.042	0.988
Lacunar volume	-0.058	0.988	-0.464	0.201	-0.427	0.429
GM volume	-0.261	0.740	0.419	0.645	0.253	0.772
Lacune count	0.075	0.988	-0.509	0.201	-0.426	0.429
CMB count	0.166	0.780	-0.115	0.905	-0.318	0.711
FA median in NAWM	-0.067	0.958	0.419	0.429	0.341	0.726
FA median in WML	0.413	0.429	0.121	0.905	0.052	0.958
MD peak height in NAWM	0.485	0.430	0.225	0.764	0.135	0.905
MD peak height in WML	0.097	0.905	0.443	0.392	0.007	0.988
FW median in NAWM	-0.104	0.905	-0.305	0.568	0.081	0.958
FW median in WML	-0.218	0.740	-0.354	0.429	-0.342	0.645
FW FA median in NAWM	-0.103	0.905	0.006	0.988	0.437	0.520
FW FA median in WML	0.146	0.896	-0.146	0.905	0.099	0.905
FW MD peak height in NAWM	0.315	0.740	0.562	0.174	-0.207	0.780
FW MD peak height in WML	0.056	0.958	0.049	0.958	-0.166	0.807

Table 3.10: Linear models of associations between various MRI markers and LTM, controlled for sex, age, and premorbid IQ. All volumetric measures were also controlled for ICV. Table shows standardised β coefficients and p values. Significant p values are shown in bold.

3.8 Discussion

3.8.1 Demographics

Our sporadic SVD and healthy control participants had similar ages, with means of 70.9 and 66.4 years respectively (Table 3.1). This is similar to the SVD populations described in the literature (Lawrence et al., 2014, Croall et al., 2017, van Norden et al., 2012, Inzitari et al., 2009). The CADASIL group had a significantly younger mean age of 51.9 years. This difference in age therefore needed to be taken into consideration when comparing our CADASIL and control groups. We controlled for age in both this chapter and subsequent chapters, but this may not have accounted for all of the variation and is a limiting factor in this study.

The participants were a well-educated population with similar mean years of schooling across all groups (13.4 years for healthy controls, 13.0 years for sporadic SVD and 14.1 years for CADASIL) (Table 3.1). They also were a predominantly white British population, which may limit the reproducibility of the results across other ethnic groups.

The average BMI of the participants was similar across the groups (26.3 for healthy controls, 27.9 for sporadic SVD and 28.8 for CADASIL) (Table 3.1). Theses means fall into the overweight population. However, the average BMI of UK men in 2014 was 27.4 and women was 27.0, so these numbers are similar to the UK averages (NCDRF, 2016).

The prevalence of the neurological risk factors of depression and migraine were recorded (Table 3.1). Depression had similar prevalence across the groups but migraine was significantly higher in the CADASIL group. This result is to be expected, as migraine is a common symptom in CADASIL (Tan and Markus, 2016).

3.8.2 Conventional MRI markers

Various parameters were taken from the MR images, which characterises the disease burden in the participants (Table 3.2). Brain volume was significantly higher in the

CADASIL population compared to control, even when taking account of age and sex. This finding is in contrast to previous studies, which have either shown no difference in brain volume between CADASIL and control (De Guio et al., 2015), or a reduction in brain volume in the CADASIL group (Rossi Espagnet et al., 2012). It could be that the age-adjustment did not account for all of the age variation between the groups. Previous studies have shown there is on average a 5% loss of brain tissue per decade (Peters, 2006), so age is an important factor when studying brain volume. Interestingly, we did not see any significant difference between the brain volumes of sporadic SVD and controls (Table 3.2). This is also inconsistent with previous studies, which have shown there to be a lower brain volume in sporadic SVD compared to age-matched controls (Nitkunan et al., 2011, O'Brien et al., 2001). It is likely that our group numbers were too low to detect a difference.

GM volume was no different between the groups (Table 3.2). This was again in contrast to the literature, where studies have shown significantly reduced GM volume in SVD compared to control (Li et al., 2017a, Liu et al., 2014a). However, it probably has the same explanation as for brain volume, where our participant numbers may have been too low to detect a significant difference. CSF was significantly higher in the sporadic SVD group compared to control. CSF volume has previously been shown to increase with age (Malko et al., 1991) and has recently been suggested that it could be used as a simple, but sensitive, imaging marker of brain atrophy due to the close association between CSF volume and atrophy (De Vis et al., 2016). Our study would provide evidence in favour of this, as we found a significant difference in CSF volume between sporadic SVD and control, but not in brain volume or GM volume, suggesting it may be a more sensitive measure for brain atrophy.

We found the WM in the sporadic SVD and CADASIL groups to be significantly higher than in the control group (Table 3.2). This is probably due to the fact that some of the WMLs, for patients with severe SVD, extend into the GM. Therefore, when the total WM is calculated from the NAWM and WML; this increases the overall volume of the WM. This has been noted in previously in the literature with no definite outcome established for this problem (Wardlaw et al., 2013a, Li et al., 2018a). The hyperintense regions still represent damaged tissue and are a part of the WML that

originated in the WM and so it is difficult not to include them, even though they technically spread beyond the limits of the WM border.

There was significantly higher volume of WML, lacune count and CMB count in the sporadic SVD and CADASIL participants compared to control (Table 3.2). These features are key neuroimaging features of SVD (Wardlaw et al., 2013c) and therefore it is to be expected that our patient groups would have significantly more of these markers compared to our healthy control group. The figures reported in Table 3.2 are similar to those reported by previous studies, suggesting our sporadic SVD and CADASIL groups express the typical features of SVD as seen in previous studies (van Leijsen et al., 2017, Lawrence et al., 2013, Croall et al., 2017, Chabriat et al., 1998).

3.8.3 DTI

FA and MD values were extracted using the histogram analysis technique; this technique is widely used in the literature and shown to correlate strongly with disease severity (Della Nave et al., 2007, Croall et al., 2017).

When comparing sporadic SVD with control, we found a significant difference between the FA values for median and peak location, but not peak height, in the NAWM. On the contrary, we found a significant difference in the FA peak height, but not the median or peak location, in the WML. For MD, there was a significant difference in all the parameters in the NAWM, but only peak height in the WML. The FA values for NAWM are consistent with previous work, where median and peak location, were significantly different in SVD from control (Lawrence et al., 2013). MD values are less consistent with previous work, as Lawrence et al. showed all MD values to be significantly different from control, whereas we have not seen this. However, we did see a trend for all of the MD parameters to be different from control, and due to our study having much lower numbers of participants, it is likely that our numbers were not high enough to reach significance in this instance.

In the CADASIL group, there was a significant difference between all of the FA NAWM parameters compared to control. For the FA values in the WML, the finding mirrored the sporadic SVD group, where only peak height was significantly different. With regards to MD, all of the parameters for NAWM and WML were significant in CADASIL compared to control. This closely reflects the previous literature, where all of the histogram parameters were found to be significantly different from control (Molko et al., 2002).

We then investigated the FW corrected DTI values and extracted them using the same histogram technique; values are shown in Table 3.4. In the sporadic SVD group, the FW median value in the NAWM was significantly higher compared to control. All of the FW parameters from the WML were significantly different from control. In the CADASIL group, all of the FW parameters in the NAWM and WML were significantly different from control. This is similar to the result of Duering et al., where FW was significantly higher in sporadic SVD and CADASIL compared to control (Duering et al., 2018).

The FW adjusted FA values followed a similar pattern to the non-adjusted values in the sporadic SVD group: FA median in the NAWM was still significantly different from control, with all of the FA values in the WML found to be significantly different from control. In the CADASIL group, the FW adjustment meant that all of the FA parameters in the WML were now significantly different from control.

The FW adjusted MD values were also similar to the non-adjusted values. The same pattern existed for sporadic SVD and CADASIL groups, where only the median value in the NAWM was now significantly different from control, but all of the WML parameters were significantly different from control.

This is the first time the histogram analysis has been applied to FW corrected DTI values, and therefore the specific values cannot be compared with the literature. However, it would seem that even with FW correction, there is still a significant difference in many of the DTI parameters of FA and MD in sporadic SVD and CADASIL compared to control, suggesting that if you remove the FW component

and leave only the component representing ultrastructural WM, you still see a difference from control. Therefore, is likely ultrastructural WM damage occurring in sporadic SVD and CADASIL. Further work is required to fully investigate the application of FW DTI to sporadic SVD, which is beyond the scope of this thesis.

3.8.4 Cognition

The cognitive profile of sporadic SVD has been extensively researched and consistently seen as a deficit in EF and PS, with little change in memory (Lawrence et al., 2013, McPherson and Cummings, 1996, Zhou and Jia, 2009). The cognitive profile is similar in CADASIL. However, they have also been seen to have additional memory problems (Charlton et al., 2006b). We did not see a significant deficit in EF in any of our groups (Table 3.5). However, we did see a significant deficit in PS in both the sporadic SVD group and the CADASIL group, and a deficit in LTM in the CADASIL group.

Brain volume, and in particular GM volume, has previously been associated with EF in sporadic SVD patients (Nitkunan et al., 2011, Lawrence et al., 2013). In our study, GM volume was only significantly associated with EF in the CADASIL group, and not in the sporadic SVD or control groups (Table 3.8). There were no association between brain volume and EF for any of the groups. Studies have also found brain volume and GM volume to be associated with PS (Lawrence et al., 2013, Croall et al., 2017). We found no association of brain volume or GM volume with PS across any of the groups (Table 3.8). However, we did find an association between GM volume and GC for both the sporadic SVD and CADASIL groups (Table 3.6). This highlights the important role of GM atrophy in in the cognitive deficits seen in SVD, which is in agreement with previous work (Lambert et al., 2015, Smith et al., 2015).

Interestingly, WML was not significantly correlated with cognition in our results (Tables 3.6-3.10). This is not an unexpected finding, as there is discrepancy in the literature with some studies that have found an association with cognition (Yamawaki et al., 2015, Croall et al., 2017) and some studies have not (Lawrence et al., 2013). Our results, and other non-significant results in the literature, do have a general trend

for higher WML volume and lower cognition scores, so it is likely that there is a small association that cannot be detected without large sample sizes.

Lacune count and volume were not associated with any of the cognitive indices in our data (Table 3.6-10). In the literature, lacune count is continually a highly significant predictor for a range of cognitive tests in SVD patients (Arboix, 2011, Smith et al., 2015, Croall et al., 2017, Blanco-Rojas et al., 2013, Vermeer et al., 2003). It is likely that again the small sample sizes make it difficult to detect this significance in our data.

CMB count was not associated with any cognitive indices (Tables 3.6-10). There are some discrepancies in the literature as to whether CMB are associated with cognition; some studies have found there is no association (Lawrence et al., 2013, Smith et al., 2015), whereas others have found an association with cognitive decline (Patel et al., 2013, Akoudad et al., 2016, Zhang et al., 2018). Therefore, it is not unexpected that we did not find this association.

DTI parameters have repeatedly been shown to correlate with cognition, more specifically EF and PS (Lawrence et al., 2013, Croall et al., 2017, D'Souza et al., 2018). FA median in the NAWM was associated with GC (Table 3.6), EF (Table 3.7) and PS (Table 3.8) in the CADASIL group. FA median in the NAWM was associated with GC in the sporadic SVD group (Table 3.10).

The FW technique has been recently applied to a sporadic SVD population and found that FW itself was highly correlated with PS (Duering et al., 2018). We found a similar result in our data, where the FW value itself was associated with GC (Table 3.6) and PS (Table 3.8) in the NAWM of the sporadic SVD group. FW corrected FA median values showed a similar pattern to uncorrected FA values, showing a significant association with GC (Table 3.6), EF (Table 3.7) and PS (Table 3.8) the CADASIL group. FW corrected values seemed to have a higher significance value in comparison to the uncorrected values, suggesting they may be a 'cleaner' way of extracting the measurement. However, they did not show any additional associations with cognition that had not already been seen with the uncorrected FA and MD

values. As the application for this technique to an SVD population is limited, more research is required to determine if these results are representative within an SVD population.

3.9 Summary of Findings

This chapter has addressed the following areas:

- Age was similar between the sporadic SVD and control groups, but was significantly lower in CADASIL compared to control
- Sporadic SVD and CADASIL patients showed a significantly higher load of the conventional MRI markers of WMLs, lacunes and CMBs compared to control
- Sporadic SVD and CADASIL participants showed significant differences in FA and MD compared to control, as both uncorrected and FW corrected values
- Sporadic SVD and CADASIL participants showed significantly higher FW compared to control
- Sporadic SVD and CADASIL participants showed deficits in PS, whilst CADASIL participants also showed a deficit in LTM
- GM volume was associated with GC in the sporadic SVD group and EF and GC in the CADASIL group
- Both uncorrected and FW corrected FA median values in the NAWM showed a correlation with GC in the sporadic SVD group and with EF, PS and GC in the CADASIL group

This chapter has provided an overview of the demographics and explored the prevalence of the conventional MRI markers, DTI markers and cognitive scores in our sporadic SVD and CADASIL populations. We have also explored the relationship between the various MRI and DTI markers with cognition. Our end-points can now be used for the next stage of this project, to determine their association with BBB permeability and microglia activation in SVD.

Chapter 4: BBB permeability – Group differences and Associations with Imaging and Cognition

4.1 Introduction

4.1.1 Aims of the Chapter

The previous chapter described the conventional MRI and DTI markers collected from our control, sporadic SVD and CADASIL groups and investigated them with cognition. This chapter explores BBB permeability in our participants and looks at the following specific questions:

- Is there a difference in BBB permeability between sporadic SVD and control groups? Does this difference occur globally or focally?
- Is there a difference in BBB permeability between CADASIL and control groups? Does this difference occur globally or focally?
- Is there a difference in BBB permeability in the NAWM and WML? Is this pattern the same across all groups?
- Is there a spatial pattern of increased BBB permeability in close proximity to WMLs?
- Is BBB permeability associated with conventional MRI markers, DTI markers and cognition?

The main hypothesis of this chapter is:

- BBB permeability will be significantly higher in the sporadic SVD and CADASIL patients compared to our healthy controls.

Exploratory outcomes beyond the main hypotheses are:

- Investigate if BBB permeability is different in the NAWM compared to WML
- Investigate if BBB permeability is increased in close proximity to WMLs
- Investigate if there is a relationship between BBB permeability and conventional MRI markers, DTI markers and cognition

4.1.2 BBB permeability in SVD

As discussed in Chapter One, BBB permeability is thought to be involved in SVD. Many studies have shown an increase in BBB permeability in SVD patients compared to controls (Wardlaw et al., 2003, Wardlaw et al., 2009, Topakian et al., 2010, Huisa et al., 2015, Zhang et al., 2017, Wardlaw et al., 2017). Additionally, cross-sectional studies have looked at the association between BBB permeability and WML volume. The majority of studies have found an association with WML volume (Topakian et al., 2010, Zhang et al., 2019, Li et al., 2017c, Wardlaw et al., 2017), but this relationship has not been found in all studies (Huisa et al., 2015). A limited number of studies have also looked at the relationship between cognitive function and BBB permeability cross-sectionally and have found an association with cognitive deficits (Hanyu et al., 2002, Zhang et al., 2019).

Based on all of this evidence, it is widely accepted that BBB permeability is in some way involved in SVD. However, the challenge is determining if BBB permeability is an initial causal part of SVD pathogenesis or if it is simply a consequence of the disease. It is also possible that increased permeability is a mixture of the two, where it is triggered as a consequential process but does then exacerbate the disease further. If increased BBB permeability can be shown to be pathological in SVD, it would be a possible target for therapeutics.

A small number of follow-up studies have looked at whether baseline BBB permeability can predict future damage. Follow-up studies are the only way to determine for definite if increased permeability is a causal mechanism in SVD. Huisa et al. found that only 11% of voxels that showed high permeability at baseline progressed to WML at follow-up (Huisa et al., 2015). However, looking from a cognitive point of view, Wardlaw et al. found that high BBB permeability at baseline led to worsened functional outcome 3 years on (Wardlaw et al., 2013b).

More recent studies have tried to further our understanding of the pathogenesis by looking at BBB permeability in brain regions where WMLs tend to grow, namely the rim around the existing WML. This region has been described as the 'penumbra' of the WMLs, after DTI changes were shown to occur in this area (Maillard et al., 2011).

Penumbras have long been investigated in acute stroke. The concept of the penumbra in ischaemic stroke is that this region is tissue that has been affected by the ischaemia but is salvageable if the cause of the ischaemia can be removed in time (Paciaroni et al., 2009). It is unknown if a penumbra exists around WMLs, but if it could be identified then this could be an area to target with therapeutics to prevent WML growth. Studies investigating BBB permeability in this penumbra region have yielded conflicting results, with Wardlaw et al. finding that permeability increased in a linear fashion to be lowest in the NAWM, steadily increasing to peak permeability in the WML (Wardlaw et al., 2017); whilst Huisa et al. found that permeability in the WML penumbra was higher than in the WML, but equivalent to the permeability in the rest of the NAWM (Huisa et al., 2015).

Previous studies are consistent that there is increased BBB permeability in SVD. However, longitudinal studies have so far provided conflicting results for a role of BBB permeability in the pathogenesis and the penumbra evidence is mixed and inconclusive. Further cross-sectional and follow-up studies that compare BBB permeability with a range of imaging and clinical outcomes are required to help unravel the role for BBB permeability in SVD.

4.1.3 DCE-MRI for BBB permeability

In recent years, there has been an increased use of DCE-MRI to assess BBB permeability. However, there has been variability in the approaches and the findings in the literature. The main challenge in SVD is that the permeability changes are subtle and therefore require sensitive techniques to be able to detect this change above the noise (Wardlaw et al., 2017). Further, BBB permeability has also been seen to increase with normal ageing (Erdő et al., 2017), and therefore this factors in additional difficulties for picking it up as pathological process. In contrast, the BBB permeability changes in acute stroke are much more pronounced and easier to detect (Yang and Rosenberg, 2011). However, it is widely agreed that DCE-MRI is the most evolved and promising technique for obtaining accurate BBB permeability values in SVD (Thrippleton et al., 2019).

In DCE-MRI, gadolinium is injected and the leakage of the gadolinium through the vessel wall is detected through a T1 shortening effect on the tissue protons (Taheri et al., 2011b).

The evolution of the DCE-MRI technique can be seen in the literature. Early studies simply looked at the change in the T1 signal. One study took patients with a CSF/albumin ratio indicative of increased BBB permeability and investigated MR signal changes in the WML, but found no significant changes (Bronge and Wahlund, 2000). However, another study using a similar technique found there was an increased permeability in the WML of patients compared to age matched controls (Hanyu et al., 2002). The inconclusive nature of these studies is likely due to the limited sensitivity of the technique they were using, which is not appropriate for detecting subtle permeability changes.

The technique then progressed to use a mixed model of signal enhancement to quantify the amount of gadolinium. Comparing lacunar vs. cortical stroke with this technique showed an increase in the lacunar stroke patients in the CSF (Wardlaw et al., 2008) and the WM (Wardlaw et al., 2009).

The area under the signal enhancement curve was the next progression of this technique, where mean signal intensity change was taken for 30 minutes post-injection and plotted against time. Permeability was seen to be increased in the NAWM with this technique in SVD patients compared to control (Topakian et al., 2010).

An improvement to the technique allowed researchers to use fast T1 mapping to measure more subtle BBB leakage, thought to be important in SVD (Hanyu et al., 2002). The new technique used only a quarter of the standard gadolinium dose, which was found to have both adequate washout from the blood and change in the MRI signal intensity over 25 minutes (Taheri et al., 2011b). Taheri et al. also found that this dose causes faster 1/T1 changes than at higher concentrations, providing a more sensitive measure. Pharmacokinetic modelling could then be used to separate the

vascular and extravascular components and allow for quantitative estimates of the BBB leakage rate.

The introduction of Patlak modelling was then apparent as the pharmacokinetic model of choice for many studies. Recent studies have further justified its application for monitoring low-level leakage in diseases such as SVD (Heye et al., 2016). The progression of the technique to this point meant that permeability could now be mapped to individual voxels and be studied in individual patients rather than in groups. Permeability in the WM was shown to be higher in patients compared to controls (Taheri et al., 2011a, Huisa et al., 2015). Later studies replicated this data, finding increased leakage in the NAWM, WM and GM in SVD patients compared to controls (Zhang et al., 2017).

4.1.4 Global vs. Focal BBB permeability

SVD is a heterogeneous disease with large clinical variation between patients. SVD contains many points of focal damage, due to individual WMLs and lacunar infarcts, which damage specific areas of the brain (Ter Telgte et al., 2018). However, this focal damage can then lead to downstream global changes in brain networks and structure, plus triggering many inflammatory cascades that will have downstream effects in other brain regions. There has been evidence from wider ischaemic stroke research suggesting that focal damage can lead to permeability changes in remote regions, which does have clinical implications (Liu et al., 2018a). Therefore, its important that both global and focal permeability are taken into consideration, as they may have distinct roles in the pathogenesis.

This combination of focal and global effects may underlie the heterogeneity seen in SVD and explain why quantification of focal WMLs and the lacunes does not perfectly correlate with symptoms (Gouw et al., 2011). The recent advances in DCE-MRI techniques mean it is now possible to generate permeability values for every voxel in the brain, allowing various measurements to be taken. Therefore, permeability can be looked at from both a global and a focal perspective to understand the relative contribution to SVD.

4.2 Methods

There were 19 controls, 19 sporadic SVD and 19 CADASIL participants who received BBB permeability imaging and so were included in this chapter. Methodology was described in Chapter Two.

4.2.1 Defining BBB permeability Values

Global mean permeability was defined as the mean permeability of all voxels in the ROI. Hotspot mean permeability was defined as the mean permeability of all voxels above the 'normal' threshold in the ROI, calculated from our control subjects and defined as any voxel above 6.5×10^{-4} L/g min. Global and hotspot mean permeability were expressed as L/g min. The hotspot permeability volume was expressed as a percentage (%) of the voxels that showed permeability values above the threshold within the given ROI.

Penumbra values were defined as a 3mm rim around the WMLs. Global means, hotspot means and hotspot volumes were calculated in the same way as described above.

4.2.2 Statistical Analysis

Group differences between BBB permeability values for sporadic SVD and control and CADASIL and control were analysed using the ANCOVA test and were controlled for age and sex. Pairs of comparisons were adjusted using Bonferroni. If there was a significant difference seen, an ANCOVA controlling for the cardiovascular risk factors of hypertension, hyperlipidaemia, type 2 diabetes and smoking was performed to see if the significance was still present. None of the BBB permeability parameters were normally distributed so were all transformed to meet normality assumptions of parametric statistical tests. The global permeability measures of WM, NAWM and WML were all transformed with cube root. The mean hotspot permeability measures of WM, NAWM and WML were log transformed; WM and NAWM with base:10 constant:10^{-6} and WML with base:10 constant:10^{-3}.

Hotspot permeability volume measure for WM, NAWM and WML were all transformed with cube root.

Comparisons between the BBB permeability values of the NAWM and WML were performed using Wilcoxon signed rank tests for paired non-parametric data. These tests were performed on the raw untransformed values. P values were corrected for multiple comparisons using FDR.

Group differences in the penumbra permeability values between sporadic SVD and control and CADASIL and control were analysed using ANCOVA tests and were controlled for age and sex. Pairs of comparisons were adjusted using Bonferroni. If there was a significant difference seen, a further ANCOVA controlling for the cardiovascular risk factors was performed to see if the significance was still present. All penumbra values were transformed with a cube root to meet normality assumptions.

Comparisons between permeability values for the NAWM and WML and the penumbra permeability values were carried out using the Wilcoxon signed rank tests for paired non-parametric data. These tests were performed on the raw untransformed values. P values were corrected for multiple comparisons using FDR.

Multivariate linear models were used to investigate the association between permeability parameters (independent) and imaging markers (dependent), controlled for age and sex. If the imaging parameter was a volumetric measure, then ICV was also used as a control. When significant associations were seen, a further linear model controlling for the cardiovascular risk factors was performed to see if the significance was still present. Permeability parameters were transformed in the same way detailed earlier to meet normality assumptions. Imaging markers were transformed if required, with the same transforms as described in Chapter Three. P values were adjusted for multiple comparisons with FDR.

Multivariate linear models were also used to investigate if permeability parameters (independent) were significantly associated with cognitive indices (dependent). These

analyses were controlled for age, sex and premorbid IQ. Permeability parameters were transformed in the same way as detailed earlier to meet normality assumptions. P values were adjusted for multiple comparisons with FDR.

4.3 Results

4.3.1 Group Differences

Permeability values in the WM, NAWM and WML were compared between the sporadic SVD and control groups and the CADASIL and control groups. Example images showing regions of significant permeability in a representative image from each of the groups is shown in Figure 4.1.

Mean global permeability was compared between groups in Figure 4.2. In the WM, the global permeability was significantly higher in sporadic SVD group compared to control, when controlled for age and sex ($p<0.001$ ($p=0.001$ when adjusted for multiple comparisons)). The significance was still present when controlled for cardiovascular risk factors ($p=0.001$). In the NAWM, a similar pattern was seen, where global permeability was significantly higher in the sporadic SVD group compared to control when controlled for age and sex ($p<0.001$ ($p<0.001$ when adjusted for multiple comparisons)) and cardiovascular risk factors ($p<0.001$). Finally, global permeability in the WML was compared between groups, with a significantly higher global permeability seen in the sporadic SVD group compared to control when controlled for age and sex ($p<0.001$ ($p<0.001$ when adjusted for multiple comparisons)) and cardiovascular risk factors ($p<0.001$). In the CADASIL group, the pattern was quite different, with no significant difference from the control group seen in the mean global permeability of the whole WM, NAWM or WML.

The mean permeability of the hotspots was compared between groups in Figure 4.3. In the WM and NAWM, the mean permeability of the hotspots was not significantly different between sporadic SVD and control group. In the WML, the mean permeability of the hotspots was significantly higher in the sporadic SVD group compared to control when controlled for age and sex ($p=0.004$ ($p=0.009$ when adjusted for multiple comparisons)) and cardiovascular risk factors ($p=0.004$). The CADASIL group had no significant difference from control for the mean value of the permeability hotspots in the WM, NAWM or WML.

Finally, the volume of the permeability hotspots was compared between groups, as shown in Figure 4.4. In the WM, the volume of the permeability hotspots was significantly higher in sporadic SVD compared to control when controlled for age and sex (p=0.004 (p=0.010 when adjusted for multiple comparisons)) and cardiovascular risk factors (p=0.007). In the NAWM, the same pattern was seen where the volume of permeability hotspots was also significantly higher in the sporadic SVD group compared to control when controlled for age and sex (p=0.003 (p=0.007 when adjusted for multiple comparisons)) and cardiovascular risk factors (p=0.006). The WML also followed the same pattern, with an increased volume of permeability hotspot in the sporadic SVD group compared to control when controlled for age and sex (p=0.002 (p=0.004 when adjusted for multiple comparisons)) and cardiovascular risk factors (p=0.002). The CADASIL group was not significantly different from control for the volume of the permeability hotspots present in the WM, NAWM or WML.
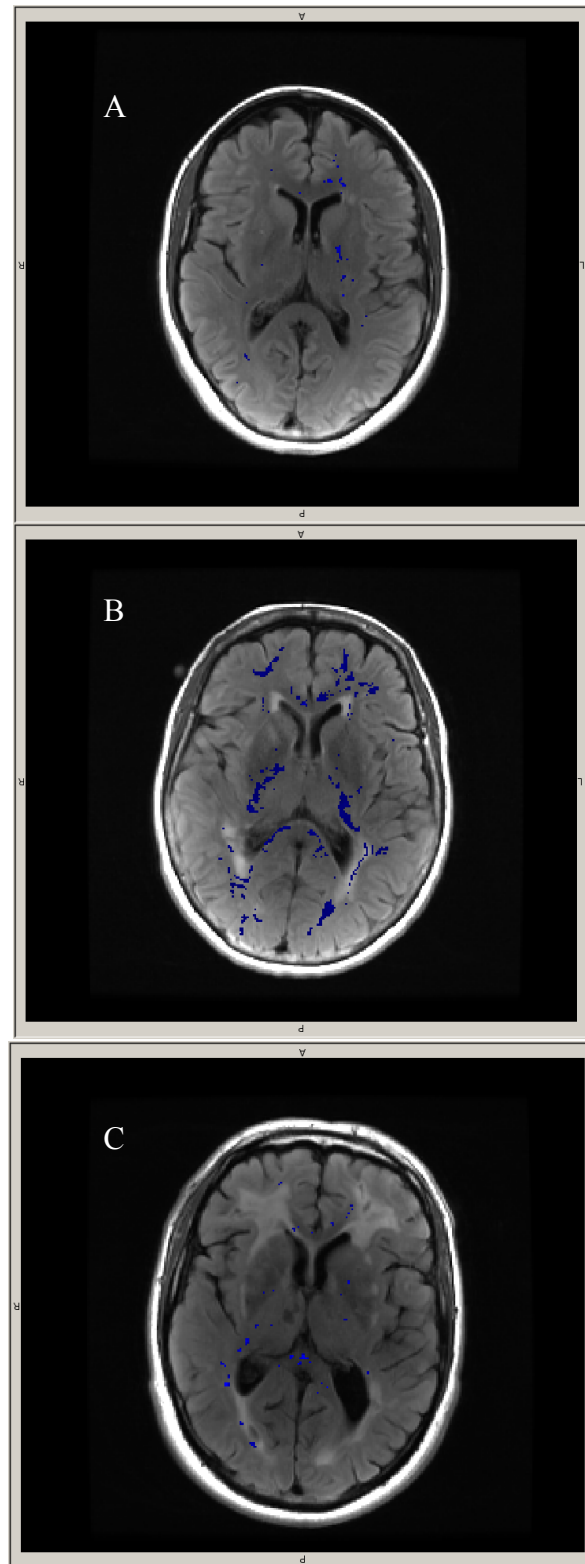
Figure 4.1: Example images of BBB permeability hotspots (blue) overlayed onto T2 FLAIR scans. A) Control. B) Sporadic SVD. C) CADASIL.
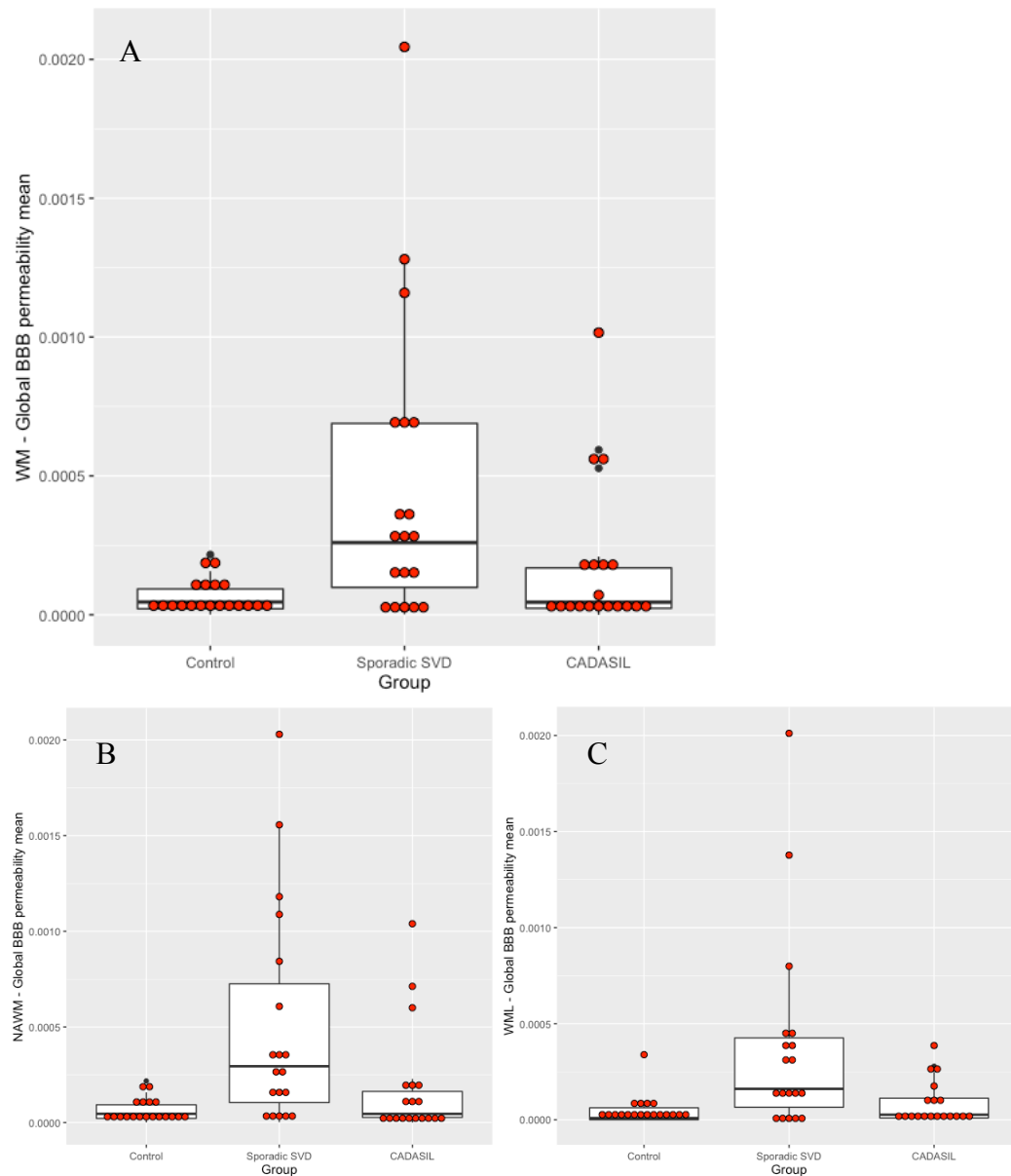
Figure 4.2: Mean global permeability (L/g min) of the WM, NAWM and WML. Group comparisons were controlled for age and sex.

A) Permeability in the WM was significantly higher in the sporadic SVD group compared to control (p=0.001). There was no significant difference between the CADASIL group and control (p=0.443).

B) Permeability in the NAWM was significantly higher in the sporadic SVD group compared to control (p<0.001). There was no difference between CADASIL and control (p=0.344).

C) Permeability in the WML was significantly higher in sporadic SVD compared to control (p<0.001). There was no significant difference between CADASIL and control groups (p=0.133).
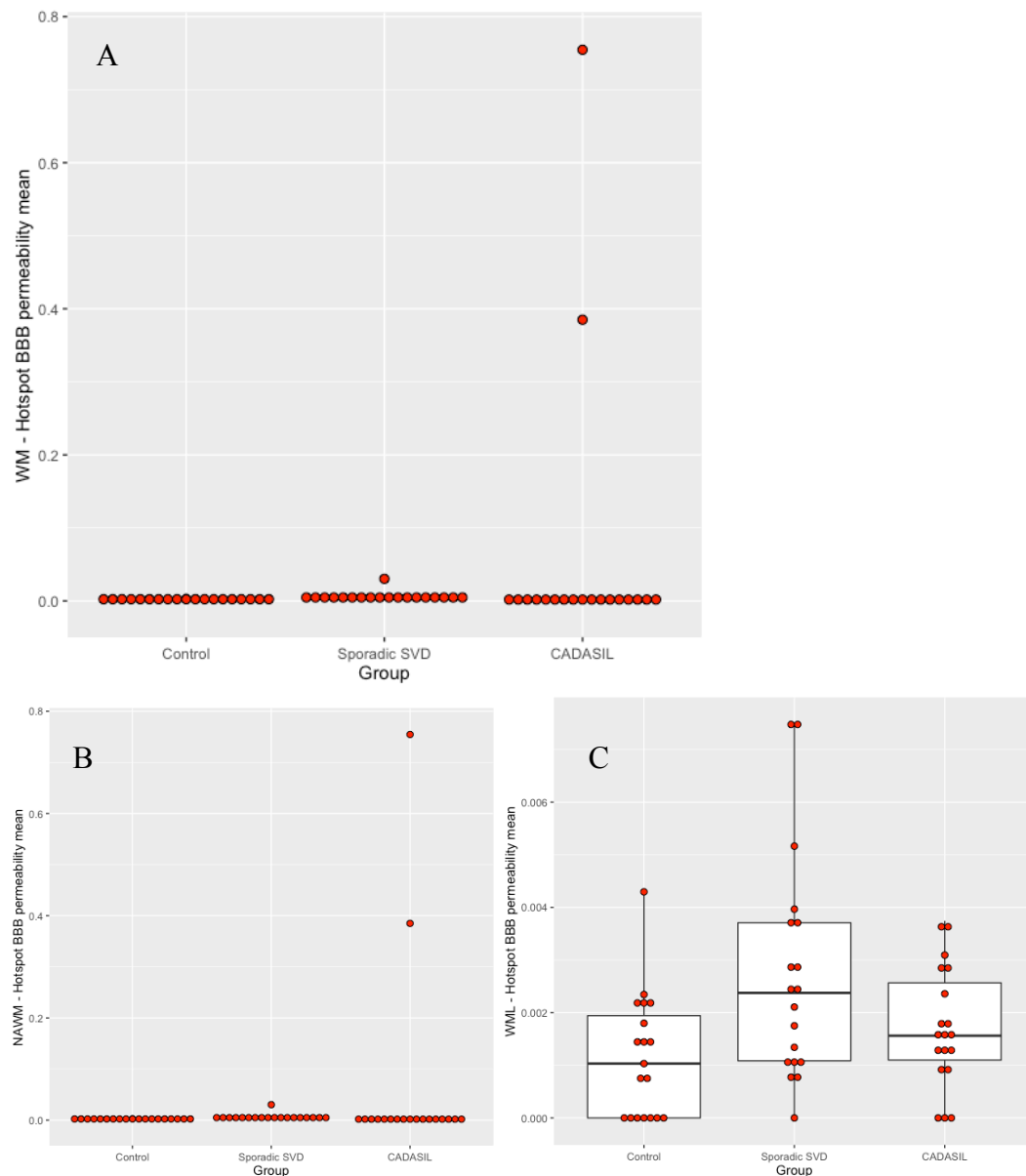
Figure 4.3: Mean hotspot permeability (L/g min) of the WM, NAWM and WML. Group comparisons were controlled for age and sex.

A) There was no significant difference in the hotspot mean permeability in the WM of the sporadic SVD group compared to control (p=0.104) or the CADASIL group compared to control (p=0.794).

B) There was no significant difference in the hotspot mean permeability in the NAWM of the sporadic SVD group compared to control (p=0.074) or CADASIL group compared to control (p=1.000).

C) Hotspot mean permeability in the WML of the sporadic SVD group was significantly higher than control (p=0.009). There was no significant difference between CADASIL and control (p=0.250).
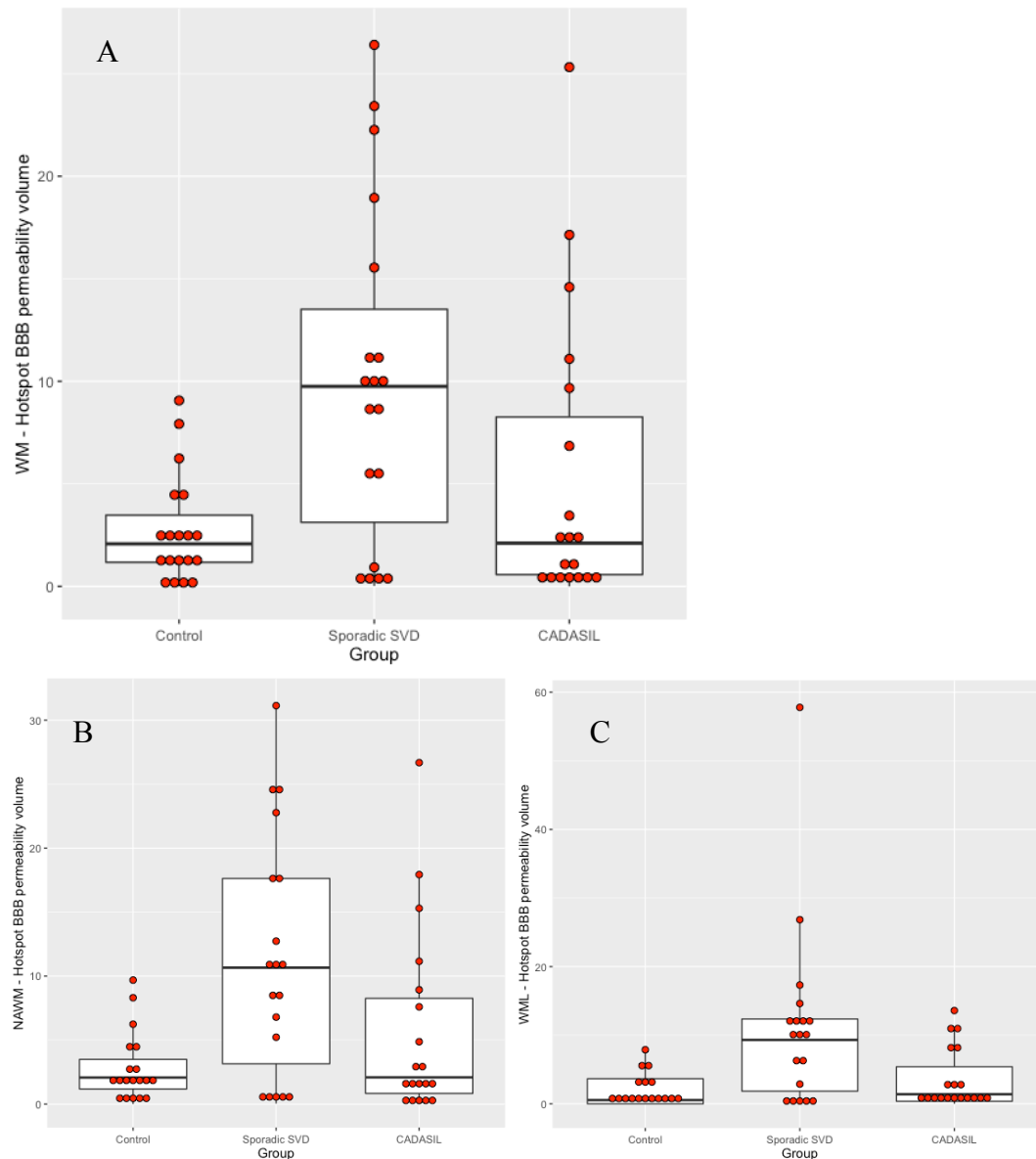
Figure 4.4: Hotspot permeability volume (%) of the WM, NAWM and WML. All analyses were controlled for age and sex.

A) Hotspot permeability volume of the WM was significantly higher in the sporadic SVD group compared to control (p=0.010). There was no significant difference between CADASIL and control (p=1.000).

B) Hotspot permeability volume of the NAWM was significantly higher in the sporadic SVD compared to control (p=0.007). There was no significant difference between CADASIL and control (p=0.869).

C) Hotspot permeability volume of the WML was significantly higher in sporadic SVD compared to control (p=0.004). There was no significant difference between CADASIL and control (p=0.508).

4.3.2 NAWM vs. WML

The permeability values in the NAWM and WML were compared within the individual groups, to see if there was a significant difference between them (Table 4.1).

In the control group, the NAWM values were consistently significantly higher than the WML values for the global permeability mean value (p=0.008), hotspot permeability mean value (p=0.008) and hotspot permeability volume (p=0.024).

In the sporadic SVD group, NAWM values were significantly higher than the WML values for the global permeability mean (p=0.024) and hotspot permeability mean (p=<0.001), but no different for the hotspot permeability volumes.

In the CADASIL group, the NAWM values were significantly higher than the WML values for the global permeability mean (p=0.008), hotspot permeability mean (p=0.022) and the hotspot permeability volume (p=0.016).

Group	Imaging parameter	NAWM		WML		P value
		Median	IQR	Median	IQR	
Control	Global permeability mean (x10^3, L/g min)	0.046	0.071	0.009	0.062	**0.008**
Control	Hotspot permeability mean (x10^3, L/g min)	1.977	1.183	1.033	1.943	**0.008**
Control	Hotspot permeability volume (%)	2.074	2.314	0.543	3.661	**0.024**
Sporadic SVD	Global permeability mean (x10^3, L/g min)	0.295	0.620	0.161	0.361	**0.024**
Sporadic SVD	Hotspot permeability mean (x10^3, L/g min)	3.397	3.036	2.376	2.624	**<0.001**
Sporadic SVD	Hotspot permeability volume (%)	10.660	14.480	9.314	10.518	0.709
CADASIL	Global permeability mean (x10^3, L/g min)	0.046	0.136	0.026	0.103	**0.008**
CADASIL	Hotspot permeability mean (x10^3, L/g min)	2.009	1.541	1.562	1.468	**0.022**
CADASIL	Hotspot permeability volume (%)	2.088	7.429	1.393	5.027	**0.016**

Table 4.1: Pairwise comparisons of BBB permeability in the NAWM and WML. Significant p values are shown in bold.

4.3.3 WML Penumbra

BBB permeability values from the penumbra were calculated and compared between the sporadic SVD and control groups and the CADASIL and control groups.

Values of global BBB permeability within the penumbra are shown and compared in Figure 4.5. The global permeability of the sporadic SVD group was significantly higher than control when controlled for age and sex ($p=0.003$ ($p=0.006$ when adjusted for multiple comparisons)) and controlled for cardiovascular risk factors ($p=0.003$). In the CADASIL group, the global BBB permeability values were not significantly different from control.

Mean values of the BBB permeability hotspots from the penumbra were compared in Figure 4.6. The mean value of the permeability hotspots was significantly higher in the sporadic SVD group compared to control when controlled for age and sex ($p=0.002$ ($p=0.004$ when adjusted for multiple comparisons)) and cardiovascular risk factors ($p=0.003$). In the CADASIL group, the mean values of the BBB permeability hotspots were not significantly different from control.

Finally, the volumes of the BBB permeability hotspots within the penumbras were compared, shown in Figure 4.7. In the sporadic SVD group, the volume of permeability hotspots in the penumbra was significantly larger than control when adjusted for age and sex ($p=0.009$ ($p=0.018$ when adjusted for multiple comparisons)) and cardiovascular risk factors ($p=0.011$). In the CADASIL group, there was no significant difference from control for the volume of the BBB permeability hotspots in the penumbra.
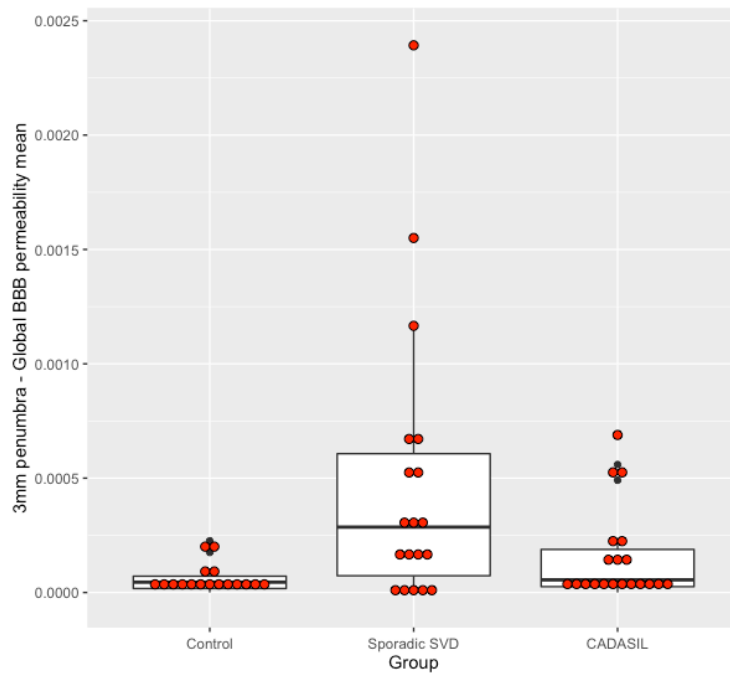
Figure 4.5: Global mean BBB permeability (L/g min) in the penumbra was compared between groups when controlled for age and sex. The penumbra mean was significantly higher in SVD compared to control (p=0.006). CADASIL was no different from control (p=0.263).
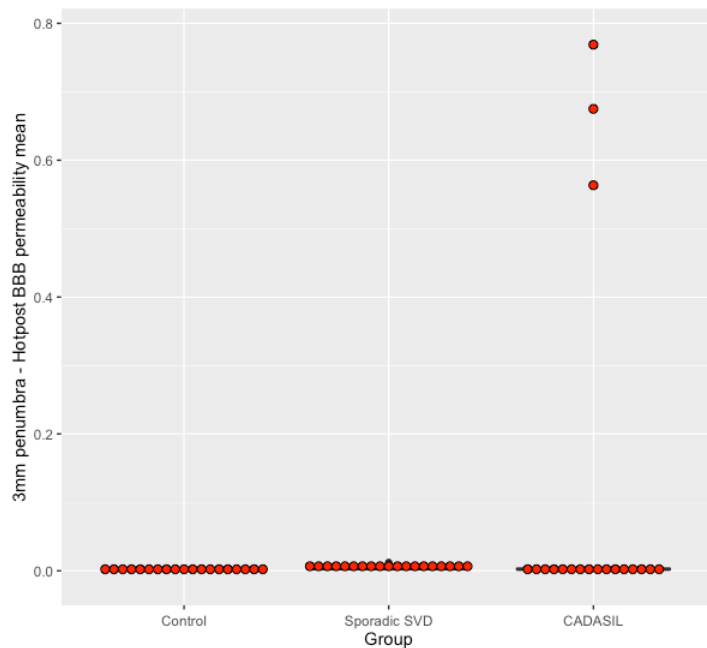
Figure 4.6: The mean value of the BBB permeability hotspots (L/g min) in the penumbra were compared between the groups, controlling for age and sex. The mean of the hotspots was significantly higher in the sporadic SVD group compared to control (p=0.004) and in the CADASIL compared to control (p=0.067).
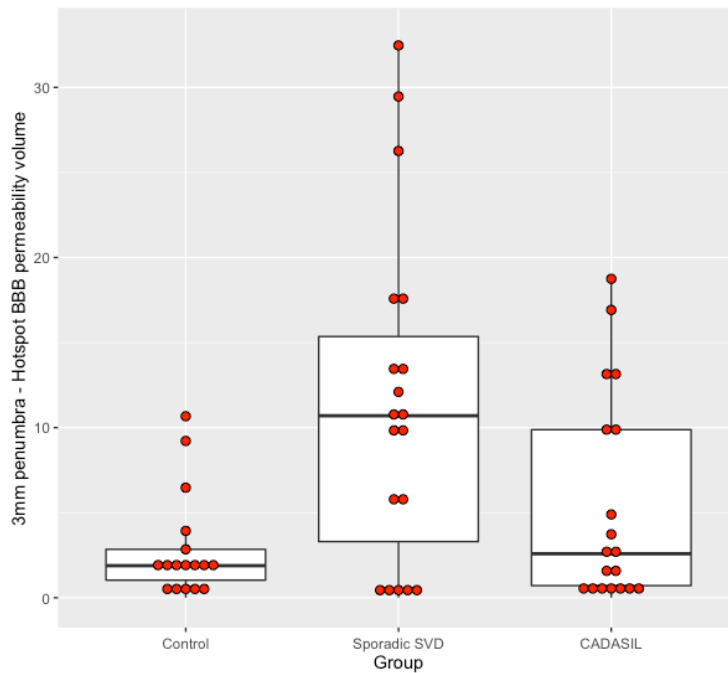
Figure 4.7: The volume of the BBB permeability hotspots (%) in the penumbra were compared between the groups, controlling for age and sex. The volume of the hotspots was significantly higher in sporadic SVD compared to control (p=0.018). There was no difference between CADASIL and control (p=0.947).

Penumbra values were then compared with corresponding NAWM and WML values, to see if they were significantly different in permeability to these regions, shown in Table 4.2.

Within the control group, penumbra values were similar to all corresponding NAWM and WML values except for the hotspot permeability in the WML. The mean value of the permeability hotspots in the penumbra was significantly higher than in the WML (p=0.003).

In the sporadic SVD group, the penumbra values were similar to the corresponding NAWM and WML for the global permeability mean and the volume of the permeability hotspots. However, when comparing to the mean value of the permeability hotspots, the penumbra values were significantly lower than the NAWM (p=0.025), but significantly higher than WML (p=0.002).

Within the CADASIL group, the penumbra values were similar to the NAWM values, but significantly higher than the WML values. The global permeability mean of the penumbra was significantly higher than in the WML (p=0.003). The hotspot mean of the penumbra was also significantly higher than the WML (p=0.010) and the hotspot volume of the penumbra was significantly higher than the WML (p=0.004).

Group	Permeability measurement	Permeability measurement		Penumbra measurement		P value
		Median	IQR	Median	IQR	
Control	NAWM mean (x10^3 L/g min)	0.046	0.071	0.045	0.054	0.984
	WML mean (x10^3 L/g min)	0.009	0.062	0.045	0.054	0.118
	NAWM hotspot mean (x10^3 L/g min)	1.977	1.183	1.664	1.548	0.204
	WML hotspot mean (x10^3 L/g min)	1.033	1.943	1.664	1.548	**0.003**
	NAWM hotspot volume (%)	2.074	2.314	1.885	1.810	0.984
	WML hotspot volume (%)	0.543	3.661	1.885	1.810	0.118
Sporadic SVD	NAWM mean (x10^3 L/g min)	0.295	0.620	0.286	0.534	0.488
	WML mean (x10^3 L/g min)	0.161	0.361	0.286	0.534	0.204
	NAWM hotspot mean (x10^3 L/g min)	3.397	3.036	2.783	3.007	**0.025**
	WML hotspot mean (x10^3 L/g min)	2.376	2.624	2.783	3.007	**0.002**
	NAWM hotspot volume (%)	10.660	14.480	10.699	12.054	0.984
	WML hotspot volume (%)	9.314	10.518	10.699	12.054	0.488
CADASIL	NAWM mean (x10^3 L/g min)	0.046	0.136	0.055	0.163	0.488
	WML mean (x10^3 L/g min)	0.026	0.103	0.055	0.163	**0.003**
	NAWM hotspot mean (x10^3 L/g min)	2.009	1.541	2.187	1.764	0.649
	WML hotspot mean (x10^3 L/g min)	1.562	1.468	2.187	1.764	**0.010**
	NAWM hotspot volume (%)	2.088	7.429	2.585	9.167	0.508
	WML hotspot volume (%)	1.393	5.027	2.585	9.167	**0.004**

Table 4.2: Pairwise comparisons for the individual groups for the global mean permeability values, hotspot mean permeability values and hotspot permeability volume with equivalent penumbra values. Significant p values are shown in bold.

4.3.4 WMLs

Associations between BBB permeability parameters and WML volume are shown in Table 4.3. There was a significant association between the mean value of the permeability hotspots in the WML of the control group and total WML volume when controlled for age, sex and ICV (β =0.718, p<0.001 (p=0.009 when adjusted for multiple comparisons). This significance was still present when additionally controlled for the cardiovascular risk factors (β =0.677, p=0.013). There were no other significant associations seen between the BBB permeability parameters and WML volume.

Permeability value	Brain region	Control		Sporadic SVD		CADASIL	
		β	P value	β	P value	β	P value
Global mean	**NAWM**	0.334	0.545	0.241	0.570	-0.438	0.104
	WML	0.581	0.063	-0.077	0.768	-0.089	0.753
Hotspot mean	**NAWM**	0.271	0.570	0.184	0.640	-0.250	0.570
	WML	**0.718**	**0.009**	0.159	0.640	0.101	0.753
Hotspot volume	**NAWM**	0.341	0.545	0.154	0.640	-0.195	0.614
	WML	0.594	0.063	-0.176	0.640	-0.049	0.813

Table 4.3: Associations between BBB permeability and WML volume when adjusted for age, sex and ICV. Table shows standardised β coefficients and p values. Significant p values are shown in bold.

4.3.5 Lacunar Infarcts

Lacunar infarcts were measured as lacune volume and as lacune count. Lacune volume was compared with the measures of BBB permeability in the different groups (Table 4.4) and none of the parameters were significantly associated with lacune volume. Similarly, lacune count was compared with the various measures of BBB permeability in the different groups (Table 4.5) and also showed that lacune count was not significantly associated with any of them.

Permeability value	Brain region	Control		Sporadic SVD		CADASIL	
		β	P value	β	P value	β	P value
Global mean	NAWM	0.006	0.978	0.213	0.978	-0.336	0.575
	WML	0.009	0.978	0.138	0.978	-0.448	0.281
Hotspot mean	NAWM	0.010	0.978	0.094	0.978	0.096	0.978
	WML	0.044	0.978	0.280	0.978	-0.121	0.978
Hotspot volume	NAWM	0.007	0.978	0.181	0.978	-0.389	0.407
	WML	0.000	0.998	0.060	0.978	-0.490	0.276

Table 4.4: Associations between BBB permeability and lacune volume when adjusted for age, sex and ICV. Table shows standardised β coefficients and p values. Significant p values are shown in bold.

Permeability value	Brain region	Control		Sporadic SVD		CADASIL	
		β	P value	β	P value	β	P value
Global mean	NAWM	-0.007	0.962	0.307	0.694	-0.396	0.290
	WML	-0.002	0.976	0.199	0.797	-0.534	0.062
Hotspot mean	NAWM	0.027	0.897	-0.031	0.962	0.131	0.845
	WML	0.051	0.784	0.282	0.709	-0.202	0.784
Hotspot volume	NAWM	-0.010	0.962	0.352	0.668	-0.465	0.140
	WML	-0.012	0.962	0.173	0.845	-0.564	0.060

Table 4.5: Associations between BBB permeability and lacune count when adjusted for age and sex. Table shows standardised β coefficients and p values. Significant p values are shown in bold.

4.3.6 CMBs

The associations between CMB count with BBB permeability parameters for the different groups is shown in Table 4.6. There were no significant associations seen.

Permeability value	Brain region	Control		Sporadic SVD		CADASIL	
		β	P value	β	P value	β	P value
Global mean	NAWM	-0.045	0.587	0.281	0.420	-0.211	0.420
	WML	-0.061	0.420	0.402	0.420	-0.256	0.420
Hotspot mean	NAWM	0.018	0.808	-0.127	0.737	0.020	0.902
	WML	-0.077	0.420	0.318	0.420	-0.298	0.420
Hotspot volume	NAWM	-0.027	0.737	0.326	0.420	-0.244	0.420
	WML	-0.072	0.420	0.399	0.420	-0.244	0.420

Table 4.6: Associations between BBB permeability and CMB count when adjusted for age and sex. Table shows standardised β coefficients and p values. Significant p values are shown in bold.

4.3.7 Brain Volume

The associations between the BBB permeability parameters and brain volume are shown in Table 4.7; there were no significant associations seen. The associations between BBB permeability parameters and GM volume are then shown in Table 4.8; again, there were no significant associations seen.

Permeability value	Brain region	Control		Sporadic SVD		CADASIL	
		β	P value	β	P value	β	P value
Global mean	NAWM	-0.021	0.980	-0.019	0.980	0.270	0.980
	WML	0.046	0.980	0.010	0.980	0.369	0.903
Hotspot mean	NAWM	-0.012	0.980	0.063	0.980	-0.073	0.980
	WML	0.040	0.980	0.004	0.980	0.121	0.980
Hotspot volume	NAWM	-0.052	0.980	-0.059	0.980	0.239	0.980
	WML	-0.059	0.980	-0.008	0.980	0.309	0.954

Table 4.7: Associations between BBB permeability and brain volume when adjusted for age, sex and ICV. Table shows standardised β coefficients and p values. Significant p values are shown in bold.

Permeability value	Brain region	Control		Sporadic SVD		CADASIL	
		β	P value	β	P value	β	P value
Global mean	**NAWM**	-0.123	0.799	-0.222	0.710	0.580	0.078
	WML	0.028	0.891	-0.071	0.799	0.517	0.109
Hotspot mean	**NAWM**	-0.068	0.799	0.140	0.799	0.176	0.799
	WML	-0.065	0.799	-0.226	0.710	0.204	0.799
Hotspot volume	**NAWM**	-0.095	0.799	-0.286	0.640	0.452	0.152
	WML	-0.099	0.799	-0.077	0.799	0.448	0.152

Table 4.8: Associations between BBB permeability and GM volume when adjusted for age, sex and ICV. Table shows standardised β coefficients and p values. Significant p values are shown in bold.

4.3.8 FA

The association between FA median and the BBB permeability parameters are shown for the NAWM in Table 4.9 and for the WML in Table 4.10. A higher FA median in the NAWM was associated with global permeability of the NAWM in the CADASIL group when adjusted for age and sex (β=0.543, p=0.002 (p=0.031 when adjusted for multiple comparisons)). When adjusted for all of the cardiovascular risk factors, the association was still significant (β=0515, p=0.019). No other parameters were associated with FA median in the NAWM or the WML for any of the groups.

Permeability value	Brain region	Control		Sporadic SVD		CADASIL	
		β	P value	β	P value	β	P value
Global mean	NAWM	-0.067	0.865	-0.506	0.233	**0.543**	**0.031**
	WML	-0.104	0.821	-0.218	0.671	0.326	0.304
Hotspot mean	NAWM	-0.299	0.349	-0.037	0.898	0.316	0.304
	WML	-0.288	0.349	-0.360	0.349	0.154	0.671
Hotspot volume	NAWM	-0.049	0.875	-0.528	0.233	0.392	0.233
	WML	-0.077	0.865	-0.181	0.730	0.297	0.304

Table 4.9: Associations between BBB permeability and FA NAWM median when adjusted for age and sex. Table shows standardised β coefficients and p values. Significant p values are shown in bold.

Permeability value	Brain region	Control		Sporadic SVD		CADASIL	
		β	P value	β	P value	β	P value
Global mean	NAWM	-0.058	0.828	-0.101	0.828	-0.311	0.828
	WML	-0.209	0.828	-0.107	0.828	-0.080	0.828
Hotspot mean	NAWM	-0.424	0.828	0.263	0.828	0.091	0.828
	WML	-0.227	0.828	-0.236	0.828	-0.241	0.828
Hotspot volume	NAWM	-0.137	0.828	-0.160	0.828	-0.282	0.828
	WML	-0.128	0.828	-0.080	0.828	-0.056	0.828

Table 4.10: Associations between BBB permeability and FA WML median when adjusted for age and sex. Table shows standardised β coefficients and p values. Significant p values are shown in bold.

4.3.9 MD

Associations between MD peak height and BBB permeability parameters are shown for NAWM in Table 4.11 and WML in Table 4.12. There were no associations between any of the BBB permeability parameters and the MD peak height in the NAWM for any of the groups. However, there was a significant negative association

between the global mean value of BBB permeability in the WML and MD peak height in the WML in the control group when adjusted for age and sex (β=-0.675, p=0.003 (p=0.027 when adjusted for multiple comparisons)). The significance was still present after adjusting for cardiovascular risk factors (β=-0.583, p=0.021). Similarly, there was significant negative association between the mean value of the BBB permeability hotspots in the WML and MD peak height in the WML in the control group when adjusted for age and sex (β=-0.830, p<0.001 (p=0.001 when adjusting for multiple comparisons)). The significance was still present after adjusting for cardiovascular risk factors (β=-0.742, p=0.003).

Permeability value	Brain region	Control		Sporadic SVD		CADASIL	
		β	P value	β	P value	β	P value
Global mean	**NAWM**	-0.196	0.855	0.225	0.855	0.194	0.855
	WML	-0.118	0.942	0.236	0.855	0.069	0.942
Hotspot mean	**NAWM**	-0.109	0.942	0.386	0.855	0.277	0.855
	WML	-0.042	0.984	0.000	0.999	-0.013	0.999
Hotspot volume	**NAWM**	-0.175	0.855	0.116	0.942	0.071	0.942
	WML	-0.070	0.942	0.201	0.914	0.027	0.999

Table 4.11: Associations between BBB permeability and MD NAWM peak height when adjusted for age and sex. Table shows standardised β coefficients and p values. Significant p values are shown in bold.

Permeability value	Brain region	Control		Sporadic SVD		CADASIL	
		β	P value	β	P value	β	P value
Global mean	NAWM	-0.420	0.324	0.220	0.626	0.020	0.940
	WML	**-0.675**	**0.027**	0.315	0.443	-0.056	0.877
Hotspot mean	NAWM	-0.405	0.324	0.305	0.456	0.114	0.790
	WML	**-0.830**	**0.001**	0.207	0.626	-0.149	0.790
Hotspot volume	NAWM	-0.418	0.324	0.107	0.790	-0.157	0.790
	WML	-0.639	0.060	0.270	0.539	-0.098	0.790

Table 4.12: Associations between BBB permeability and MD WML peak height when adjusted for age and sex. Table shows standardised β coefficients and p values. Significant p values are shown in bold.

4.3.10 FW

Associations between FW median and BBB permeability parameters are shown for NAWM in Table 4.13 and WML in Table 4.14. There was no association between any of the BBB permeability parameters and either of the FW values for any of the groups.

Permeability value	Brain region	Control		Sporadic SVD		CADASIL	
		β	P value	β	P value	β	P value
Global mean	NAWM	0.097	0.782	0.333	0.782	-0.238	0.782
	WML	0.189	0.782	0.165	0.782	-0.088	0.782
Hotspot mean	NAWM	0.122	0.782	0.012	0.963	-0.261	0.782
	WML	0.238	0.782	0.278	0.782	-0.077	0.782
Hotspot volume	NAWM	0.048	0.867	0.380	0.782	-0.144	0.782
	WML	0.148	0.782	0.149	0.782	-0.072	0.782

Table 4.13: Associations between BBB permeability and FW NAWM median when adjusted for age and sex. Table shows standardised β coefficients and p values. Significant p values are shown in bold.

Permeability value	Brain region	Control		Sporadic SVD		CADASIL	
		β	P value	β	P value	β	P value
Global mean	NAWM	0.078	0.899	-0.159	0.860	-0.197	0.769
	WML	0.293	0.703	-0.283	0.703	0.020	0.931
Hotspot mean	NAWM	0.346	0.633	-0.413	0.633	-0.420	0.578
	WML	0.368	0.633	-0.149	0.860	0.164	0.790
Hotspot volume	NAWM	0.117	0.899	-0.024	0.931	0.068	0.899
	WML	0.440	0.633	-0.237	0.769	0.052	0.899

Table 4.14: Associations between BBB permeability and FW WML median when adjusted for age and sex. Table shows standardised β coefficients and p values. Significant p values are shown in bold.

4.3.11 FW adjusted FA

Associations between FW adjusted FA median and BBB permeability parameters are shown for NAWM in Table 4.15 and WML in Table 4.16. There was a significant negative association between the volume of the BBB permeability hotspots in the NAWM and the FW adjusted FA median in the NAWM in the sporadic SVD group (β=-0.672, p=0.005 (p=0.045 when adjusted for multiple comparisons)). This association was still present after adjusting for cardiovascular risk factors (β=-0.671, p=0.012). In the CADASIL group, there was a significant positive association between the global mean value of BBB permeability of the NAWM and the FW adjusted FA median in the NAWM (β=0.614, p<0.001 (p=0.009 when adjusted for multiple comparisons)). This association was still present after adjusting for cardiovascular risk factors (β=0.593, p=0.008). There were no significant associations between any of the other permeability parameters with the FW adjusted FA values in the NAWM and WML.

Permeability value	Brain region	Control		Sporadic SVD		CADASIL	
		β	P value	β	P value	β	P value
Global mean	NAWM	-0.005	0.981	-0.522	0.126	**0.614**	**0.009**
	WML	-0.098	0.775	-0.474	0.135	0.376	0.135
Hotspot mean	NAWM	-0.198	0.525	0.168	0.706	0.377	0.135
	WML	-0.286	0.291	-0.469	0.135	0.172	0.583
Hotspot volume	NAWM	0.039	0.919	**-0.672**	**0.045**	0.447	0.125
	WML	-0.035	0.919	-0.563	0.126	0.347	0.146

Table 4.15: Associations between BBB permeability and FW adjusted FA NAWM median when adjusted for age and sex. Table shows standardised β coefficients and p values. Significant p values are shown in bold.

Permeability value	Brain region	Control		Sporadic SVD		CADASIL	
		β	P value	β	P value	β	P value
Global mean	NAWM	-0.206	0.695	-0.228	0.695	-0.490	0.467
	WML	-0.190	0.695	-0.273	0.695	-0.064	0.855
Hotspot mean	NAWM	-0.576	0.217	0.198	0.695	-0.098	0.806
	WML	-0.145	0.737	-0.344	0.695	-0.180	0.695
Hotspot volume	NAWM	-0.352	0.695	-0.257	0.695	-0.285	0.695
	WML	-0.112	0.806	-0.227	0.695	0.004	0.989

Table 4.16: Associations between BBB permeability and FW adjusted WML median when adjusted for age and sex. Table shows standardised β coefficients and p values. Significant p values are shown in bold.

4.3.12 FW adjusted MD

Associations between FW adjusted MD peak height and BBB permeability parameters are shown for NAWM in Table 4.17 and WML in Table 4.18. There was no association between any of the BBB permeability parameters and the FW adjusted MD peak height values in the NAWM. There was a significant negative association

between the mean value of the BBB permeability hotspots in the WML and the FW adjusted MD peak height in the WML in the control group (β=-0.725, p=0.001 (p=0.017 when adjusted for multiple comparisons)). This association was still present after adjusting for cardiovascular risk factors (β=-0.665, p=0.019). There were no significant associations between any of the other permeability parameters with the FW adjusted MD values in the WML.

Permeability value	Brain region	Control		Sporadic SVD		CADASIL	
		β	P value	β	P value	β	P value
Global mean	NAWM	0.192	0.427	0.273	0.427	-0.334	0.360
	WML	0.307	0.353	0.507	0.353	-0.299	0.360
Hotspot mean	NAWM	0.100	0.660	0.077	0.821	0.000	0.999
	WML	0.329	0.353	0.310	0.425	-0.160	0.584
Hotspot volume	NAWM	0.116	0.631	0.275	0.427	-0.277	0.397
	WML	0.281	0.360	0.497	0.353	-0.242	0.425

Table 4.17: Associations between BBB permeability and FW adjusted MD NAWM peak height when adjusted for age and sex. Table shows standardised β coefficients and p values. Significant p values are shown in bold.

Permeability value	Brain region	Control		Sporadic SVD		CADASIL	
		β	P value	β	P value	β	P value
Global mean	NAWM	-0.311	0.680	-0.120	0.859	0.358	0.680
	WML	-0.582	0.103	-0.111	0.859	-0.046	0.861
Hotspot mean	NAWM	-0.253	0.680	-0.304	0.680	0.061	0.861
	WML	**-0.725**	**0.017**	-0.083	0.859	-0.252	0.680
Hotspot volume	NAWM	-0.289	0.680	-0.114	0.859	0.078	0.859
	WML	-0.566	0.145	-0.139	0.859	-0.097	0.859

Table 4.18: Associations between BBB permeability and FW adjusted MD WML peak height when adjusted for age and sex. Table shows standardised β coefficients and p values. Significant p values are shown in bold.

4.3.13 Cognition

The association between BBB permeability parameters and GC can be seen in Table 4.19. The associations between BBB permeability parameters and the various cognitive domains of EF, PS, WoM and LTM can be found in Tables 4.20, 4.21, 4.22 and 4.23 respectively. There was no association between any of the BBB permeability parameters in any of the groups with cognition.

Permeability value	Brain region	Control		Sporadic SVD		CADASIL	
		β	P value	β	P value	β	P value
Global mean	NAWM	-0.169	0.551	-0.149	0.561	0.586	0.118
	WML	-0.275	0.328	0.037	0.945	0.459	0.278
Hotspot mean	NAWM	-0.227	0.441	0.006	0.977	0.325	0.440
	WML	-0.149	0.561	-0.064	0.891	0.417	0.288
Hotspot volume	NAWM	-0.211	0.441	-0.237	0.441	0.473	0.278
	WML	-0.160	0.551	-0.012	0.977	0.410	0.288

Table 4.19: Associations between BBB permeability and GC when adjusted for age, sex and premorbid IQ. Table shows standardised β coefficients and p values. Significant p values are shown in bold.

Permeability value	Brain region	Control		Sporadic SVD		CADASIL	
		β	P value	β	P value	β	P value
Global mean	NAWM	-0.244	0.463	-0.229	0.463	0.669	0.066
	WML	-0.276	0.421	-0.124	0.684	0.561	0.101
Hotspot mean	NAWM	-0.132	0.684	-0.036	0.863	0.046	0.863
	WML	-0.187	0.587	-0.051	0.863	0.583	0.101
Hotspot volume	NAWM	-0.230	0.463	-0.357	0.227	0.569	0.101
	WML	-0.105	0.684	-0.205	0.463	0.452	0.227

Table 4.20: Associations between BBB permeability and EF when adjusted for age, sex and premorbid IQ. Table shows standardised β coefficients and p values. Significant p values are shown in bold.

Permeability value	Brain region	Control		Sporadic SVD		CADASIL	
		β	P value	β	P value	β	P value
Global mean	NAWM	-0.244	0.463	-0.229	0.463	0.669	0.066
	WML	-0.276	0.421	-0.124	0.683	0.561	0.134
Hotspot mean	NAWM	-0.142	0.683	-0.036	0.853	0.092	0.774
	WML	-0.204	0.511	-0.087	0.737	0.536	0.136
Hotspot volume	NAWM	-0.230	0.463	-0.357	0.227	0.569	0.134
	WML	-0.105	0.684	-0.205	0.463	0.452	0.227

Table 4.21: Associations between BBB permeability and PS when adjusted for age, sex and premorbid IQ. Table shows standardised β coefficients and p values. Significant p values are shown in bold.

Permeability value	Brain region	Control		Sporadic SVD		CADASIL	
		β	P value	β	P value	β	P value
Global mean	NAWM	0.029	0.950	-0.127	0.937	0.306	0.937
	WML	-0.153	0.937	-0.035	0.937	0.041	0.946
Hotspot mean	NAWM	-0.198	0.937	-0.057	0.937	0.230	0.937
	WML	-0.191	0.937	-0.097	0.937	0.152	0.937
Hotspot volume	NAWM	-0.006	0.977	-0.136	0.937	0.081	0.937
	WML	-0.072	0.937	-0.042	0.937	-0.068	0.937

Table 4.22: Associations between BBB permeability and WoM when adjusted for age, sex and premorbid IQ. Table shows standardised β coefficients and p values. Significant p values are shown in bold.

Permeability value	Brain region	Control		Sporadic SVD		CADASIL	
		β	P value	β	P value	β	P value
Global mean	**NAWM**	-0.069	0.936	-0.129	0.936	0.088	0.936
	WML	-0.181	0.936	0.211	0.936	0.060	0.936
Hotspot mean	**NAWM**	-0.141	0.936	-0.197	0.936	0.175	0.936
	WML	-0.017	0.936	0.042	0.936	0.041	0.936
Hotspot volume	**NAWM**	-0.104	0.936	-0.135	0.936	0.019	0.936
	WML	-0.142	0.936	0.216	0.936	0.069	0.936

Table 4.23: Associations between BBB permeability and LTM when adjusted for age, sex and premorbid IQ. Table shows standardised β coefficients and p values. Significant p values are shown in bold.

4.4 Discussion

This chapter has shown that there seems to be both a global and focal increase in BBB permeability in the sporadic SVD group compared to control. There does not seem to be increased permeability in the CADASIL group compared to control. Permeability was higher in the NAWM compared to the WML, with no significant increase in permeability seen in the WML penumbra. The volume of the BBB permeability hotspots in the NAWM of the sporadic SVD group was associated with FW corrected FA values in the NAWM, suggesting a higher volume of highly permeable tissue is associated with decreased WM integrity of the tissue.

4.4.1 Group Differences in Sporadic SVD vs. Control

Global permeability of the whole WM, NAWM and WML were all significantly higher in sporadic SVD compared to control (Figure 4.2), suggesting that there is a global increase in BBB permeability throughout the WM in SVD.

In the literature, many studies have compared global BBB permeability between sporadic SVD and controls, and have shown permeability to be significantly higher in the sporadic SVD group (Wardlaw et al., 2009, Topakian et al., 2010, Huisa et al., 2015, Taheri et al., 2011a). Therefore, our data is consistent with the literature, suggesting a global increase in permeability in sporadic SVD compared to control.

Hotspots were then created by filtering out all voxels that had a permeability value below a 'normal threshold' determined from our control group, to allow focal regions of high permeability to be identified. The mean value of permeability within these regions was calculated, as well as the volume of the regions. This analysis method filters out the 'noise' from normal fluctuations in permeability, and in theory should therefore only represent the pathological permeability. The mean value of the permeability hotspots in the WM and NAWM showed no significant difference between sporadic SVD and control, although there was a trend for the values to be higher (Figure 4.3). However, there was a significantly higher mean value in the permeability hotspots of sporadic SVD compared to control in the WML. The volume

of the permeability hotspots was consistently shown to be higher in the sporadic SVD group compared to the control group in the WM, NAWM and WML (Figure 4.4).

Previous studies have used a similar hotspot analysis to us, by establishing a threshold by which voxels must pass to class as having significant BBB permeability. A significant increase in the hotspot mean of sporadic SVD compared to control has been seen in the WM (Huisa et al., 2015, Taheri et al., 2011a), although not in all studies (Zhang et al., 2017). Zhang et al. found a significantly increased volume of hotspot BBB permeability leakage in sporadic SVD compared to control in the NAWM and WML (Zhang et al., 2017).

An explanation to the discrepancies shown in the literature is probably due to the methods used to establish the hotspot threshold. Huisa et al. used a previously established threshold that had given the maximum accuracy of correctly predicting control and patients (Huisa et al., 2015). Zhang et al. took positively skewed histograms of permeability and removed the 'normal distribution' part of the histogram to leave only the positively skewed values, suggested to be the high permeability values (Zhang et al., 2017). Taheri et al. used the same method as our study, taking the voxels with a value greater than the 95th centile of the permeability distribution from the NAWM of the control population (Taheri et al., 2011a). Interestingly, the control permeability value from the Taheri et al. paper is around half of the value from our study (3×10^{-4} L/g min compared to 6.5×10^{-4} L/g min). This may be due to the use of elderly controls in our study, who naturally have higher levels of BBB permeability.

Our result and the results of previous studies would suggest that the choice of hotspot threshold can impact on the hotspot parameters. It would suggest that if a higher threshold is used then this is less likely to show a significant difference in the mean value of the hotspots, but potentially more likely to show a significant difference in the volume of the hotspots. Therefore, this must be carefully considered when drawing conclusions from the literature.

Overall, our results our consistent with the literature, showing that there is increased BBB permeability in sporadic SVD, with a significant increase in global permeability and hotspot volume throughout the NAWM and WML, compared to control.

4.4.2 Group Differences in CADASIL vs. Control

In CADASIL, the involvement of BBB permeability in the mechanism is less clear. The CADASIL group showed no significant difference in BBB permeability from the control group for any of the parameters (Figures 4.2-4).

There were two severe outliers in the CADASIL group for the mean value of the BBB permeability hotspots in the WM and NAWM, which can be seen in Figure 4.3. There was no obvious reason to exclude these outliers and therefore they were left in for the analysis. However, we did rerun the analysis without these outliers to see if they were skewing the results. This analysis can be found in Appendix A; the analysis shows no difference in the pattern of the results to when the outliers are left in. Removing the outliers still shows no significant difference in the mean value of the BBB permeability hotspots between the CADASIL and control groups in the WM (Figure A.1) or the NAWM (Figure A.2).

The CADASIL literature on BBB permeability is limited. In an early study, Dichgans et al. found elevated protein content and an elevated CSF/serum albumin ratio in CADASIL patients, suggesting there is an increased permeability of the BBB (Dichgans et al., 1999). Other studies of CADASIL patients have shown changes in pericytes (Dziewulska and Lewandowska, 2012) and an increase in circulating biomarkers of endothelial cell dysfunction (Pescini et al., 2017, Rufa et al., 2008), also suggesting an increase in BBB permeability. However, when BBB permeability was measured in CADASIL mice models, an increased permeability was not seen (Cognat et al., 2014, Joutel et al., 2010).

The literature is conflicting, but would suggest that there is a role for increased BBB permeability in CADASIL patients. One explanation for the lack of difference seen in our study could be that our CADASIL participants were significantly younger than

controls (Table 3.1). BBB permeability is known to increase with age (Mooradian and McCuskey, 1992, Farrall, 2009, Goodall et al., 2018), and therefore this could be influencing the results. The analyses were controlled for age, but the relationship may be more complicated than the analyses account for, with potentially a step effect rather than a linear effect. Age-matched controls should be used in future studies to see if there is still no group difference seen.

Looking closely at the graphs, it seems that CADASIL has a wide range of permeability values, with some values closer to the levels seen in sporadic SVD, whilst others are more similar to control (Figures 4.2-4). Potentially, this could be due to the fact that our CADASIL participants had a wide range of disease severity, with some patients in an early stage where they may have no symptoms, whilst others are late stage having experienced major symptoms such as stroke.

The unclear nature of the role of BBB permeability in CADASIL and the high spread of values seen, led us to investigate permeability within the CADASIL group specifically (Appendix B). We compared the permeability between patients who were over 55, had a stroke history and had migraine history. The results showed that there was a significant difference between the global mean permeability of the NAWM in patients who had a stroke compared to those who had not (Table B.4). Interestingly, BBB permeability was higher in patients who had not experienced a stroke, suggesting that maybe BBB permeability has a role in CADASIL pre-stroke. It is important to note that this data uses very low group numbers and therefore it is impossible to fully explore the role of BBB permeability in CADASIL without a larger sample size and broader range of clinical symptoms.

Our data does not show an obvious role for BBB permeability in CADASIL. However, it suggests that BBB permeability could be worth investigating further in the CADASIL population. Future studies should compare CADASIL BBB permeability with age matched controls, to see if this is influencing the lack of association seen in our study. Additionally, they should investigate permeability in various stages of CADASIL disease, to see if the role of permeability is dependent on the disease time-course.

4.4.3 NAWM vs. WML

We performed pairwise comparisons on the permeability values in the NAWM and WML, to see if there was a significant difference (Table 4.1). In the control and CADASIL participants, the permeability in the NAWM was consistently significantly higher than in the WML for the three measures of permeability (global mean, hotspot mean and hotspot volume). In the sporadic SVD group, permeability in the NAWM was significantly higher than in the WML for the global mean and hotspot mean, however the volume of hotspot permeability was not significantly different between the NAWM and WML.

The difference in permeability in the NAWM and WML has been explored previously in the literature, with little consensus. Huisa et al. reported similar results to ours, where there is significantly more permeability in the NAWM compared to the WML (Huisa et al., 2015). However, other studies have shown the opposite, with significantly higher permeability in the WML compared to NAWM (Wardlaw et al., 2017, Heye et al., 2016). Other studies have reported no significant difference between NAWM and WML permeability (Bronge and Wahlund, 2000). Some studies have reported values for NAWM and WML permeability in the text without performing statistical comparisons between the two; Zhang et al. reported NAWM permeability as higher (Zhang et al., 2017), whilst others report WML permeability as higher (Hanyu et al., 2002, Li et al., 2018b).

The discrepancies in the literature are confusing and make it difficult to interpret the data. The likely source for the discrepancies is due to differing imaging techniques, analysis and normalisation methods. A recent paper by Thrippleton et al. has attempted to bring together a consensus with recommendations for usage of DCE-MRI technique for BBB leakage in SVD to try to reduce some of this discrepancy in the data and allow studies to be more easily interpreted and compared with one another (Thrippleton et al., 2019).

The pattern of permeability in the NAWM and WML is important to establish, as this would help to provide evidence for or against the pathogenic role of BBB permeability in SVD. If the consensus were that permeability is more evident in the

WML then this would suggest it is more of a secondary process to damage. However, if the consensus were that there is higher BBB permeability in the NAWM, as shown in our study, this would suggest that permeability could be involved in the formation of WML from previously NAWM and is therefore pathogenic.

4.4.4 WML Penumbra

There is a growing interest in the SVD field in the penumbra of the WML (Maillard et al., 2011). Studies have shown that approximately 80% of new WML voxels represent extensions of existing WML (Maillard et al., 2012). DTI studies have suggested that there is disrupted WM integrity beyond the area of the WMLs and within the NAWM (Lee et al., 2009), and that these changes are associated with increased WML growth at follow-up (de Groot et al., 2013). This body of research has led to the hypothesis that there may be changes in BBB permeability in the penumbra of the WMLs, which pre-empts WML growth.

We took a 3mm penumbra of the WML and measured the BBB permeability in this region. We then compared between the groups to see if there were differences between our patients and controls (Figures 4.5-7). We found that the penumbra followed a similar pattern to the rest of the WM, where the permeability was significantly increased in the sporadic SVD group compared to control. The CADASIL group was not significantly different from control. We repeated the analysis removing the outliers in the CADASIL group and found the results to follow the same pattern (Figure A.3).

We then went on to compare the penumbra permeability values to the NAWM and WML permeability values within the individual groups (Table 4.2). In the control group, the mean value of the hotspots in the penumbra were significantly higher than the mean value of the hotspots in the WML, but similar to the NAWM. Penumbra values were similar to the global mean and volume of the hotspots in the NAWM and WML. In the sporadic SVD group, the mean value of the hotspots in the penumbra was significantly higher than the mean value of the hotspots in the WML, but significantly lower than the NAWM. Again, penumbra values were similar to the

global mean and volume of the hotspots in the NAWM and WML. In the CADASIL group, penumbra values were significantly higher than WML values, but were similar to NAWM values for the global mean, hotspot mean and hotspot volume. The results are slightly confusing, but the overall pattern suggests that the penumbra permeability values are similar to the NAWM, but higher than the WML.

We repeated this penumbra analysis with a 6mm penumbra, and found that this yielded the same pattern of results. The results of the 6mm penumbra can be found in Appendix C. The 6mm penumbra contained the same outliers in the CADASIL group as the 3mm penumbra, therefore the analysis was also repeated without these outliers (Figure A.4) and found to have the same pattern of results.

Only two previous studies have investigated the penumbra of the WML, which is probably due to the fact that the techniques have only become sophisticated enough to do so quite recently. Huisa et al. created a 4mm rim around the WMLs (of which 2mm was WML and 2mm was the adjoining NAWM and investigated the permeability in this area. They found that 51% of the total permeability voxels were located in the 4mm rim, 9% in the core of the WML and 49% in the NAWM (Huisa et al., 2015). These results were similar the results from our study, suggesting that the penumbra does have higher permeability compared to the WML, but not compared to the rest of the NAWM.

Wardlaw et al. reported a very different pattern of permeability, where there was higher permeability in the WML compared to the NAWM (Wardlaw et al., 2017). They found an interesting observation that the permeability increased with proximity to the WML, suggesting that there may be some permeability changes in the penumbra of the WMLs.

More studies with higher numbers are required which investigate the penumbra of the WML to validate the findings. Ideally, these further studies would use a consensus protocol so that results of future studies can be directly compared to try to minimise discrepancies in methods and make results easier to interpret between studies.

4.4.5 Association with WML Volume

WML volume was found to be significantly associated with mean permeability of the hotspots in the WML of the control group (Table 4.3). There was also a trend, which did not reach significance once corrected for multiple comparisons, for WML volume to be associated with both the global permeability mean and volume of the permeability hotspots in the WMLs of the control group. This association was not seen in the sporadic SVD or CADASIL groups.

The association of WML volume with WML permeability in the control group, but not the sporadic SVD or CADASIL groups, is an interesting finding. One explanation could be that BBB permeability is important for WML progression at early stages of the disease. Our healthy control group was comprised of an elderly population, where most of them had some degree of WML on their MRI scan, and therefore they could be seen as a very early-stage pre-symptomatic SVD population. Our SVD group, on the other hand, is quite a severe population, with inclusion criteria of confluent WML and lacunar stroke. Our CADASIL group is also a severe population, with the highest mean WML volume of all of the groups in this study (Table 3.2). Therefore, if BBB permeability is involved in WML growth, it could be that this is only detectable in early stages of the disease, whereas in later stages of the disease, when there are many pathological processes occurring, there is too much noise to see the association. This explanation could be supported by the current literature, where studies using a lacunar stroke population (with no inclusion criteria for WML volume) (Wardlaw et al., 2017, Topakian et al., 2010, Zhang et al., 2017) and non-SVD populations (Li et al., 2018b) showed a correlation between WML volume and BBB leakage, whereas a study using a more severe SVD population, defined by both WML volume and lacunar stroke, did not show this association (Huisa et al., 2015).

Unfortunately, our study has relatively small group sizes, which makes it difficult to examine these associations within the groups. To fully understand the role of BBB permeability in WML growth, larger longitudinal studies that map the WML progression from early to late stage SVD are required to see if the participants with higher BBB permeability at baseline have increased WML growth at follow-up.

4.4.6 Associations with Lacunes, CMBs and Brain Volume

The control and sporadic SVD groups were not significantly associated with any other imaging markers of lacune number or volume, CMB number, brain volume or GM volume (Tables 4.4-.8). Lacune and CMB number were shown to be significantly associated with BBB leakage in one recent study of SVD patients (Li et al., 2018b). However, this association could be mediated by the fact that patients with higher WML volume are likely to have a more severe phenotype, and therefore have higher numbers of lacunes and CMBs. An ordinal SVD score, which combines the presence of lacunes, WMLs, CMBs and perivascular spaces was also found to be significantly associated with BBB permeability (Li et al., 2018b). To the best of my knowledge, an association between BBB permeability and brain volume or GM volume has never previously been reported in the literature.

The lack of association between permeability and these parameters would suggest that BBB permeability is not directly involved in the pathological mechanisms of lacune formation, CMB formation or GM atrophy. However, we cannot rule out a causal relationship, where BBB permeability may influence the subsequent development of lacune formation, CMB formation or atrophy. Longitudinal studies are required to fully understand this.

4.4.7 Associations with FA in the sporadic SVD group

In the SVD group, a higher volume of permeability hotspots in the NAWM was associated with a lower FA in the NAWM, after adjustment for FW (Table 4.15). Interestingly, this association was not significant before the FW adjustment (Table 4.9).

Reductions in FA manifest in the histogram as a lower median and peak location, and a increased peak height due to the increased frequency of lower FA values. In turn, this causes a greater rightward tail of the distribution (more positive skew) and more pronounced peak (greater kurtosis) (Zeestraten et al., 2016). Median has been used widely in the literature as the most useful FA histogram parameter, with a decrease in

FA median corresponding to damage to the WM ultrastructure and a more severe disease phenotype (Brookes et al., 2014, Croall et al., 2017).

In the sporadic SVD group, our results suggest that a higher volume of high permeability voxels in the NAWM are associated with a reduction in NAWM FA, indicating a reduction in the directionality of diffusion tensor and therefore suggesting a disruption of the WM fibres. The fact that the association is only present after FW correction, would suggest that the association is specific to changes in the WM fibres themselves.

An association between BBB permeability and FA in the NAWM in SVD has not previously been reported in the literature. However, an association between NAWM FA and WML growth has been shown, where NAWM regions with lower FA were shown to be more likely to progress to WML (de Groot et al., 2013). Therefore, this association could suggest that an increased volume of BBB permeability in the NAWM could be involved in disruption of the WM fibres in the NAWM, which may progress to WML in the future. This would need to be explored by following up the patients over time to see if brain regions with high BBB permeability and/or low FA at baseline progress to WMLs at follow-up.

4.4.8 Associations with FA in the CADASIL group
Higher global permeability in the NAWM was associated with a higher FA median in the NAWM in the CADASIL group (Table 4.9). After FW correction, the same pattern was seen with a stronger association (Table 4.15). The association seen between BBB permeability and FA in the CADASIL group is opposite to that seen in the sporadic SVD group. The association suggests that CADASIL patients with higher overall NAWM permeability had a higher FA and therefore more intact WM axonal fibres in the NAWM.

As this is the first time this technique has been applied to CADASIL patients, there is no existing literature to compare our results to. Looking at the CADASIL subgroup analysis of Appendix B, global mean permeability of the NAWM was significantly

higher in CADASIL patients with no history of stroke (Table B.4). Further, non-stroke CADASIL patients also had a higher FA NAWM median (Table B.3). Therefore, stroke history could be mediating the effect that we are seeing, where BBB permeability is higher in CADASIL before the first stroke occurs, which happens to coincide with a lower severity disease phenotype shown by the higher FA NAWM median. Interestingly, this association was not seen for older vs. younger patients, or for patients with a history of migraine compared to those without (Table B.2 and B.6).

Further studies are needed with higher sample sizes to investigate the role of BBB permeability in CADASIL. If BBB permeability is important in the pre-stroke stages of the CADASIL disease process, then it could be a process to target with therapeutics, to slow down the disease progression before the severe symptoms occur.

4.4.9 Associations with MD in the Control group
A lower MD peak height in the WML was associated with a higher global and hotspot mean of BBB permeability of the WML in the control group (Table 4.12). Hotspot BBB mean was still associated after FW adjustment (Table 4.18).

MD peak height has previously been shown to be the most sensitive MD histogram parameter for detecting SVD severity and progression (Zeestraten et al., 2016) and therefore has been the most widely used in studies (Lawrence et al., 2013, Croall et al., 2017). MD histogram distributions represent ultrastructural WM damage that manifests as increases in diffusivity; this means that pathological tissue results in a higher median and peak location but a lower peak height, as higher diffusivity values are identified with greater frequency (Zeestraten et al., 2016). Increases in diffusivity values causes the rightward tail of the distribution to become broader, increasing the positive skew. Therefore a negative association between MD peak height and BBB permeability suggests that there is higher WML BBB permeability in the control participants with increased ultrastructural damage in the WML. The same association was present when using the FW corrected MD peak height values (Table 4.18). This is important as the FW correction reduces the effect of oedema caused by BBB permeability and vacuolization within myelin sheaths. This allows MD to represent

microstructural tissue damage, such as axonal degeneration and loss of WM fibre organisation, more specifically. This association was not seen for the sporadic SVD or CADASIL groups.

Once again, if we take our control group as an early stage pre-clinical asymptomatic SVD group with mild WMLs, then this would provide further evidence that BBB permeability of the WML may have a role early on, contributing to the microstructural tissue damage. MD has been investigated in studies of BBB permeability but the parameters have not been directly compared to one another (Munoz Maniega et al., 2017). Therefore, we cannot compare our results to the literature. Further studies are needed to investigate the role of BBB permeability in early stage SVD, and whether it is a pathological process that is occurring in the WML to disrupt the WM fibres and lead to WML growth.

4.4.10 Associations with Cognition

None of the BBB permeability parameters were significantly associated with any of cognitive parameters across any of the groups (Tables 4.19-23).

Cognition has only been investigated in relation to BBB permeability in a small number of studies. An early study by Hanyu et al. used the MMSE and found that there was a significant correlation between worsened MMSE score and increased BBB permeability (Hanyu et al., 2002). A later study by Zhang et al. used more intensive cognitive testing and found that a higher leakage rate in the NAWM was associated with lower EF and PS scores in healthy controls, but not in SVD patients (Zhang et al., 2019). Wardlaw et al. looked at functional outcome using the Oxford Handicap Score, 3 years after quantifying BBB permeability, and found that higher basal ganglia BBB permeability at baseline was associated with poorer functional outcome (Wardlaw et al., 2013b).

More studies with higher participant numbers and more comprehensive testing are required to see if cognition is associated with BBB permeability in sporadic SVD and control patients. Further, testing cognitive change across time is likely a more

interesting end-point to explore, as if BBB permeability is pathological then it would be expected to associated with decreasing cognition over time, even if there is no association seen cross-sectionally.

4.4.11 Limitations

DCE-MRI techniques are the most established and widely agreed method for imaging BBB permeability in human subjects. However, the technique is not without limitations.

The largest limitation in terms of data interpretation lies in the variety of ways that the data can be analysed. Differing methods here have led to discrepancies in results and have limited the progression of the field. A recent paper has suggested recommendations about how to use and analyse DCE-MRI for BBB permeability in SVD to try to reduce these discrepancies (Thrippleton et al., 2019).

The nature of DCE-MRI means the method is reliant on an intravenous injection of gadolinium. This limits the subjects that can take part in the study, as some cannot have gadolinium due to kidney failure. It also means that every participant must endure the invasive implanting of the venous line for the injection, which can be a deterrent and lead to problems with recruitment. Further, the scan time for DCE-MRI is long and many participants struggle to tolerate this, further limiting those who are willing to take part.

An emerging option for imaging BBB permeability, which could reduce some of these limitations, is arterial spin labelling based methods. Multicompartmental modelling of the arterial spin labeling signal provides a potential route to measuring BBB permeability to water, with a new method for estimating global water BBB permeability recently proposed (Lin et al., 2018). Currently, sensitivity limitations mean the technique does not have the capability of DCE-MRI but hopefully in coming years, increasing technological advances will improve the methodology and application to BBB permeability in SVD.

4.5 Summary of Findings

Returning to the aims of this chapter, the following areas have been addressed:

1. Global BBB permeability was significantly higher in sporadic SVD compared to control, in the whole WM, NAWM and WML

2. The volume of the BBB permeability hotspots was significantly higher in sporadic SVD compared to control, in the whole WM, NAWM and WML

3. BBB permeability in the CADASIL group was not significantly different from controls for any of the parameters or regions

4. BBB permeability was higher in the NAWM compared to the WML

5. The permeability in the penumbra of the WML had similar permeability to the NAWM, but was significantly higher than the WML permeability

6. BBB permeability in the WMLs of the control group was associated with increased WML volume and decreased MD peak height in the WML, suggesting higher permeability is associated with microstructural tissue damage

7. BBB permeability in the NAWM of the SVD group was associated with decreased FA median of the tissue, suggesting a higher permeability is associated with disruption of WM fibre organisation

8. BBB permeability in the NAWM of the CADASIL group was associated with increased FA median of the tissue, suggesting a higher permeability is associated with increased WM fibre integrity

9. BBB permeability was not associated with any of the cognitive parameters in any of the groups

This chapter has investigated BBB permeability between the groups and in comparison to the other end-points collected in the study. The next chapter will investigate PK binding, as a representation of microglia activation, and the relationship with the imaging and cognitive end-points.

Chapter 5: PK binding – Group Differences and Associations with Imaging and Cognition

5.1 Introduction

5.1.1 Aims of the Chapter

The previous chapter explored differences in BBB permeability measures between the patient and control groups. Chapter Four also looked at the relationship of BBB permeability with conventional MRI markers and cognition. This chapter looks at PK binding as a measure of microglia activation to answer similar questions:

- Is there a difference in PK binding between sporadic SVD and control groups? Does this difference occur globally or focally?
- Is there a difference in PK binding between CADASIL and control groups? Does this difference occur globally or focally?
- Is there a difference in PK binding in the NAWM and WML? Is this pattern the same across all groups?
- Is there a spatial pattern of increased PK binding in close proximity to WMLs?
- Is PK binding associated with conventional MRI markers, DTI markers and cognition?

The main hypothesis of this chapter is:

- PK binding will be significantly higher in the sporadic SVD and CADASIL patients compared to our healthy controls.

Exploratory outcomes beyond the main hypotheses are:

- Investigate if PK binding is different in the NAWM compared to WML
- Investigate if PK binding is increased in close proximity to WMLs
- Investigate if there is a relationship between PK binding and conventional MRI markers, DTI markers and cognition

5.1.2 Neuroinflammation in SVD

Inflammation is vital for survival, defending the body from invaders by eliminating the injurious agent and removing the damaged tissue components so that the body can begin to heal. However, many chronic diseases have shown a detrimental role for inflammation, where the immune system recognises a normal component of the body as foreign and attacks it. Further, chronic inflammation can lead to the generation of oxidative stress and production of free radical molecules that are damaging. A pathogenic role for inflammation has been suggested in SVD (Low et al., 2019, Fu and Yan, 2018).

Many of the studies investigating inflammation in SVD to date, have focused on inflammatory biomarkers from the blood (Low et al., 2019). As discussed in Chapter One, SVD etiology primarily occurs in the brain, and therefore microglia and astrocytes are the cells responsible for the immune response. Typically, microglia are activated first, initiating morphological changes and expression and release of pro-inflammatory mediators and other signaling molecules (Russo and McGavern, 2015). Therefore, measures of blood biomarkers are far from optimal for exploring the role of neuroinflammation in SVD.

There has been some post-mortem work that has investigated the presence of microglia in SVD. However, the results have been conflicting. Early studies suggested that higher levels of microglia were present in the WML of SVD patients (Tomimoto et al., 1996, Young et al., 2008). Later studies then showed that there is also increased microglia in the NAWM (Simpson et al., 2007b, Forsberg et al., 2018). In CADASIL, only one post-mortem study has investigated microglia and found there was no change compared to control (Brennan-Krohn et al., 2010). Post-mortem studies tend to be of a severe late-stage disease phenotype, and may not represent the pathology occurring earlier on. Microglia activation is likely to be a dynamic process, which may have varying roles throughout the SVD pathology, which may mean that post-mortem studies are not as relevant to early and mid-stage disease.

Techniques to image neuroinflammation have surged over the past 15 years, as accurate imaging of neuroinflammation can be used for diagnosis and monitoring, as

154

well as guide the development of novel treatments for a range of diseases (Albrecht et al., 2016). PET is by far the most commonly used technique for imaging neuroinflammation, with a growing range of tracers continually being developed to allow for new and improved targeting.

PET inflammation studies have the potential to answer many questions on the pathogenesis of SVD. PET can be used to investigate neuroinflammation both cross-sectionally, in comparison to a control group, and longitudinally, to investigate the effect of baseline neuroinflammation on disease progression. PET methods can be used to understand global changes in neuroinflammation, but also more focal changes by investigating where the inflammatory regions are on a voxel-by-voxel basis. They can be used to investigate whether neuroinflammation is more prevalent in WML or NAWM and whether the penumbra of the WMLs is important, in the same way that DCE-MRI explored BBB permeability in Chapter Four.

5.1.3 TSPO PET imaging

PET methods that target neuroinflammation primarily focus on TSPO, a five transmembrane domain protein situated in the outer mitochondrial membrane. In the healthy CNS, TSPO is constitutively expressed by multiple cell types, including glia and neurons, at low levels (Cosenza-Nashat et al., 2009). However, during neuroinflammation, TSPO is upregulated predominantly, if not exclusively, in glia cells (Chen and Guilarte, 2008). The specific cell expressing TSPO is a point of controversy for TSPO imaging, as technically it could be both microglia and astrocytes. It is impossible to know the relative contribution of microglia and astrocytes to TSPO and it is probably dependent on many factors, including the disease being investigated and the time-course of inflammation in that disease. This is something to consider when comparing TSPO expression across studies, as it may not be measuring the same composition of cells. Despite this, many studies reference the increased PK binding to TSPO as increased microglia activation (Janssen et al., 2018).

PK is the most widely used TSPO imaging agent. However, PK has low brain penetrance and high nonspecific binding, which limits signal to background ratio (SBR) and the ability of the tracer to detect subtle PET signals related to glial activation (Venneti et al., 2006). Second generation TSPO ligands have been generated, including [C^{11}]PBR28, [F^{18}]DPA-714, [F^{18}]FEPPA, [C^{11}]DAA1106, [F^{18}]PBR06, and [F^{18}]PBR111. These ligands possess much higher signal-to-background ratio (SBR) than PK and have been used to image glial activation in a number of pathologies including psychiatric disorders (van der Doef et al., 2015), amyotrophic lateral sclerosis (Zurcher et al., 2015) and chronic pain (Loggia et al., 2015).

Unfortunately, all second-generation TSPO ligands are confounded by the existence of two binding sites: one with high affinity and one with low affinity (Owen et al., 2010). Individual subjects have differential expression of the binding sites, making it difficult to compare TSPO binding of second-generation ligands between individuals. For example, among people of European ancestry, ~50% express only high affinity sites, ~10% express only low affinity sites and ~40% express equal numbers of high and low affinity sites (Kreisl et al., 2013). This makes impossible to know if a group difference is due to pathological differences or simply a difference in binding sites. However, recent advances in genetics have identified a single nucleotide polymorphism in the TSPO gene (*Ala147Thr*) (Owen et al., 2012), which fully predicts the binding site, so now this can be added into the recruitment strategy to match subjects by genotype for this imaging (Mizrahi et al., 2012). However, this would require genotyping of subjects prior to recruitment, which is expensive and time consuming, and adds an extra layer of complexity into often already complex studies. Therefore, PK is currently still the best option for TSPO imaging.

5.1.4 PET Analysis

PET analysis requires an estimation of specific binding of the ligand to the molecule of interest. The gold standard for PET is kinetic modelling with arterial sampling, with a plasma AIF and correction for plasma free fraction (Gunn et al., 2001). This is an invasive procedure that is uncomfortable for the patients. Additionally, this method

has substantial variability with TSPO. This is thought to be due to high PK binding to the plasma protein α1-acid glycoprotein, which is up regulated in inflammatory states (Lockhart et al., 2003). This is expected to be the same for the second-generation ligands but has not been directly investigated. Therefore, outcome estimation of specific binding is difficult using arterial sampling with TSPO ligands and other methods have been developed.

Alternative methods include SRTM and the use of semi-quantitative measures (Scott et al., 2017). These methods have been validated and shown to provide accurate values (Logan et al., 1996, Lammertsma and Hume, 1996). SRTM involves taking a brain region as the reference region, from which the other region values are derived. Technically, the reference tissue should be a region where there is no specific binding of the ligand. However, for many ligands, including PK, a true reference tissue does not exist in the brain. Therefore, a 'pseudo-reference region' can be used, which contains low levels of TSPO and is thought to have consistent TSPO binding across participants. Lyoo et al. used the cerebellum as an anatomically defined pseudo-reference region; comparing the use of this reference region to arterial sampling methods, they found the cerebellum pseudo-reference region to provide more accurate results (Lyoo et al., 2015). Data-driven techniques have now been adopted that can identify voxels across the brain with TACs mirroring those of controls, as an automatic way of extracting a reference tissue input function (Turkheimer et al., 2007). The technique uses supervised cluster analysis the TAC of each voxel as a sum of the kinetics of 4 predefined tissues (normal GM and WM and the 2 sources of specific binding, activated microglia and vasculature) obtained from control subjects. The reference kinetic can then be obtained by averaging the whole brain, whilst each pixel TAC is weighted by its normal index of the reference region of the GM or WM.

The SRTM technique means that an arterial line does not need to be placed in the patient, minimising patient discomfort. Further, this method helps to correct for the within-subject signal differences caused by the TSPO genotype of the individual patient (Coughlin et al., 2014). However, it is important that the methods are fully validated in the individual study population and that the reference region is carefully chosen, so that accurate results can be obtained.

5.1.5 Global vs. Focal Inflammation

As discussed in Chapter Four, SVD is a heterogeneous disease with many points of focal damage in the brain due to individual WMLs and lacunar infarcts. However, this then leads to many downstream global changes to networks and structure (Ter Telgte et al., 2018). Inflammation after acute stroke has been well-documented as a primarily focal event leading to secondary global changes (Shi et al., 2019). Primary focal inflammation occurs immediately after stroke onset in the region of the lesion and is often irreversible. Cells affected by the injury trigger a cascade of secondary events including BBB damage, excitotoxicity, oxidative stress, microvascular failure and mitochondrial disturbance, all of which promote secondary brain injury (Fu et al., 2015). The contribution of global vs. focal inflammation to SVD is debated in the literature, but it is important to differentiate between the processes as they are probably representative of very different inflammatory cascades (Kawabori and Yenari, 2015).

Global inflammatory measures can be calculated from PET imaging, by taking the mean binding for an ROI, such as NAWM and WML. Focal inflammation is slightly more difficult, as PET imaging techniques are notorious for having low spatial resolution and therefore making it difficult to assess changes in small ROIs. However, with this technique we can identify hotspots, which are voxels above the 'normal' threshold, determined from a control group of patients. The location of these hotspots may be important, but also the volume of them will give a representative estimation of the focal inflammation occurring in our population.

5.2 Methods

There were 17 controls, 16 sporadic SVD and 14 CADASIL who received PK PET imaging and so were included in this chapter. Methodology was described in Chapter Two.

5.2.1 Defining PK binding Values

Global mean PK binding was defined as the mean PK binding of all voxels in the ROI. Hotspot mean PK binding was defined as the mean PK binding of all voxels above the 'normal' threshold, calculated from our control subjects in the same way as for the permeability data, and defined as voxel that was above 0.135 (ratio of the reference region, no units). The hotspot PK binding volume was expressed as a percentage (%) of the voxels that showed PK binding values above the threshold within the given ROI.

Penumbra values were defined as a 3mm rim around the WMLs. Global means, hotspot means and hotspot volumes were calculated in the same way as described above.

5.2.2 Statistical Analysis

All group differences were analysed using an ANCOVA test, comparing between sporadic SVD and control groups, and between CADASIL and control groups. All analyses were controlled for age and sex. Pairs of comparisons were adjusted using Bonferroni. If there was a significant difference seen, additional controlling for cardiovascular risk factors of hypertension, hyperlipidaemia, type 2 diabetes and smoking was performed to determine if results remained significant. Some of the PK binding parameters were not normally distributed so they were transformed to meet normality assumptions. The global PK binding measures of WM, NAWM and WML were log transformed (base:10 constant:10^{-1}). The mean hotspot PK binding measures of WM and NAWM met normality assumptions, however WML did not so was transformed by squaring. The hotspot volume of WM and NAWM did not meet

normality so they were log transformed (base:10). Hotspot volume of WML also did not meet normality so was log transformed (base:10 constant:10^{-1}).

Comparisons between the PK binding values of the NAWM and WML were performed using Wilcoxon signed rank tests for paired non-parametric data. These tests were performed on the raw untransformed values. P values were corrected for multiple comparisons using FDR.

PK binding values in the penumbra were also analysed using ANCOVAs, comparing between sporadic SVD and control groups, and CADASIL and control groups. Pairs of comparisons were adjusted using Bonferroni. If there was a significant difference seen, then a further ANCOVA controlling for the cardiovascular risk factors was performed, to see if the significance was still present. Global mean PK binding values for the penumbra met normality assumptions. Hotspot mean PK binding values for the penumbra did not meet normality assumptions so were log transformed (base:10). Hotspot PK binding volumes for the penumbra also did not meet normality assumptions so were log transformed (base:10).

Comparisons between PK binding values for the various brain regions and the corresponding penumbra value were carried out using the Wilcoxon signed rank tests for paired non-parametric data. These tests were performed on the raw untransformed values. P values were corrected for multiple comparisons using FDR.

Multivariate linear models were then used to investigate the association between PK binding parameters (independent) and imaging markers (dependent), controlled for age and sex. If the imaging parameter was a volumetric measure, then ICV was also used as a control. For significant associations, a further linear model with the cardiovascular risk factors was also used to see if the significance was still present. If required, PK binding parameters were transformed in the same way as detailed earlier, to meet normality assumptions. Imaging markers were also transformed if required, using the same transforms as described in Chapter Three. P values were adjusted for multiple comparisons with FDR.

Multivariate linear models were also used to investigate if PK binding parameters (independent) were significantly associated with cognitive indices (dependent). These analyses were controlled for age, sex and premorbid IQ. For any of the PK binding parameters that do not fit normality assumptions, the same transforms as detailed earlier were used. P values were adjusted for multiple comparisons with FDR.

5.3 Results

5.3.1 Group Differences

PK binding values in the WM, NAWM and WML were calculated for each individual patient and comparisons were made between the sporadic SVD and control groups, and between the CADASIL and control groups. Representative images from each of the groups showing hotspots of significant PK binding are shown in Figure 5.1.

Global PK binding for each group is shown in Figure 5.2. There was no significant difference in the global PK binding between the sporadic SVD and control group or the CADASIL control group in the WM, NAWM or the WML.

The mean values of the PK binding hotspots are shown for the different groups in Figure 5.3. In the WM, there was a significantly higher mean in the PK binding hotspots in the sporadic SVD group compared to control when controlled for age and sex ($p < 0.001$ ($p < 0.001$ when adjusted for multiple comparisons)) and cardiovascular risk factors ($p < 0.001$). The mean PK binding hotspot values in the WM were also significantly higher in CADASIL compared to control when controlled for age and sex ($p = 0.007$ ($p = 0.015$ when adjusted for multiple comparisons)) and cardiovascular risk factors ($p = 0.006$). In the NAWM, the mean binding hotspot value was significantly higher in sporadic SVD compared to control when controlling for age and sex ($p < 0.001$ ($p < 0.001$ when adjusted for multiple comparisons)) and cardiovascular risk factors ($p < 0.001$). However, the mean binding hotspot value in the NAWM was not significantly different in CADASIL compared to control. In the WML, the mean binding hotspot value was significantly higher in the sporadic SVD group compared to control when controlling for age and sex ($p < 0.001$ ($p < 0.001$ when adjusted for multiple comparisons)) and cardiovascular risk factors ($p < 0.001$). Similarly, the mean binding hotspot value in the WML was significantly higher in CADASIL compared to control, when controlling for both age and sex ($p < 0.001$ ($p < 0.001$ when adjusted for multiple comparisons)) and cardiovascular risk factors ($p < 0.001$).

162

The volumes of the PK binding hotspots were compared between groups in Figure 5.4. In the WM, the volume of the hotspots was not significantly different between sporadic SVD and control or between CADASIL and control. However, in the NAWM the volume of the PK binding hotspots was significantly higher in the sporadic SVD compared to control when controlled for age and sex ($p=0.001$ ($p=0.003$ when adjusted for multiple comparisons)) and cardiovascular risk factors ($p=0.001$). There was no significant difference in the volume of the NAWM hotspots in the CADASIL group compared to control. In the WML, the volume of the hotspots in the sporadic SVD group was significantly higher than control when controlled for age and sex ($p=0.002$ ($p=0.003$ when adjusted for multiple comparisons)) and cardiovascular risk factors ($p=0.002$). This was mirrored in the CADASIL group, where the volume of the hotspots in the WML was significantly higher than control when controlled for age and sex ($p<0.001$ ($p<0.001$ when adjusted for multiple comparisons)) and cardiovascular risk factors ($p<0.001$).
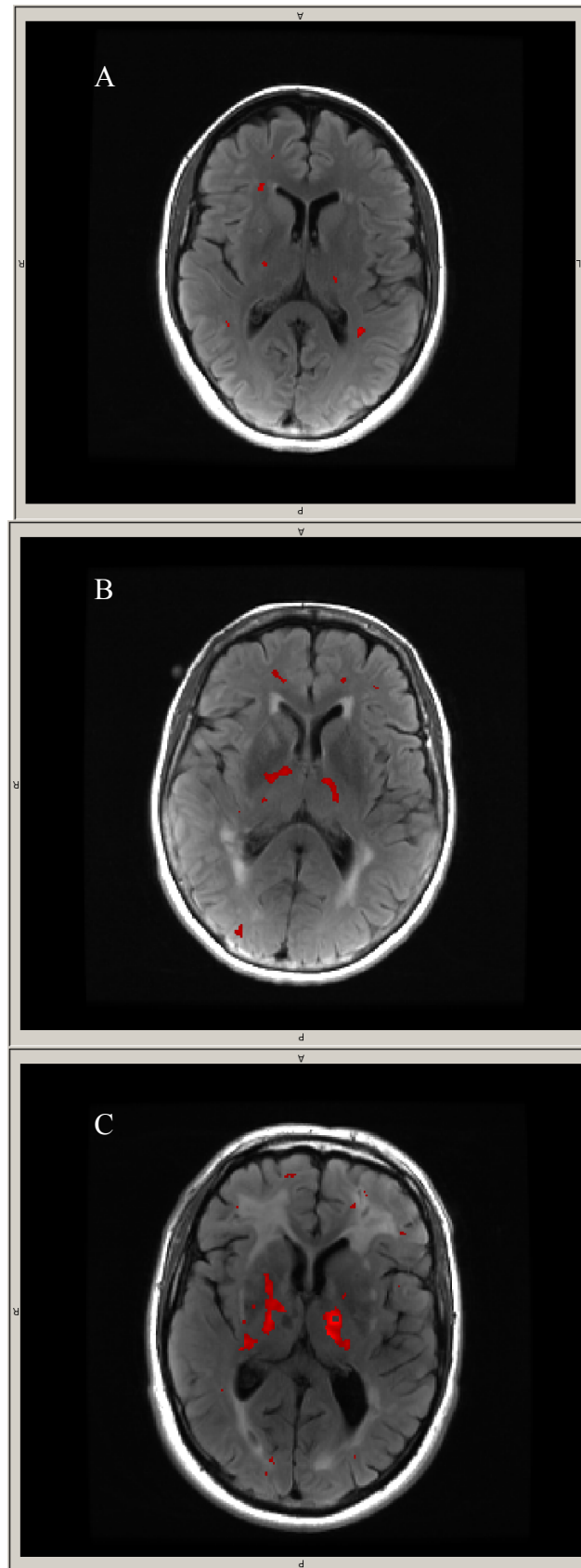
Figure 5.1: Example images of PK binding hotspots (red) overlayed onto T2 FLAIR scans. A) Control. B) Sporadic SVD. C) CADASIL.
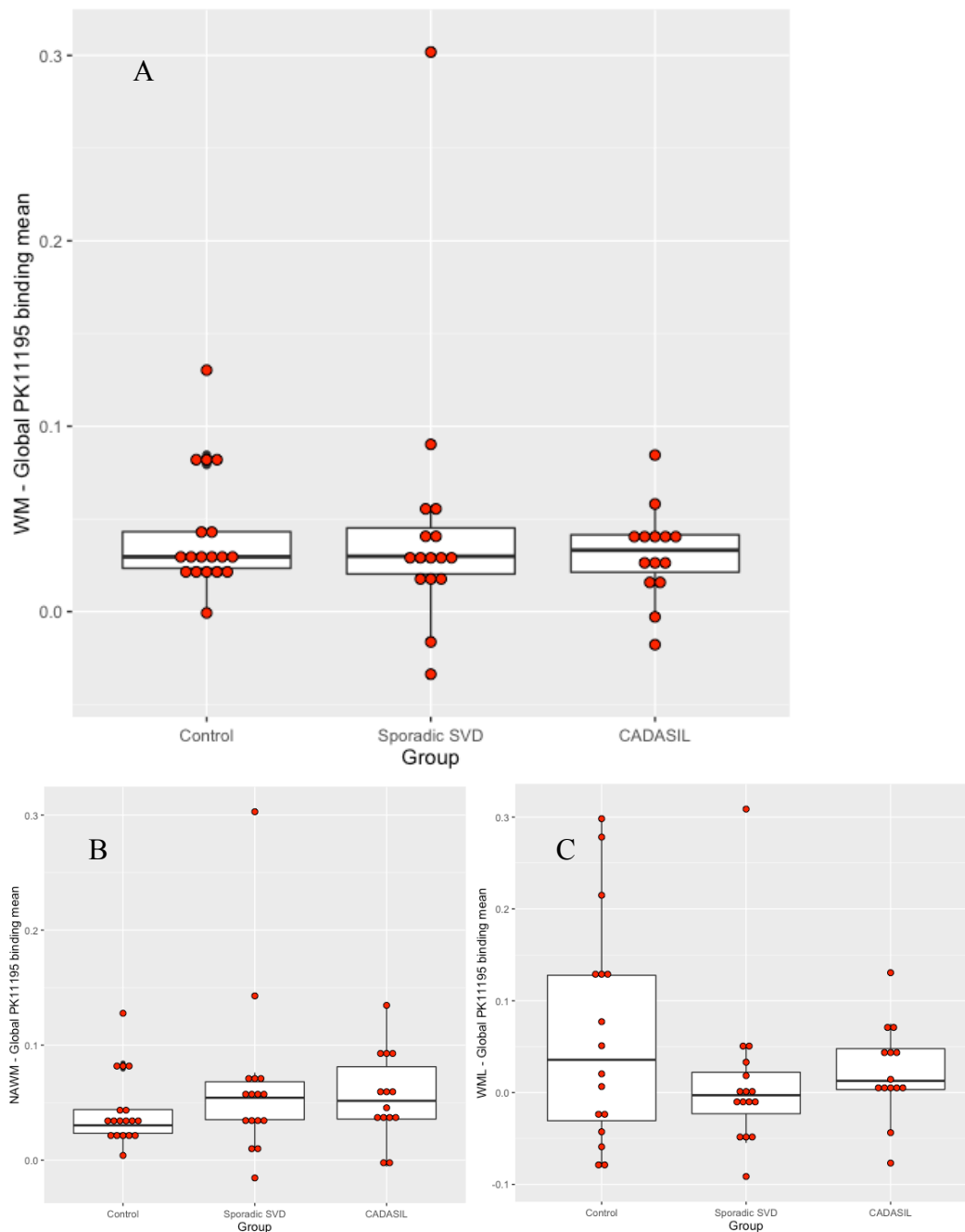
Figure 5.2: Mean global PK binding in the WM, NAWM and WML controlled for age and sex.

A) Global mean PK binding in the WM was not significantly different between sporadic SVD and control (p=1.000) or CADASIL and control (p=0.566).

B) Global mean PK binding in the NAWM was not significantly different between sporadic SVD and control (p=0.571) or CADASIL and control (p=0.615).

C) Global mean PK binding in the WML was not significantly different between sporadic SVD and control (p=0.753) or CADASIL and control (p=1.000).
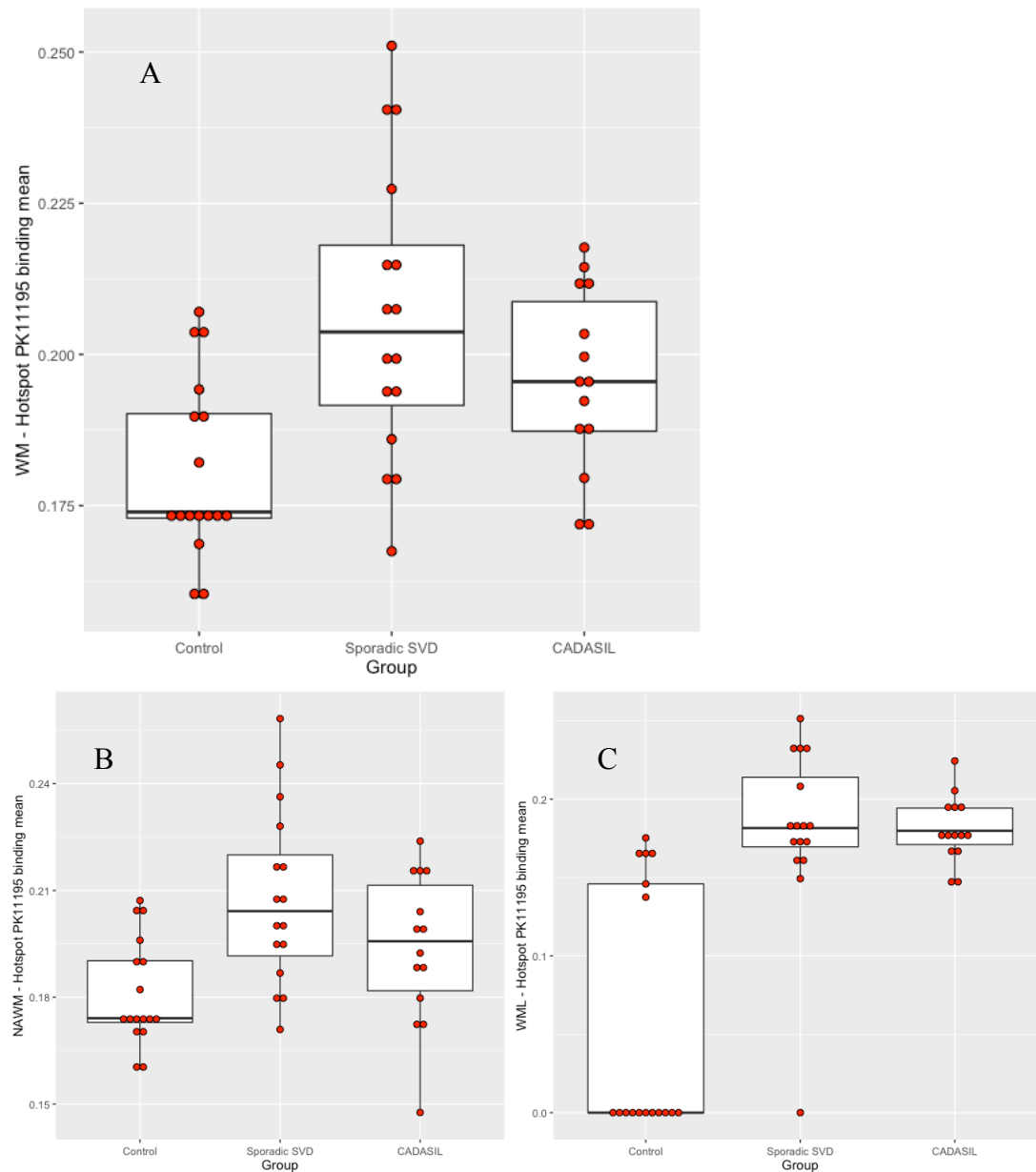
Figure 5.3: Hotspot mean PK binding in the WM, NAWM and WML, controlled for age and sex.

A) Hotspot mean PK binding in the WM was significantly higher in the sporadic SVD group compared to control (p<0.001) and in the CADASIL group compared to control (p=0.015).

B) Hotspot mean PK binding in the NAWM was significantly higher in the sporadic SVD group compared to control (p<0.001). However, it was not significantly different in the CADASIL group compared to control (p=0.117).

C) Hotspot volume of PK binding in the WML was significantly higher in the sporadic SVD group compared to control (p<0.001) and in the CADASIL group compared to control (p<0.001).
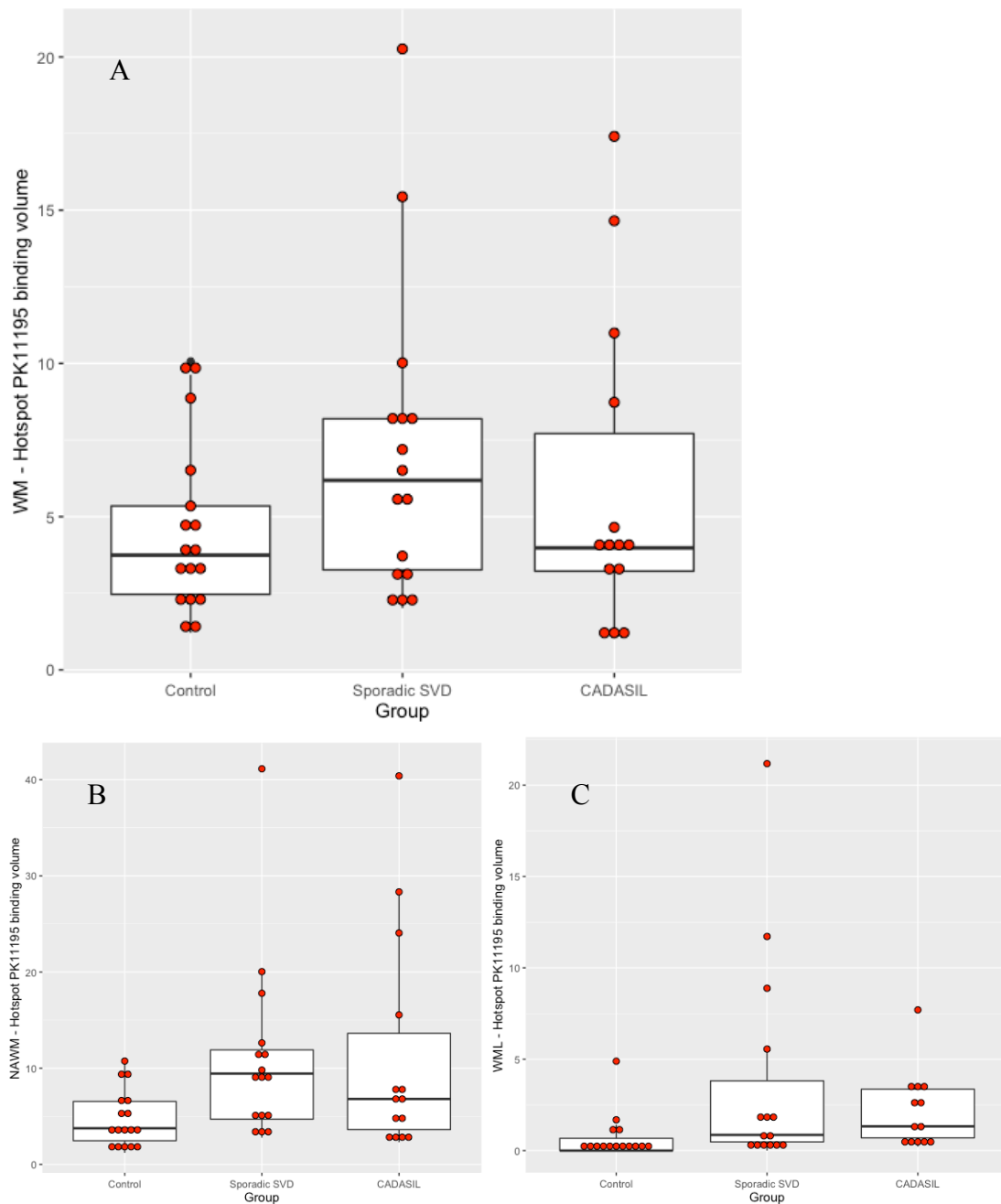
Figure 5.4: Hotspot volume of PK binding (%) in the WM, NAWM and WML.

A) Hotspot volume of PK binding in the WM was not significantly different between sporadic SVD and control (p=0.123) or CADASIL and control (p=1.000).

B) Hotspot volume of PK binding in the NAWM was significantly higher in sporadic SVD compared to control (p=0.003). However, it was not significantly different in CADASIL compared to control (p=0.073).

C) Hotspot volume of PK binding in the WML was significantly higher in the sporadic SVD group compared to control (p=0.003) and in the CADASIL group compared to control (p<0.001).

5.3.2 NAWM vs. WML

Pairwise comparisons between the NAWM PK binding values and corresponding WML values are shown in Table 5.1.

In the control group, there was no significant difference in the global PK binding mean between the NAWM and WML. However, there was a significantly higher mean of the PK binding hotspots in NAWM compared to WML ($p<0.001$) and significantly higher volume of the PK binding hotspots in NAWM compared to WML ($p<0.001$).

In the sporadic SVD, there was significantly higher PK binding in the NAWM compared to WML when investigating global binding mean ($p=0.003$), hotspot binding mean ($p=0.007$) and hotspot binding volume ($p=0.003$).

In the CADASIL group, there was no significant difference in the global PK binding mean between the NAWM and WML. However, there was a significantly higher mean of the PK binding hotspots in the NAWM compared to WML ($p=0.021$) and significantly higher volume of the PK binding hotspots in NAWM compared to WML ($p=0.007$).

Group	Imaging parameter	NAWM		WML		P value
		Median	IQR	Median	IQR	
Control	Global PK binding mean	0.030	0.021	0.036	0.158	0.900
Control	Hotspot PK binding mean	0.174	0.017	0.000	0.146	**<0.001**
Control	Hotspot PK binding volume (%)	3.761	4.085	0.000	0.671	**<0.001**
Sporadic SVD	Global PK binding mean	0.054	0.033	-0.003	0.045	**0.003**
Sporadic SVD	Hotspot PK binding mean	0.204	0.028	0.182	0.044	**0.007**
Sporadic SVD	Hotspot PK binding volume (%)	9.442	7.199	0.858	3.341	**0.003**
CADASIL	Global PK binding mean	0.052	0.045	0.013	0.044	0.134
CADASIL	Hotspot PK binding mean	0.196	0.030	0.180	0.023	**0.021**
CADASIL	Hotspot PK binding volume (%)	6.805	10.004	1.327	2.665	**0.007**

Table 5.1: Comparisons of PK binding in the NAWM and WML. Significant p values are shown in bold.

5.3.3 WML Penumbra

PK binding values from the penumbras were calculated and compared between the sporadic SVD and control groups, and between the CADASIL and control groups. Global mean binding values were compared, as well as the mean and volume of the PK binding hotspots.

Global mean PK binding in the penumbra was compared between the groups in Figure 5.5. The global mean PK binding in the penumbra was not significantly different between sporadic SVD and control groups or the CADASIL and control groups.

Mean values of the PK binding hotspots in the penumbra were then compared between groups in Figure 5.6. There was no significant difference in the mean binding values of the hotspots in the penumbra of the sporadic SVD group compared to control. However, the mean values of the PK binding hotspots were significantly higher in the CADASIL penumbra compared to control when controlling for age and sex ($p=0.003$ ($p=0.007$ when adjusted for multiple comparisons)) and cardiovascular risk factors ($p=0.005$).

The volumes of the PK binding hotspots were compared in the penumbras in Figure 5.7. There was no significant difference in the volume of the PK binding hotspots in the penumbra between the sporadic SVD and control groups or the CADASIL and control groups.
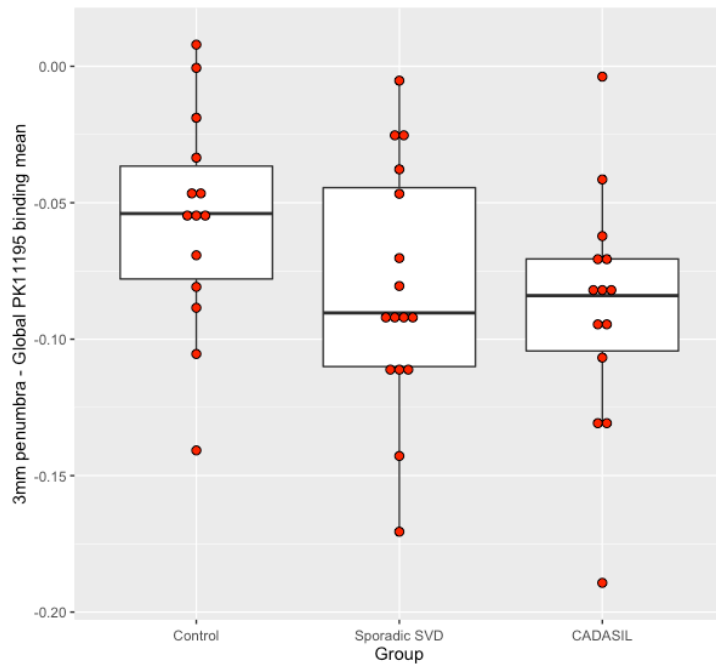
Figure 5.5: Global mean PK binding of the penumbra regions were compared between groups when controlled for age and sex. Global mean binding values were no different in sporadic SVD and control groups (p=0.248). There was also no difference between CADASIL and control (p=0.100).
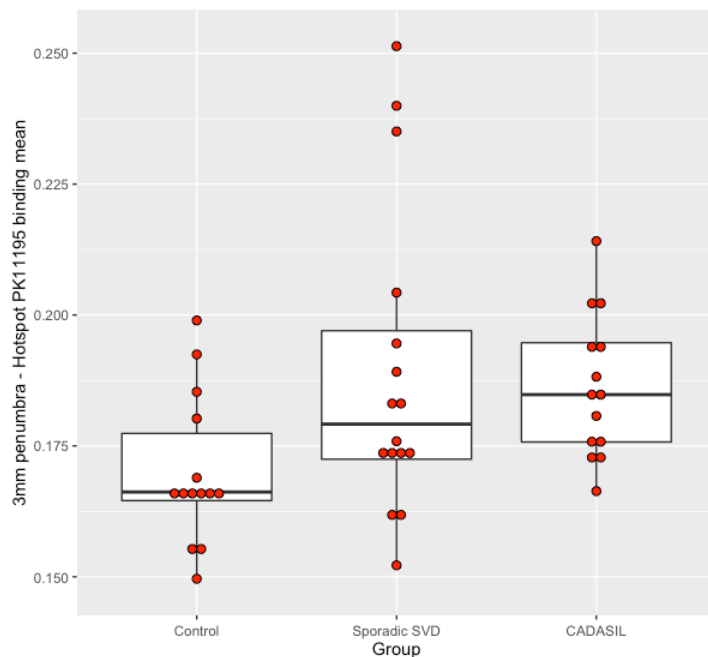
Figure 5.6: Mean values of the PK binding hotspots in the penumbras were compared between the groups, controlling for age and sex. Hotspot mean binding values were not significantly higher in sporadic SVD compared to control (p=0.060). However, they were significantly higher in CADASIL compared to control (p=0.007).
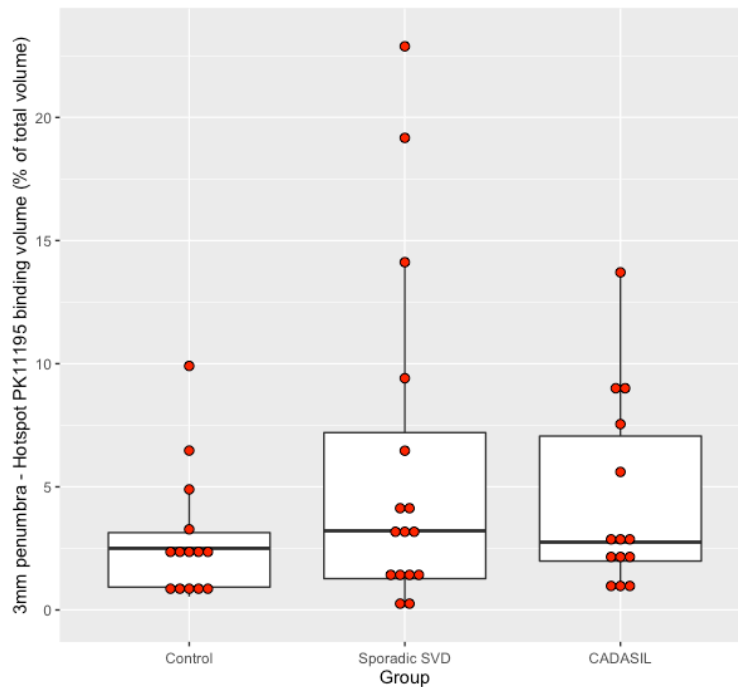
Figure 5.7: Volumes of the PK binding hotspots in the penumbras (%) were compared between the groups. Hotspot volumes were not significantly different between sporadic SVD and control (p=0.762). There was also no difference between CADASIL and control (p=0.352).

Penumbra values were compared with corresponding NAWM and WML values in Table 5.2. In the control group, penumbra values were significantly lower than global mean PK binding values in the NAWM (p<0.001) and WML (p<0.001). Mean values of the PK binding hotspots were significantly lower in the penumbra in comparison to the NAWM (p<0.001), but significantly higher than the WML (p=0.001). The same pattern was present for the volume of the PK binding hotspots, with penumbra values significantly lower than NAWM (p=0.001), but higher than WML (p<0.001).

In the sporadic SVD group, the global mean binding of the penumbra was significantly lower than NAWM (p<0.001) and WML (p<0.001). The mean values of the PK binding hotspots within the penumbra were significantly lower than in the NAWM (p=0.004), but no different from the WML. The volume of the PK binding

hotspots in the penumbra was significantly lower than the NAWM (p=0.011), but significantly higher than the WML (p=0.042).

In the CADASIL group, penumbra values were significantly lower than both NAWM (p<0.001) and WML (p<0.001) values for global mean PK binding. They were similar to NAWM and WML for mean values of the PK binding hotspots. The volume of the PK binding hotspots in the penumbra was significantly lower than the NAWM (p=0.001), but significantly higher than the WML (p=0.018).

Group	PK binding measurement	Mean PK binding		Mean Penumbra		P value
		Median	IQR	Median	IQR	
Control	NAWM mean	0.030	0.021	-0.054	0.041	**<0.001**
	WML mean	0.036	0.158	-0.054	0.041	**<0.001**
	NAWM hotspot mean	0.174	0.017	0.166	0.013	**<0.001**
	WML hotspot mean	0.000	0.146	0.166	0.013	**0.001**
	NAWM volume (%)	3.761	4.085	2.501	2.213	**0.001**
	WML volume (%)	0.000	0.671	2.501	2.213	**<0.001**
Sporadic SVD	NAWM mean	0.054	0.033	-0.090	0.066	**<0.001**
	WML mean	-0.003	0.045	-0.090	0.066	**<0.001**
	NAWM hotspot mean	0.204	0.028	0.179	0.025	**0.004**
	WML hotspot mean	0.182	0.044	0.179	0.025	0.348
	NAWM volume (%)	9.442	7.199	3.212	5.930	**0.011**
	WML volume (%)	0.858	3.341	3.212	5.930	**0.042**
CADASIL	NAWM mean	0.052	0.045	-0.084	0.034	**<0.001**
	WML mean	0.013	0.044	-0.084	0.034	**<0.001**
	NAWM hotspot mean	0.196	0.030	0.185	0.019	0.117
	WML hotspot mean	0.180	0.023	0.185	0.019	0.205
	NAWM volume (%)	6.805	10.004	2.754	5.076	**0.001**
	WML volume (%)	1.327	2.665	2.754	5.076	**0.028**

Table 5.2: Pairwise comparisons for the individual groups for the global mean PK binding values, hotspot mean PK binding values and hotspot PK binding volume with equivalent penumbra values. Significant p values are shown in bold.

5.3.4 WMLs

Associations between the PK binding parameters and WML volume are shown in Table 5.3. In the control group, the volume of the PK binding hotspots in the NAWM was significantly associated with the volume of the WMLs when controlled for age and sex (β=0.835, p=0.002 (p=0.035 when adjusted for multiple comparisons)). When the analysis was rerun accounting for all of the cardiovascular risk factors, the significance was still present (β=0.838, p=0.017). All other PK binding parameters were not significant. In the sporadic SVD and CADASIL groups, none of the PK binding parameters were significantly associated with WML volume.

PK value	Brain region	Control		Sporadic SVD		CADASIL	
		β	P value	β	P value	β	P value
Global mean	**NAWM**	0.385	0.478	0.236	0.640	0.281	0.485
	WML	-0.199	0.640	-0.083	0.837	0.215	0.640
Hotspot mean	**NAWM**	0.650	0.074	0.203	0.640	0.155	0.640
	WML	0.580	0.074	-0.157	0.772	-0.064	0.838
Hotspot volume	**NAWM**	**0.835**	**0.035**	0.537	0.215	0.266	0.478
	WML	0.503	0.154	-0.218	0.640	0.090	0.820

Table 5.3: Associations between PK binding and WML volume when adjusted for age, sex and ICV. Table shows standardised β coefficients and p values. Significant p values are shown in bold.

5.3.5 Lacunar Infarcts

Lacunar infarcts were measured as lacune volume and as lacune count. Lacune volume was compared with the measures of PK binding in the different groups (Table 5.4), but none of the parameters were found to be significantly associated with lacune volume. Similarly, lacune count was compared with the various measures of PK binding in the different groups (Table 5.5), but no significant associations were seen.

175

PK value	Brain region	Control		Sporadic SVD		CADASIL	
		β	P value	β	P value	β	P value
Global mean	NAWM	-0.078	0.728	-0.195	0.756	0.271	0.756
	WML	-0.122	0.728	-0.513	0.728	-0.179	0.756
Hotspot mean	NAWM	0.076	0.728	-0.113	0.760	0.345	0.728
	WML	-0.032	0.760	-0.108	0.760	0.274	0.756
Hotspot volume	NAWM	0.074	0.756	-0.109	0.760	0.348	0.728
	WML	-0.056	0.756	-0.435	0.728	0.198	0.756

Table 5.4: Associations between PK binding and lacune volume when adjusted for age, sex and ICV. Table shows standardised β coefficients and p values. Significant p values are shown in bold.

PK value	Brain region	Control		Sporadic SVD		CADASIL	
		β	P value	β	P value	β	P value
Global mean	NAWM	-0.049	0.716	-0.122	0.803	0.262	0.716
	WML	-0.133	0.607	-0.519	0.607	-0.213	0.716
Hotspot mean	NAWM	0.084	0.607	0.009	0.978	0.329	0.607
	WML	-0.036	0.758	0.012	0.978	0.314	0.716
Hotspot volume	NAWM	0.093	0.607	0.044	0.978	0.386	0.607
	WML	-0.050	0.716	-0.396	0.607	0.275	0.716

Table 5.5: Associations between PK binding and lacune count when adjusted for age and sex. Table shows standardised β coefficients and p values. Significant p values are shown in bold.

5.3.6 CMBs

The association between CMB count for the different group with PK binding parameters is shown in Table 5.6. There were no significant associations seen with any of the PK parameters.

PK value	Brain region	Control		Sporadic SVD		CADASIL	
		β	P value	β	P value	β	P value
Global mean	NAWM	-0.027	0.745	-0.176	0.704	0.354	0.388
	WML	-0.053	0.704	-0.499	0.381	-0.151	0.704
Hotspot mean	NAWM	-0.055	0.704	-0.424	0.388	-0.124	0.704
	WML	-0.047	0.704	-0.519	0.381	0.624	0.381
Hotspot volume	NAWM	-0.042	0.704	-0.488	0.381	-0.025	0.922
	WML	-0.054	0.704	-0.795	0.064	0.412	0.425

Table 5.6: Associations between PK binding and CMB count when adjusted for age and sex. Table shows standardised β coefficients and p values. Significant p values are shown in bold.

5.3.7 Brain Volume

The association between the PK binding parameters and brain volume are shown in Table 5.7. There were no associations with any of the parameters in any of the groups. The association between PK binding parameters and GM volume are then shown in Table 5.8. Similar to brain volume, there were no significant associations seen.

PK value	Brain region	Control		Sporadic SVD		CADASIL	
		β	P value	β	P value	β	P value
Global mean	NAWM	-0.071	0.855	0.263	0.416	-0.329	0.724
	WML	0.010	0.985	0.412	0.156	0.319	0.724
Hotspot mean	NAWM	-0.112	0.731	0.021	0.985	-0.586	0.416
	WML	-0.093	0.734	0.059	0.920	-0.385	0.724
Hotspot volume	NAWM	0.004	0.985	0.138	0.724	-0.492	0.416
	WML	-0.213	0.416	0.256	0.455	-0.441	0.724

Table 5.7: Associations between PK binding and brain volume when adjusted for age, sex and ICV. Table shows standardised β coefficients and p values. Significant p values are shown in bold.

PK value	Brain region	Control		Sporadic SVD		CADASIL	
		β	P value	β	P value	β	P value
Global mean	NAWM	-0.085	0.775	-0.091	0.775	-0.542	0.274
	WML	-0.112	0.775	0.430	0.230	0.457	0.358
Hotspot mean	NAWM	-0.305	0.358	-0.460	0.230	-0.611	0.230
	WML	-0.217	0.459	-0.271	0.459	-0.559	0.367
Hotspot volume	NAWM	-0.119	0.775	-0.453	0.230	-0.537	0.230
	WML	-0.341	0.285	0.047	0.862	-0.672	0.230

Table 5.8: Associations between PK binding and GM volume when adjusted for age, sex and ICV. Table shows standardised β coefficients and p values. Significant p values are shown in bold.

5.3.8 FA

The associations between FA median and the PK binding parameters are shown for the NAWM in Table 5.9 and for the WML in Table 5.10. There were no associations between any of the PK binding parameters and FA in any of the groups.

PK value	Brain region	Control		Sporadic SVD		CADASIL	
		β	P value	β	P value	β	P value
Global mean	NAWM	-0.118	0.677	0.007	0.979	-0.461	0.227
	WML	0.204	0.443	0.284	0.443	0.518	0.227
Hotspot mean	NAWM	-0.289	0.405	-0.336	0.405	-0.253	0.434
	WML	-0.317	0.405	0.283	0.443	-0.706	0.227
Hotspot volume	NAWM	-0.397	0.405	-0.339	0.405	-0.340	0.405
	WML	-0.288	0.405	0.390	0.405	-0.602	0.227

Table 5.9: Associations between PK and FA NAWM median when adjusted for age and sex. Table shows standardised β coefficients and p values. Significant p values are shown in bold.

PK value	Brain region	Control		Sporadic SVD		CADASIL	
		β	P value	β	P value	β	P value
Global mean	NAWM	0.035	0.949	-0.280	0.949	0.156	0.949
	WML	-0.428	0.949	0.176	0.949	0.311	0.949
Hotspot mean	NAWM	-0.021	0.949	0.032	0.949	-0.374	0.949
	WML	-0.082	0.949	-0.022	0.949	0.133	0.949
Hotspot volume	NAWM	-0.053	0.949	0.093	0.949	-0.094	0.949
	WML	-0.032	0.949	0.093	0.949	-0.074	0.949

Table 5.10: Associations between PK binding and FA WML median when adjusted for age and sex. Table shows standardised β coefficients and p values. Significant p values are shown in bold.

5.3.9 MD

Associations between MD peak height and PK binding parameters are shown for NAWM in Table 5.11 and WML in Table 5.12. There were no associations between any of the PK binding parameters and the MD peak height in the NAWM in any of the groups. There was a significant negative association between PK binding hotspot volume in the NAWM and MD peak height in the WML in the control group when controlled for age and sex (β=-0.864, p=0.003 (p=0.043 when adjusted for multiple comparisons)). The significance was still present after adjusting for cardiovascular risk factors (β=-0.787, p=0.046).

PK value	Brain region	Control		Sporadic SVD		CADASIL	
		β	P value	β	P value	β	P value
Global mean	NAWM	-0.298	0.580	0.036	0.898	-0.200	0.694
	WML	-0.179	0.694	0.242	0.694	0.540	0.580
Hotspot mean	NAWM	-0.035	0.898	0.133	0.857	-0.183	0.694
	WML	-0.255	0.694	0.099	0.866	-0.529	0.580
Hotspot volume	NAWM	-0.244	0.694	0.107	0.866	-0.156	0.732
	WML	-0.230	0.694	0.288	0.694	-0.451	0.580

Table 5.11: Associations between PK binding and MD NAWM peak height when adjusted for age and sex. Table shows standardised β coefficients and p values. Significant p values are shown in bold.

PK value	Brain region	Control		Sporadic SVD		CADASIL	
		β	P value	β	P value	β	P value
Global mean	NAWM	-0.434	0.307	0.172	0.631	0.389	0.386
	WML	0.241	0.562	0.531	0.133	-0.208	0.664
Hotspot mean	NAWM	-0.665	0.100	0.495	0.157	-0.297	0.536
	WML	-0.590	0.102	0.271	0.547	-0.137	0.792
Hotspot volume	NAWM	**-0.864**	**0.043**	0.151	0.665	0.055	0.859
	WML	-0.511	0.186	0.656	0.092	0.428	0.433

Table 5.12: Associations between PK binding and MD WML peak height when adjusted for age and sex. Table shows standardised β coefficients and p values. Significant p values are shown in bold.

5.3.10 FW

Associations between FW median and PK binding parameters are shown for the NAWM in Table 5.13 and WML in Table 5.14. There were no associations seen between any of the PK binding parameters and either of the FW values for any of the groups.

PK value	Brain region	Control		Sporadic SVD		CADASIL	
		β	P value	β	P value	β	P value
Global mean	NAWM	0.292	0.808	-0.156	0.808	0.050	0.814
	WML	-0.129	0.808	-0.198	0.808	-0.415	0.570
Hotspot mean	NAWM	-0.076	0.809	-0.116	0.808	0.163	0.808
	WML	0.226	0.808	-0.307	0.808	0.499	0.570
Hotspot volume	NAWM	0.262	0.808	-0.155	0.808	0.086	0.808
	WML	0.182	0.808	-0.421	0.808	0.248	0.808

Table 5.13: Associations between PK binding and FW NAWM median when adjusted for age and sex. Table shows standardised β coefficients and p values. Significant p values are shown in bold.

PK value	Brain region	Control		Sporadic SVD		CADASIL	
		β	P value	β	P value	β	P value
Global mean	NAWM	-0.020	0.986	0.182	0.910	0.049	0.986
	WML	-0.129	0.910	-0.518	0.910	-0.103	0.910
Hotspot mean	NAWM	-0.015	0.986	-0.005	0.986	0.290	0.910
	WML	0.150	0.910	0.316	0.910	0.212	0.910
Hotspot volume	NAWM	0.164	0.910	0.123	0.910	0.240	0.910
	WML	0.182	0.910	-0.223	0.910	0.149	0.910

Table 5.14: Associations between PK binding and FW WML median when adjusted for age and sex. Table shows standardised β coefficients and p values. Significant p values are shown in bold.

5.3.11 FW adjusted FA

Associations between FW adjusted FA median and PK binding parameters are shown for NAWM in Table 5.15 and WML in Table 5.16. There was no association between any of the PK binding parameters and either of the FW adjusted FA median values for any of the groups.

PK value	Brain region	Control		Sporadic SVD		CADASIL	
		β	P value	β	P value	β	P value
Global mean	NAWM	-0.079	0.832	-0.148	0.754	-0.527	0.206
	WML	0.267	0.394	-0.074	0.833	0.543	0.257
Hotspot mean	NAWM	-0.221	0.490	-0.422	0.394	-0.253	0.490
	WML	-0.253	0.441	-0.087	0.833	-0.746	0.206
Hotspot volume	NAWM	-0.349	0.394	-0.450	0.394	-0.382	0.394
	WML	-0.206	0.490	-0.164	0.754	-0.634	0.206

Table 5.15: Associations between PK binding and FW adjusted FA NAWM median when adjusted for age and sex. Table shows standardised β coefficients and p values. Significant p values are shown in bold.

PK value	Brain region	Control		Sporadic SVD		CADASIL	
		β	P value	β	P value	β	P value
Global mean	NAWM	-0.028	0.923	-0.364	0.923	0.054	0.923
	WML	-0.596	0.359	-0.233	0.923	0.331	0.923
Hotspot mean	NAWM	-0.059	0.923	-0.163	0.923	-0.254	0.923
	WML	-0.160	0.923	0.058	0.923	0.473	0.923
Hotspot volume	NAWM	0.046	0.923	-0.111	0.923	-0.056	0.923
	WML	-0.080	0.923	-0.195	0.923	-0.123	0.923

Table 5.16: Associations between PK binding and FW adjusted WML median when adjusted for age and sex. Table shows standardised β coefficients and p values. Significant p values are shown in bold.

5.3.12 FW adjusted MD

Associations between FW adjusted MD peak height and PK binding parameters are shown for NAWM in Table 5.17 and WML in Table 5.18. There was no association between any of the PK binding parameters and the FW adjusted MD peak height values in the NAWM. There was a significant negative association between PK

182

binding hotspot volume in the NAWM and FW adjusted MD peak height in the WML in the control group (β=-0.930, p=0.005 (p=0.006 when adjusted for multiple comparisons)). This significance was still present after adjusting for cardiovascular risk factors (β=-0.880, p=0.004).

PK value	Brain region	Control		Sporadic SVD		CADASIL	
		β	P value	β	P value	β	P value
Global mean	NAWM	0.013	0.997	-0.030	0.997	0.384	0.706
	WML	0.040	0.997	0.276	0.852	-0.201	0.964
Hotspot mean	NAWM	0.265	0.768	0.295	0.852	0.158	0.964
	WML	0.012	0.997	0.480	0.706	0.011	0.997
Hotspot volume	NAWM	0.001	0.997	0.174	0.964	0.492	0.706
	WML	-0.002	0.997	0.548	0.706	0.389	0.768

Table 5.17: Associations between PK binding and FW adjusted MD NAWM peak height when adjusted for age and sex. Table shows standardised β coefficients and p values. Significant p values are shown in bold.

PK value	Brain region	Control		Sporadic SVD		CADASIL	
		β	P value	β	P value	β	P value
Global mean	NAWM	-0.456	0.279	0.324	0.430	-0.024	0.937
	WML	0.302	0.434	-0.210	0.559	-0.485	0.296
Hotspot mean	NAWM	-0.676	0.098	0.476	0.279	-0.239	0.503
	WML	-0.579	0.122	0.634	0.180	0.039	0.937
Hotspot volume	NAWM	**-0.930**	**0.006**	0.336	0.434	-0.256	0.496
	WML	-0.515	0.180	0.283	0.496	0.430	0.430

Table 5.18: Associations between PK binding and FW adjusted MD WML peak height when adjusted for age and sex. Table shows standardised β coefficients and p values. Significant p values are shown in bold.

5.3.13 Cognition

The association between PK binding parameters and GC can be seen in Table 4.19.
The associations between PK binding parameters and the various cognitive domains
of EF, PS, WoM and LTM can be found in Tables 5.20, 5.21, 5.22 and 5.23
respectively. There was no association between any of the PK binding parameters in
any of the groups with cognition.

PK value	Brain region	Control		Sporadic SVD		CADASIL	
		β	P value	β	P value	β	P value
Global mean	**NAWM**	-0.082	0.901	0.098	0.901	-0.457	0.531
	WML	-0.185	0.789	0.149	0.901	0.598	0.342
Hotspot mean	**NAWM**	-0.033	0.977	-0.107	0.901	0.016	0.977
	WML	-0.050	0.926	0.073	0.926	-0.899	0.075
Hotspot volume	**NAWM**	-0.103	0.901	0.008	0.977	-0.272	0.901
	WML	0.095	0.901	0.136	0.901	-0.780	0.194

Table 5.19: Associations between PK binding and GC when adjusted for age, sex and
premorbid IQ. Table shows standardised β coefficients and p values. Significant p
values are shown in bold.

PK value	Brain region	Control		Sporadic SVD		CADASIL	
		β	P value	β	P value	β	P value
Global mean	**NAWM**	-0.212	0.742	0.093	0.742	-0.415	0.742
	WML	0.144	0.742	-0.085	0.766	0.350	0.742
Hotspot mean	**NAWM**	-0.141	0.742	-0.052	0.861	-0.262	0.742
	WML	-0.108	0.742	0.116	0.742	-0.989	0.083
Hotspot volume	**NAWM**	-0.271	0.742	0.139	0.742	-0.364	0.742
	WML	0.093	0.742	-0.020	0.921	-0.684	0.732

Table 5.20: Associations between PK binding and EF when adjusted for age, sex and
premorbid IQ. Table shows standardised β coefficients and p values. Significant p
values are shown in bold.

PK value	Brain region	Control		Sporadic SVD		CADASIL	
		β	P value	β	P value	β	P value
Global mean	NAWM	0.235	0.752	0.102	0.863	-0.298	0.752
	WML	-0.438	0.607	0.231	0.752	0.786	0.100
Hotspot mean	NAWM	0.088	0.863	0.005	0.989	0.161	0.787
	WML	-0.288	0.752	0.291	0.752	-0.834	0.101
Hotspot volume	NAWM	0.206	0.752	0.267	0.752	-0.070	0.863
	WML	-0.229	0.752	0.286	0.752	-0.575	0.607

Table 5.21: Associations between PK binding and PS when adjusted for age, sex and premorbid IQ. Table shows standardised β coefficients and p values. Significant p values are shown in bold.

PK value	Brain region	Control		Sporadic SVD		CADASIL	
		β	P value	β	P value	β	P value
Global mean	NAWM	-0.006	0.982	0.154	0.616	-0.434	0.531
	WML	-0.064	0.982	0.130	0.747	0.044	0.982
Hotspot mean	NAWM	-0.026	0.982	-0.230	0.616	0.018	0.982
	WML	0.180	0.747	-0.108	0.833	-0.366	0.616
Hotspot volume	NAWM	0.028	0.982	-0.240	0.616	-0.327	0.616
	WML	0.334	0.531	0.055	0.982	-0.654	0.342

Table 5.22: Associations between PK binding and WoM when adjusted for age, sex and premorbid IQ. Table shows standardised β coefficients and p values. Significant p values are shown in bold.

PK value	Brain region	Control		Sporadic SVD		CADASIL	
		β	P value	β	P value	β	P value
Global mean	**NAWM**	-0.112	0.896	-0.060	0.896	-0.482	0.280
	WML	-0.308	0.499	0.279	0.514	0.464	0.325
Hotspot mean	**NAWM**	0.027	0.917	-0.088	0.896	0.198	0.788
	WML	-0.050	0.896	-0.117	0.896	-0.373	0.499
Hotspot volume	**NAWM**	0.028	0.917	-0.240	0.499	-0.327	0.499
	WML	0.334	0.325	0.055	0.896	-0.654	0.280

Table 5.23: Associations between PK binding and LTM when adjusted for age, sex and premorbid IQ. Table shows standardised β coefficients and p values. Significant p values are shown in bold.

5.4 Discussion

Taking PK binding as a marker of microglia activation, this chapter has shown that there are increased regions of hotspot microglia activation in the NAWM and WML of the sporadic SVD group compared to control. There were also increased hotspots of microglia activation in the WML of the CADASIL group compared to control. However, there was not a significant increase in global microglia activation in sporadic SVD or CADASIL compared to control. Microglia activation was higher in the NAWM compared to the WML, with no significant increase in microglia activation seen in the WML penumbra.

5.4.1 Global Group Differences

Global PK binding was not significantly different between the sporadic SVD and control groups or the CADASIL and control groups in the whole WM, NAWM or WML (Figure 5.2).

The main reason behind this result is likely the analysis techniques that used in this study. As described in Chapter Two, we used the SRTM approach to quantify BP_{ND} in the WM (Lammertsma and Hume, 1996), and then weighted each pixel TAC to its 'normal' WM index. The GM was originally used as the reference region but was found to be unreliable in this cohort. However, it is questionable as to whether there is any 'normal' tissue in the WM of the SVD populations, and therefore this is probably why we cannot detect a global change here, even if there is one. As PK imaging has not previously been performed in an SVD population, we cannot compare this with previous studies.

PK imaging for microglia activation has been performed in other neurological disorders. Multiple sclerosis (MS) PK studies have a fairly consistent method, using the SRTM to quantify BP_{ND} in the GM as the reference region (Airas et al., 2018). These studies have shown mixed results, where some showed that global binding in the NAWM was increased compared to control (Politis et al., 2012, Rissanen et al.,

2014, Giannetti et al., 2015, Rissanen et al., 2018) whilst others have found no significant group difference (Debruyne et al., 2003).

PK imaging has also been used in Alzheimer's disease, where results have been inconsistent. The SRTM approach is the method of choice in Alzheimer's disease (Gunn et al., 1997). Early studies found there was increased PK tracer uptake in Alzheimer's patients compared to controls (Cagnin et al., 2001, Edison et al., 2008, Yokokura et al., 2011). However, later studies have not seen this significant group difference (Schuitemaker et al., 2013).

Ischaemic stroke studies have also used PK to investigate the role of microglia after an acute infarct. In ischaemic stroke, there are more options for the reference region, as stroke causes a focal infarct and therefore non-infarcted tissue can be used as a reference region. Most studies take the cerebellum as the reference region. There was found to be no increase in PK binding in acute stroke patients compared to controls within the first 72 hours but there was a significant difference at 1 week, which is still evident at 30 days, although it has declined (Price et al., 2006, Gerhard et al., 2005). The evidence from acute stroke suggests that microglia activation is a very dynamic process that can change dramatically over the course of a few days.

Taking all of this work together, it is obvious that the analysis technique for different studies is dependent on the individual pathology of the disease. Further, the mixed results seen in MS, Alzheimer's disease and ischaemic stroke, suggest that even when a consistent analysis technique is used, studies can still show differing results. Using the WM as the reference region in SVD has shown no global group difference in PK binding. As further PET techniques are developed, there may be a better way of analysing this data, which reveals a group difference. Alternatively, the dynamic nature of microglia activation could mean that a global difference can only be detected during certain stages of the disease pathogenesis. Longitudinal studies that track microglia activation over time would be needed to establish this. On the other hand, it could be that there truly is no global difference in microglia activation in SVD, or the effect is so subtle that it cannot be detected by PK imaging.

5.4.2 Focal Group Differences

Hotspots were created, which investigated the voxels above a threshold, established from the normal control group. The mean and volume of these hotspots was calculated and compared between groups.

In the sporadic SVD group, the mean and volume of hotspot PK binding were significantly higher than control in the NAWM and WML (Figure 5.3-4). The mean hotspot PK binding was also significantly higher in the whole WM of the sporadic SVD group compared to control. Interestingly, the volume of the PK binding hotspots in the WM was not significantly different from control. Investigating this further, it seems as though the standard deviation in the control group is increased in the WM compared to in the NAWM or WML separately. This is probably because the controls with the most extensive and highest binding in the NAWM also had the most extensive and highest binding the WML, and therefore when these regions are combined, this has lead to a large range of values across the group.

In the CADASIL group, the mean and volume of the PK binding hotspots was significantly higher in the WML of the CADASIL group compared control (Figures 5.3-4). The hotspot relationships seen in the WM and NAWM were slightly more complicated. In the WM, the mean, but not the volume, of the PK binding hotspots was significantly higher in the CADASIL group compared to control (Figure 5.3). The lack of association seen between the WM volumes is probably due to the same explanation as above, where the standard deviation of the control group was much higher in the WM. In the NAWM, neither the mean nor the volume of the PK binding hotspots was significantly different from control, even though there was a trend for them to be higher than the control group. The lack of association seen in the NAWM is probably due to the small group size of the CADASIL group; we had a particularly high failure rate of PET ligand production in the CADASIL group, meaning we were only able to get PK imaging in 14 participants, limiting the power of our results.

The investigation of focal inflammatory hotspots has not been widely used in the literature. However, one study of Alzheimer's disease did use a similar technique to look at clusters of hotspot voxels. They found there was a significantly higher volume

189

of hotspots in the occipital lobe in Alzheimer's disease compared to healthy controls (Schuitemaker et al., 2013). Similarly to in our study, they did not find a significant difference with the conventional global analyses. The authors suggested that this is because microglial activation is a subtle phenomenon in Alzheimer's. A focal analysis was also used in a cognitive healthy elderly population; similarly they were found to have a significantly higher volume of PK binding hotspots compared to a younger population (Kumar et al., 2012).

There is significant overlap between Alzheimer's disease and SVD, with many elderly patients having some degree of both pathologies (Liu et al., 2018b). Therefore, the similarities between our results and the Alzheimer's and elderly cohorts suggest that there may be a focal role for microglia activation in the disease pathologies. Follow-up data is needed to determine whether these focal regions of inflammation are pathological by seeing if SVD-related pathology, such as WML growth, develops in these regions.

5.4.4 NAWM vs. WML

We found that the mean and volume of the PK binding hotspots were higher in the NAWM than in the WML for control, sporadic SVD and CADASIL groups (Table 5.1). Global mean PK binding values were significantly higher in the NAWM compared to the WML in the sporadic SVD group, but there was no significant difference between NAWM and WML for control or CADASIL groups.

This result is in contrast to post-mortem studies of SVD, where they have reported significantly higher markers of microglia in the WMLs compared to in the NAWM (Simpson et al., 2007b, McAleese et al., 2016). However, as discussed above, this may be because post mortem studies are measuring end-stage disease whereas our study is looking at earlier stages.

PK studies of MS, however, have found a similar result to our study, where there was a higher level of PK binding in the NAWM compared to WML (Debruyne et al., 2003). In MS, this has been suggested to represent 'preactive lesions', thought to be a

result of alterations in brain homeostasis leading to microglial activation in NAWM (van Horssen et al., 2012). Early studies elucidated that this damage does not necessarily indicate irreversible damage or impaired function of brain tissue and even suggested that it could be a protective response to the damage (Graumann et al., 2003, Heppner et al., 2005). However, more recent studies have shown that higher microglia activation in the NAWM was associated with a higher risk of developing MS at 2 years, suggesting that this process is pathological (Giannetti et al., 2015). Therefore, a similar process could be occurring in SVD, where the inflammation is spreading away from the WMLs and into the NAWM to represent regions that are undergoing pathological processes prior to progressing into WMLs.

PK studies in acute stroke have investigated microglia activation both in and around the infarct and have reported various trends. Price et al. studied PK binding over time after acute stroke and suggested that the PK binding begins in the infarct and it is only during the later sub-acute phase that the peri-infarct zone shows increased uptake (Price et al., 2006). However, a later study by Gulyas et al. found no significant difference in PK binding in the ischaemic core compared to the peri-infarct area one month after acute stroke (Gulyas et al., 2012). PK binding has been shown to be increased in the contralateral hemisphere after the sub-acute phase, suggesting the neuroinflammation continues to extend out from the infarct (Gerhard et al., 2005, Pappata et al., 2000). Further, studies investigating specific fibre tracts found that there was PK binding seen in the WM tract if a lesion had occurred at some point on the tract, suggesting this may be a method by which the inflammation spreads (Radlinska et al., 2009).

The acute infarcts seen in ischaemic stroke are different to the WMLs seen in SVD, as the WMLs are not caused by a single acute event, rather by chronic hypoxia. However, the WMLs of SVD still represent focal damage to the tissue and often occur within the WM tracts. Therefore, in SVD it is likely that a similar process of inflammation spreading along the WM tracts also occurs and this may be why we are seeing higher levels of microglial activation in the NAWM. The comparatively lower inflammation in the WML may be because the WMLs in SVD are usually not acute or recent. Therefore, the inflammatory processes that occur here may only be temporary

and as time goes on and the WML becomes inactive, the inflammatory processes may spread away from the insult and into the NAWM.

Further studies that investigate changes in the PK binding in both the NAWM and WML over time are required to see whether a temporal relationship is occurring here and provide further insight into what is happening in the pathogensis of SVD.

5.4.5 WML Penumbra

We had hypothesised that the penumbra PK binding values would be significantly higher if microglia activation is involved in the pathogenesis of SVD, as these regions are the most likely place for new WMLs to form (Maillard et al., 2011).

First, we investigated the PK binding in the penumbra between the sporadic SVD and control groups, and the CADASIL and control groups. The mean of the PK binding hotspots was significantly higher in the sporadic SVD penumbra compared to control (Figure 5.6). However, there was no significant difference between the groups for the volume of the hotspots or the global PK binding (Figure 5.5 and 5.7). There was no significant difference between CADASIL and control for any of the penumbra PK binding values. It was unclear as to whether the significant increase seen in the mean of the PK binding hotspots in the sporadic SVD group was because the penumbra had significantly higher microglia activation, or because the sporadic SVD brain was in a heightened inflammatory state more generally.

Therefore, we then compared the penumbra PK binding values to the respective NAWM and WML values, within the individual groups. The global PK binding values showed a similar pattern across the different groups where the global PK binding in the penumbra was significantly lower than the global PK binding in the NAWM or the WML (Table 5.2).

The mean values of the PK binding hotspots showed different trends in different groups. In the control group, the mean binding of the PK hotspot was significantly lower in the penumbra than in the NAWM values but significantly higher than in the

192

WML (Tables 5.2). In the sporadic SVD group, the mean binding of the PK hotspot was also significantly lower in the penumbra than in the NAWM, but was similar to the WML (Tables 5.2). In the CADASIL group, the penumbra values were similar to both the NAWM and WML (Tables 5.2).

Finally, looking at the volume of the PK binding hotspots in the penumbra, there was a similar trend across all of the groups. The volume of the PK binding hotspots was significantly lower than in the NAWM, but significantly higher than the WML for all of the groups (Tables 5.2).

We repeated this analysis with a 6mm penumbra, to see if that resulted in the same patterns as the 3mm penumbra. The patterns were similar across all analysis, and can be found in Appendix C.

These results are slightly confusing, but suggest that in general, the penumbra of the WMLs have lower global PK binding than the NAWM or the WML. Whereas, the hotspot PK binding is lower than the NAWM but higher than the WML.

Acute stroke studies have also investigated the penumbra around the infarct, where the importance of this region has been long established. A study of acute stroke found that on day 6 after acute infarct, there is a rim of increased PK binding around the infarct (Ramsay et al., 1992). However, this was not seen in all studies; a more recent study looking at patients in the sub-acute and early chronic stages after stroke found there was no significant increase in PK binding at these time-points, suggesting no significant increase in microglia activation in the penumbra region (Morris et al., 2018). A study looking at the penumbra of intracerebral haemorrages 4-28 days after stroke also had confusing results, with some patients showing increased PK binding and others not (Abid et al., 2018).

The results seen here are difficult to draw conclusions from. However, the lower global PK binding that was seen in the penumbra of all groups compared to the NAWM and WML suggests that there is less overall activated microglia in the WML penumbra. Taken together, the PK binding hotspot results suggests that the values

seen in the penumbra are generally higher than those in the WML, but lower than those in the NAWM. This may be due to partial volume effects, as resolution of PET imaging is poor and so a 3mm or 6mm penumbra may be too small to give accurate read-outs. A better option for exploring the penumbra of WMLs would probably be to look at post-mortem data, and to see if there are cells there that are positive for activated microglia. However, this still comes with limitations, as this would be representative of end-stage SVD, which may not be as relevant to early and mid-stage processes.

5.4.6 Associations with WML Volume and MD

The volume of the PK hotspots in the NAWM of the control group was associated with WML volume (Table 5.3). Further, the volume of the PK hotspots in the NAWM of the control group was significantly associated with a lower MD peak height in the WML. As discussed in Chapter Four, MD peak height is the most sensitive histogram parameter for SVD severity and progression, with a lower peak height representative of higher diffusivity and increased ultrastructural damage in the WM (Zeestraten et al., 2016). Therefore, this association suggests that a higher volume of inflammation in the NAWM is associated with increased WML volume and increased ultrastructural damage in the control subject WMLs. These associations were not evident in any of the other groups.

The significant association in the control group, but not the sporadic SVD or CADASIL group, may be relevant if the control group can be seen as an asymptomatic 'early SVD' population, due to the fact that they are an elderly cohort. It could be that later down the line, the inflammatory mechanisms have become too complex due to the widespread damage, and therefore these associations become lost in the noise.

As PK imaging has not been previously reported in relation to WML in an SVD or healthy elderly cohort, it is therefore difficult to put this finding into context. One study of MS patients found that there was a correlation between PK binding in the NAWM and WML volume (Giannetti et al., 2015) but, to the best of my knowledge,

there have been no other reports of this in the literature. Further, as this was the only significant association seen as a result of many analyses performed, this finding needs to be treated with caution and reproduced in a larger sample size to be confirmed.

5.4.7 Associations with Lacunes, CMBs, Brain Volume and FA

There was no association between PK binding and lacune volume (Table 5.4), lacune number (Table 5.5), CMB number (Table 5.6), brain volume (Table 5.7), GM volume (Table 5.8) or any of the FA parameters (Tables 5.9, 5.19, 5.15 and 5.16) in any of the groups. This would suggest that microglia activation is not involved in the underlying pathology leading to these imaging characteristics. Alternatively, it may be that there is a temporal relationship between microglia activation and these parameters (i.e. one predicts another) and a single time-point analysis, as we have done in this study, is not able to see this relationship. Longitudinal studies are required to investigate if there is a temporal relationship between microglia activation and these imaging parameters.

5.4.8 Association with Cognition

PK binding was not associated with GC in any of the groups (Table 5.19). Further, when investigating the individual cognitive indices, there was no correlation between cognition and EF (Table 5.20), PS (Table 5.21), WoM (Table 5.22) or LTM (Table 5.23) in any of the groups.

PK binding and cognition have been previously studied in Alzheimer's disease and mild cognitive impairment, where there was also found to be no correlation with cognitive function (Schuitemaker et al., 2013, Okello et al., 2009). However, when analysing regions in more detail, one study did find an association between MMSE and PK binding in the posterior cingulate gyrus, parietal and frontal cortical regions (Edison et al., 2008), whilst another found an association between LTM and PK binding in the precuneus (Passamonti et al., 2018). Further, a recent study used PK PET and functional MRI to establish a relationship between increased PK binding and disruption of network function (Passamonti et al., 2019). Passamonti et al. showed that, in Alzheimer's disease, patients with a higher association between these two

parameters had decreased cognitive function. This suggests that microglia activation may be mediating cognition through decreased functional connectivity of networks.

Our results suggests that there is no direct association between cognition and microglia activation cross-sectionally. However, there could be a longitudinal association where microglia activation is causative of underlying damage, leading to a greater decline in cognition over time. Follow-up studies are needed to see if baseline microglia activation can predict a larger decline in cognition at follow-up.

5.4.9 Limitations

The use of PK imaging to provide in vivo quantification and localisation of neuroinflammation in patient populations offers great scope of application, to further our understanding of the role of microglia activation across many diseases. A key limitation of this study is the lack of previous studies investigating PK imaging in SVD, as this has meant we could not compare our results to previous literature and have no repeat scanning, so do not know how reproducible these values are.

PK imaging itself is not without limitations, the key ones being low brain bioavailability and poor signal-to-noise due to high nonspecific binding (Largeau et al., 2017). Further, the short half-life of carbon-11 means that the tracer must be produced just before required. This brings a certain amount of unpredictability into the study, as the tracers can fail last minute or not pass quality control.

Another important limitation of PK is that it is non-specific for activated microglia, as TSPO is expressed by multiple types of immune cells including astrocytes (Lavisse et al., 2012). It is impossible to differentiate between these cell types during the PK imaging. So, although many studies reference 'activated microglia' when discussing PK results, really the results may also be representative of other cell types.

Further, inflammation itself is a very dynamic process and PK imaging only supplies us with a snapshot of this process. Repeat scanning is necessary to track the dynamics and fully understand the process, but this is difficult due to radiation doses and costs.

In addition to these, there are other limitations that are general to PET imaging, that must be kept in mind when designing a study and interpreting the results. To quantify the data, a reference region is required to be able to calculate the ligand binding relative to the reference region (Alam et al., 2017). In states of disease, there often is no brain region free from pathology, and therefore it can be difficult to find an appropriate reference region for this purpose. Therefore, techniques vary between studies (Airas et al., 2015) and this needs to be kept in mind when evaluating and comparing the literature.

PET imaging also has notoriously poor spatial resolution, which makes it difficult to image small brain regions and leads to issues with partial volume. With improving technology, the spatial resolution of PET should continue to improve. However, due to the fundamental physics of PET cameras, the spatial resolution will always be limited (Moses, 2011).

Other general PET limitations include cost and patient willingness to participate. The cost of PET tracers and scanner time is high, and means that studies often end up with a relatively low sample size that can make results difficult to interpret. Finally, the reality that PET involves a radioactive injection that leads to an increased risk of cancer makes it imperfect for use in research studies and can make it difficult to recruit patients to PET research.

5.5 Summary of Findings

Returning to the aims of this chapter, the following areas have been addressed:

1. Global PK binding was not significantly different in the sporadic SVD or CADASIL groups compared to control in the WM, NAWM or WML

2. The mean of the PK binding hotspots was significantly higher in the WM, NAWM and WML of the sporadic SVD patients compared to control; the volume of the PK binding hotspots was also significantly higher in the NAWM and WML of the sporadic SVD group compared to control

3. The mean of the PK binding hotspots was significantly higher in CADASIL group compared to control in the WM and WML; the volume of the PK binding hotspots was significantly higher in the WML

4. Global PK binding in the penumbra was lower than in the NAWM or WML across all of the groups

5. Hotspot PK binding in the penumbra was generally lower than NAWM but higher than in the WML across the groups

6. PK binding volume in the NAWM of the control group was associated with increased WML volume and decreased MD peak height in the WML, suggesting increased WML severity is associated with increased volume of microglia activation elsewhere

7. PK binding was not associated with any of the cognitive parameters in any of the groups

This chapter has investigated PK binding between the groups and in comparison to the other end-points collected in the study. The next chapter will investigate the relationship between BBB permeability and PK binding.

Chapter 6: Relationship between BBB permeability and PK binding

6.1 Introduction

6.1.1 Aims of the Chapter

The previous chapters explored BBB permeability and PK binding separately, by comparing them between the patient and control groups, and also exploring the relationship with imaging and cognitive markers. This chapter now looks at the relationship between BBB permeability and PK binding and investigates the following specific questions:

- Is there a correlation between BBB permeability and PK binding in the control, sporadic SVD and CADASIL groups?
- Is there a significant difference in the spatial distribution of BBB permeability and PK binding between groups?
- Is there an association between the spatial overlap of BBB permeability and PK binding in individual groups?

The main hypotheses of this chapter are:

- BBB permeability and PK binding will be significantly correlated in the sporadic SVD, CADASIL and healthy control groups
- There will be a significant spatial overlap between regions of increased BBB permeability and increased PK binding in the sporadic SVD and CADASIL groups

6.1.2 Hypothesised Mechanism of BBB Permeability and Inflammation

The evidence for the presence of increased BBB permeability and PK binding in SVD were outlined in Chapters 4 and 5. However, we have not yet investigated the relationship between BBB permeability and PK binding. The hypothesised cascade of events linking BBB permeability and inflammation to SVD pathophysiology can be seen in Figure 1.1 (Rosenberg, 2018).

The full hypothesised mechanism underlying the pathogenesis of SVD can be found in Chapter One. However, briefly, underlying pathology of the small vessels is thought to trigger an inflammatory response through up-regulation of HIF-1α (Rosenberg, 2018). HIF-1α then leads to a recruitment of macrophages and activation of microglia. These cells release proteases and free radicals in the process of remodelling the damaged vessels. These free radicals and proteases then break down the fibrotic basal lamina, disrupt tight junction proteins to lead to increase in BBB permeability, and attack myelinated fibres.

6.1.3 Evidence for BBB Permeability and Inflammation in the Pathogenesis of SVD
Animal studies of SVD, where SHR/SP rats undergo unilateral carotid artery occlusion and are fed a low protein high salt diet to induce WMLs and cognitive deficits, have investigated the link between BBB permeability and inflammation in more detail (Jalal et al., 2012, Kaiser et al., 2014).

The WMLs in these rats contain reactive astrocytes and activated microglia (Jalal et al., 2012). Additionally, these rats are seen to have increased BBB permeability and decreased tight junction proteins in the vascular endothelial cells (Yang et al., 2018). Taking this further, co-labelling of MMP-9 and immunoglobulin G found they were localised to similar regions, suggesting MMP-9 may be associated with BBB disruption (Jalal et al., 2015).

Jalal et al. found that treatment with minocycline, an anti-inflammatory agent with many actions including MMP-9 inhibition, led to significantly reduced WML size and improved cognition (Jalal et al., 2015). Minocycline almost entirely blocked BBB leakage and enhanced the protein levels of the tight junctions, facilitating repair (Yang et al., 2018). Interestingly, more recent studies have used MMP-9 specific drugs and found that they do not have this ability of minocycline (Raz et al., 2018). Therefore, it has now been suggested that the beneficial action of minocycline may not be through MMP-9 specifically, but through a broader effect on inflammation

involving suppression of microglia (Giuliani et al., 2005) or through multiple MMPs (Jin et al., 2013, Machado et al., 2006).

These animal studies provide evidence for BBB permeability and inflammation in the pathogenesis of SVD, resulting in damage to the WM that leads to WML formation and cognitive deficits. They suggest that broader inflammatory mechanisms need to be examined, to understand the protective effects of minocycline that have been seen in the animal model.

6.2 Methods

There were 16 controls, 15 sporadic SVD and 13 CADASIL who received both BBB permeability and PK PET imaging and so were included in this chapter. Most of the methodology was described in Chapter 2.

6.2.1 Voxel-based Analysis

Binary maps were created of voxels of significant BBB permeability and PK binding by thresholding the data, as described previously to generate the hotspot maps. To create the overlap maps, these binary maps were then added to produce maps of overlap voxels, voxels with just BBB permeability, voxels with just PK binding and voxels with neither BBB permeability nor PK binding. The total number of voxels in the WM, NAWM and WML were then extracted.

6.2.2 Statistical Analysis

Spearman's rank correlation test was used to test all of the correlations between BBB permeability and respective PK binding values. P values were adjusted for multiple comparisons using FDR.

Chi squared tests were then used to assess the homogeneity of the permeability and PK binding on a voxel-by-voxel basis for all regions of all groups. The test of homogeneity investigates the distributions, to see if the frequency of overlap voxels, permeability voxels, PK binding voxels and voxels with neither permeability nor PK binding follows a similar distribution across the groups.

Chi squared tests were then again used to assess the independence of BBB permeability and PK binding on a voxel-by-voxel basis for all regions for all groups, except for the WML of the control group. The WML of the control group had an expected frequency of <5 in one of the cells, and therefore did not meet the assumptions of the chi-squared test. Therefore, a Fisher's exact test was used here.

6.3 Results

6.3.1 Correlation between BBB Permeability and PK binding

Correlation matrices of BBB permeability and PK binding associations can be seen in Tables 6.1-3. Table 6.1 shows the associations in the WM, Table 6.2 shows associations in the NAWM and Table 6.3 shows associations in the WML. There were no associations seen between the parameters for any of the regions in any of the groups.

A

Control		PK		
		Global mean	**Hotspot mean**	**Hotspot volume**
BBB	**Global mean**	0.43	0.07	0.22
	Hotspot mean	0.41	0.22	0.27
	Hotspot volume	0.45	-0.01	0.12

B

Sporadic SVD		PK		
		Global mean	**Hotspot mean**	**Hotspot volume**
BBB	**Global mean**	0.3	0.24	-0.01
	Hotspot mean	0.28	0.57	0.28
	Hotspot volume	0.2	-0.1	-0.25

C

CADASIL		PK		
		Global mean	**Hotspot mean**	**Hotspot volume**
BBB	**Global mean**	0.25	-0.37	-0.19
	Hotspot mean	0.52	-0.12	0.29
	Hotspot volume	0.04	-0.27	-0.27

*p<0.05, **p<0.01, ***p<0.001

Table 6.1: Correlation matrices of Spearman's Rho values for associations between BBB permeability and PK binding parameters in the WM. 1) Control. 2) Sporadic SVD. 3) CADASIL.

A

Control		PK		
		Global mean	**Hotspot mean**	**Hotspot volume**
BBB	**Global mean**	0.36	0.08	0.18
	Hotspot mean	0.36	0.19	0.25
	Hotspot volume	0.39	0	0.1

B

Sporadic SVD		PK		
		Global mean	**Hotspot mean**	**Hotspot volume**
BBB	**Global mean**	-0.05	0.25	-0.18
	Hotspot mean	-0.3	0.39	0.15
	Hotspot volume	0.07	0.05	-0.29

C

CADASIL		PK		
		Global mean	**Hotspot mean**	**Hotspot volume**
BBB	**Global mean**	-0.41	-0.13	-0.24
	Hotspot mean	0.11	0.02	0.14
	Hotspot volume	-0.38	0.03	-0.19

*p<0.05, **p<0.01, ***p<0.001

Table 6.2: Correlation matrices of Spearman's Rho values for associations between BBB permeability and PK binding parameters in the NAWM. 1) Control. 2) Sporadic SVD. 3) CADASIL.

A

Control		PK		
		Global mean	Hotspot mean	Hotspot volume
BBB	Global mean	0.18	0.32	0.24
	Hotspot mean	0.06	0.33	0.29
	Hotspot volume	0.18	0.17	0.21

B

Sporadic SVD		PK		
		Global mean	Hotspot mean	Hotspot volume
BBB	Global mean	0.28	-0.52	-0.52
	Hotspot mean	0.4	-0.33	-0.4
	Hotspot volume	0.16	-0.29	-0.32

C

CADASIL		PK		
		Global mean	Hotspot mean	Hotspot volume
BBB	Global mean	0.59	-0.6	-0.58
	Hotspot mean	0.25	-0.64	-0.41
	Hotspot volume	0.46	-0.44	-0.41

*p<0.05, **p<0.01, ***p<0.001

Table 6.3: Correlation matrices of Spearman's Rho values for associations between BBB permeability and PK binding parameters in the WML. 1) Control. 2) Sporadic SVD. 3) CADASIL.

6.3.2 Distribution of BBB permeability PK binding Voxels

Example images of the regions of increased BBB permeability and PK binding are shown in Figure 6.2.

The distribution of the voxels are shown as percentages for each of the groups for the WM (Figure 6.3), NAWM (Figure 6.4) and WML (Figure 6.5). Tests of homogeneity showed a significant difference in the distribution of the voxels between the groups in the WM ($p<0.001$), NAWM ($p<0.001$) and WML ($p<0.001$).
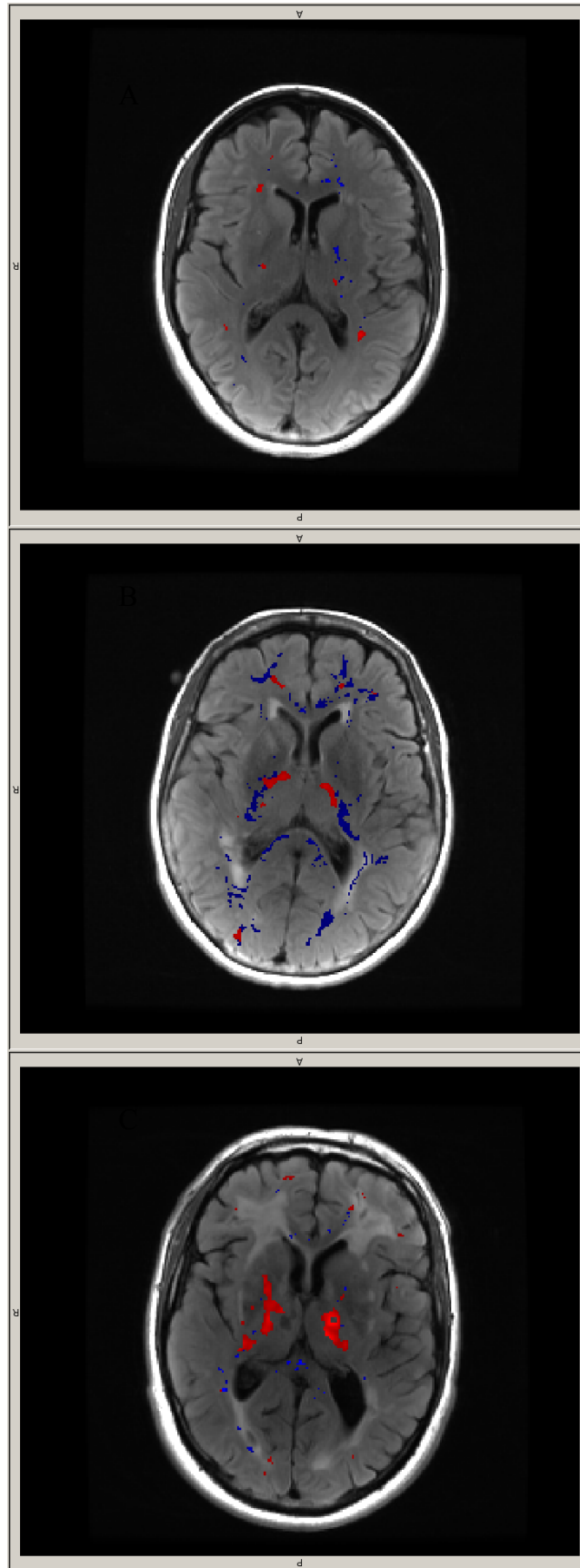
Figure 6.2: Example images of permeability (blue) and PK hotspots (red) overlayed onto T2 FLAIR scans. A) Control. B) Sporadic SVD. C) CADASIL.
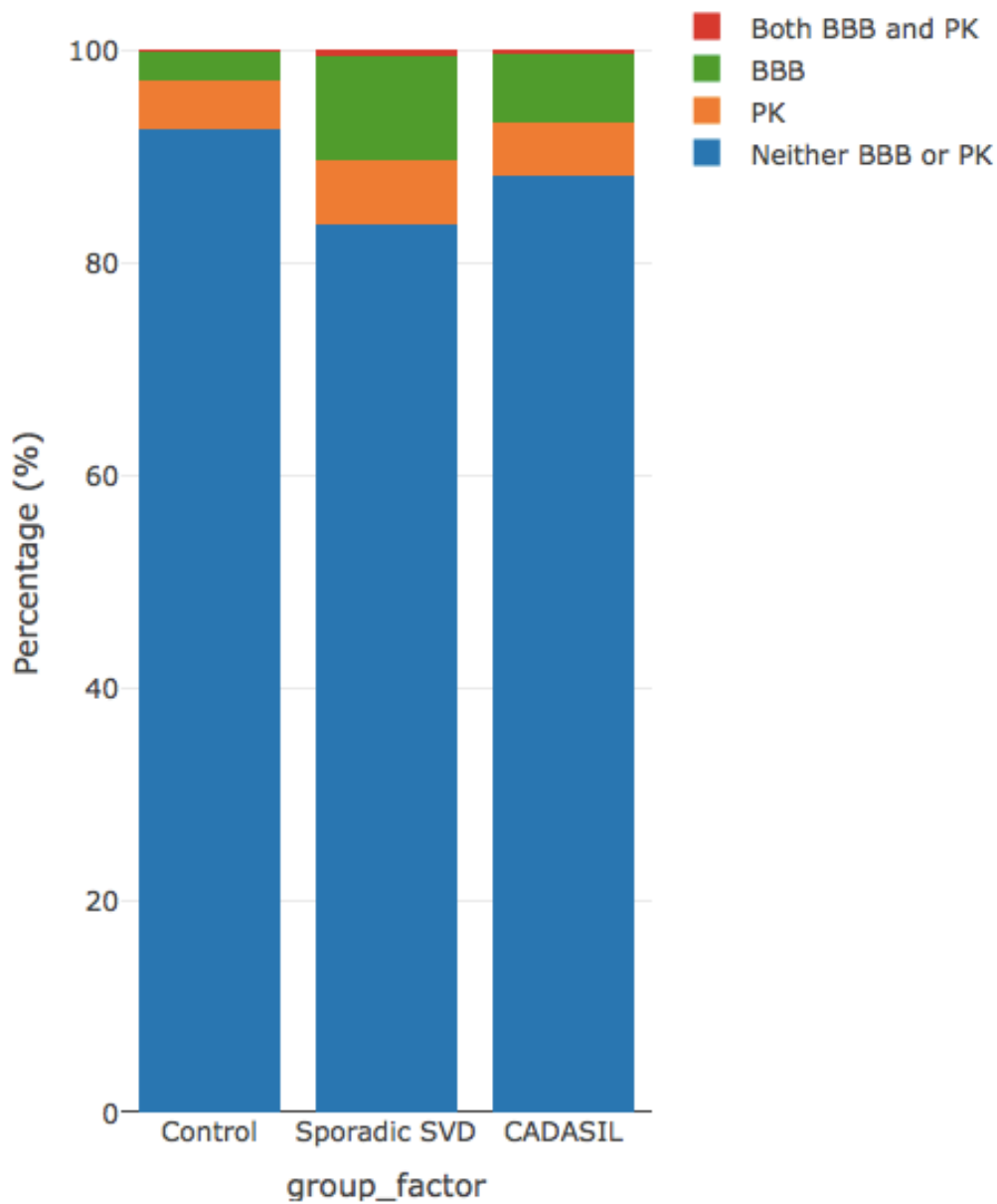
Figure 6.3: Distributions of the voxels in the WM for each group, displayed as a percentage. The control group was made up of 0.14% overlap, 2.61% BBB, 4.54% PK binding and 92.59% neither. The sporadic SVD group was made up of 0.46% overlap, 9.83% BBB, 5.98% PK binding and 83.3% neither. The CADASIL group was made up of 0.19% overlap, 6.47% BBB, 5.05% PK binding and 88.12% neither. There was a significant difference in the distribution between the groups (p<0.001).
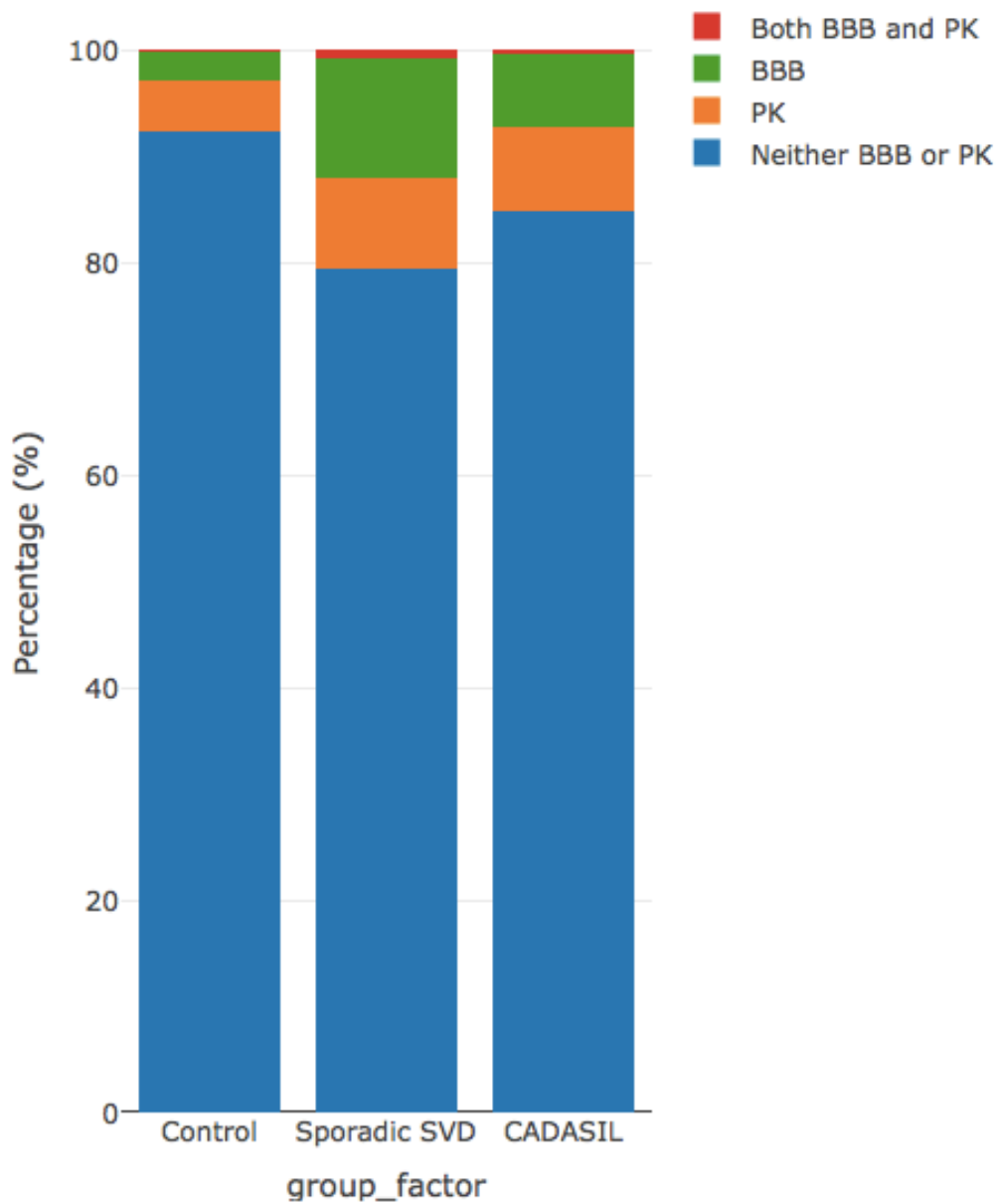
Figure 6.4: Distributions of the voxels in the NAWM for each group, displayed as a percentage. The control group was made up of 0.14% overlap, 2.66% BBB, 4.71% PK binding and 92.35% neither. The sporadic SVD group was made up of 0.71% overlap, 11.31% BBB, 8.34% PK binding and 78.87% neither. The CADASIL group was made up of 0.27% overlap, 6.93% BBB, 7.77% PK binding and 84.76% neither. There was a significant difference in the distribution between the groups ($p<0.001$).
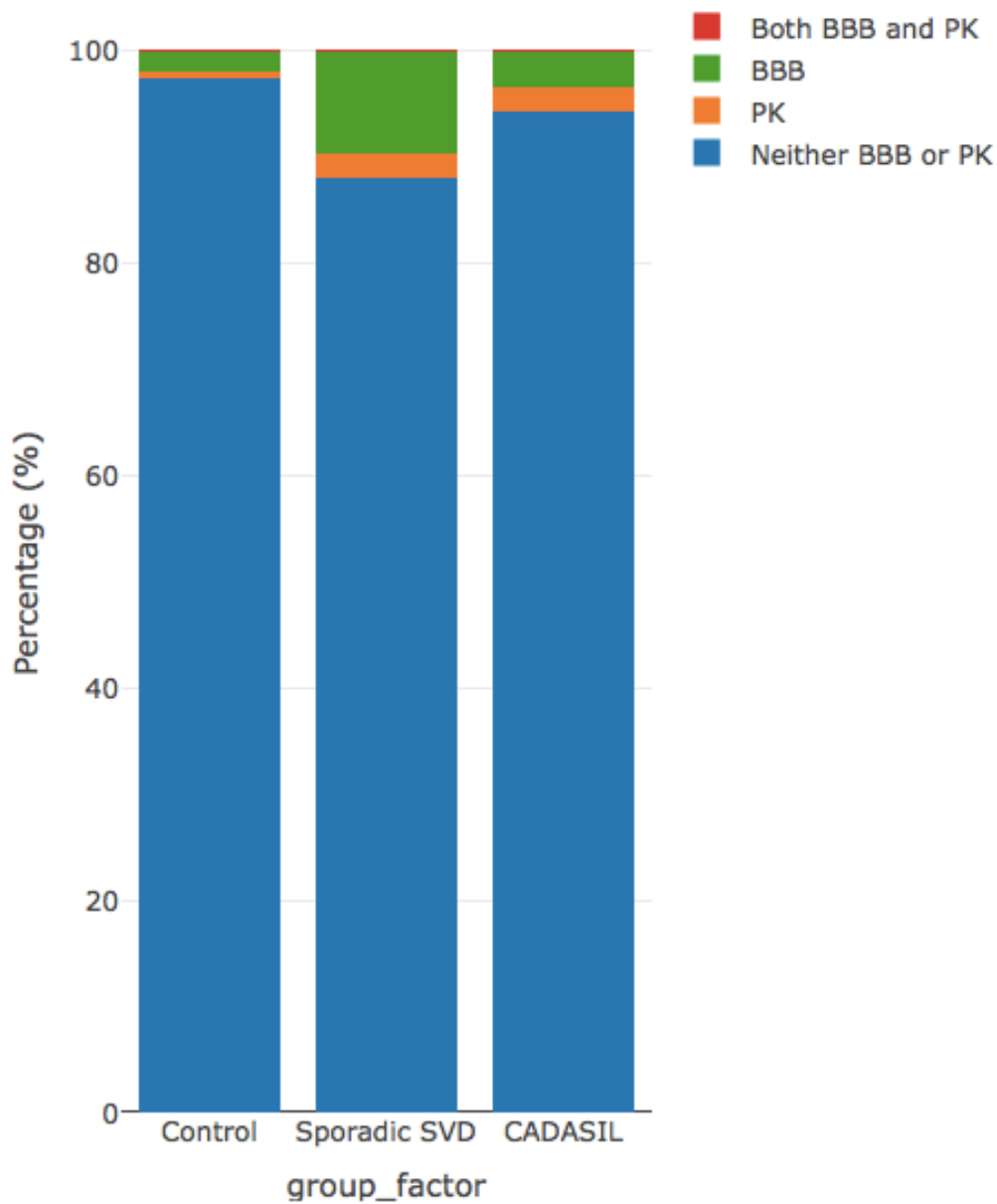
Figure 6.5: Distributions of the voxels in the WML for each group, displayed as a percentage. The control group was made up of 0.01% overlap, 1.83% BBB, 0.61% PK binding and 97.53% neither. The sporadic SVD group was made up of 0.31% overlap, 9.59% BBB, 2.22% PK binding and 87.93% neither. The CADASIL group was made up of 0.07% overlap, 3.40% BBB, 2.15% PK binding and 94.31% neither. There was a significant difference in the distribution between the groups (p<0.001).

6.3.3 Overlap Analysis of BBB permeability and PK binding Voxels

Tests of independence were used within the groups, to see if there was a significantly different distribution of voxels compared to chance.

In the control group, there was no significant difference from chance for the distribution of the voxels in the WM, NAWM or the WML (Table 6.4).

In the sporadic SVD group, the number of voxels with both significantly high permeability and inflammation was significantly lower than expected by chance in the WM ($p<0.001$), NAWM ($p<0.001$) and WML ($p<0.001$) (Table 6.5).

In the CADASIL group, the number of voxels with both significantly high permeability and inflammation was significantly lower than expected by chance in the WM ($p<0.001$) and NAWM ($p<0.001$) (Table 6.6). However, there was no significant difference in the distribution to what is expected by chance in the WML.

A

	Inflammation	No inflammation	Total
Permeability	908 (858)	16400 (16450)	17308
No permeability	28562 (28612)	548812 (548762)	577374
Total	29470	565212	594682

B

	Inflammation	No inflammation	Total
Permeability	904 (861)	15976 (16019)	16880
No permeability	28194 (28237)	525415 (525372)	553609
Total	29098	541391	570489

C

	Inflammation	No inflammation	Total
Permeability	4 (4)	424 (424)	428
No permeability	198 (198)	19467 (19467)	19665
Total	202	19891	20093

Table 6.4: Contingency tables of observed (expected) values for the number of voxels with significant permeability and PK binding in the control group. A) WM (p=0.074). B) NAWM (p=0.127). C) WML (p=1.000).

A

	Inflammation	No inflammation	Total
Permeability	4191 (5454)	62007 (60744)	66198
No permeability	45966 (44703)	496583 (497846)	542549
Total	50157	558590	608747

B

	Inflammation	No inflammation	Total
Permeability	4019 (5845)	51315 (49489)	55334
No permeability	38252 (36426)	306556 (308382)	344808
Total	42271	357871	400142

C

	Inflammation	No inflammation	Total
Permeability	256 (335)	10608 (10529)	10864
No permeability	4883 (4804)	151019 (151098)	155902
Total	5139	161627	166766

Table 6.5: Contingency tables of observed (expected) values for the number of voxels with significant permeability and PK binding in the sporadic SVD group. A) WM (p<0.001). B) NAWM (p<0.001). C) WML (p<0.001).

A

	Inflammation	No inflammation	Total
Permeability	1052 (2188)	32828 (31692)	33880
No permeability	35060 (33924)	490291 (491427)	525351
Total	36112	523119	559231

B

	Inflammation	No inflammation	Total
Permeability	931 (2321)	24727 (23337)	25658
No permeability	28861 (27471)	274888 (276278)	303749
Total	29792	299615	329407

C

	Inflammation	No inflammation	Total
Permeability	215 (234)	8007 (7988)	8222
No permeability	6905 (6886)	235518 (235537)	242423
Total	7120	243525	250645

Table 6.6: Contingency tables of observed (expected) values for the number of voxels with significant permeability and PK binding in the CADASIL group. A) WM ($p < 0.001$). B) NAWM ($p < 0.001$). C) WML ($p = 0.210$).

6.4 Discussion

This chapter has shown that there is no relationship between the amount of BBB permeability and PK binding present. There was no significant spatial overlap in regions of significant BBB permeability and PK binding in the control group. However, in the sporadic SVD and CADASIL groups, the spatial locations of BBB permeability and PK binding are significantly distinct from one another in the whole WM and NAWM.

6.4.1 Correlating BBB permeability and PK binding

Associations between the BBB permeability and PK binding values were performed and displayed for the WM (Table 6.1), NAWM (Table 6.2) and WML (Table 6.3). There were no associations seen between any of the parameters in any of the groups.

Correlations were also explored between the BBB permeability and PK binding values for all of the groups combined, shown in Appendix D. This did find one significant correlation between the global PK binding and the mean value of the BBB permeability hotspots in the WM (Table D.1). However, no other correlations were seen and so it is likely that this was simply due to chance.

The lack of correlations was surprising, as we expected that patients with more severe disease would have increased PK binding and BBB permeability, which would mean the two parameters would correlate with one another. However, it seems the relationship is not as linear as expected.

It is difficult to put these findings into context of the literature, as PK binding for microglia activation and DCE-MRI for BBB permeability have not before been reported in an SVD population. Studies have investigated biomarkers of BBB permeability and inflammation SVD. However, only a very limited number have correlated these outcomes together, as most correlate instead with disease progression (Cipollini et al., 2019). Staszewski et al. used ICAM-1, a marker of endothelial inflammation, which could be considered a surrogate marker of BBB permeability;

they found a correlation with the inflammatory marker PF4, but not IL-1, TNF-α, IL6 or CRP (Staszewski et al., 2019). This study therefore also suggests that the cross-sectional relationship between BBB permeability and inflammation may not be linear. However, this study used blood biomarkers rather than neuroinflammatory markers and therefore only has limited similarities to our study.

PK binding and DCE-MRI has been investigated in acute intracerebral haemorrhage, where again, there was not a clear relationship between PK binding and permeability (Abid et al., 2018). Abid et al. found a consistent increased BBB permeability around the haematoma, but microglia activation only present in this region in some of the patients. This suggests that microglia activation is a dynamic process, which may have fast-moving timescales after stroke.

Larger studies in this area that investigate both the temporal and spatial overlap between inflammation and BBB permeability are needed to help understand the underlying pathophysiology of SVD. The latest developments in PET/MR technology have now made it possible to visualise these two processes in the same patients, and these techniques now need to be utilised for longitudinal follow-up of patients to improve our understanding of the complex relationship between these two important mechanisms.

6.4.2 BBB permeability and PK binding Distributions

There was a significant difference in the spatial distributions of the voxels across the different groups in the WM (Figure 6.3), NAWM (Figure 6.4) and WML (Figure 6.5).

The distribution of voxels followed a similar pattern to that seen in Chapters 4 and 5, where sporadic SVD and CADASIL had a higher volume of BBB permeability and PK binding, compared to control. Therefore, there were a higher number of voxels with significant BBB permeability and PK binding in the sporadic SVD and CADASIL groups, compared to control. This then means that we would expect to see a higher number of overlap voxels in the sporadic SVD and CADASIL groups compared to control, just by chance. Therefore, just because the relative number of

overlap voxels is higher in sporadic SVD and CADASIL groups, it does not mean that we can conclude that there is a spatial relationship between BBB permeability and PK binding in disease. A test that explores the spatial independence of BBB permeability and PK binding voxels from one another within each group is required to see if the amount of overlap voxels is significantly different from chance.

6.4.3 Spatial Analysis of BBB permeability and PK binding

Within each group, we analysed the distribution of overlap voxels, just BBB permeability voxels, just PK binding voxels and voxels with neither PK binding nor permeability, to see if the number of overlap voxels was equivalent to that expected by chance. In the control group, we found that there was no significant overlap, and therefore the spatial distribution of BBB permeability and PK binding was no different to chance in the WM, NAWM and WML (Table 6.4). However, in the sporadic SVD group, we found that there was significantly less overlap then you would expect by chance in the WM, NAWM and WML (Table 6.5). This finding was mirrored by the CADASIL group in the WM and NAWM, although the WML was not significantly different from chance (Table 6.6).

This finding is very interesting and unexpected, and suggests that the two processes are spatially distinct from one another. As the data here is cross-sectional, it could be that the activated microglia and increased BBB permeability occur at distinct stages of the pathological process, and so when taking a cross-sectional snapshot, you only see one of the pathologies, as it evolves through the mechanistic pathway over time. Both BBB permeability and microglia activation are both thought to be highly dynamic processes, although the detailed timescale of these dynamics has not been investigated (Shi and Wardlaw, 2016). Further follow-up scans are required to determine the timescale of voxels and whether they can transition from an inflammatory to permeability state, and vice versa, and whether permeability or inflammatory voxels eventually become WML.

Another explanation could be that, due to the anatomy of the brain, microglia activation does not occur near regions of BBB permeability, so even though they were

involved in the same pathological cascade, they could communicate through signalling proteins but remain spatially distinct from one another. Post-mortem studies have looked at investigating these pathologies together. A recent study showed that vascular bagging, where the space between the vessel wall and external collagenous membrane of small vessels becomes widened due to BBB leakage, and activated microglia were both present throughout the WMLs and in the neighbouring WM areas (Forsberg et al., 2018). Microglia were found to be particularly concentrated around damaged vessels, whilst vascular bagging was found more generally throughout the brain, with Forsberg et al. hypothesising it developed in the frontoparietal and temporal WM primarily. As increasingly high resolution imaging techniques develop, it should become more accessible to image these pathologies in vivo and localise them both anatomically and functionally.

The final option could be that the two pathologies are unrelated in SVD. This would contradict the previous animal studies, but may be the case if a pathological mechanism involving both pathologies cannot be established in human studies.

6.4.4 Limitations

The largest technical limitation of this study was the resolution of the images, which had a voxel size of 2.0 x 2.0 x 3 mm. At this resolution, we cannot measure these processes on a cellular level, and so are incorporating thousands of cells into every voxel, making it a crude measurement of the underlying processes. The cross-sectional nature of this study also limits the interpretation of the data, as we cannot know if these proposed pathological processes are causative of one another, or of damage to the WM.

As imaging techniques and technology improve, higher resolution scans will likely become available that will be able to investigate this process in more detail. High-resolution longitudinal imaging studies are needed to monitor the dynamics of microglia activation and BBB permeability in SVD, and the progression to WML and clinical symptoms, to understand if these mechanisms are involved in the pathological processes underlying the disease.

6.5 Summary of Findings

Returning to the aims of this chapter, the following areas have been addressed:

1. The amount of BBB permeability and PK binding were not significantly correlated
2. The distribution of voxels was significantly different between groups, with a higher proportion of BBB permeability and PK binding voxels in the sporadic SVD and CADASIL groups compared to control
3. In the control group, the number of overlap voxels (with both significant permeability and PK binding) was no different to chance
4. In the sporadic SVD and CADASIL groups, the number of overlap voxels was significantly lower than chance would suggest in the WM and NAWM; in the sporadic SVD, this pattern also exists in the WML

This chapter has explored the relationship between BBB permeability and PK binding, and the spatial overlap between the two. The next chapter will investigate inflammatory biomarkers in SVD, and their relation to BBB permeability and PK binding.

Chapter 7: Blood Biomarkers in SVD and their Relationship with BBB permeability and PK binding

7.1 Introduction

7.1.1 Aims of the Chapter

The previous chapters have explored BBB permeability and PK binding separately in relation to imaging markers and cognitive markers, and also in relation to one another. This chapter will investigate various serum biomarkers and explore differences between groups and the relationship between the biomarkers and BBB permeability and PK binding. The biomarkers studied in this chapter fall into the categories of inflammatory markers, MMPs and endothelial cell activation markers. This chapter will address the following specific questions:

- Are blood biomarkers increased in SVD patients compared to controls?
- Are blood biomarkers increased in CADASIL patients compared to controls?
- Are blood biomarkers associated with increased permeability, quantified from DCE-MRI?
- Are blood biomarkers associated with increased microglia activation, quantified from PET PK binding?

Exploratory hypotheses in this chapter are:

- Biomarkers will be increased in sporadic SVD patients and CADASIL patients compared to controls
- MMPs and markers of endothelial cell activation will be associated with increased BBB permeability
- Markers of inflammation will be associated with increased PK binding

7.1.2 Blood Biomarkers

Blood biomarkers provide simple measures that can be used in research as clinical trial end-points and in the clinic for diagnosis and tracking of disease progression (Kamtchum-Tatuene and Jickling, 2019), whilst also helping to further understand the

pathogenesis of a disease. Biomarker techniques tend to use labelled antibodies to tag the protein of interest and give a readout, which can then be quantified (Nimse et al., 2016). In the field of neurology, the relevance of blood biomarkers is debatable, as blood biomarkers are a reflection of systemic processes and may not be representative of what is happening in the CNS (Polivka et al., 2016).

There is a complex mechanistic pathway involved in the underlying pathology of SVD, which has not been fully characterised. There has been shown to be an inflammatory response involving microglia, neurons, astrocytes and endothelial cell release of pro-inflammatory markers (Rosenberg, 2018). This triggers inflammatory cascades both within the brain and within the vessel walls, leading to a breakdown in BBB integrity, which increases its permeability. Therefore, markers of this cascade may be present systemically.

The pathogenesis is easiest to be explored in animal models, where pathways and processes can be easily manipulated and measured (Chesselet and Carmichael, 2012). Much of the current literature has focused on ischaemic events to investigate neuroinflammation (Kawabori and Yenari, 2015). The literature tends to focus on either focal ischaemia, such as the result of a stroke, or global ischaemia, such as the result of a heart attack (Traystman, 2003). There is also literature on neurodegenerative disorders, such as Alzheimer's disease and MS (Chen et al., 2016). Focal acute mechanisms are relevant to SVD pathology as SVD is associated with lacunar stroke from acute blockage of the small vessels. However, the mechanisms are likely to be more complex in SVD, as SVD is also associated with chronic hypoxia due to small vessel damage, which may be more related to the global ischaemic and neurodegenerative mechanisms. This introduction will review the key neuroinflammatory mechanisms from the literature that have the most relevance to SVD pathology.

7.1.3 Inflammation

During acute ischaemia, cells become hyperactive or die, resulting in a release of glutamate and excitotoxicity (Terasaki et al., 2014). Excitotoxicity in chronic

ischaemia, such as SVD, has not been studied as widely as acute ischaemia. However, evidence suggests that chronic ischaemia also leads to an increase in glutamate, and that even a 10% increase in glutamate is enough to activate pathological cascades (Lewerenz and Maher, 2015)

ROS are released from the brain and immune cells in response to excitotoxicity, leading to oxidative stress. An inflammatory response is also triggered both centrally and peripherally; microglial activation in the brain triggers various inflammatory cascades, opening the BBB and allowing activated blood-borne immune cells, such as neutrophils and T-cells, to infiltrate.

Pro-inflammatory cytokines TNF-α, interleukin 1 (IL-1) and interleukin 6 (IL-6) are all released by activated cells including neurons, astrocytes, microglia and endothelial cells (Yang and Rosenberg, 2015, Doll et al., 2014). This can also trigger a wider systemic inflammatory response throughout the body.

TNF-α precursor is membrane bound and cleaved by TNF-α converting enzyme (TACE) to release the soluble form of TNF-α that can bind to TNFR1 or TNFR2 (Liu et al., 1996). Virtually all cell types and tissues express TNFR1, which has an intracellular death domain, in which the adaptor protein TNFR-associated death domain protein (TRADD) can interact and elicit signalling for cell death or cell survival through recruitment of other adaptor proteins such as caspase-8 and FAS (Pobezinskaya and Liu, 2012). TNFR2 is mostly linked to the nuclear factor kappa-light-chain-enhancer of activated B cells (NF-κB) mediated inflammatory pathway (Rothe et al., 1995). Activation of the NF-κB pathway is commonly used as an indicator of inflammation in ischaemic stroke studies (Majid, 2014). Therefore, TNF-α can lead to cell death and inflammation, depending on which receptor it is bound to and which cascades are activated.

IL-1 exists as a family of 11 members, but IL-1α and IL-1β are the most important in the context of stroke (Sobowale et al., 2016). Both IL-1α and IL-1β are created as precursor proteins, which undergo cleavage into their active forms. IL-1α has some biological activity in its precursor state, whereas IL-1β is biologically inactive until it

is cleaved by caspase-1 (Thornberry et al., 1992). Both IL-1α and IL-1β produce their biological effects through binding to IL-1R1 which associates with the IL-1R1 accessory protein (IL-1RAcP) and initiates intracellular signalling (Korherr et al., 1997). IL-1 can also potentiate inflammation by activating microglia, increasing leukocyte infiltration and increasing breakdown of the BBB.

Another important member of the IL-1 family in the context of stroke is IL-18. IL-18 is a pro-inflammatory cytokine acting in both acquired and innate immunity and playing a crucial role in the inflammatory cascade (Yuen et al., 2007). IL-18 is also related to the atherosclerotic plaque propagation and instability. IL-18 acts as a modifier for the immune response through inducing cytokine gene expression and T helper cell differentiation, activating natural killer cells (Sedimbi et al., 2013).

IL-6 is an interleukin that can have both pro-inflammatory and anti-inflammatory effects (Rothaug et al., 2016). IL-6 induces the hepatic acute phase response and is involved in lymphocyte and monocyte differentiation. IL-6 is an activator of the Janus Kinase (JAK)/signal transducer and activator of transcription (STAT) signalling pathway, which has many effects including increasing astrogliosis and angiogenesis for tissue remodelling and recovery after ischaemia (Erta et al., 2012). Other IL-6 mechanisms include inhibiting TNF-α, inducing apoptosis in neutrophils and recruiting monocytes and T-cells (Marz et al., 1996).

CHI3L1, also known as YKL-40, is a plasma protein produced by various cell-types including macrophages, vascular smooth muscle cells and some types of cancer cells (Kazakova and Sarafian, 2009, Renkema et al., 1998, Schultz and Johansen, 2010, Shao, 2013). The precise function of CHI3L1 is not fully understood, but it is thought to be involved in tissue remodelling during inflammation and in the angiogenic processes mediating infiltration, differentiation and maturation of macrophages and is therefore considered a marker of inflammation (Shao, 2013, Rathcke and Vestergaard, 2009, Rehli et al., 2003, Rehli et al., 1997). It was originally thought to only be associated with macrophages, but recent studies suggest it is abundant in astrocytes and microglial cells also, making it a key player in neuroinflammation (Bonneh-Barkay et al., 2010).

Inflammation in the CNS and vasculature can trigger a global inflammatory response seen by generic markers of inflammation. CRP is a biomarker of systemic inflammation, secreted by hepatocytes in response to cytokines, such as IL-6, IL1 and TNF-α (Chandra et al., 2014). CRP is not disease specific but is a sensitive marker produced in response to tissue injury, infectious agents, immunological stimuli and inflammation.

7.1.4 MMPs

Microglia, macrophages, infiltrating neutrophils, TNF-α and IL-1β are all involved in the transcription of MMPs. MMPs are a family of 26 extracellular and intracellular matrix-degrading enzymes that are important in development, tumour growth, brain development and injury (Rosenberg, 2016). In recent years, MMPs have become a point of interest for ischaemic stroke, after studies revealed that they have an important role in acute ischaemia (Yang and Rosenberg, 2015). Interest in MMPs in neurodegenerative disorders has also increased recently, with a role for them established in Alzheimer's disease, Parkinson's disease, ALS, Huntington's disease and MS (Brkic et al., 2015).

Extracellular matrix is the primary site of MMP action, but they are also involved in releasing molecules from the cell surface, cell signalling and cell death (Yong, 2005). MMPs act at several sites in the neurovascular unit, regulating the permeability of the BBB. Their major site of action is on the proteins in the basal lamina and the tight junction proteins, but studies indicate they can also act intracellularly (Yang et al., 2007, Yang et al., 2010). Tissue inhibitors of metalloproteinases (TIMPs) are endogenous inhibitors of MMPs and, to date, four of them have been identified (Brew and Nagase, 2010). Once MMPs are activated, they are generally rapidly inactivated by a series of mechanisms that mainly involve the four TIMPs (Yang and Rosenberg, 2015).

MMP-2 and MMP-14 are constitutive enzymes, present in latent forms under normal conditions, which are initially activated in hypoxic/ischaemic injury (Yong et al.,

2001). MMP-2 and MMP-14 are present in brain cells, particularly in astrocytes where the foot processes are connected to the endothelial cells (Yang and Rosenberg, 2015). The activation of the constitutive enzymes is strictly controlled in a spatially specific manner, close to the site of activation. The biological basis for this is that MMP-2 and MMP-14 are activated in a trimolecular complex with metalloproteinase inhibitor-2 (TIMP-2). MMP-14 is bound to the membrane and therefore the activated MMP-2 is also connected to the membrane so the activity of the enzyme is constrained to the region close to the activation site and prevents MMP-2 doing extensive damage. MMP-2 initiates disruption of the basal lamina proteins and opening of the tight junction proteins, increasing permeability of the BBB (Yang et al., 2007). If the hypoxic stress is short-lived and there is no further MMP activation, then this initial phase is reversible and there can be a restoration of the basal lamina integrity (Rosenberg, 2016).

If hypoxia progresses, as it is thought to do in SVD, the inducible enzymes of MMP-3 and MMP-9 are released and activated (Yang and Rosenberg, 2015). The inducible enzymes have a much wider spread effect and are not constrained to only act close to the site of action, so this can lead to more extensive tissue damage. Microglia, macrophages and infiltrating neutrophils are the primary sources of MMP-3 and MMP-9. Cytokines activate the transcription sites leading to the formation of latent forms of the inducible enzymes, and then nitrosylation and other free radicals lead to their activation. This leads to major irreversible damage to the cerebral vessels with vasogenic oedema. Matrix metalloproteinase-8 (MMP-8) and matrix metalloproteinase-13 (MMP-13) are also involved in injury cascades (Cuadrado et al., 2009), with MMP-8 having a critical role in mediating microglial activation through modulation of TNF-α activity (Yang and Rosenberg, 2015). Both MMPs and cytokines may be expressed in the blood during an inflammatory response to injury and infection.

7.1.5 Endothelial Cell Activation

Endothelial cells make up a key component of the BBB, with particular importance given to their tight junctions. Markers of endothelial cell activation have been

measured and seen to increase in ischaemic stroke (Cherian et al., 2003), neurodegeneration (Maiuolo et al., 2018) and SVD specifically (Poggesi et al., 2016). Markers of endothelial cell activation are predominantly cellular adhesion molecules.

Tight junctions are a key to the function of endothelial cells and the BBB. Tight junctions consist of three integral membrane proteins: claudin, occluding and junctional adhesion molecules (JAM), as well as several cytoplasmic accessory proteins including ZO-1, cingulin, CDH5, platelet endothelial cell adhesion molecule-1 (PECAM-1), activated leukocyte cell adhesion molecule (ALCAM), ICAM-1 and vascular cell adhesion molecule 1 (VCAM-1) (Yu et al., 2015). These proteins are key to seal the cell-cell contacts of endothelial cells and therefore have an important role in BBB permeability (Luissint et al., 2012).

During injury, one of the most important events is the adhesion of leukocytes to the endothelium, which precedes their emigration to the tissues and is central to the inflammatory process (Panés et al., 1999). The recruitment of leukocytes and platelets in the cerebral microvascular is widely regarded as a rate-limiting step in the inflammatory response associated with cerebral hypoxia/ischaemia (Yilmaz and Granger, 2008). In response to hypoxia/ischaemia (or other inflammatory insult), the cerebral endothelium expresses high levels of adhesion molecules to recruit large numbers of leukocytes. The interaction appears to be largely mediated by P-selectin expressed on endothelial cells, which engages with circulating cells (Ishikawa et al., 2003). Firm adhesion is then mediated by an interaction between ITGB2 on leukocytes with ICAM-1 on cerebral endothelial cells (Liu and Kubes, 2003). Studies of acute ischaemia have shown that P-selectin upregulation occurs as early as 15 minutes following ischaemic insult, with increased E-selectin expression occurring within 2 hours (Zhang et al., 1998). Additional adhesion molecules have also been shown to partake in the transmigrational process of leukocytes, including ALCAM (Cayrol et al., 2008).

Platelet adhesion seems to occur through a leukocyte independent method, and a leukocyte-dependent method. Increased leukocyte adhesion is accompanied by the recruitment of platelets (Ishikawa et al., 2004), and the leukocyte-dependent methods

involves the binding of platelet-associated P-selectin to its ligand P-selectin glycoprotein ligand 1 (PSGL-1) on leukocytes, which in turn utilise endothelial cell P-selectin to create a platform on which leukocytes can establish a firm adhesion with ICAM-1, independent of ITGB2 (Yilmaz and Granger, 2008). Platelet independent method involves the binding of glycoprotein receptors to various ligands expressed on the surface of endothelial cells such as vWF, ICAM-1 and P-selectin (Tailor et al., 2005). vWF, released during endothelial cell activation can also bind to the glycoprotein receptors to bind platelets to the endothelium.

Interestingly, the effect of P-selectin seems to differ in focal versus global cerebral ischaemia, and therefore the role that it would have in SVD is unclear. Blocking P-selectin in either model reduces leukocyte-endothelium interaction. However, in focal iscahemia, knockout mice of P-selectin had reduced neurological deficits compared to control (Connolly et al., 1997), suggesting P-selectin has detrimental effects. However, in global cerebral ischaemia, blocking P-selectin reduced survival (Lehmberg et al., 2006), suggesting a protective role.

7.1.6 Relation to SVD

The hypothesised cascade thought to be occurring in SVD can be seen in Figure 7.1. The evidence for the involvement of these mechanisms in SVD has predominantly come from studies of ischaemic stroke and neurodegeneration. Therefore, the relevance of these mechanisms to SVD specifically is unclear. Animal models of SVD have hypothesised that these mechanisms are occurring (Jalal et al., 2012, Kaiser et al., 2014), but the number of studies that have investigated this in SVD is far fewer than for ischaemic stroke or neurodegeneration. It is important to see if these mechanisms are occurring in human SVD, to understand their role in the pathophysiology.
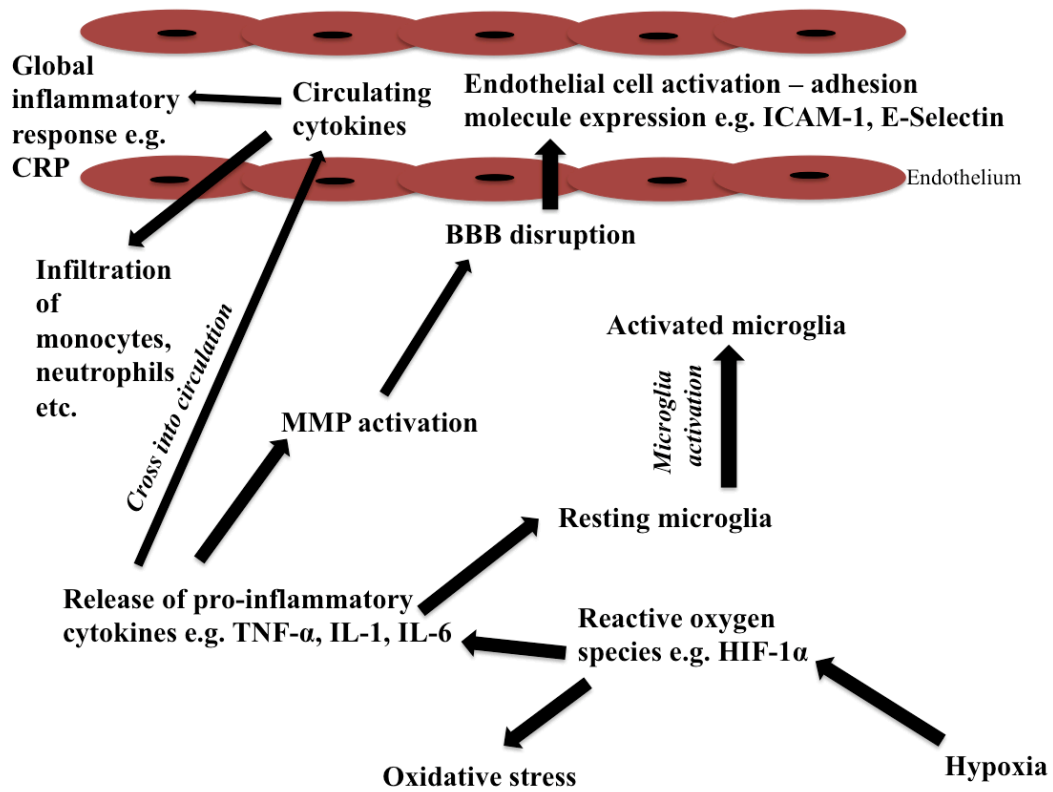
Figure 7.1: Hypothesised cascade occurring in SVD where the initial response of hypoxia leads to ROS activation, and the release of pro-inflammatory cytokines. These then activate microglia, MMPs and initiate a global inflammatory response. MMPs then lead to BBB disruption and endothelial cell activation.

7.2 Methods

Serum samples were taken from 20 controls, 20 sporadic SVD and 20 CADASIL patients and were used for the group comparisons. A DCE-MRI scan was carried out in 19 controls, 19 sporadic SVD and 19 CADASIL patients and was used to compare the blood biomarkers with BBB permeability. PK PET was taken from 17 controls, 16 sporadic SVD and 14 CADASIL patients and was used to compare the blood biomarkers with microglia activation.

The majority of the methodology for this chapter is discussed in Chapter Two.

7.2.1 Biomarkers

As discussed in Chapter Two, the sample analysis carried out by Olink Proteomics and the Core Biochemical Assay Laboratory at Addenbrooke's Hospital, which together provided a total of 93 biomarker quantifications from our serum samples. To decide which were useful to investigate, we used hypothesis driven methods from the literature detailed in the introduction, to understand which biomarkers are likely be involved in SVD. The biomarkers we investigated are as follows:

- **Inflammation:** TNF-R1, TNF-R2, FAS, IL1-RT1, IL-6Rα, IL-18BP, CRP and CHI3L1
- **MMPs**: MMP-2, MMP-3, MMP-9 and TIMP-4
- **Endothelial cell activation:** E-selectin, P-selectin, ITGB2, vWF, CDH5, JAM-A, PECAM-1 and ALCAM

7.2.2 Statistical Analysis

ANCOVA analyses were used to compare between sporadic SVD and control, and between CADASIL and control. ANCOVAs were performed between the sporadic SVD and control groups and the CADASIL and control groups, controlled for age and sex. Pairs of comparisons were adjusted using Bonferroni. If significance was seen then the analysis was then repeated controlling for the cardiovascular risk factors of

hypertension, hyperlipidaemia, type 2 diabetes and smoking, to see if the significance was still present.

Most of the biomarkers met assumptions of normality. However, TIMP-4, vWF, CRP and CHI3L1 did not meet normality assumptions, and were therefore log transformed (base:10) prior to analysis.

Multivariate linear models were used to investigate the associations between individual biomarkers (independent) and BBB permeability or PK binding parameters (dependent), controlled for sex and age. When significant associations were seen, a further linear model controlling for the cardiovascular risk factors was performed to see if the significance was still present. Biomarkers were transformed in the same way as detailed above and BBB permeability and PK binding parameters were transformed in the same way as detailed in Chapters Four and Five respectively. They were corrected for multiple comparisons with FDR.

7.3 Results

7.3.1 Inflammation

Mean values and group comparisons for each of the inflammatory markers are shown in Table 7.1. TNFR1 was significantly higher in sporadic SVD compared to control when controlled for age and sex (p=0.002 (p=0.003 when adjusted for multiple comparisons)) and cardiovascular risk factors (p=0.002). Similarly, TNFR2 was also significantly higher in sporadic SVD compared to control when controlled for age and sex (p=0.001 (p=0.003 when adjusted for multiple comparisons)) and cardiovascular risk factors (p=0.002). There was no significant difference between CADASIL and control groups for TNFR1 or TNFR2.

FAS was significantly higher in sporadic SVD compared to control when controlled for age and sex (p=0.020 (p=0.040 when adjusted for multiple comparisons)) and cardiovascular risk factors (p=0.019). There was no significant difference between CADASIL and control.

IL1-RT1 was significantly higher in sporadic SVD compared to control when controlled for age and sex (p=0.002 (p=0.004 when adjusted for multiple comparisons)) and cardiovascular risk factors (p=0.001). Similarly IL-18BP was significantly higher in sporadic SVD compared to control when controlled for age and sex (p<0.001 (p<0.001 when adjusted for multiple comparisons)) and cardiovascular risk factors (p<0.001). There was no significant difference between sporadic SVD and control for IL-6Rα. There was no significant difference between CADASIL and control for IL1-RT1, IL-6Rα or IL-18BP.

CRP was not significantly different between sporadic SVD and control or between CADASIL and control. Similarly, CHI3LT was not significantly higher in sporadic SVD compared to control or CADASIL compared to control

	Control		Sporadic SVD		CADASIL		SVD vs. control	CADASIL vs. control
	Mean	SD	Mean	SD	Mean	SD	P value	P value
TNFR1	6.98	0.37	7.34	0.36	6.98	0.33	**0.003**	1.000
TNFR2	6.00	0.39	6.35	0.28	6.03	0.41	**0.003**	1.000
FAS	6.38	0.31	6.63	0.38	6.20	0.34	**0.040**	0.199
IL1-RT1	6.67	0.31	6.97	0.30	6.62	0.34	**0.004**	1.000
IL-6Rα	12.24	0.46	12.42	0.36	12.39	0.43	0.356	0.581
IL-18BP	6.21	0.32	6.57	0.27	6.23	0.33	**<0.001**	1.000
CRP	3.91	3.44	2.84	1.98	4.38	4.71	0.510	1.000
CHI3L1	4.68	0.83	5.26	0.93	4.56	0.75	0.062	1.000

Table 7.1: Group comparisons between the inflammatory markers were performed, controlling for age and sex. Comparisons were performed between the sporadic SVD and control groups, and the CADASIL and control groups. Significant p values are shown in bold.

7.3.2 MMPs

Mean values and group comparisons for each of the MMPs are shown in Table 7.3. MMP-2 was significantly higher in the sporadic SVD group compared to control when controlled for age and sex (p=0.016 (p=0.033 when adjusted for multiple comparisons)) and cardiovascular risk factors (p=0.014). There was no significant difference in MMP-2 levels between CADASIL and control. MMP-3 was not significantly different between sporadic SVD and control, or CADASIL and control. There was no significant difference in MMP-9 levels between sporadic SVD and control or CADASIL and control. Similarly, TIMP-4 was not significantly different between sporadic SVD and control or CADASIL and control.

	Control		Sporadic SVD		CADASIL		SVD vs. control	CADASIL vs. control
	Mean	SD	Mean	SD	Mean	SD	P value	P value
MMP-2	4.08	0.38	4.38	0.39	3.93	0.35	**0.033**	0.385
MMP-3	8.30	0.64	8.37	0.72	8.26	0.69	1.000	1.000
MMP-9	6.81	0.62	7.11	0.62	7.22	0.48	0.286	0.056
TIMP-4	3.60	0.52	3.88	0.47	3.68	0.63	0.111	1.000

Table 7.3: Group comparisons between the MMPs were performed, controlling for age and sex. Comparisons were performed between the sporadic SVD and control groups, and the CADASIL and control groups. Significant p values are shown in bold.

7.3.3 Endothelial Cell Activation

Mean values and group comparisons for each of the markers of endothelial cell activation are shown in Table 7.4. E-selectin was significantly higher in the sporadic SVD group compared to control when controlled for age and sex (p=0.007 (p=0.014 when adjusted for multiple comparisons)) and cardiovascular risk factors (p=0.006). There was no significant difference in the CADASIL group. P-selectin and ITGB2 both were not significantly different between the sporadic SVD and control or the CADASIL and control groups.

vWF, CDH5 and JAM-A were not significantly different between the sporadic SVD
and control groups or the CADASIL and control groups.

PECAM-1 was significantly higher in the sporadic SVD group compared to control
when controlling for age and sex (p=0.002 (p=0.003 when adjusted for multiple
comparisons)) and cardiovascular risk factors (p=0.001). ALCAM was also
significantly higher in the sporadic SVD group compared to control when controlling
for age and sex (p=0.004 (p=0.007 when adjusted for multiple comparisons)) and
cardiovascular risk factors (p=0.003). However, there was no significant difference in
PECAM-1 or ALCAM in the CADASIL group compared to control.

	Control		Sporadic SVD		CADASIL		SVD vs. control	CADASIL vs. control
	Mean	SD	Mean	SD	Mean	SD	P value	P value
E-selectin	12.14	0.50	12.60	0.50	12.31	0.76	**0.014**	0.861
P-selectin	10.93	0.53	11.14	0.40	10.94	0.48	0.293	1.000
ITGB2	5.21	0.43	5.43	0.37	5.32	0.43	0.125	0.828
vWF	8.45	0.75	8.46	0.73	8.00	0.66	1.000	0.090
CDH5	4.88	0.43	5.05	0.30	4.94	0.36	0.302	1.000
JAM-A	4.53	0.42	4.65	0.33	4.59	0.33	0.577	1.000
PECAM-1	4.68	0.83	5.26	0.93	4.56	0.75	**0.003**	1.000
ALCAM	7.70	0.40	8.02	0.33	7.76	0.32	**0.007**	1.000

Table 7.4: Group comparisons between the endothelial cell activation markers were
performed, controlling for age and sex. Comparisons were performed between the
sporadic SVD and control groups, and the CADASIL and control groups. Significant
p values are shown in bold.

7.3.4 Biomarkers and BBB permeability in the sporadic SVD group

Linear models were used to investigate the association between the inflammatory biomarkers and the BBB permeability parameters in the sporadic SVD group (Table 7.5). TNFR1 was significantly negatively associated with both global permeability (β =-0.792, p=0.009 (p=0.039 when adjusted for multiple comparisons)) and the volume of the permeability hotspots (β=-0.813, p=0.005 (p=0.028 when adjusted for multiple comparisons)) in the NAWM. When controlled for cardiovascular risk factors, the significance was still present with global permeability (β =-0.973, p<0.001) and hotspot permeability volume (β =-1.079, p=0.002). Similarly, TNFR2 was significantly negatively associated with both global permeability (β =-0.785, p=0.008 (p=0.039 when adjusted for multiple comparisons)) and the volume of the permeability hotspots (β=-0.759, p=0.007 (p=0.028 when adjusted for multiple comparisons)) in the NAWM. When controlled for cardiovascular risk factors, the significance was still present with the global permeability (β =-0.835, p=0.007) and hotspot permeability volume (β =-0.842, p=0.013). None of the other inflammatory biomarkers were significantly associated with the BBB permeability in the NAWM. None of the inflammatory biomarkers were significantly associated with BBB permeability in the WML.

Linear models were used to investigate the association between MMPs and BBB permeability parameters in the sporadic SVD group (Table 7.6). There was no significant association between any of the MMPs and any of the BBB permeability parameters in the NAWM or the WML.

Linear models were then used to investigate the association between the markers of endothelial cell activation and BBB permeability parameters in the sporadic SVD group (Table 7.7). There was no significant association between any of the markers of endothelial cell activation and the markers of BBB permeability in the NAWM or the WML.

A

NAWM	Global		Hotspot mean		Hotspot volume	
Biomarker	β	P value	β	P value	β	P value
TNFR1	**-0.792**	**0.039**	-0.260	0.740	**-0.813**	**0.028**
TNFR2	**-0.785**	**0.039**	-0.147	0.740	**-0.759**	**0.028**
FAS	-0.303	0.437	0.244	0.740	-0.338	0.395
IL1-RT1	-0.008	0.992	0.135	0.740	-0.071	0.892
IL-6Rα	-0.422	0.193	-0.451	0.479	-0.260	0.478
IL-18BP	-0.621	0.135	0.049	0.881	-0.679	0.060
CRP	0.003	0.992	-0.167	0.740	0.033	0.892
CHI3L1	0.201	0.601	0.392	0.479	-0.068	0.892

B

WML	Global		Hotspot mean		Hotspot volume	
Biomarker	β	P value	β	P value	β	P value
TNFR1	-0.756	0.086	-0.301	0.447	-0.759	0.080
TNFR2	-0.700	0.086	-0.583	0.243	-0.632	0.088
FAS	-0.279	0.504	-0.273	0.447	-0.227	0.754
IL1-RT1	0.016	0.956	-0.054	0.857	-0.032	0.912
IL-6Rα	-0.285	0.504	-0.259	0.447	-0.182	0.754
IL-18BP	-0.659	0.099	-0.619	0.243	-0.643	0.088
CRP	0.135	0.676	0.213	0.447	0.109	0.865
CHI3L1	0.151	0.676	0.319	0.447	-0.080	0.865

Table 7.5. Linear models showing standardised β coefficients and p values for the associations between the inflammatory markers and the BBB permeability values in the NAWM (A) and the WML (B) for the sporadic SVD group. Significant p-values are shown in bold.

A

NAWM	Global		Hotspot mean		Hotspot volume	
Biomarker	β	P value	β	P value	β	P value
MMP-2	-0.303	0.505	0.067	0.954	-0.359	0.229
MMP-3	-0.187	0.505	0.351	0.609	-0.368	0.229
MMP-9	-0.173	0.505	-0.248	0.609	-0.174	0.470
TIMP-4	-0.340	0.505	-0.015	0.954	-0.461	0.229

B

WML	Global		Hotspot mean		Hotspot volume	
Biomarker	β	P value	β	P value	β	P value
MMP-2	-0.301	0.559	-0.271	0.680	-0.305	0.502
MMP-3	-0.081	0.793	-0.092	0.744	-0.175	0.688
MMP-9	-0.067	0.793	0.143	0.744	-0.082	0.736
TIMP-4	-0.382	0.559	-0.257	0.680	-0.457	0.268

Table 7.6. Linear models showing standardised β coefficients and p values for the associations between the MMPs and the BBB permeability values in the NAWM (A) and the WML (B) for the sporadic SVD group. Significant p-values are shown in bold.

A

NAWM	Global		Hotspot mean		Hotspot volume	
Biomarker	β	P value	β	P value	β	P value
E-selectin	0.354	0.562	0.124	0.886	0.226	0.582
P-selectin	0.162	0.727	0.275	0.886	-0.144	0.582
vWF	-0.257	0.727	0.131	0.886	-0.320	0.582
ITGB2	-0.052	0.851	0.307	0.886	-0.197	0.582
CDH5	-0.123	0.727	0.074	0.886	-0.140	0.582
PECAM-1	-0.204	0.727	0.118	0.886	-0.332	0.582
ALCAM	-0.453	0.562	0.034	0.905	-0.474	0.523

B

WML	Global		Hotspot mean		Hotspot volume	
Biomarker	β	P value	β	P value	β	P value
E-selectin	0.417	0.476	0.456	0.302	0.258	0.482
P-selectin	-0.084	0.861	0.397	0.302	-0.351	0.390
vWF	-0.356	0.476	-0.246	0.672	-0.381	0.390
ITGB2	0.049	0.861	-0.044	0.873	-0.048	0.858
CDH5	-0.053	0.861	-0.149	0.767	-0.050	0.858
PECAM-1	-0.215	0.861	-0.131	0.811	-0.302	0.482
ALCAM	-0.396	0.476	-0.465	0.302	-0.380	0.390

Table 7.7. Linear models showing standardised β coefficients and p values for the associations between the endothelial cell activation markers and the BBB permeability values in the NAWM (A) and the WML (B) for the sporadic SVD group. Significant p-values are shown in bold.

7.3.5 Biomarkers and PK binding in the sporadic SVD group

Linear models were used to investigate the association between the markers of inflammation and PK binding parameters in the sporadic SVD group (Table 7.8). There was no significant association between any of the markers of inflammation and the any of PK binding values in the NAWM or the WML.

Linear models were then used to investigate the association between MMPs and PK binding parameters in the sporadic SVD group (Table 7.9). There were no association between any of the MMPs and any of the PK binding parameters in the NAWM. However, there was a significant positive association between MMP-3 and the mean value of the PK binding hotspots in the WML (β =0.568, p=0.012 (p=0.049 when adjusted for multiple comparisons)). This significance was still present when controlled for cardiovascular risk factors (β =0.850, p=0.010). There was no significant association between any of the other MMPs and any of the PK binding values in the WML.

Linear models were then used to investigate the association between the markers of endothelial cell activation and PK binding parameters in the sporadic SVD group (Table 7.10). There was no significant association between any of the markers of endothelial cell activation and the markers of PK binding in the NAWM or the WML.

A

NAWM	Global		Hotspot mean		Hotspot volume	
Biomarker	β	P value	β	P value	β	P value
TNFR1	0.517	0.452	0.667	0.182	0.624	0.300
TNFR2	0.450	0.452	0.650	0.182	0.537	0.300
FAS	0.447	0.452	0.482	0.182	0.261	0.530
IL1-RT1	0.648	0.360	0.167	0.604	0.046	0.883
IL-6Rα	-0.016	0.959	-0.225	0.479	-0.145	0.682
IL-18BP	0.710	0.360	0.659	0.182	0.567	0.300
CRP	0.300	0.452	0.360	0.270	0.449	0.300
CHI3L1	-0.073	0.950	0.483	0.182	0.349	0.383

B

WML	Global		Hotspot mean		Hotspot volume	
Biomarker	β	P value	β	P value	β	P value
TNFR1	-0.013	0.976	0.648	0.149	0.594	0.270
TNFR2	0.003	0.994	0.758	0.097	0.740	0.189
FAS	0.243	0.439	0.558	0.097	0.705	0.105
IL1-RT1	0.272	0.390	0.428	0.169	0.484	0.232
IL-6Rα	-0.303	0.266	-0.052	0.838	-0.172	0.622
IL-18BP	0.267	0.504	0.554	0.169	0.694	0.189
CRP	-0.177	0.537	0.536	0.097	0.330	0.338
CHI3L1	-0.126	0.685	0.353	0.228	0.088	0.783

Table 7.8. Linear models showing standardised β coefficients and p values for the associations between the inflammation markers and the PK binding values in the NAWM (A) and the WML (B) for the sporadic SVD group. Significant p-values are shown in bold.

A

NAWM	Global		Hotspot mean		Hotspot volume	
Biomarker	β	**P value**	β	**P value**	β	**P value**
MMP-2	0.276	0.880	0.244	0.565	0.038	0.902
MMP-3	0.074	0.880	0.387	0.565	0.258	0.902
MMP-9	-0.045	0.880	-0.156	0.565	-0.188	0.902
TIMP-4	0.159	0.880	0.310	0.565	0.109	0.902

B

WML	Global		Hotspot mean		Hotspot volume	
Biomarker	β	**P value**	β	**P value**	β	**P value**
MMP-2	0.175	0.800	0.335	0.376	0.271	0.510
MMP-3	0.093	0.800	**0.568**	**0.049**	0.451	0.429
MMP-9	-0.068	0.800	-0.261	0.376	-0.301	0.510
TIMP-4	0.094	0.800	0.079	0.786	0.083	0.809

Table 7.9. Linear models showing standardised β coefficients and p values for the associations between the MMPs and the PK binding values in the NAWM (A) and the WML (B) for the sporadic SVD group. Significant p-values are shown in bold.

A

NAWM	Global		Hotspot mean		Hotspot volume	
Biomarker	β	**P value**	β	**P value**	β	**P value**
E-selectin	-0.337	0.529	0.168	0.814	0.015	0.969
P-selectin	-0.141	0.788	0.283	0.708	0.306	0.775
vWF	-0.186	0.788	-0.043	0.887	-0.277	0.775
ITGB2	0.406	0.529	0.465	0.708	0.408	0.775
CDH5	0.632	0.139	0.228	0.708	0.079	0.969
PECAM-1	0.726	0.244	0.426	0.708	-0.015	0.969
ALCAM	0.084	0.809	-0.079	0.887	-0.018	0.969

B

WML	Global		Hotspot mean		Hotspot volume	
Biomarker	β	**P value**	β	**P value**	β	**P value**
E-selectin	-0.155	0.904	-0.234	0.549	-0.254	0.579
P-selectin	0.008	0.980	-0.354	0.332	-0.403	0.368
vWF	-0.358	0.571	0.024	0.930	-0.201	0.613
ITGB2	0.390	0.571	0.464	0.241	0.686	0.123
CDH5	0.311	0.571	0.469	0.241	0.533	0.128
PECAM-1	0.133	0.904	0.550	0.241	0.531	0.368
ALCAM	-0.090	0.904	0.049	0.930	-0.067	0.833

Table 7.10. Linear models showing standardised β coefficients and p values for the associations between the endothelial cell activation markers and the PK binding values in the NAWM (A) and the WML (B) for the sporadic SVD group. Significant p-values are shown in bold.

7.3.6 Biomarkers and BBB permeability in the CADASIL group

Linear models were used to investigate the association between the markers of inflammation and BBB permeability parameters in the CADASIL group (Table 7.11). There was no significant association between any of the markers of inflammation and the any of BBB permeability values in the NAWM or the WML.

Linear models were then used to investigate the association between MMPs and BBB permeability parameters in the CADASIL group (Table 7.12). There was a significant negative association between TIMP-4 and the mean value of the BBB permeability hotspots in the NAWM (β =-0.707, p=0.004 (p=0.014 when adjusted for multiple comparisons)). This significance was still present when controlled for cardiovascular risk factors (β =-0.825, p=0.001). There was no significant association between any other MMPs and BBB permeability in the NAWM, and there was no association with any of the BBB permeability parameters in the WML.

Linear models were used to investigate the association between the markers of endothelial cell activation and BBB permeability parameters in the CADASIL group (Table 7.13). There was no significant association between any of the markers of endothelial cell activation and the any of BBB permeability values in the NAWM or the WML.

A

NAWM	Global		Hotspot mean		Hotspot volume	
Biomarker	β	P value	β	P value	β	P value
TNFR1	-0.380	0.338	-0.156	0.940	-0.214	0.567
TNFR2	-0.247	0.586	-0.050	0.940	-0.258	0.567
FAS	-0.208	0.586	0.073	0.940	-0.069	0.799
IL1-RT1	0.168	0.586	-0.021	0.940	0.207	0.567
IL-6Rα	-0.184	0.586	-0.119	0.940	-0.302	0.567
IL-18BP	0.061	0.818	0.095	0.940	0.109	0.783
CRP	-0.558	0.188	-0.245	0.940	-0.381	0.567
CHI3L1	-0.496	0.188	-0.379	0.940	-0.369	0.567

B

WML	Global		Hotspot mean		Hotspot volume	
Biomarker	β	P value	β	P value	β	P value
TNFR1	-0.161	0.760	0.025	0.950	-0.106	0.688
TNFR2	-0.219	0.760	-0.112	0.950	-0.176	0.678
FAS	0.083	0.760	0.134	0.950	0.145	0.678
IL1-RT1	0.136	0.760	-0.016	0.950	0.190	0.678
IL-6Rα	-0.396	0.454	-0.255	0.950	-0.386	0.586
IL-18BP	0.115	0.760	0.137	0.950	0.151	0.678
CRP	-0.334	0.580	-0.077	0.950	-0.295	0.678
CHI3L1	-0.469	0.454	-0.253	0.950	-0.383	0.586

Table 7.11. Linear models showing standardised β coefficients and p values for the associations between the inflammation markers and the BBB permeability values in the NAWM (A) and the WML (B) for the CADASIL group. Significant p-values are shown in bold.

A

NAWM	Global		Hotspot mean		Hotspot volume	
Biomarker	β	P value	β	P value	β	P value
MMP-2	0.181	0.485	-0.203	0.452	0.013	0.961
MMP-3	-0.326	0.456	-0.557	0.156	-0.379	0.365
MMP-9	-0.563	0.075	-0.432	0.156	-0.416	0.259
TIMP-4	-0.537	0.075	**-0.707**	**0.014**	-0.448	0.259

B

WML	Global		Hotspot mean		Hotspot volume	
Biomarker	β	P value	β	P value	β	P value
MMP-2	-0.102	0.701	-0.291	0.318	-0.103	0.700
MMP-3	-0.367	0.390	-0.339	0.318	-0.389	0.355
MMP-9	-0.439	0.220	-0.341	0.318	-0.356	0.355
TIMP-4	-0.598	0.083	-0.499	0.214	-0.525	0.196

Table 7.12. Linear models showing standardised β coefficients and p values for the associations between MMPs and the BBB permeability values in the NAWM (A) and the WML (B) for the CADASIL group. Significant p-values are shown in bold.

A

NAWM	Global		Hotspot mean		Hotspot volume	
Biomarker	β	**P value**	β	**P value**	β	**P value**
E-selectin	-0.561	0.114	-0.424	0.422	-0.489	0.316
P-selectin	0.000	0.999	0.346	0.481	0.379	0.388
vWF	0.109	0.999	-0.450	0.422	0.173	0.823
ITGB2	-0.048	0.999	0.215	0.508	0.033	0.905
CDH5	0.466	0.268	-0.020	0.946	0.435	0.373
PECAM-1	0.063	0.999	-0.240	0.508	0.076	0.905
ALCAM	0.115	0.999	0.276	0.503	0.139	0.823

B

WML	Global		Hotspot mean		Hotspot volume	
Biomarker	β	**P value**	β	**P value**	β	**P value**
E-selectin	-0.378	0.468	-0.377	0.432	-0.315	0.515
P-selectin	0.353	0.468	0.494	0.401	0.462	0.434
vWF	0.162	0.761	0.137	0.860	0.125	0.737
ITGB2	0.083	0.761	0.202	0.829	0.117	0.737
CDH5	0.418	0.468	0.075	0.915	0.420	0.434
PECAM-1	0.104	0.761	-0.003	0.991	0.094	0.737
ALCAM	0.082	0.761	0.179	0.829	0.104	0.737

Table 7.13. Linear models showing standardised β coefficients and p values for the associations between the endothelial cell activation markers and the BBB permeability values in the NAWM (A) and the WML (B) for the CADASIL group. Significant p-values are shown in bold.

7.3.7 Biomarkers and PK binding in the CADASIL group

Linear models were used to investigate the association between the markers of inflammation and PK binding parameters in the CADASIL group (Table 7.14). There was no significant association between any of the markers of inflammation and the any of PK binding values in the NAWM or the WML.

Linear models were then used to investigate the association between MMPs and PK binding parameters in the CADASIL group (Table 7.15). There was no significant association between any of the MMPs and PK binding in the NAWM. There was a significant positive association between MMP-9 and the mean value of the PK binding hotspots in the WML (β =0.558, p=0.018 (p=0.037 when adjusted for multiple comparisons)). This significance was still present when controlled for cardiovascular risk factors (β =0.770, p=0.022). There was also a significant positive association between TIMP-4 and the mean value of the PK binding hotspots in the WML (β =0.499, p=0.018 (p=0.037 when adjusted for multiple comparisons)). This significance was still present when controlled for cardiovascular risk factors (β =0.516, p=0.047). There was no significant association between any of the other MMPs with the mean of the PK binding hotspots in the WML.

Linear models were then used to investigate the association between markers of endothelial cell activation and PK binding parameters in the CADASIL group (Table 7.16). There was a significant negative association between PECAM-1 and the mean value of the PK binding hotspots (β =-0.779, p=0.004 (p=0.031 when adjusted for multiple comparisons)). This significance was still present when controlled for cardiovascular risk factors (β =-0.773, p=0.006). There was no significant association between any of the other endothelial cell activation biomarkers and the PK binding in the NAWM. There was no significant association between any of the endothelial cell activation biomarkers and the PK binding in the WML.

A

NAWM	Global		Hotspot mean		Hotspot volume	
Biomarker	β	P value	β	P value	β	P value
TNFR1	0.118	0.892	-0.287	0.856	-0.104	0.898
TNFR2	0.180	0.892	-0.180	0.856	-0.059	0.898
FAS	0.216	0.892	-0.059	0.856	0.079	0.898
IL1-RT1	0.171	0.892	-0.276	0.856	-0.087	0.898
IL-6Rα	0.169	0.892	-0.074	0.856	-0.042	0.898
IL-18BP	-0.084	0.892	-0.387	0.856	-0.291	0.898
CRP	-0.044	0.892	0.076	0.856	-0.176	0.898
CHI3L1	0.115	0.892	0.202	0.856	-0.122	0.898

B

WML	Global		Hotspot mean		Hotspot volume	
Biomarker	β	P value	β	P value	β	P value
TNFR1	-0.250	0.772	0.054	0.940	0.205	0.745
TNFR2	-0.245	0.772	0.044	0.940	0.287	0.745
FAS	-0.067	0.815	-0.018	0.940	0.169	0.745
IL1-RT1	-0.096	0.815	-0.086	0.940	0.285	0.745
IL-6Rα	-0.364	0.757	0.072	0.940	0.330	0.745
IL-18BP	-0.081	0.815	-0.145	0.940	0.045	0.903
CRP	-0.164	0.815	0.480	0.080	-0.035	0.903
CHI3L1	-0.388	0.757	0.559	0.076	0.222	0.745

Table 7.14. Linear models showing standardised β coefficients and p values for the associations between the inflammation biomarkers and the PK binding values in the NAWM (A) and the WML (B) for the CADASIL group. Significant p-values are shown in bold.

A

NAWM	Global		Hotspot mean		Hotspot volume	
Biomarker	β	**P value**	β	**P value**	β	**P value**
MMP-2	0.113	0.843	-0.305	0.439	-0.124	0.805
MMP-3	0.277	0.843	-0.583	0.439	-0.544	0.805
MMP-9	0.074	0.843	-0.015	0.968	-0.093	0.805
TIMP-4	0.301	0.843	-0.425	0.439	-0.274	0.805

B

WML	Global		Hotspot mean		Hotspot volume	
Biomarker	β	**P value**	β	**P value**	β	**P value**
MMP-2	-0.309	0.259	-0.076	0.743	0.438	0.200
MMP-3	-0.602	0.209	0.314	0.513	0.562	0.238
MMP-9	-0.587	0.137	**0.558**	**0.037**	0.417	0.238
TIMP-4	-0.494	0.137	**0.499**	**0.037**	0.483	0.200

Table 7.15. Linear models showing standardised β coefficients and p values for the associations between the MMPs and the PK binding values in the NAWM (A) and the WML (B) for the CADASIL group. Significant p-values are shown in bold.

A

NAWM	Global		Hotspot mean		Hotspot volume	
Biomarker	β	P value	β	P value	β	P value
E-selectin	0.067	0.963	-0.453	0.272	-0.226	0.872
P-selectin	0.208	0.963	0.146	0.813	0.171	0.872
vWF	-0.367	0.963	-0.571	0.170	-0.778	0.032
ITGB2	-0.015	0.963	-0.179	0.812	-0.106	0.872
CDH5	-0.286	0.963	-0.534	0.170	-0.495	0.244
PECAM-1	-0.246	0.963	**-0.779**	**0.031**	-0.558	0.244
ALCAM	0.042	0.963	-0.039	0.901	0.043	0.894

B

WML	Global		Hotspot mean		Hotspot volume	
Biomarker	β	P value	β	P value	β	P value
E-selectin	-0.466	0.625	0.326	0.609	0.333	0.983
P-selectin	0.219	0.877	-0.040	0.884	0.130	0.983
vWF	-0.333	0.707	0.125	0.841	-0.156	0.983
ITGB2	0.016	0.956	-0.193	0.793	-0.006	0.983
CDH5	-0.131	0.902	-0.173	0.793	-0.012	0.983
PECAM-1	-0.295	0.707	-0.052	0.884	0.042	0.983
ALCAM	0.052	0.956	-0.297	0.609	0.109	0.983

Table 7.16. Linear models showing standardised β coefficients and p values for the associations between the endothelial cell activation biomarkers and the PK binding values in the NAWM (A) and the WML (B) for the CADASIL group. Significant p-values are shown in bold.

7.4 Discussion

This chapter reported an increase in the biomarkers TNFR1, TNFR2, IL1-RT1, IL-18BP, FAS and MMP-2 in sporadic SVD compared to control, suggesting that inflammation, MMPs and endothelial cell activation are involved in sporadic SVD. None of the biomarkers were significantly increased in CADASIL compared to control. TNFR1 and TNFR2 were both negatively associated with BBB permeability in the NAWM of sporadic SVD patients, whilst MMP-3 was significantly associated with PK binding in the WML. In the CADASIL group, TIMP-4 was significantly negatively associated with BBB permeability in the NAWM, but positively associated with PK binding in the WML. MMP-9 was also positively associated with PK binding in the WML and PECAM-1 was negatively associated with PK binding in the NAWM in the CADASIL group.

7.4.1 Inflammatory Biomarkers in sporadic SVD

Five out of the eight inflammatory biomarkers tested were found to be significantly elevated in SVD compared to control (Table 7.1). These biomarkers were TNFR1, TNFR2, FAS, IL1-RT1 and IL-18BP. TNFR1 and TNFR2 were significantly negative correlated with the global permeability and volume of the permeability hotspots in the NAWM (Table 7.5). Interestingly, none of the inflammatory biomarkers were associated with any of the PK binding parameters (Table 7.8).

TNFR1 and TNFR2 are the two cell membrane receptors of TNF-α (Faustman and Davis, 2010). We found both TNFR1 and TNFR2 were significantly elevated in our sporadic SVD group compared to controls. TNFR1 has not been previously studied in SVD, however, TNFR2 has been studied and has been significantly correlated with levels of CMBs, but not with lacunes or WMLs (Shoamanesh et al., 2015). Much of the previous SVD literature has focused on circulating levels of TNF-α itself and found it was significantly higher in lacunar stroke patients compared to non-stroke (Wiseman et al., 2014) and in vascular dementia patients compared to control (Tarkowski et al., 1999). Further, TNF-α has been associated with increased age and

hypertension in an SVD population (Wang et al., 2016) and with future vascular events in a longitudinal study (Boehme et al., 2016).

We found also found TNFR1 and TNFR2 to be negatively associated with the global mean and hotspot volume of BBB permeability in the NAWM. These results would suggest that higher levels of TNFR1 and TNFR2 are associated with lower levels of BBB permeability. TNFR1 and TNFR2 have been shown to be the mediators of transport of TNF-α across the BBB (Pan and Kastin, 2002). Therefore, one explanation for our finding could be that when there are higher levels of BBB permeability, TNFR1 and TNFR2 may be down-regulated as they are no longer required to transport TNF-α into the brain. An alternative explanation comes from some interesting work, which suggests pre-treatment of TNF-α is neuroprotective in animal models of ischaemic stroke (Nawashiro et al., 1997). Further, knocking out TNFR1 and TNFR2 receptors in mice was shown to exacerbate damage after ischaemic stroke (Bruce et al., 1996, Gary et al., 1998, Marchetti et al., 2004). Therefore, this increase in TNFR1 and TNFR2 may actually be protective against increased BBB permeability. As this is the first study to show this association, we must be cautious not to over-interpret the findings. However, our study does suggest that there is a role for the receptors of TNF-α in SVD disease pathogenesis, and further studies with larger numbers should investigate this further and see if these results can be replicated.

FAS levels were increased in sporadic SVD compared to control (Table 7.2). The increase in FAS suggests a role for apoptosis in sporadic SVD. FAS has not been previously investigated in SVD, but has been shown to be increased in mild ischaemic models (Wetzel et al., 2008). FAS had no association with BBB permeability or PK binding in sporadic SVD, suggesting it may not be involved in these pathogenic mechanisms and may instead by a resultant process of the ongoing damage occurring in SVD.

IL1-RT1 is a receptor for IL-1 and was significantly increased in sporadic SVD compared to control. Animal studies have suggested that this receptor is rapidly upregulated after stroke (Wang et al., 1997). Blood levels of IL1-RT1 have not been

studied in SVD. However, IL-1 has been studied in both its α and β forms. Interestingly, WML and lacune count were not associated with IL-1α (Staszewski et al., 2018) or IL-1β (Baune et al., 2009). However, our results would suggest an upregulation of IL1-RT1 in SVD.

IL-18BP, an antagonist of IL-18, was significantly increased in sporadic SVD compared to control. IL-18BP has not been reported in SVD, but IL-18BP was shown to improve neurological recovery in studies of experimental head injury (Yatsiv et al., 2002) and hyperoxia-induced brain injury (Felderhoff-Mueser et al., 2005), through its effects of blocking IL-18. IL-18 itself has been seen to be increased in type 2 diabetes (Aso et al., 2003), obesity (Esposito et al., 2002), stress (Sugama and Conti, 2008) and Alzheimer's disease (Ojala et al., 2009). IL-18 was also shown to be significantly associated with the number of CMBs (Miwa et al., 2011). Therefore, the upregulation of IL-18BP in SVD could be suggested to be a response of the immune system to act as natural protection against IL-18.

CHI3L1 was not significantly elevated in sporadic SVD compared to control and was not associated with any of the BBB permeability or PK binding parameters. CHI3L1 has never been investigated in sporadic SVD previously. However, it has been shown to have a role in type 2 diabetes (Di Rosa and Malaguarnera, 2016), large artery stroke (Chen et al., 2017) and intracerebral haemorrhage (Jiang et al., 2014). Further, elevated CHI3L1 in the general population was found to be associated with a two-fold increased risk of ischaemic stroke (Kjaergaard et al., 2015). It was also associated with worsened outcomes after ischaemic stroke (Rathcke et al., 2012) and heart failure (Harutyunyan et al., 2012). Therefore, CHI3L1 is likely to be a more general risk factor for cardiovascular disease rather than a marker for SVD specifically.

Interestingly, CRP was not seen to be significantly elevated in sporadic SVD compared to control or associated with any of the BBB permeability of PK binding parameters. CRP is the most widely studied marker of systemic inflammation, shown to be elevated in lacunar stroke compared to non-stroke (Wiseman et al., 2014). Cross-sectionally, CRP has been associated with WML volume (van Dijk et al., 2005, Wright et al., 2009, Raz et al., 2012, Satizabal et al., 2012, Rizzi et al., 2014) and

lacune count (Hoshi et al., 2005, Yoshida et al., 2009, Mitaki et al., 2016, Hilal et al., 2018), with greater progression of WML also associated with higher CRP levels at baseline (van Dijk et al., 2005). However, some studies have found that CRP is not associated with WMLs (Gunstad et al., 2006, Schmidt et al., 2006, Wada et al., 2008, Wersching et al., 2010, Wada et al., 2011, Rouhl et al., 2012, Aribisala et al., 2014) or with lacune count (van Dijk et al., 2005, Schmidt et al., 2006, Gottesman et al., 2009, Wada et al., 2011, Rouhl et al., 2012, Nylander et al., 2015, Shoamanesh et al., 2015). It is interesting that we did not see elevated CRP levels in the sporadic SVD group compared to control, as this is contradictory to the literature. It may be that the numbers from this study were too low to detect a difference; CRP is influenced by inflammatory responses occurring throughout the body and therefore it is possible that this noise makes it difficult to see the group difference with low numbers.

IL-6Rα was not seen to be significantly elevated in sporadic SVD compared to control and was also not associated with BBB permeability or PK binding. IL-6Rα is part of the receptor for IL-6, which binds to IL-6 with low affinity but does not produce a signal. After ischaemic stroke, IL-6Rα was seen to remain unchanged whilst IL-6 concentration significantly rose (Acalovschi et al., 2003). IL-6Rα has never before been reported in an SVD population. IL-6 itself has been widely reported in the literature and associated with WMLs (Fornage et al., 2008, Satizabal et al., 2012), lacunes (Hoshi et al., 2005, Yoshida et al., 2009) and CMBs (Shoamanesh et al., 2015, Miwa et al., 2011). However, not all studies have reported significant association between IL-6 and WMLs (Jefferson et al., 2007, Baune et al., 2009, Aribisala et al., 2014, Kim et al., 2014, Shoamanesh et al., 2015), lacunes (Baune et al., 2009, Satizabal et al., 2012, Shoamanesh et al., 2015) or CMBs (Lu et al., 2017). It has also been associated with SVD progression, defined as an increase in WMLs or development or new lacunes (Staszewski et al., 2018). The discrepancies with IL-6 here can be explained by the fact we were measuring the IL-6Rα, which is a subunit of the receptor, and therefore may not upregulate in the same way IL-6 has been seen to.

Our results suggest a role for TNFR1, TNFR2, FAS, IL1-RT1 and IL-18BP in sporadic SVD, suggesting that sporadic SVD is associated with a systemic

inflammatory response. Further, our results suggest a common pathogenesis between TNFR1 and TNFR2 with BBB permeability, which should be further explored.

7.4.2 Inflammatory Biomarkers in CADASIL

None of the inflammatory biomarkers were significantly increased in CADASIL patients compared to control (Table 7.1) and none of the biomarkers were significantly associated with BBB permeability (Table 7.11) or PK binding (Table 7.14).

CRP has been previously reported in CADASIL and the result mirrored that of our study, where levels were not significantly different from control (Campolo et al., 2013). I*n vitro* experiments of Notch3 signalling have suggested an associated with FAS-mediated apoptosis (Yamamoto et al., 2011). FAS signalling is a major apoptotic pathway in vascular smooth muscle cells, and therefore it has been suggested that, under normal conditions Notch3 signalling blocks FAS-mediated apoptosis (Wang et al., 2002). Therefore, Wang et al. suggested that in CADASIL, there may be increased FAS-dependent apoptosis of vascular smooth muscle cells. As TNF-α is the major activator of FAS-mediated apoptosis through TNFR1, then we may have expected to see an increase in TNFR1 and FAS in CADASIL. However, this was not the case in our study.

The result that none of the inflammatory biomarkers were elevated in CADASIL or related to BBB permeability or PK binding could be related to the finding that BBB permeability is not significantly elevated in CADASIL (Figure 4.1-3), and therefore there may be neuroinflammatory responses occurring that are restricted to the CNS, as the BBB is too intact to allow them to spill into the periphery. It is also important to note that many of these inflammatory biomarkers have been associated with ageing, and are thought to increase with age (Singh and Newman, 2011). Our CADASIL group is significantly younger than our control group (Table 3.1) and therefore, although we did control for age in our analyses, they may not have taken into account all of this variation and an age-matched control group is important to validate this finding. Finally, it could be that inflammation is not as important in CADASIL

256

disease pathogenesis and so we do not see the same elevation of circulating biomarkers as we do in sporadic SVD.

7.4.3 MMPs in sporadic SVD

MMP-2 was significantly increased in sporadic SVD compared to control (Table 7.3). MMP-3 was positively associated with increased mean value of the PK binding hotspots in the WML (Table 7.9).

MMP-2 was significantly increased in sporadic SVD in our study, but was not associated with BBB permeability or PK binding. Candelario-Jalil et al. previously investigated MMP-2 as an index in SVD, where CSF and plasma values were taken and indexed against albumin; they found a reduction in the MMP-2 index in vascular cognitive impairment patients (Candelario-Jalil et al., 2011). Another study found that MMP-2 could separate SVD from Alzheimer's disease (Bjerke et al., 2011). MMP-2 is known to affect the tight junctions of the BBB, increasing permeability. However, it was originally hypothesised to be most important in acute stroke, with less importance in chronic diseases, but this evidence would suggest that MMP-2 is still elevated and therefore is likely to be involved in SVD.

MMP-3 was not upregulated in sporadic SVD compared to control, but it was significantly associated with the mean value of the PK binding hotspots in the WML. MMP-3 is an inducible MMP, along with MMP-9, and has been shown to be elevated in patients with vascular cognitive impairment (Candelario-Jalil et al., 2011). MMP-3s role is predominantly tissue breakdown during the injury phase and angiogenesis in the recovery phase (Rosenberg, 2016). Importantly, it has also been shown to activate microglia (Connolly et al., 2016), which may explain the role between elevated MMP-3 and increased PK binding. The lack of increase in SVD compared to control suggests MMP-3 is not overly important in SVD pathology, but may still be useful as a general anti-inflammatory target to reduce microglia activation.

We did not found a difference in TIMP-4 levels between sporadic SVD and control and no association with PK binding or BBB permeability. Interestingly TIMP-4 has

been investigated in SVD previously and was found to be associated with atrophy, WMLs and total SVD burden (Arba et al., 2019b). TIMP-4 inhibits a wide range of MMPs, with protective effects on remodelling of extracellular matrix (Leco et al., 1997). However, our study would suggest that TIMP-4 does not have a large role in SVD.

We did not find an increase in MMP-9 in our study and also found no association between MMP-9 and any of the BBB permeability of PK binding values. The role of MMP-9 in SVD is controversial in the literature. Early studies showed that MMP-9 was elevated in vascular dementia compared to controls (Adair et al., 2004). MMP-9 was also seen to be associated with WMLs (Kim et al., 2014, Romero et al., 2010) and CMBs (Koh et al., 2011, Lu et al., 2017). However, a more recent study in vascular cognitive impairment did not show an increase in MMP-9 compared to controls (Candelario-Jalil et al., 2011). Further, MMP-9 was not seen to be associated with lacunar infarcts (Yoshida et al., 2009, Romero et al., 2010). These negative results were then mirrored in a recent animal study of the SVD rat model, which showed no beneficial outcome of blocking MMP-9 (Raz et al., 2018). These results suggest that MMP-9 may not be as important in SVD as originally thought and may not be the best therapeutic target for SVD.

Taken together, our results suggest there may be a role for MMP-2 and MMP-3 in the pathogenesis of sporadic SVD. However, the limited associations seen between MMPs and BBB permeability and PK binding is unexpected, as in the original hypothesis for this study, MMPs were the mediating factor between the inflammatory response and the opening of the BBB. These results suggest that potentially MMPs are not as important as originally thought, and some of the other more general inflammatory biomarkers may be more useful to target with therapeutics to slow down disease pathogenesis.

7.4.4 MMPs in CADASIL

None of the MMPs were significantly elevated in CADASIL compared to control (Table 7.3). TIMP-4 was significantly negatively associated with the mean value of

the BBB permeability hotspots in the NAWM (Table 7.12). MMP-9 and TIMP-4 were then significantly positively associated with the mean value of the PK binding hotspots in the WML (Table 7.15).

TIMP-4 was negatively associated with the mean BBB permeability of the hotspots in the NAWM, but positively associated with the mean PK binding of the hotspots in the WML. The *TIMP-4* gene has been previously shown to be upregulated in CADASIL, and has been suggested to be important for its role in vascular inflammation (Pippucci et al., 2015). TIMPs are endogenous inhibitors of MMPs, so this result would suggest that when TIMP-4 is reduced, BBB permeability is increased, which could be due to the inhibiting effects of TIMP-4 on the MMPs being reduced.

MMP-9 was seen to be significantly associated with increased mean of the PK binding hotspot in the WML. Previously, intense immune staining to MMP-9 has been seen in CADASIL (Dziewulska et al., 2017). MMP-9 is produced by microglia and therefore this could explain this finding (Könnecke and Bechmann, 2013). This result would suggest that MMP-9 potentially has more of a role in CADASIL than in sporadic SVD.

MMP-2 and MMP-3 were not seen to be elevated in CADASIL or have a significant association with BBB permeability or PK binding. Interestingly, MMP-2 has previously been shown to have intense staining in CADASIL, whereas MMP-3 has not (Dziewulska et al., 2017). Our results would suggest that neither of them have a significant role in the pathogenesis of CADASIL.

Overall, this evidence would suggest that MMP-9 and TIMP-4 might be involved in the disease pathogenesis, even though none of the MMPs were increased in CADASIL compared to controls. Similarly to discussed above, it could be that the lack of BBB permeability seen in CADASIL means that these processes cannot be picked up systemically, but may still be occurring centrally. Studies that investigate the CSF or perform post-mortem studies are required to explore if these processes are occurring in the CNS.

7.4.5 Endothelial Cell Activation Biomarkers in sporadic SVD

Three out of the seven total endothelial cell activation markers were significantly elevated in sporadic SVD: E-selectin, PECAM-1 and ALCAM (Table 7.4). None of the endothelial cell activation markers were significantly associated with BBB permeability or PK binding (Table 7.10 and 7.13).

We found increased E-selectin in sporadic SVD compared to control, but no increase in P-selectin. E-selectin and P-selectin are soluble adhesion molecules. E-selectin is expressed purely on endothelial cells, whilst P-selectin is expressed on both endothelial cells and platelets. Both E-selectin and P-selectin have previously been seen to be elevated in cerebrovascular disease, with P-selectin associated with severity of WMLs (Fassbender et al., 1999, de Leeuw et al., 2002). E-selectin was seen to be elevated in lacunar stroke patients compared to controls (Kozuka et al., 2002), but this finding has not been replicated in other studies when comparing with control (Tuttolomondo et al., 2009b) or other stroke subtypes (Tuttolomondo et al., 2009a, Beer et al., 2011). P-selectin results have been mixed, with some studies finding it to be increased in lacunar stroke patients compared to controls (Kozuka et al., 2002), and some finding no difference (Ilhan et al., 2010). The activation of P-selectin is fast, whereas E-selectin is only activated 2 hours after ischaemic injury, suggesting that E-selectin may have more of a role in chronic disease, whereas P-selectin may be more involved in acute injury. Our results suggest that E-selectin has a role in the pathogenesis of sporadic SVD and should be further investigated.

We found a significantly higher circulating PECAM-1 in SVD patients compared to controls. PECAM-1 is expressed on leukocytes, platelets and endothelial cells and required for migration of leukocytes (Muller et al., 1993). Levels of PECAM-1 have been shown to be increased in both MS and ischaemic stroke (Kalinowska and Losy, 2006). Further, circulating PECAM-1 has previously been associated with increased atherosclerotic cerebral infarction risk (Song et al., 2015). Early studies linked an increased PECAM-1 to an increase in BBB permeability (Kalinowska and Losy, 2006). However, more recent studies in MS have built on this relationship, and suggested that PECAM-1 has a protective role of stabilising the BBB (Wimmer et al., 2019). Interestingly, it was not directly associated with BBB permeability levels in

sporadic SVD in our study, which would suggest that there may be other factors mediating the relationship between PECAM-1 and BBB permeability. Nonetheless, the upregulation of PECAM-1 in SVD suggests an activation of the endothelium is occurring and it is a biomarker that could be explored further.

We found a significantly higher circulating ALCAM in SVD patients compared to controls. ALCAM, also known as CD166, is upregulated substantially during inflammation and replaces VCAM-1 during transmigration of leukocytes across CNS endothelium (Cayrol et al., 2008). Studies of ischaemic stroke found that ALCAM levels measured during the stroke are associated with long-term mortality in those patients (Smedbakken et al., 2011). Follow-up data would be useful to see if ALCAM can predict similar outcomes in sporadic SVD patients.

There was no significant difference between vWF in the sporadic SVD and control groups and no association between vWF and BBB permeability or PK binding. Meta-analysis of vWF studies found that it was significantly higher in lacunar stroke vs. healthy controls, but was significantly lower compared to the non-lacunar stroke subtypes of atherothrombotic and cardioembolic stroke (Wiseman et al., 2014). vWF has also been associated cross-sectionally with WMLs (Kearney-Schwartz et al., 2009, Wada et al., 2011) and lacunes (Kario et al., 1996, Gottesman et al., 2009). vWF was also associated with increased WML and lacunes longitudinally (Arba et al., 2019a). However, other studies have not seen an association with WMLs (Knottnerus et al., 2010) or lacunes (Wada et al., 2011). It may be that our group sizes were not large enough to detect a difference between sporadic SVD and control groups or it may be that vWF is not as important in the disease pathogenesis as suggested by these earlier studies.

ITGB2 was not found to be significantly different between the sporadic SVD and control group or the CADASIL and control group. ITGB2 has not previously been investigated in SVD. However, ICAM-1 has been widely investigated. During an inflammatory response, ICAM-1 and ITGB2 form a complex to allow recruitment of leukocytes to the endothelial cells and therefore you would expect a relationship between these markers (Liu and Kubes, 2003). ICAM-1 has been associated with

increased WML (Hassan et al., 2003, Markus et al., 2005, Tchalla et al., 2015, Shoamanesh et al., 2015) and lacunes (Rouhl et al., 2012, Shoamanesh et al., 2015). One study also found ICAM-1 to be associated with longitudinal presence of WMLs, but not with lacunes (Arba et al., 2019a). However, not all studies have seen an association between ICAM-1 and SVD markers, with some showing no association with WMLs (de Leeuw et al., 2002, Jefferson et al., 2007, Rouhl et al., 2012) or lacunes (Hassan et al., 2003). Further studies are required that measure both ITGB2 and ICAM-1 to see if they are upregulated in SVD.

JAM-A, also known as soluble F11 receptor, was also found not to be significantly different between the sporadic SVD and control groups or CADASIL and control groups. It was also found not to be associated with BBB permeability or PK binding. JAM-A has been shown to redistribute from tight junctions to the apical cell surface where it mediates immune cell adhesion, upon inflammatory stimulation of endothelial cells, suggesting it may be detectable in circulation (Kummer and Ebnet, 2018). It has been shown to have increasing circulating levels in hypertension (Ong et al., 2009), atherosclerosis (Cavusoglu et al., 2007) and haemodialysis patients (Salifu et al., 2007). However, a more recent study found that there was no increase in serum JAM-A in MS or ischaemic stroke patients, suggesting that JAM-A may not be released from endothelial cells in pro-inflammatory states, as originally thought (Haarmann et al., 2010). These results from MS and stroke patients would reflect our results, where JAM-A was not increased in the serum of sporadic SVD or CADASIL patients compared to control.

CDH5, also known as VE-cadherin, was not significantly different between sporadic SVD and control groups. Circulating CDH5 has not been investigated in SVD, but was found to be elevated in patients with type 2 diabetes (Koga et al., 2005) and acute ischaemic stroke (Li and Qin, 2015). However, our results would suggest it does not have a role in SVD.

Overall, there does seem to be a role for E-selectin, PECAM-1 and ALCAM in SVD. Interestingly, none of the endothelial cell activation markers were significantly

associated with BBB permeability or PK binding, which would suggest they may not be directly involved in the pathogenesis.

7.4.6 Endothelial Cell Activation Biomarkers in CADASIL

None of the endothelial cell activation biomarkers were significantly different between CADASIL and control (Table 7.4). PECAM-1 was significantly negatively associated with the mean value of the PK binding hotspots in the NAWM (Table 7.16)

PECAM-1 was the only endothelial cell activation biomarker to have any relationship in the CADASIL group, showing a negative association with PK binding in the NAWM. Elevated PECAM-1 is thought to be beneficial in MS, through contributing to the regulation of BBB integrity and T-cell migration, with absence of PECAM-1 increasing the migration of T-cells across the BBB transcellular pathway (Wimmer et al., 2019). Therefore, potentially PECAM-1 is protective in CADASIL, and a reduction of it is leading to an increased activation of microglia.

Interestingly, we found no difference between vWF in the CADASIL group compared to control. vWF has been studied previously in CADASIL specifically, in a post-mortem study where they showed an accumulation of vWF in the small vessel walls, suggesting vWF permeates these sites and is involved in the pathogenesis of CADASIL (Zhang et al., 2012). More recently, a study of serum biomarkers in CADASIL found that vWF was significantly elevated in the serum compared to controls (Pescini et al., 2017). The lack of a difference found in this study is likely to be due to the low subject numbers used, and vWF should be further investigated in a larger samples size to see if this finding can be replicated.

None of the other markers of endothelial cell activation have been previously investigated in CADASIL (Poggesi et al., 2016). The general lack of endothelial cell activation elevation in CADASIL was an unexpected finding. It would suggest that endothelial cells might not have an important role in CADASIL disease pathogenesis.

Further, combining this with the lack of increased BBB permeability seen in the CADASIL group, it would suggest a limited role for endothelial cells in CADASIL.

7.4.7 Limitations

The key limitation of this analysis is that the biomarkers were taken from serum samples, yet we are using them to hypothesise about mechanisms occurring in the vasculature and CNS. In reality, these samples are representing systemic increases in various biomarkers, and not any subtle changes that would be occurring in the CNS. Therefore, it is important to critique any generalisation to CNS mechanisms. Future work could omit some of these limitations by taking biomarkers from the CSF, to reduce the systemic processes, which interfere with biomarkers taken from the serum.

Although this work was primarily focused on furthering our understanding of the disease pathogenesis, there is application of this work for disease diagnosis and progression, as we found many serum biomarkers were raised in our SVD cohort. Therefore, further studies should be carried out to see if any of these biomarkers are specific enough for this purpose, as this could reduce scan costs and increase the availability and accessibility of SVD diagnosis and tracking.

7.5 Summary of Findings

Returning to the aims of this chapter, the following areas have been addressed:

1. The inflammatory biomarkers of TNF-R1, TNF-R2, FAS, IL1-RT1 and IL-18BP were significantly increased in sporadic SVD compared to control
2. MMP-2 was significantly increased in sporadic SVD compared to control
3. E-selectin, PECAM-1 and ALCAM, markers of endothelial cell activation, were significantly increased in sporadic SVD compared to control
4. None of the biomarkers were increased in CADASIL compared to control
5. TNFR1 and TNFR2 were significantly negatively associated with global mean BBB permeability and the volume of the BBB permeability hotspots in the NAWM in the sporadic SVD group
6. MMP-3 was significantly positive associated with the mean value of the PK binding hotspots in the WML in the sporadic SVD group
7. TIMP-4 was significantly negatively associated with the mean value of the BBB permeability hotspots in the NAWM and positively associated with the mean value of the PK binding hotspots in the WML in CADASIL
8. MMP-9 was significantly positively associated with the mean value of the PK binding hotspots in the WML in CADASIL
9. PECAM-1 was significantly negatively associated with the mean value of the PK binding hotspots in the NAWM in CADASIL

This chapter has investigated blood biomarkers and their group differences and relevance to BBB permeability and PK binding. The next chapter will take all of the findings of this thesis and put them into context of the wider literature and implications for the field.

Chapter 8: General Discussion and Future Work

8.1 Summary of Work

This thesis considers the pathogenesis of SVD and whether, using MR and PET imaging techniques, the underlying mechanisms of BBB permeability and microglia activation have a role in the disease. This thesis looks at both BBB permeability and microglia activation as separate concepts in comparison to imaging markers, cognitive markers and circulating biomarkers, as well as looking at the relationship between the two.

8.1.1 Pathogenesis of sporadic SVD

The mechanisms linking sporadic SVD to the parenchyma damage are heterogeneous and unclear. As outlined in Chapter One, the cardiovascular risk factors, environmental factors and genetic factors accumulated throughout life are thought to damage the small vessels, leading to inadequate blood supply to the brain regions (Marstrand et al., 2002, O'Sullivan et al., 2002). This hypoperfusion leads to a hypoxic response, causing free radical production, microglia activation, triggering of inflammatory cascades (including MMPs) and increased BBB permeability (Rosenberg et al., 2014). These mechanisms may then lead to further tissue damage through actions of the inflammatory molecules and increased extravasation of blood components through the BBB. This then leads to the characteristic SVD imaging markers that we see using conventional MRI and DTI, and the manifesting of clinical symptoms.

Many studies have investigated the above mechanisms and found associations between them and the imaging or clinical outcomes. However, very few studies have looked at multiple pathogenic mechanisms simultaneously to understand their relationship with one another. Our study looked at microglia activation with BBB permeability, in combination with serum biomarkers, to try to understand how these complex mechanisms fit into the underlying disease pathogenesis. The exact methods

used are outlined in Chapter Two and the characteristics of the patient and control populations are described in Chapter Three.

Chapter Four studied BBB permeability as an individual concept, in a similar way to how it had been studied previously (Cuadrado-Godia et al., 2018). Firstly, we provided evidence that there is an increase in BBB permeability in sporadic SVD compared to controls. We showed a significant increase in global BBB permeability in the NAWM and WML. Further, we showed increased focal permeability in sporadic SVD compared to control, by showing an increased volume of BBB permeability hotspots in the NAWM and WML.

We then investigated whether BBB permeability was associated with current characteristic imaging markers of SVD. Within the sporadic SVD group, we did not find an association between BBB permeability and WMLs, lacunes or CMBs. However, we did find that increased volume of significant BBB permeability in the NAWM was associated with increased FA, suggesting that the presence of higher areas of permeability is associated with disruption of WM fibres in the NAWM. We also found higher levels of permeability in the NAWM compared to the WML. Taken together, this data suggests a role for BBB permeability in the NAWM, where it may precede WML formation. However, without follow-up data, this cannot be concluded.

In Chapter Five, microglia activation was explored as an individual concept. PET imaging of PK binding was used to measure microglia activation. We found there were increased hotspots of microglia activation in sporadic SVD compared to control, with a significantly increased mean value and volume in the NAWM and WML.

We found that microglia activation was not associated with any of the clinical SVD characteristics of WMLs, lacunes, CMBs or DTI parameters in the sporadic SVD group. Focal hotspots of microglia activation were consistently increased in the NAWM compared to the WML. Similarly to BBB permeability, this could again suggest that microglia activation is involved in the mechanism turning NAWM into WML, although again, this cannot be proved without follow-up data.

The most interesting and unexpected result of the study came from Chapter Six, where we examined the relationship between the BBB permeability and microglia activation. We found no correlation between the two, and spatial analysis showed that voxels of significant BBB permeability and microglia activation were significantly independent of one another. This provides evidence that BBB permeability and microglia activation are occurring as distinct mechanisms within the pathogenic process within a single time-point. However, what we cannot determine from these results, is whether they are causative of one another; in other words, whether an area of high microglia activation will go on to become an area of high BBB permeability, or vice versa. Alternatively, they may be completely separate disease mechanisms, which are not involved in the same pathogenic pathway. Follow-up studies are needed, which scan patients repeatedly to see the change in these dynamic processes over time, which will clarify whether they are causative of one other, of WML formation or of neither.

Finally, Chapter Seven investigated various circulating biomarkers. We found evidence suggesting a role for the TNF-α receptors and cytokines within the IL-1 family in sporadic SVD, representative of a systemic inflammatory response. Further, we found an increase in MMP-2 in sporadic SVD compared to control. There was also an increase in various markers of endothelial cell activation, including E-selectin, PECAM-1 and ALCAM, suggestive of endothelial cells in an inflammatory state, which may contribute to BBB permeability. TNFR1 and TNFR2 were negatively associated with BBB permeability, suggesting an opposing regulation between the TNF-α receptors and BBB permeability. MMP-3 was associated with microglia activation, suggesting a role in SVD.

These markers show that there do seem to be underlying mechanisms occurring that may link BBB permeability and neuroinflammation together in SVD. They would therefore provide evidence that the results of Chapter Six, where BBB permeability and microglia activation were spatially distinct, are due to different brain regions being at varying stages in the pathogenic pathway, rather than the processes being functionally independent of one-another.

Taken together, our results suggest a role for BBB permeability and microglia activation in sporadic SVD. They suggest that the processes are spatially independent at a single time-point. However, there do seem to be underlying inflammatory processes occurring that may be linking BBB permeability and microglia activation together, suggesting that they may be involved in the same mechanism.

8.1.2 Pathogenesis of CADASIL

The mechanism underlying CADASIL is also unclear. As described in Chapter One, CADASIL is a genetic disease and therefore the initial damage to the small vessels is predominantly due to genetic causes through a mutation in *Notch3* (Papakonstantinou et al., 2019), although this can still be worsened by risk factors (Adib-Samii et al., 2010). Studies have suggested that, although different initial processes damage the small vessels, the underlying mechanism that occurs as a result of the damaged vessels may be broadly similar to the sporadic condition (Poggesi et al., 2016). This is important to establish, as if a common mechanism exists then future treatments can be shared between sporadic SVD and CADASIL. Therefore, briefly, in CADASIL it is thought that *Notch3* mutations lead to a degeneration of the vasculature through effects on many cells, predominantly vascular smooth muscle cells (Coupland et al., 2018). Hypoxia then occurs and follows a similar pathway to sporadic SVD, with free radical production, microglia activation, activation of inflammatory cascades and increase in BBB permeability. However, very few studies have investigated the underling mechanism in CADASIL, making work within this area very novel. Chapter Two outlined the methods used in this study and Chapter Three described the CADASIL and control populations.

In Chapter Four, we investigated BBB permeability in CADASIL and found that it was not significantly different from controls. This finding was in contrast to sporadic SVD, where BBB permeability was seen to increase compared to controls. BBB permeability had no relation to any of the characteristic SVD imaging markers of WMLs, lacunes or CMBs in the CADASIL group and no association with cognition. Therefore, this study would not provide evidence for increased BBB permeability in CADASIL.

We then moved to investigate microglia activation in CADASIL in Chapter Five. We found there was a significantly higher mean and volume of hotspot microglia activation in the WMLs of CADASIL patients compared to control. The association was not significant in the NAWM, although there was a non-significant trend for the mean and volume of the hotspot microglia activation to be increased in CADASIL compared to control. We saw no associations between the amount of microglia activation and any of the SVD imaging markers of WMLs, lacunes or CMBs, and also no association with cognition within the CADASIL group. This work suggests that microglia activation is increased in patients with CADASIL; however, its role in the pathophysiology of the disease is unclear.

Chapter Six compared the relationship between BBB permeability and microglia activation. This chapter showed a similar pattern across the sporadic SVD and CADASIL groups, which was that BBB permeability and microglia activation were not consistently correlated with one-another and that voxels of significant BBB permeability and microglia activation were significantly independent of one another spatially. This suggests that either the two mechanisms are not related, or that they are two parts of a dynamic process that occur at separate time-points, and therefore cross-sectional data will be unable to establish the relationship.

Chapter Seven then investigated circulating biomarkers in CADASIL. None of the biomarkers were significantly elevated in CADASIL compared to control. Additionally, none of the inflammatory markers were associated with any of the BBB permeability or microglia activation parameters. This could suggest that these inflammatory markers are involved in increasing BBB permeability, and their absence in CADASIL is why we do not see the same increase in BBB permeability as we see in sporadic SVD. Alternatively, it could be that, as we are measuring these markers systemically, the lack of increased permeability seen in CADASIL makes it more difficult for the markers to travel from their site of origin in the CNS, into the circulation. Therefore, the same inflammatory processes may be occurring in the CNS in sporadic SVD and CADASIL, but in sporadic SVD the increased permeability allows the markers to be picked up systemically, whereas in CADASIL they are

confined to the CNS. MMP-9 and TIMP-4 were shown to be associated with BBB permeability and microglia activation, suggesting MMPs may be involved in the pathogenesis. PECAM-1 was also negatively associated with microglia activation, suggesting a protective role against increasing inflammation.

Further studies are required to understand the inflammatory response occurring in CADASIL, and why we do not see the same increase in BBB permeability as we do in sporadic SVD.

Taken together, our results suggest that there is a role for activated microglia in CADASIL. They suggest that there is not an obvious role for BBB permeability, and there is a spatial independence between activated microglia and BBB permeability at a single time-point. The results also suggest that there are no systemic inflammatory mechanisms occurring in CADASIL.

8.2 Ongoing and future work

8.2.1 Follow-up of Patients

The fact that the data from this study is cross-sectional and taken at a single time-point makes it impossible to be certain of the role of these mechanisms in SVD pathogenesis. The mechanisms of BBB permeability and activated microglia can only be proven to be pathogenic if they can be shown to lead to damage to the brain tissue at a later stage. Therefore, all the patients from this study will be followed up one year later, where they will undergo a further clinical MRI scan and cognitive tests. The key markers we are interested in monitoring the change of are WML volume and the DTI parameters FA and MD.

WML growth and DTI changes over the follow-up period will be calculated. These will then be analysed in comparison to the baseline levels of BBB permeability and PK binding, to see if patients who had higher permeability or binding at baseline, seem to have increased progression of WMLs or increased FA and MD at follow-up.

The analysis will then be expanded to see if the regions classified as hotspot BBB permeability or hotspot PK binding at baseline, have progressed to become WML or have obtained a significant change in FA or MD one-year on. This analysis will also be repeated in reverse, where follow-up MRI scans will be marked for WMLs, with baseline lesions subtracted, to create a mask of new WMLs that have occurred in that one-year period. The amount of BBB permeability and PK binding that was present at baseline in the new WMLs will be calculated to see if the levels were higher than in the rest of the brain.

The cognitive decline seen over the one-year period will also be calculated and compared to baseline levels of BBB permeability and PK binding, to see if there is a clinical application to this.

The greatest limitation of this is that the one-year period of follow-up is not a long amount of time, and therefore detectable changes in this time period may not be seen.

272

If this is the case, then a decision may be made to follow-up patients up again at a later time-point.

Further, as these follow-up studies will not repeat the DCE-MRI or PK PET scans, they do not help to answer the question about the dynamics of the SVD pathogenic mechanism. If the follow-up scans do show BBB permeability and/or microglia activation to be pathogenic, a study investigating the dynamics of the processes could be very useful to improve our understanding and help with time-course and administration of future treatments.

8.2.2 Clinical Trial

This study has led to the start of a clinical trial utilising the same imaging techniques, cognitive tests and biomarkers used in this study. The clinical trial is based on an animal study of SVD, where minocycline was shown to reduce the size of WMLs (Jalal et al., 2015). The mechanism of action of minocycline is controversial, with Jalal et al. originally suggesting it acted through MMP-9, but later determining that this is unlikely to be the case (Raz et al., 2018). The many anti-inflammatory mechanisms of minocycline make it difficult to determine which action is protective in SVD. Therefore, if the drug is found to be effective in SVD patients, then further *in vitro* and *in vivo* studies will be required to fully understand the therapeutic mechanism of action.

The clinical trial will scan patients with DCE-MRI and PK PET at baseline and after 3 months of treatment with minocycline, to see if this reduces the amount of BBB permeability and microglia activation seen. The patients will then continue treatment for one year, where they will be scanned again with just a clinical MRI scan, to see if treatment with minocycline reduces WML growth and DTI changes in comparison to a placebo. If successful this trial could provide the first treatment for SVD that targets the underlying mechanism.

8.3 Conclusion

SVD is responsible for a third of all strokes and is the leading cause of vascular dementia (O'Brien and Thomas, 2015). Research is increasingly suggesting that SVD underlies age-related cognitive decline in the elderly, making it the most prevalent neurological disorder ever described (Thompson and Hakim, 2009). The growing ageing population of the UK means that this disease will continue to increase costs to the economy and affect the lives of hundreds of thousands of people. With no current treatments that treat the underlying mechanism, research into the pathogenesis of SVD is vital to discover new targets for therapeutics.

The findings from this thesis have potential clinical and research implications. From an imaging perspective, we have shown that simultaneous PET/MR imaging can be carried out in an SVD patient population, and can provide quantification and spatial localisation of BBB permeability and microglia activation. Clinical trials investigating the impact of future therapeutics on these disease mechanisms can use this technology as suitable end-points to measure the therapeutic impact.

The biological findings from this study have confirmed a role for BBB permeability and microglia activation in sporadic SVD, whilst paving the way for future research into the dynamics of these processes. This study has provided the first indication that microglia activation is an important mechanism in CADASIL, and the implications this may have for disease treatment. We have also shown an array of blood biomarkers that seem to be increased in sporadic SVD that provide new insights into the pathophysiology and have the potential to be utilised as clinical trial end-points or for both diagnosis and management of disease progression. Further, *in vivo* and *in vitro* work can build on these findings to understand the link between microglia activation and BBB permeability, which can then be translated into the clinic.

SVD is a heterogeneous disease with an array of neuroimaging features and associated symptoms manifesting from a complex underlying mechanistic pathway. Improving our knowledge of the disease pathogenesis will allow for novel

therapeutics that target these mechanisms to be tested, and allow us to slow down, or even reverse, the disease progression and resulting clinical symptoms.

Appendix A: Mean value of BBB permeability Hotspots - Analysis with Outliers Removed

Two outliers were removed for the hotspot permeability mean values (both WM and NAWM), whilst three outliers were removed for the hotspot permeability mean penumbra values (both 3mm and 6mm penumbras). These outliers did not have an obvious reason to be removed but they were higher than can be reasonably expected and so are likely due to artifact.

A.1 Statistical Analysis

Statistical analysis was carried out in the same way as described in the main chapter. Briefly, group differences between hotspot mean values for sporadic SVD and control and CADASIL and control were analysed using the ANCOVA test and were controlled for age and sex. Pairs of comparisons were adjusted using Bonferroni. If there was a significant difference seen, an ANCOVA controlling for the cardiovascular risk factors of hypertension, hyperlipidaemia, type 2 diabetes and smoking was performed to see if the significance was still present.

All parameters met normality assumptions after removal of the outliers.

A.2 Results

A.2.1 Group Differences

There was no significant difference in the mean value of the BBB permeability hotspots in the WM between the sporadic SVD and control groups or the CADASIL and control groups (Figure A.1). There was also no significant difference in the mean value of the BBB permeability hotspots in the NAWM between the sporadic SVD and control groups or the CADASIL and control groups (Figure A.2).
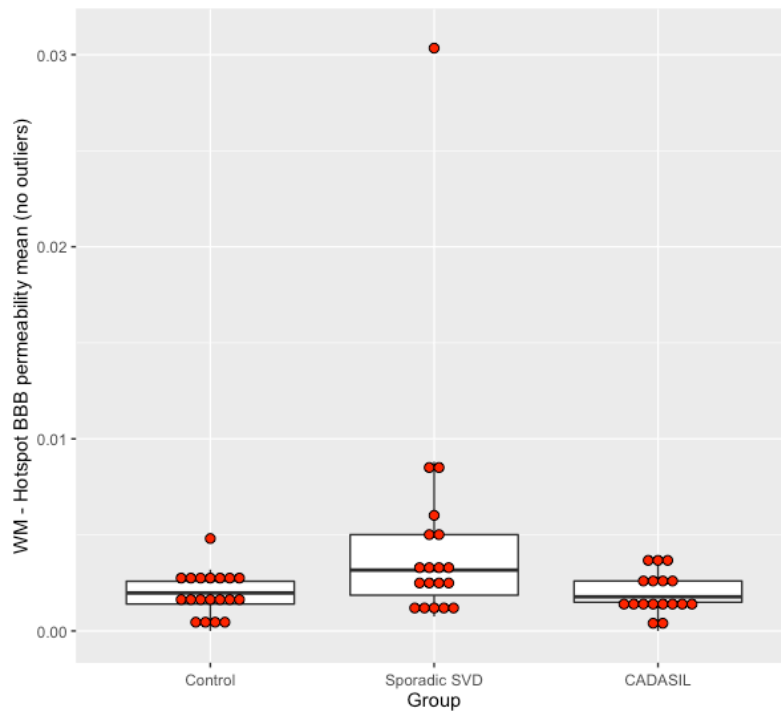
Figure A.1: There was no significant difference in the hotspot mean permeability in the WM of the sporadic SVD group compared to control (p=0.123) or the CADASIL group compared to control (p=1.000).
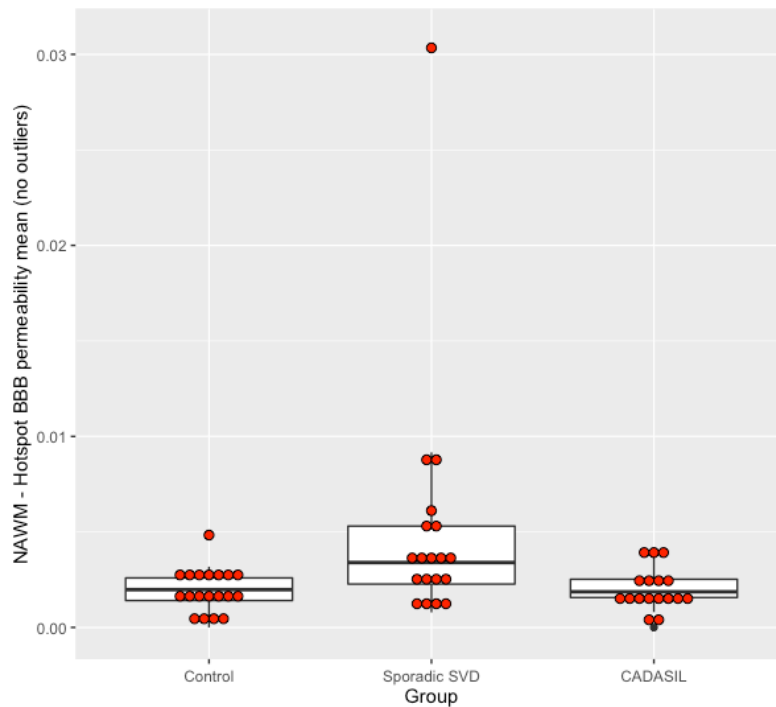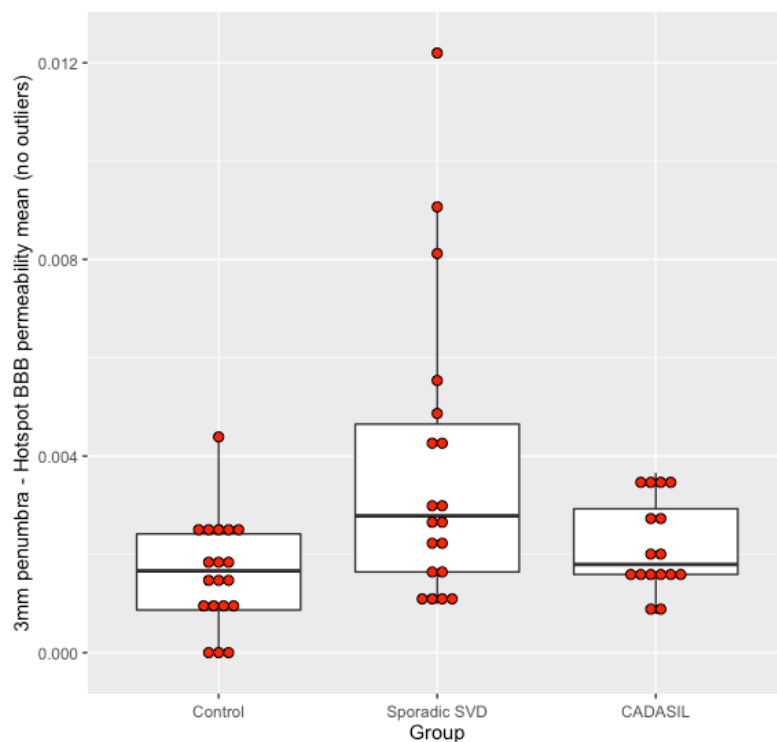

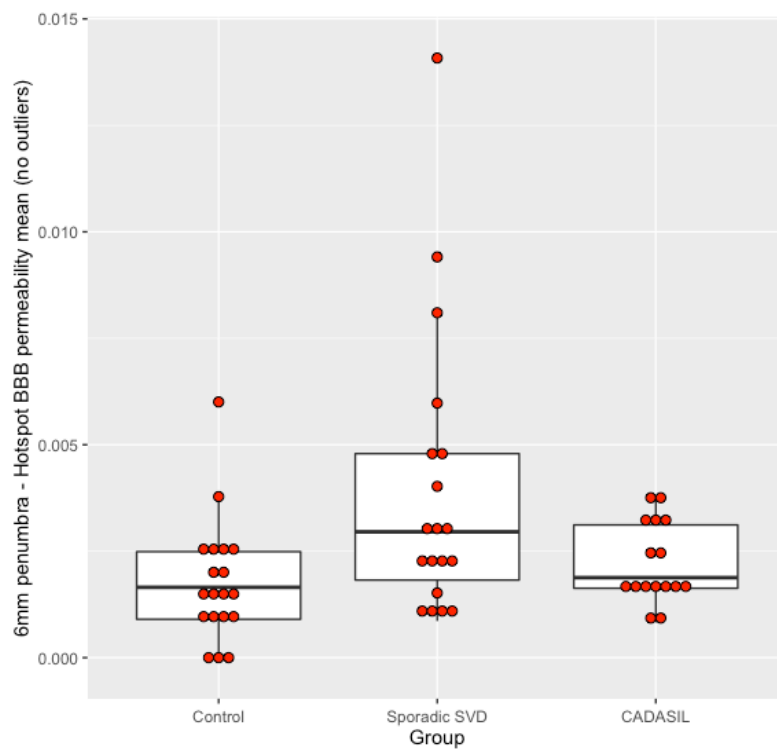
Figure A.2: There was no significant difference in the hotspot mean permeability in the NAWM of the sporadic SVD group compared to control (p=0.090) or the CADASIL group compared to control (p=1.000).

A.2.2 WML Penumbra Group Difference

There was a significantly higher mean value of the BBB permeability hotspots in the 3mm penumbra of the sporadic SVD group compared to control (p=0.004 (p=0.007 when adjusted for multiple comparisons) (Figure A.3). However, there was no significant difference in the mean value of the BBB permeability hotspots between the CADASIL and control groups.

There was a significantly higher mean value of the BBB permeability hotspots in the 6mm penumbra of the sporadic SVD group compared to control (p=0.009 (p=0.018 when adjusted for multiple comparisons)) (Figure A.4). However, there was no significant difference in the mean value of the BBB permeability hotspots between the CADASIL and control groups.

Figure A.3: There was a significant difference in the hotspot mean permeability in the 3mm penumbra of the sporadic SVD group compared to control (p=0.007). However, there was no significant difference in the CADASIL group compared to control (p=0.194).

Figure A.4: There was a significant difference in the hotspot mean permeability in the 6mm penumbra of the sporadic SVD group compared to control (p=0.018). However, there was no significant difference in the CADASIL group compared to control (p=0.516).

Appendix B: BBB permeability in CADASIL

An analysis was carried out comparing the amount of BBB permeability in the CADASIL group between various symptoms.

B.1 Statistical analysis

Mann-Whitney U tests for non-parametric data were used to compare the imaging parameters and BBB permeability parameters for CADASIL patients by age, stroke history and migraine history.

B.2 Results

B.2.1 Age

Comparisons between the imaging markers for CADASIL patients over 55 vs. under 55 are shown in Table B.1. Brain volume and GM volume were not significantly different between the groups. WML volume was significantly higher in the over 55 group compared to under 55 (p=0.017). The groups had similar lacune volume, lacune number and CMB number. All of the DTI parameters of FA and MD were similar between the groups.

Comparisons between the BBB permeability values between patients over 55 vs. under 55 are shown in Table B.2. There was no significant difference in any of the BBB permeability parameters of global mean, hotspot mean or hotspot volume between the groups.

Imaging Parameter	Median [Q1, Q3]		P value
	Over 55 (n=9)	Under 55 (n=11)	
Brain volume (% of ICV)	76.03 [73.77, 79.96]	70.73 [68.48, 80.62]	0.470
GM volume (% of ICV)	40.04 [35.59, 43.46]	40.85 [40.10, 46.54]	0.305
WML volume (% of ICV)	5.25 [2.72, 6.91]	2.40 [1.54, 3.47]	**0.017**
Lacune volume (% of ICV)	0.06 [0.02, 0.10]	0.00 [0.00, 0.05]	0.099
Number of lacunes	3.00 [2.00, 8.00]	0.00 [0.00, 6.00]	0.157
Number of CMBs	1.00 [0.00, 2.00]	0.00 [0.00, 6.00]	0.647
FA NAWM median	0.28 [0.24, 0.33]	0.34 [0.31, 0.35]	0.053
FA WML median	0.19 [0.18, 0.22]	0.20 [0.17, 0.23]	0.732
MD NAWM peak height*	10.26 [8.79, 11.95]	12.43 [10.46, 13.71]	0.074
MD WML peak height*	6.96 [6.17, 7.36]	6.43 [6.01, 7.38]	0.849
FW NAWM median	0.35 [0.33, 0.37]	0.30 [0.28, 0.35]	0.063
FW WML median	0.61 [0.56, 0.65]	0.54 [0.53, 0.57]	0.184
FW FA NAWM median	0.21 [0.18, 0.23]	0.23 [0.23, 0.25]	0.063
FW FA WMH median	0.18 [0.18, 0.19]	0.20 [0.18, 0.21]	0.342
FW MD NAWM peak height*	2.31 [2.20, 2.66]	2.57 [2.37, 2.73]	0.305
FW MD WML peak height*	2.78 [2.30, 2.91]	2.58 [2.15, 2.82]	0.425

*$(\times 10^3)$

Table B.1: Comparisons of imaging parameters of CADASIL patients over 55 years of age compared to under 55 years of age.

Permeability value	Brain Region	Median [Q1, Q3]		P value
		Over 55 (n=8)	Under 55 (n=11)	
Global mean (x10³)	**NAWM**	0.05 [0.02, 0.18]	0.05 [0.03, 0.15]	0.804
	WML	0.01 [0.01, 0.10]	0.04 [0.01, 0.11]	0.408
Hotspot mean (x10³)	**NAWM**	2.46 [2.27, 2.89]	1.78 [1.55, 2.87]	0.160
	WML	2.07 [1.15, 2.85]	1.37 [1.10, 1.71]	0.408
Hotspot volume	**NAWM**	1.19 [0.39, 5.04]	2.85 [1.30, 8.26]	0.364
	WML	0.59 [0.19, 4.63]	1.71 [0.72, 5.40]	0.408

Table B.2: Comparisons of permeability parameters of CADASIL patients over 55 years of age compared to under 55 years of age.

B.2.2 Stroke

Comparisons were made for imaging markers between CADASIL patients who had experienced a stroke and those who had not in Table B.3. Brain volume, GM volume, WML volume, lacune volume, lacune number and CMB number were not significantly different between the groups. FA median in the NAWM was significantly lower in patients who had experienced a stroke compared to those who had not (p=0.017). FW adjusted FA median followed the same pattern and was significantly lower in those who had experienced a stroke (p=0.014). MD peak height in the WML was also significantly lower in patients who had experienced a stroke compared to those who had not (p=0.031). FW median in the WML was significantly higher in those who had experienced a stroke compared to those who had not (p=0.037).

Comparisons between the BBB permeability parameters between CADASIL patients who had experienced a stroke and those who had not are shown in Table B.4. BBB permeability in the NAWM was significantly higher in those who had not experienced a stroke compared to those who had (p=0.021). None of the other parameters were significantly different.

Imaging parameter	Median [Q1, Q3]		P
	Stroke (n=8)	Non-Stroke (n=12)	value
Brain volume (% of ICV)	73.43 [69.97, 77.94]	77.92 [70.06, 81.38]	0.589
GM volume (% of ICV)	39.65 [35.36, 40.20]	44.27 [40.73, 46.19]	0.064
WML volume (% of ICV)	4.40 [2.39, 7.31]	2.66 [1.04, 3.70]	0.143
Lacune volume (% of ICV)	0.09 [0.01, 0.11]	0.00 [0.00, 0.03]	0.202
Number of lacunes	8.00 [1.50, 10.00]	0.50 [0.00, 3.00]	0.188
Number of CMBs	4.50 [0.00, 22.50]	0.00 [0.00, 1.25]	0.076
FA NAWM median	0.28 [0.27, 0.30]	0.35 [0.32, 0.36]	**0.017**
FA WML median	0.20 [0.18, 0.20]	0.21 [0.17, 0.24]	0.537
MD NAWM peak height*	10.16 [9.36, 10.95]	12.56 [10.23, 13.50]	0.076
MD WML peak height*	6.30 [5.65, 6.66]	7.34 [6.41, 8.00]	**0.031**
FW NAWM median	0.35 [0.35, 0.37]	0.31 [0.29, 0.34]	0.076
FW WML median	0.62 [0.58, 0.66]	0.54 [0.50, 0.57]	**0.037**
FW FA NAWM median	0.21 [0.20, 0.22]	0.24 [0.23, 0.25]	**0.014**
FW FA WMH median	0.19 [0.18, 0.20]	0.18 [0.18, 0.21]	0.643
FW MD NAWM peak height*	2.34 [2.18, 2.61]	2.55 [2.30, 2.71]	0.355
FW MD WML peak height*	2.47 [2.20, 2.87]	2.71 [2.19, 3.07]	0.700

*$(\times 10^3)$

Table B.3: Comparisons of imaging parameters of CADASIL patients who have and have not experienced stroke.

Permeability value	Brain Region	Median [Q1, Q3]		P value
		Stroke (n=8)	Non-Stroke (n=11)	
Global mean ($\times 10^3$)	**NAWM**	0.02 [0.01, 0.06]	0.08 [0.04, 0.38]	**0.021**
	WML	0.01 [0.00, 0.06]	0.04 [0.02, 0.11]	0.116
Hotspot mean ($\times 10^3$)	**NAWM**	1.94 [1.72, 2.43]	2.36 [1.67, 3.90]	0.68
	WML	1.39 [0.90, 2.04]	1.63 [1.19, 2.64]	0.563
Hotspot volume	**NAWM**	0.89 [0.38, 3.35]	3.00 [1.63, 11.45]	0.099
	WML	0.45 [0.11, 3.26]	2.23 [1.09, 5.40]	0.215

Table B.4: Comparisons of permeability parameters of CADASIL patients who have and have not experienced stroke.

B.2.3 Migraine

Comparisons of imaging parameters between CADASIL patients who had experienced a migraine vs. those who had not, is shown in Table B.5. Brain volume, GM volume and WML volume were not significantly different between groups. However, lacunes were significantly higher in those who had not experienced migraine compared to those who had in both volume (p=0.015) and count (p=0.031). Number of CMBs was not significantly different between the groups. None of the DTI parameters were significantly different between the groups.

Comparisons of the BBB permeability values between CADASIL patients who had experienced a migraine and those who had not is shown in Table B.6. There was no significant difference in any of the permeability parameters between the groups.

Imaging parameter	Median [Q1, Q3]		P value
	Migraine (n=16)	Non-Migraine (n=4)	
Brain volume (% of ICV)	75.40 [70.06, 80.26]	75.34 [64.15, 80.88]	0.925
GM volume (% of ICV)	41.98 [38.93, 45.83]	39.65 [34.08, 44.05]	0.450
WML volume (% of ICV)	2.53 [1.77, 4.10]	4.83 [3.34, 6.72]	0.131
Lacune volume (% of ICV)	0.00 [0.00, 0.04]	0.13 [0.10, 0.15]	**0.015**
Number of lacunes	0.50 [0.00, 4.25]	10.50 [6.75, 14.25]	**0.031**
Number of CMBs	0.00 [0.00, 5.50]	1.00 [0.00, 16.50]	0.717
FA NAWM median	0.33 [0.30, 0.35]	0.28 [0.27, 0.30]	0.219
FA WML median	0.20 [0.18, 0.24]	0.19 [0.17, 0.20]	0.299
MD NAWM peak height*	11.61 [9.75, 13.21]	10.97 [9.50, 11.56]	0.450
MD WML peak height*	7.03 [6.29, 7.50]	6.01 [5.51, 6.58]	0.131
FW NAWM median	0.32 [0.29, 0.36]	0.35 [0.35, 0.37]	0.108
FW WML median	0.54 [0.52, 0.63]	0.60 [0.59, 0.64]	0.156
FW FA NAWM median	0.23 [0.22, 0.25]	0.21 [0.20, 0.23]	0.299
FW FA WMH median	0.19 [0.18, 0.21]	0.18 [0.17, 0.19]	0.219
FW MD NAWM peak height*	2.55 [2.25, 2.67]	2.34 [2.11, 2.53]	0.345
FW MD WML peak height*	2.68 [2.20, 3.00]	2.45 [2.19, 2.74]	0.571

*($\times 10^3$)

Table B.5: Comparisons of imaging parameters of CADASIL patients who have and have not experienced migraine.

Permeability value	Brain Region	Median [Q1, Q3]		P value
		Migraine (n=16)	Non-Migraine (n=3)	
Global mean ($\times 10^3$)	**NAWM**	0.06 [0.03, 0.16]	0.03 [0.02, 0.37]	0.911
	WML	0.03 [0.01, 0.11]	0.02 [0.01, 0.15]	0.823
Hotspot mean ($\times 10^3$)	**NAWM**	1.85 [1.56, 2.52]	3.96 [3.17, 194.48]	0.057
	WML	1.55 [1.15, 1.94]	2.77 [1.39, 2.93]	0.654
Hotspot volume	**NAWM**	2.47 [0.97, 7.93]	1.22 [0.61, 9.57]	0.823
	WML	1.55 [0.44, 4.38]	0.68 [0.34, 4.80]	0.654

Table B.6: Comparisons of permeability parameters of CADASIL patients who have and have not experienced migraine.

Appendix C: 6mm WML Penumbra

A 6mm penumbra was drawn around the WMLs to see if this followed the same patterns seen with the 3mm penumbra.

C.1 Statistical Analysis

Group differences in the penumbra values between sporadic SVD and control and between CADASIL and control were analysed using ANCOVA tests and were controlled for age and sex. Pairs of comparisons were adjusted using Bonferroni. If there was a significant difference seen, a further ANCOVA controlling for the cardiovascular risk factors was performed to see if the significance was still present.

Comparisons between permeability or PK binding values for the NAWM and WML and the penumbra permeability or PK binding values were carried out using the Wilcoxon signed rank tests for paired non-parametric data. These tests were performed on the raw untransformed values. P values were corrected for multiple comparisons using FDR.

All permeability penumbra values were transformed with a cube root to meet normality assumptions. Global mean PK binding values for the 6mm penumbra met normality assumptions. Hotspot mean PK binding values for the 6mm penumbra did not meet normality assumptions so were log transformed (base:10). Hotspot PK binding volumes for the 6mm penumbra also did not meet normality assumptions so were log transformed (base:10).

C.2 Results

C.2.1 BBB permeability Group Difference

Global BBB permeability values within the penumbra were compared in Figure C.1. Global permeability in the sporadic SVD group was significantly higher than control when controlled for age and sex (p=0.003 (p=0.006 when adjusted for multiple comparisons)) and cardiovascular risk factors (p=0.004). The global BBB permeability values in the penumbra were not significantly different between CADASIL and control.

Mean values of the BBB permeability hotspots were compared in Figure C.2. The mean value of the permeability hotspots was significantly higher than control when adjusted for age and sex (p=0.003 (p=0.007 when adjusted for multiple comparisons)) and cardiovascular risk factors (p=0.005). There was no significant difference between mean value of the hotspots in the penumbra between the CADASIL and the control groups.

Finally, the volumes of the BBB permeability hotspots within the penumbras were compared, shown in Figure C.3. In the sporadic SVD group, there was a significantly higher volume of hotspots compared to control when adjusted for age and sex (p=0.009 (p=0.018 when adjusted for multiple comparisons)) and cardiovascular risk factors (p=0.010). In the CADASIL group, there was no significant difference from control.
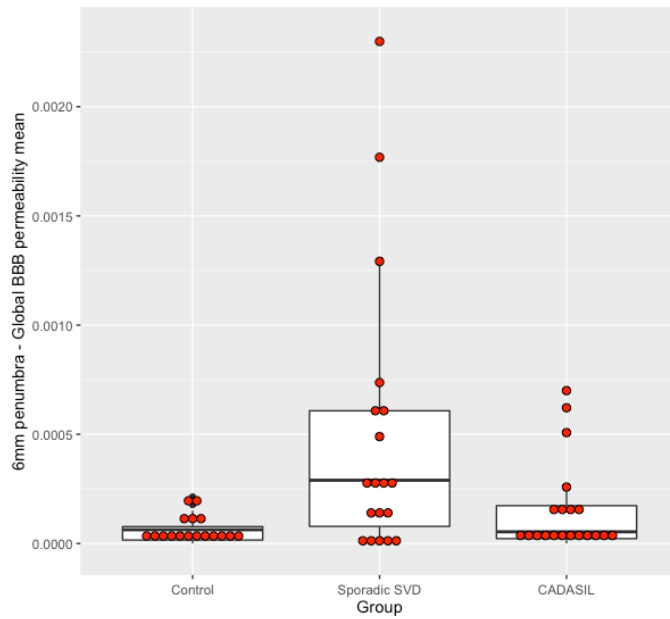
Figure C.1: Global mean values of BBB permeability from the 6mm penumbra region were compared between groups when controlled for age and sex. Global permeability mean was significantly higher in SVD compared to control (p=0.006). CADASIL was no different from control (p=0.263).
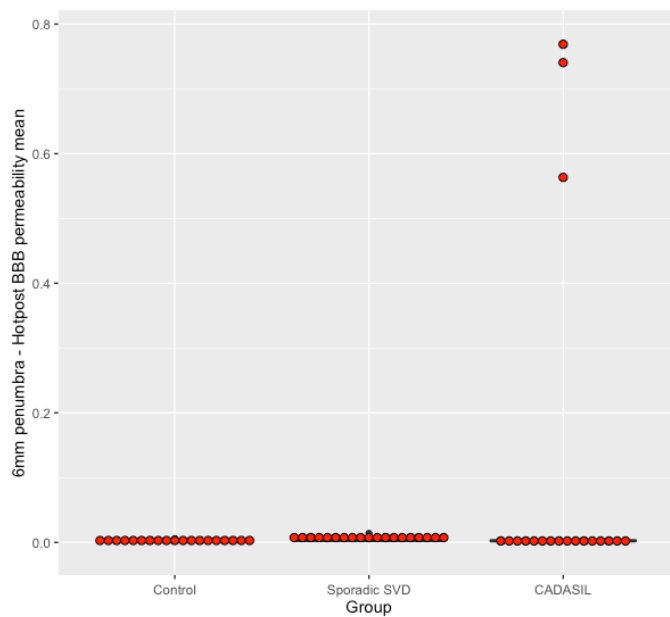
Figure C.2: Mean values of the BBB permeability hotspots from the 6mm penumbra region were compared between groups when controlled for age and sex. The mean value of the hotspots was significantly higher in the sporadic SVD group compared to control (p=0.007). There was no difference between CADASIL and control (p=0.071).
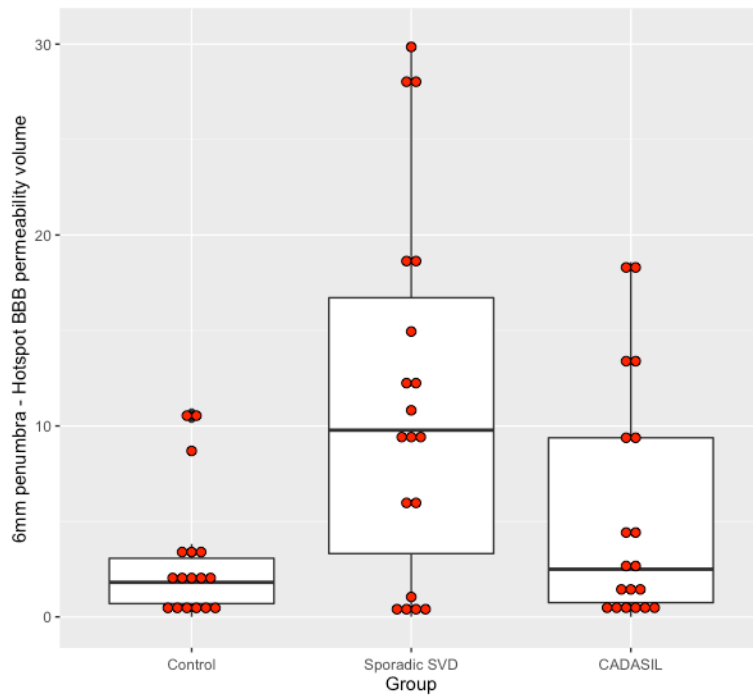
Figure C.3: The volume of the BBB permeability hotspots for the 6mm penumbra were compared between the groups. The volume was significantly higher in sporadic SVD compared to control (p=0.018). There was no difference between CADASIL and control (p=0.932).

C.2.2. BBB permeability NAWM vs. WML

Penumbra values were then compared with corresponding NAWM and WML values, to see if they were significantly different in permeability to these regions, shown in Table C.1.

Within the control group, penumbra values were similar to all corresponding NAWM and WML values except for the hotspot permeability in the WML. The mean value of the permeability hotspots in the penumbra was significantly higher than in the WML (p=0.011).

In the sporadic SVD group, the penumbra values were similar to the corresponding NAWM and WML for the global permeability mean and the volume of the permeability hotspots. However, when comparing to the mean value of the

permeability hotspots, the penumbra values were significantly lower than the NAWM (p=0.037), but significantly higher than WML (p=0.001).

Within the CADASIL group, the penumbra values were similar to the NAWM values, but significantly higher than the WML values. The global permeability mean of the penumbra was significantly higher than in the WML (p=0.004). The hotspot mean of the penumbra was also significantly higher than the WML (p=0.004) and the hotspot volume of the penumbra was significantly higher than the WML (p=0.004).

Group	Permeability measurement	Permeability measurement		Penumbra measurement		P value
		Median	IQR	Median	IQR	
Control	NAWM mean (x10^3)	0.046	0.071	0.063	0.061	0.976
	WML mean (x10^3)	0.009	0.062	0.063	0.061	0.072
	HS NAWM mean (x10^3)	1.977	1.183	1.652	1.588	0.684
	HS WML (x10^3)	1.033	1.943	1.652	1.588	**0.011**
	NAWM volume	2.074	2.314	1.811	2.372	0.976
	WML volume	0.543	3.661	1.811	2.372	0.105
Sporadic SVD	NAWM mean (x10^3)	0.295	0.620	0.290	0.529	0.713
	WML mean (x10^3)	0.161	0.361	0.290	0.529	0.146
	HS NAWM mean (x10^3)	3.397	3.036	2.955	2.968	**0.037**
	HS WML (x10^3)	2.376	2.624	2.955	2.968	**0.001**
	NAWM volume	10.660	14.480	9.780	13.400	1.000
	WML volume	9.314	10.518	9.780	13.400	0.598
CADASIL	NAWM mean (x10^3)	0.046	0.136	0.054	0.151	0.874
	WML mean (x10^3)	0.026	0.103	0.054	0.151	**0.004**
	HS NAWM mean (x10^3)	2.009	1.541	2.358	1.888	0.976
	HS WML (x10^3)	1.562	1.468	2.358	1.888	**0.004**
	NAWM volume	2.088	7.429	2.496	8.635	0.713
	WML volume	1.393	5.027	2.496	8.635	**0.004**

Table C.1: Pairwise comparisons for the individual groups for the global mean permeability values, hotspot mean permeability values and hotspot permeability volume with equivalent 6mm penumbra values. Significant p values are shown in bold.

C.2.3 PK binding Group Difference

Global PK binding in the penumbra was compared between sporadic SVD and control and CADASIL and control; there was no significant difference seen (Figure C.4).

The mean value of the PK binding hotspots was then compared between the groups in Figure C.5. The mean binding o the hotspots was significantly higher in the sporadic SVD group compared to control when controlling for age and sex (p=0.014 (p=0.029 when adjusted for multiple comparisons)) and cardiovascular risk factors (p=0.021). Further, the hotspot mean was significantly higher in CADASIL compared to control when adjusted for age and sex (p=0.005 (p=0.010 when adjusted for multiple comparisons)) and cardiovascular risk factors (p=0.005).

The volume of the PK binding hotspots was not significantly different between the 6mm penumbras (Figure C.6).
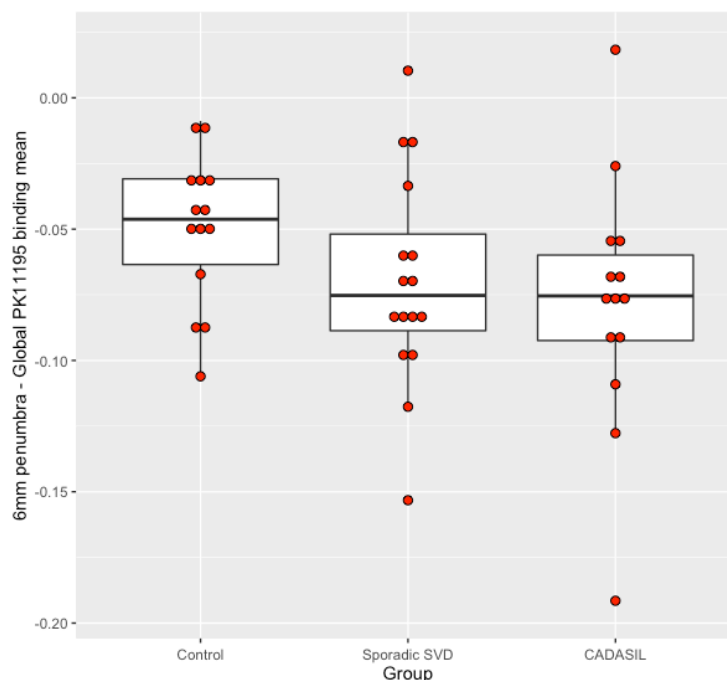
Figure C.4: The global PK binding mean was compared between the groups. The mean was not significantly different between sporadic SVD compared to control (p=0.287) or CADASIL and control (p=0.142).
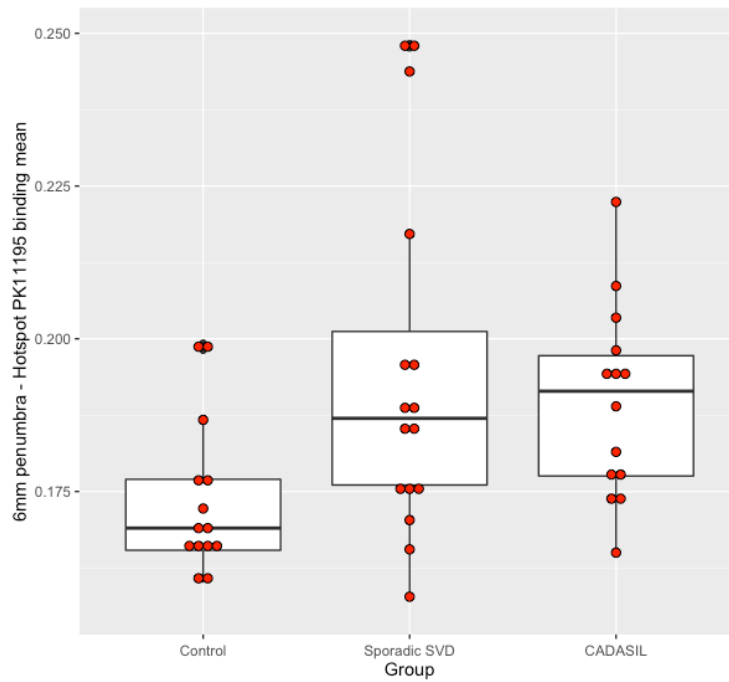
Figure C.5: The mean value of the PK binding hotspots was compared between the groups. The mean was were significantly higher in sporadic SVD compared to control (p=0.029). They were also significantly higher in CADASIL compared to control (p=0.010).
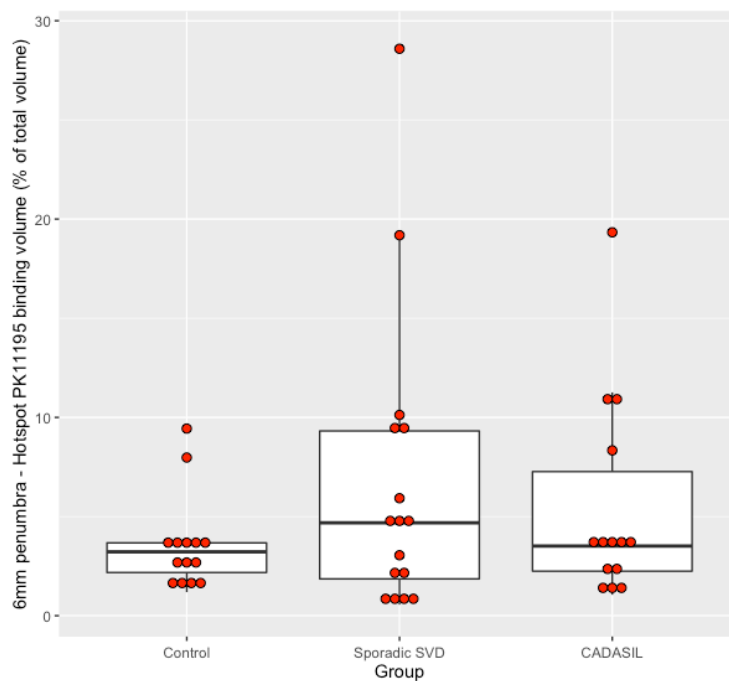
Figure C.6: The volume value of the PK binding hotspots was compared between the groups. The volume was not significantly different between sporadic SVD compared to control (p=0.783) or CADASIL and control (p=0.641).

C.2.4 PK binding NAWM vs. WML

6mm penumbra values are shown in Table C.2. In the control group, the global mean PK values of the penumbra were significantly lower than the NAWM ($p<0.001$) and WML ($p<0.001$). The mean values of the PK binding hotspots were significantly lower then NAWM values ($p<0.001$), but significantly higher than WML values ($p<0.001$). The same pattern was seen for the volume of the PK binding hotspots; with 6mm penumbra values significantly lower than NAWM ($p<0.001$), but higher than WML ($p<0.001$).

In the sporadic SVD group, global mean PK binding values in the 6mm penumbra were significantly lower than NAWM ($p<0.001$), but significantly higher than WML ($p=0.003$). The mean values of the PK binding hotspots in the penumbra were significantly lower than the NAWM value ($p=0.002$), but no different from the WML value. NAWM hotspot volume was significantly higher than 6mm penumbra ($p=0.005$), but no different from the WML value.

In the CADASIL group, 6mm penumbra values were significantly lower than both NAWM ($p<0.001$) and WML ($p<0.001$) values for global mean binding. They were similar to NAWM ($p=0.194$) and WML ($p=0.083$) for the mean value in the PK binding hotspots. 6mm penumbra values were significantly lower than NAWM ($p<0.001$), but higher than WML ($p=0.013$) for the volume of the PK binding hotspots.

Group	Permeability measurement	Mean PK binding		Mean Penumbra		P value
		Median	IQR	Median	IQR	
Control	NAWM mean	0.030	0.021	-0.046	0.033	**<0.001**
	WML mean	0.036	0.158	-0.046	0.033	**<0.001**
	HS NAWM mean	0.174	0.017	0.169	0.012	**<0.001**
	HS WML	0.000	0.146	0.169	0.012	**<0.001**
	NAWM volume	3.761	4.085	3.222	1.494	**<0.001**
	WML volume	0.000	0.671	3.222	1.494	**<0.001**
Sporadic SVD	NAWM mean	0.054	0.033	-0.075	0.037	**<0.001**
	WML mean	-0.003	0.045	-0.075	0.037	**0.003**
	HS NAWM mean	0.204	0.028	0.187	0.025	**0.002**
	HS WML	0.182	0.044	0.187	0.025	0.083
	NAWM volume	9.442	7.199	4.685	7.458	**0.005**
	WML volume	0.858	3.341	4.685	7.458	0.076
CADASIL	NAWM mean	0.052	0.045	-0.075	0.033	**<0.001**
	WML mean	0.013	0.044	-0.075	0.033	**<0.001**
	HS NAWM mean	0.196	0.030	0.191	0.020	0.194
	HS WML	0.180	0.023	0.191	0.020	0.083
	NAWM volume	6.805	10.004	3.514	5.021	**<0.001**
	WML volume	1.327	2.665	3.514	5.021	**0.013**

Table C.2: Pairwise comparisons for the individual groups for the global PK binding values, hotspot PK binding mean and hotspot PK binding volume with equivalent 6mm penumbra values. Significant p values are shown in bold.

Appendix D: Correlations between BBB permeability and PK

Correlations were investigated between the BBB permeability and PK values for all of the patients combined.

D.1 Statistical Analysis

Spearman's rank correlation test was used to test all of the correlations between BBB permeability and respective PK binding values. P values were adjusted for multiple comparisons using FDR.

D.2 Results

Correlations between all of the BBB permeability and PK binding parameters for all of the participants combined can be found in Table D.1. In the WM, there was a significant correlation seen between the global mean value from the PK binding and the mean value of the BBB permeability hotspots (Spearman's Rho = 0.41, $p<0.05$). There were no other significant correlations seen for any of the other WM values or for any of the NAWM or WML values.

A

WM		PK		
		Global mean	**Hotspot mean**	**Hotspot volume**
BBB	**Global mean**	0.27	0.21	0.08
	Hotspot mean	0.41*	0.31	0.24
	Hotspot volume	0.16	0.08	-0.05

B

NAWM		PK		
		Global mean	**Hotspot mean**	**Hotspot volume**
BBB	**Global mean**	0.11	0.28	0.11
	Hotspot mean	0.11	0.28	0.21
	Hotspot volume	0.08	0.2	0.03

C

WML		PK		
		Global mean	**Hotspot mean**	**Hotspot volume**
BBB	**Global mean**	0.15	0.08	-0.02
	Hotspot mean	0.19	-0.02	-0.01
	Hotspot volume	0.1	0.05	0.01

*p<0.05, **p<0.01, ***p<0.001

Table D.1: Correlation matrices of Spearman's Rho values for associations between BBB permeability and PK binding parameters in all the patients combined. 1) WM. 2) NAWM. 3) WML.

References

Abbott, N. J., Patabendige, A. A., Dolman, D. E., Yusof, S. R. & Begley, D. J. (2010) Structure and function of the blood-brain barrier. *Neurobiol Dis* **37(1)**:13-25.

Abbott, N. J., Ronnback, L. & Hansson, E. (2006) Astrocyte-endothelial interactions at the blood-brain barrier. *Nat Rev Neurosci* **7(1)**:41-53.

Abdelhafiz, A. H., Ahmed, S. & El Nahas, M. (2011) Microalbuminuria: marker or maker of cardiovascular disease. *Nephron Exp Nephrol* **119 Suppl 1**:e6-10.

Abid, K. A., Sobowale, O. A., Parkes, L. M., Naish, J., Parker, G. J. M., Du Plessis, D., Brough, D., Barrington, J., Allan, S. M., Hinz, R. & Parry-Jones, A. R. (2018) Assessing Inflammation in Acute Intracerebral Hemorrhage with PK11195 PET and Dynamic Contrast-Enhanced MRI. *J Neuroimaging* **28(2)**:158-161.

Acalovschi, D., Wiest, T., Hartmann, M., Farahmi, M., Mansmann, U., Auffarth, G. U., Grau, A. J., Green, F. R., Grond-Ginsbach, C. & Schwaninger, M. (2003) Multiple levels of regulation of the interleukin-6 system in stroke. *Stroke* **34(8)**:1864-9.

Adair, J. C., Charlie, J., Dencoff, J. E., Kaye, J. A., Quinn, J. F., Camicioli, R. M., Stetler-Stevenson, W. G. & Rosenberg, G. A. (2004) Measurement of gelatinase B (MMP-9) in the cerebrospinal fluid of patients with vascular dementia and Alzheimer disease. *Stroke* **35(6)**:e159-62.

Adib-Samii, P., Brice, G., Martin, R. J. & Markus, H. S. (2010) Clinical spectrum of CADASIL and the effect of cardiovascular risk factors on phenotype: study in 200 consecutively recruited individuals. *Stroke* **41(4)**:630-4.

Airas, L., Nylund, M. & Rissanen, E. (2018) Evaluation of Microglial Activation in Multiple Sclerosis Patients Using Positron Emission Tomography. *Front Neurol* **9**.

Airas, L., Rissanen, E. & Rinne, J. O. (2015) Imaging neuroinflammation in multiple sclerosis using TSPO-PET. *Clin Transl Imaging* **3(6)**:461-73.

Akiguchi, I., Tomimoto, H., Suenaga, T., Wakita, H. & Budka, H. (1998) Blood-brain barrier dysfunction in Binswanger's disease; an immunohistochemical study. *Acta Neuropathol* **95(1)**:78-84.

Akoudad, S., Wolters, F. J., Viswanathan, A., De Bruijn, R. F., Van Der Lugt, A., Hofman, A., Koudstaal, P. J., Ikram, M. A. & Vernooij, M. W. (2016) Cerebral microbleeds are associated with cognitive decline and dementia: the Rotterdam Study. *JAMA Neurol* **73(8)**:934-43.

Alafuzoff, I., Adolfsson, R., Bucht, G. & Winblad, B. (1983) Albumin and immunoglobulin in plasma and cerebrospinal fluid, and blood-cerebrospinal fluid barrier function in patients with dementia of Alzheimer type and multi-infarct dementia. *J Neurol Sci* **60(3)**:465-72.

Alam, M. M., Lee, J. & Lee, S. Y. (2017) Recent Progress in the Development of TSPO PET Ligands for Neuroinflammation Imaging in Neurological Diseases. *Nucl Med Mol Imaging* **51(4)**:283-96.

Albrecht, D. S., Granziera, C., Hooker, J. M. & Loggia, M. L. (2016) In Vivo Imaging of Human Neuroinflammation. *ACS Chem Neurosci* **7(4)**:470-83.

Aloisi, F. (2001) Immune function of microglia. *Glia* **36(2)**:165-79.

Appelman, A. P., Exalto, L. G., Van Der Graaf, Y., Biessels, G. J., Mali, W. P. & Geerlings, M. I. (2009) White matter lesions and brain atrophy: more than shared risk factors? A systematic review. *Cerebrovasc Dis* **28(3)**:227-42.

Arba, F., Giannini, A., Piccardi, B., Biagini, S., Palumbo, V., Giusti, B., Nencini, P., Maria Gori, A., Nesi, M., Pracucci, G., Bono, G., Bovi, P., Fainardi, E., Consoli, D., Nucera, A., Massaro, F., Orlandi, G., Perini, F., Tassi, R., Sessa, M., Toni, D., Abbate, R. & Inzitari, D. (2019a) Small vessel disease and biomarkers of endothelial dysfunction after ischaemic stroke. *Eur Stroke J* **4(2)**:119-126.

Arba, F., Piccardi, B., Palumbo, V., Giusti, B., Nencini, P., Gori, A. M., Sereni, A., Nesi, M., Pracucci, G., Bono, G., Bovi, P., Fainardi, E., Consoli, D., Nucera, A., Massaro, F., Orlandi, G., Perini, F., Tassi, R., Sessa, M., Toni, D., Abbate, R. & Inzitari, D. (2019b) Small Vessel Disease Is Associated with Tissue Inhibitor of Matrix Metalloproteinase-4 After Ischaemic Stroke. *Transl Stroke Res* **10(1)**:44-51.

Arba, F., Quinn, T. J., Hankey, G. J., Lees, K. R., Wardlaw, J. M., Ali, M. & Inzitari, D. (2018) Enlarged perivascular spaces and cognitive impairment after stroke and transient ischemic attack. *Int J Stroke* **13(1)**:47-56.

Arboix, A. (2011) Lacunar infarct and cognitive decline. *Expert Rev Neurother* **11(9)**:1251-4.

Aribisala, B. S., Valdes Hernandez, M. C., Royle, N. A., Morris, Z., Munoz Maniega, S., Bastin, M. E., Deary, I. J. & Wardlaw, J. M. (2013) Brain atrophy associations with white matter lesions in the ageing brain: the Lothian Birth Cohort 1936. *Eur Radiol* **23(4)**:1084-92.

Aribisala, B. S., Wiseman, S., Morris, Z., Valdes-Hernandez, M. C., Royle, N. A., Maniega, S. M., Gow, A. J., Corley, J., Bastin, M. E., Starr, J., Deary, I. J. & Wardlaw, J. M. (2014) Circulating inflammatory markers are associated with magnetic resonance imaging-visible perivascular spaces but not directly with white matter hyperintensities. *Stroke* **45(2)**:605-7.

Armao, D., Kornfeld, M., Estrada, E. Y., Grossetete, M. & Rosenberg, G. A. (1997) Neutral proteases and disruption of the blood-brain barrier in rat. *Brain Res* **767(2)**:259-64.

Armitage, P. A., Farrall, A. J., Carpenter, T. K., Doubal, F. N. & Wardlaw, J. M. (2011) Use of dynamic contrast-enhanced MRI to measure subtle blood-brain barrier abnormalities. *Magn Reson Imaging* **29(3)**:305-14.

Armulik, A., Genove, G., Mae, M., Nisancioglu, M. H., Wallgard, E., Niaudet, C., He, L., Norlin, J., Lindblom, P., Strittmatter, K., Johansson, B. R. & Betsholtz, C. (2010) Pericytes regulate the blood-brain barrier. *Nature* **468(7323)**:557-61.

Asahi, M., Wang, X., Mori, T., Sumii, T., Jung, J. C., Moskowitz, M. A., Fini, M. E. & Lo, E. H. (2001) Effects of matrix metalloproteinase-9 gene knock-out on the proteolysis of blood-brain barrier and white matter components after cerebral ischemia. *J Neurosci* **21(19)**:7724-32.

Ashburner, J. & Friston, K. J. (2005) Unified segmentation. *Neuroimage* **26(3)**:839-51.

Aso, Y., Okumura, K., Takebayashi, K., Wakabayashi, S. & Inukai, T. (2003) Relationships of plasma interleukin-18 concentrations to hyperhomocysteinemia and carotid intimal-media wall thickness in patients with type 2 diabetes. *Diabetes Care* **26(9)**:2622-7.

Assarsson, E., Lundberg, M., Holmquist, G., Bjorkesten, J., Thorsen, S. B., Ekman, D., Eriksson, A., Rennel Dickens, E., Ohlsson, S., Edfeldt, G., Andersson, A. C., Lindstedt, P., Stenvang, J., Gullberg, M. & Fredriksson, S. (2014)

Homogenous 96-plex PEA immunoassay exhibiting high sensitivity, specificity, and excellent scalability. *PLoS One* **9(4)**:e95192.

Attems, J. & Jellinger, K. A. (2014) The overlap between vascular disease and Alzheimer's disease--lessons from pathology. *BMC Med* **12**:206.

Auer, D. P., Putz, B., Gossl, C., Elbel, G., Gasser, T. & Dichgans, M. (2001) Differential lesion patterns in CADASIL and sporadic subcortical arteriosclerotic encephalopathy: MR imaging study with statistical parametric group comparison. *Radiology* **218(2)**:443-51.

Baezner, H., Blahak, C., Poggesi, A., Pantoni, L., Inzitari, D., Chabriat, H., Erkinjuntti, T., Fazekas, F., Ferro, J. M., Langhorne, P., O'brien, J., Scheltens, P., Visser, M. C., Wahlund, L. O., Waldemar, G., Wallin, A. & Hennerici, M. G. (2008) Association of gait and balance disorders with age-related white matter changes: the LADIS study. *Neurology* **70(12)**:935-42.

Bailey, E. L., Wardlaw, J. M., Graham, D., Dominiczak, A. F., Sudlow, C. L. & Smith, C. (2011) Cerebral small vessel endothelial structural changes predate hypertension in stroke-prone spontaneously hypertensive rats: a blinded, controlled immunohistochemical study of 5- to 21-week-old rats. *Neuropathol Appl Neurobiol* **37(7)**:711-26.

Bamford, J., Sandercock, P., Dennis, M., Burn, J. & Warlow, C. (1991) Classification and natural history of clinically identifiable subtypes of cerebral infarction. *Lancet* **337(8756)**:1521-6.

Bateman, R. J., Siemers, E. R., Mawuenyega, K. G., Wen, G., Browning, K. R., Sigurdson, W. C., Yarasheski, K. E., Friedrich, S. W., Demattos, R. B., May, P. C., Paul, S. M. & Holtzman, D. M. (2009) A gamma-secretase inhibitor decreases amyloid-beta production in the central nervous system. *Ann Neurol* **66(1)**:48-54.

Baune, B. T., Ponath, G., Rothermundt, M., Roesler, A. & Berger, K. (2009) Association between cytokines and cerebral MRI changes in the aging brain. *J Geriatr Psychiatry Neurol* **22(1)**:23-34.

Becker, C. E., Quinn, T. J. & Williams, A. (2019) Association Between Endothelial Cell Stabilizing Medication and Small Vessel Disease Stroke: A Case-Control Study. *Front Neurol* **10**:1029.

Beer, C., Blacker, D., Hankey, G. J. & Puddey, I. B. (2011) Association of clinical and aetiologic subtype of acute ischaemic stroke with inflammation, oxidative stress and vascular function: a cross-sectional observational study. *Med Sci Monit* **17(9)**:Cr467-73.

Bell, R. D., Winkler, E. A., Sagare, A. P., Singh, I., Larue, B., Deane, R. & Zlokovic, B. V. (2010) Pericytes control key neurovascular functions and neuronal phenotype in the adult brain and during brain aging. *Neuron* **68(3)**:409-27.

Benjamin, P., Trippier, S., Lawrence, A. J., Lambert, C., Zeestraten, E., Williams, O. A., Patel, B., Morris, R. G., Barrick, T. R., Mackinnon, A. D. & Markus, H. S. (2018) Lacunar Infarcts, but Not Perivascular Spaces, Are Predictors of Cognitive Decline in Cerebral Small-Vessel Disease. *Stroke* **49(3)**:586-593.

Bennett, D. A., Gilley, D. W., Lee, S. & Cochran, E. J. (1994) White matter changes: neurobehavioral manifestations of Binswanger's disease and clinical correlates in Alzheimer's disease. *Dementia* **5(3-4)**:148-52.

Bernbaum, M., Menon, B. K., Fick, G., Smith, E. E., Goyal, M., Frayne, R. & Coutts, S. B. (2015) Reduced blood flow in normal white matter predicts development of leukoaraiosis. *J Cereb Blood Flow Metab* **35(10)**:1610-5.

Birns, J., Jarosz, J., Markus, H. S. & Kalra, L. (2009) Cerebrovascular reactivity and dynamic autoregulation in ischaemic subcortical white matter disease. *J Neurol Neurosurg Psychiatry* **80(10)**:1093-8.

Biron, K. E., Dickstein, D. L., Gopaul, R. & Jefferies, W. A. (2011) Amyloid triggers extensive cerebral angiogenesis causing blood brain barrier permeability and hypervascularity in Alzheimer's disease. *PLoS One* **6(8)**:e23789.

Bjerke, M., Zetterberg, H., Edman, A., Blennow, K., Wallin, A. & Andreasson, U. (2011) Cerebrospinal fluid matrix metalloproteinases and tissue inhibitor of metalloproteinases in combination with subcortical and cortical biomarkers in vascular dementia and Alzheimer's disease. *J Alzheimers Dis* **27(3)**:665-76.

Blanco-Rojas, L., Arboix, A., Canovas, D., Grau-Olivares, M., Oliva Morera, J. C. & Parra, O. (2013) Cognitive profile in patients with a first-ever lacunar infarct with and without silent lacunes: a comparative study. *BMC Neurol* **13**:203.

Blennow, K., Fredman, P., Wallin, A., Gottfries, C. G., Karlsson, I., Langstrom, G., Skoog, I., Svennerholm, L. & Wikkelso, C. (1993) Protein analysis in

cerebrospinal fluid. II. Reference values derived from healthy individuals 18-88 years of age. *Eur Neurol* **33(2)**:129-33.

Boehme, A. K., Mcclure, L. A., Zhang, Y., Luna, J. M., Del Brutto, O. H., Benavente, O. R. & Elkind, M. S. (2016) Inflammatory Markers and Outcomes After Lacunar Stroke: Levels of Inflammatory Markers in Treatment of Stroke Study. *Stroke* **47(3)**:659-67.

Bolandzadeh, N., Davis, J. C., Tam, R., Handy, T. C. & Liu-Ambrose, T. (2012) The association between cognitive function and white matter lesion location in older adults: a systematic review. *BMC Neurol* **12**:126.

Bonneh-Barkay, D., Wang, G., Starkey, A., Hamilton, R. L. & Wiley, C. A. (2010) In vivo CHI3L1 (YKL-40) expression in astrocytes in acute and chronic neurological diseases. In *J Neuroinflammation*.), vol. 7, pp. 34.

Braun, H., Bueche, C. Z., Garz, C., Oldag, A., Heinze, H. J., Goertler, M., Reymann, K. G. & Schreiber, S. (2012) Stases are associated with blood-brain barrier damage and a restricted activation of coagulation in SHRSP. *J Neurol Sci* **322(1-2)**:71-6.

Brennan-Krohn, T., Salloway, S., Correia, S., Dong, M. & De La Monte, S. M. (2010) Glial Vascular Degeneration in CADASIL. *J Alzheimers Dis* **21(4)**:1393-402.

Brew, K. & Nagase, H. (2010) The tissue inhibitors of metalloproteinases (TIMPs): An ancient family with structural and functional diversity. *Biochim Biophys Acta* **1803(1)**:55-71.

Brkic, M., Balusu, S., Libert, C. & Vandenbroucke, R. E. (2015) Friends or Foes: Matrix Metalloproteinases and Their Multifaceted Roles in Neurodegenerative Diseases. *Mediators Inflamm* **2015**.

Bronge, L. & Wahlund, L. O. (2000) White matter lesions in dementia: an MRI study on blood-brain barrier dysfunction. *Dement Geriatr Cogn Disord* **11(5)**:263-7.

Brookes, R. L., Herbert, V., Lawrence, A. J., Morris, R. G. & Markus, H. S. (2014) Depression in small-vessel disease relates to white matter ultrastructural damage, not disability. *Neurology* **83(16)**:1417-23.

Bruce, A. J., Boling, W., Kindy, M. S., Peschon, J., Kraemer, P. J., Carpenter, M. K., Holtsberg, F. W. & Mattson, M. P. (1996) Altered neuronal and microglial responses to excitotoxic and ischemic brain injury in mice lacking TNF receptors. *Nat Med* **2(7)**:788-94.

Burgos, N., Cardoso, M. J., Thielemans, K., Modat, M., Pedemonte, S., Dickson, J., Barnes, A., Ahmed, R., Mahoney, C. J., Schott, J. M., Duncan, J. S., Atkinson, D., Arridge, S. R., Hutton, B. F. & Ourselin, S. (2014) Attenuation correction synthesis for hybrid PET-MR scanners: application to brain studies. *IEEE Trans Med Imaging* **33(12)**:2332-41.

Cagnin, A., Brooks, D. J., Kennedy, A. M., Gunn, R. N., Myers, R., Turkheimer, F. E., Jones, T. & Banati, R. B. (2001) In-vivo measurement of activated microglia in dementia. *Lancet* **358(9280)**:461-7.

Campolo, J., De Maria, R., Mariotti, C., Tomasello, C., Parolini, M., Frontali, M., Inzitari, D., Valenti, R., Federico, A., Taroni, F. & Parodi, O. (2013) Is the Oxidant/Antioxidant Status Altered in CADASIL Patients? *PLoS One* **8(6)**.

Candelario-Jalil, E., Thompson, J., Taheri, S., Grossetete, M., Adair, J. C., Edmonds, E., Prestopnik, J., Wills, J. & Rosenberg, G. A. (2011) Matrix metalloproteinases are associated with increased blood-brain barrier opening in vascular cognitive impairment. *Stroke* **42(5)**:1345-50.

Candiello, J., Cole, G. J. & Halfter, W. (2010) Age-dependent changes in the structure, composition and biophysical properties of a human basement membrane. *Matrix Biol* **29(5)**:402-10.

Carmelli, D., Decarli, C., Swan, G. E., Jack, L. M., Reed, T., Wolf, P. A. & Miller, B. L. (1998) Evidence for genetic variance in white matter hyperintensity volume in normal elderly male twins. *Stroke* **29(6)**:1177-81.

Carney, J. P., Townsend, D. W., Rappoport, V. & Bendriem, B. (2006) Method for transforming CT images for attenuation correction in PET/CT imaging. *Med Phys* **33(4)**:976-83.

Cavalieri, M., Schmidt, H. & Schmidt, R. (2012) Structural MRI in normal aging and Alzheimer's disease: white and black spots. *Neurodegener Dis* **10(1-4)**:253-6.

Cavallari, M., Moscufo, N., Meier, D., Skudlarski, P., Pearlson, G. D., White, W. B., Wolfson, L. & Guttmann, C. R. (2014) Thalamic fractional anisotropy predicts accrual of cerebral white matter damage in older subjects with small-vessel disease. *J Cereb Blood Flow Metab* **34(8)**:1321-7.

Cavusoglu, E., Kornecki, E., Sobocka, M. B., Babinska, A., Ehrlich, Y. H., Chopra, V., Yanamadala, S., Ruwende, C., Salifu, M. O., Clark, L. T., Eng, C., Pinsky, D. J. & Marmur, J. D. (2007) Association of plasma levels of F11

receptor/junctional adhesion molecule-A (F11R/JAM-A) with human atherosclerosis. *J Am Coll Cardiol* **50(18)**:1768-76.

Cayrol, R., Wosik, K., Berard, J. L., Dodelet-Devillers, A., Ifergan, I., Kebir, H., Haqqani, A. S., Kreymborg, K., Krug, S., Moumdjian, R., Bouthillier, A., Becher, B., Arbour, N., David, S., Stanimirovic, D. & Prat, A. (2008) Activated leukocyte cell adhesion molecule promotes leukocyte trafficking into the central nervous system. *Nat Immunol* **9(2)**:137-45.

Chabriat, H., Herve, D., Duering, M., Godin, O., Jouvent, E., Opherk, C., Alili, N., Reyes, S., Jabouley, A., Zieren, N., Guichard, J. P., Pachai, C., Vicaut, E. & Dichgans, M. (2016) Predictors of Clinical Worsening in Cerebral Autosomal Dominant Arteriopathy With Subcortical Infarcts and Leukoencephalopathy: Prospective Cohort Study. *Stroke* **47(1)**:4-11.

Chabriat, H., Levy, C., Taillia, H., Iba-Zizen, M. T., Vahedi, K., Joutel, A., Tournier-Lasserve, E. & Bousser, M. G. (1998) Patterns of MRI lesions in CADASIL. *Neurology* **51(2)**:452-7.

Chandra, P., Suman, P., Airon, H., Mukherjee, M. & Kumar, P. (2014) Prospects and advancements in C-reactive protein detection. *World J Methodol* **4(1)**:1-5.

Charidimou, A., Shams, S., Romero, J. R., Ding, J., Veltkamp, R., Horstmann, S., Eiriksdottir, G., Van Buchem, M. A., Gudnason, V., Himali, J. J., Gurol, M. E., Viswanathan, A., Imaizumi, T., Vernooij, M. W., Seshadri, S., Greenberg, S. M., Benavente, O. R., Launer, L. J. & Shoamanesh, A. (2018) Clinical significance of cerebral microbleeds on MRI: A comprehensive meta-analysis of risk of intracerebral hemorrhage, ischemic stroke, mortality, and dementia in cohort studies (v1). *Int J Stroke* **13(5)**:454-468.

Charlton, R. A., Barrick, T. R., Mcintyre, D. J., Shen, Y., O'sullivan, M., Howe, F. A., Clark, C. A., Morris, R. G. & Markus, H. S. (2006a) White matter damage on diffusion tensor imaging correlates with age-related cognitive decline. *Neurology* **66(2)**:217-22.

Charlton, R. A., Morris, R. G., Nitkunan, A. & Markus, H. S. (2006b) The cognitive profiles of CADASIL and sporadic small vessel disease. *Neurology* **66(10)**:1523-6.

Chauveau, F., Boutin, H., Van Camp, N., Dolle, F. & Tavitian, B. (2008) Nuclear imaging of neuroinflammation: a comprehensive review of [11C]PK11195 challengers. *Eur J Nucl Med Mol Imaging* **35(12)**:2304-19.

Chen, M. K. & Guilarte, T. R. (2008) Translocator protein 18 kDa (TSPO): molecular sensor of brain injury and repair. *Pharmacol Ther* **118(1)**:1-17.

Chen, W. W., Zhang, X. & Huang, W. J. (2016) Role of neuroinflammation in neurodegenerative diseases (Review). *Mol Med Rep* **13(4)**:3391-6.

Chen, X. L., Li, Q., Huang, W. S., Lin, Y. S., Xue, J., Wang, B., Jin, K. L. & Shao, B. (2017) Serum YKL-40, a prognostic marker in patients with large-artery atherosclerotic stroke. *Acta Neurol Scand* **136(2)**:97-102.

Cherian, P., Hankey, G. J., Eikelboom, J. W., Thom, J., Baker, R. I., Mcquillan, A., Staton, J. & Yi, Q. (2003) Endothelial and platelet activation in acute ischemic stroke and its etiological subtypes. *Stroke* **34(9)**:2132-7.

Chesselet, M. F. & Carmichael, S. T. (2012) Animal Models of Neurological Disorders. *Neurotherapeutics* **9(2)**:241-4.

Cho, A. H., Kim, H. R., Kim, W. & Yang, D. W. (2015) White matter hyperintensity in ischemic stroke patients: it may regress over time. *J Stroke* **17(1)**:60-6.

Choi, J. C. (2015) Genetics of Cerebral Small Vessel Disease. *J Stroke* **17(1)**:7-16.

Choi, P., Ren, M., Phan, T. G., Callisaya, M., Ly, J. V., Beare, R., Chong, W. & Srikanth, V. (2012) Silent infarcts and cerebral microbleeds modify the associations of white matter lesions with gait and postural stability: population-based study. *Stroke* **43(6)**:1505-10.

Cianchetti, C., Corona, S., Foscoliano, M., Scalas, F. & Sannio-Fancello, G. (2005) Modified Wisconsin Card Sorting Test: proposal of a supplementary scoring method. *Arch Clin Neuropsychol* **20(4)**:555-8.

Cianciolo, G., De Pascalis, A., Di Lullo, L., Ronco, C., Zannini, C. & La Manna, G. (2017) Folic Acid and Homocysteine in Chronic Kidney Disease and Cardiovascular Disease Progression: Which Comes First? *Cardiorenal Med* **7(4)**:255-266.

Cipollini, V., Troili, F. & Giubilei, F. (2019) Emerging Biomarkers in Vascular Cognitive Impairment and Dementia: From Pathophysiological Pathways to Clinical Application. *Int J Mol Sci* **20(11)**.

Clarke, R., Bennett, D., Parish, S., Lewington, S., Skeaff, M., Eussen, S. J., Lewerin, C., Stott, D. J., Armitage, J., Hankey, G. J., Lonn, E., Spence, J. D., Galan, P., De Groot, L. C., Halsey, J., Dangour, A. D., Collins, R. & Grodstein, F. (2014) Effects of homocysteine lowering with B vitamins on cognitive aging: meta-analysis of 11 trials with cognitive data on 22,000 individuals. *Am J Clin Nutr* **100(2)**:657-66.

Cognat, E., Cleophax, S., Domenga-Denier, V. & Joutel, A. (2014) Early white matter changes in CADASIL: evidence of segmental intramyelinic oedema in a pre-clinical mouse model. *Acta Neuropathol Commun* **2**.

Connolly, C., Magnusson-Lind, A., Lu, G., Wagner, P. K., Southwell, A. L., Hayden, M. R., Bjorkqvist, M. & Leavitt, B. R. (2016) Enhanced immune response to MMP3 stimulation in microglia expressing mutant huntingtin. *Neuroscience* **325**:74-88.

Connolly, E. S., Jr., Winfree, C. J., Prestigiacomo, C. J., Kim, S. C., Choudhri, T. F., Hoh, B. L., Naka, Y., Solomon, R. A. & Pinsky, D. J. (1997) Exacerbation of cerebral injury in mice that express the P-selectin gene: identification of P-selectin blockade as a new target for the treatment of stroke. *Circ Res* **81(3)**:304-10.

Cordonnier, C., Al-Shahi Salman, R. & Wardlaw, J. (2007) Spontaneous brain microbleeds: systematic review, subgroup analyses and standards for study design and reporting. *Brain* **130(Pt 8)**:1988-2003.

Cosenza-Nashat, M., Zhao, M. L., Suh, H. S., Morgan, J., Natividad, R., Morgello, S. & Lee, S. C. (2009) Expression of the translocator protein of 18 kDa by microglia, macrophages and astrocytes based on immunohistochemical localization in abnormal human brain. *Neuropathol Appl Neurobiol* **35(3)**:306-28.

Coughlan, A. K., Oddy, M. & Crawford, J. R. (2007) *The BIRT Memory and Information Processing Battery (B-MIPB)*. Wakefield, UK, The Brain Injury Rehabilitation Trust (BIRT).

Coughlin, J. M., Wang, Y., Ma, S., Yue, C., Kim, P. K., Adams, A. V., Roosa, H. V., Gage, K. L., Stathis, M., Rais, R., Rojas, C., Mcglothan, J. L., Watkins, C. C., Sacktor, N., Guilarte, T. R., Zhou, Y., Sawa, A., Slusher, B. S., Caffo, B., Kassiou, M., Endres, C. J. & Pomper, M. G. (2014) Regional brain

distribution of translocator protein using [(11)C]DPA-713 PET in individuals infected with HIV. *J Neurovirol* **20(3)**:219-32.

Coupland, K., Lendahl, U. & Karlstrom, H. (2018) Role of NOTCH3 Mutations in the Cerebral Small Vessel Disease Cerebral Autosomal Dominant Arteriopathy With Subcortical Infarcts and Leukoencephalopathy. *Stroke* **49(11)**:2793-2800.

Craggs, L. J., Hagel, C., Kuhlenbaeumer, G., Borjesson-Hanson, A., Andersen, O., Viitanen, M., Kalimo, H., Mclean, C. A., Slade, J. Y., Hall, R. A., Oakley, A. E., Yamamoto, Y., Deramecourt, V. & Kalaria, R. N. (2013) Quantitative vascular pathology and phenotyping familial and sporadic cerebral small vessel diseases. *Brain Pathol* **23(5)**:547-57.

Croall, I. D., Lohner, V., Moynihan, B., Khan, U., Hassan, A., O'brien, J. T., Morris, R. G., Tozer, D. J., Cambridge, V. C., Harkness, K., Werring, D. J., Blamire, A. M., Ford, G. A., Barrick, T. R. & Markus, H. S. (2017) Using DTI to assess white matter microstructure in cerebral small vessel disease (SVD) in multicentre studies. *Clin Sci (Lond)* **131(12)**:1361-73.

Cuadrado, E., Rosell, A., Borrell-Pages, M., Garcia-Bonilla, L., Hernandez-Guillamon, M., Ortega-Aznar, A. & Montaner, J. (2009) Matrix metalloproteinase-13 is activated and is found in the nucleus of neural cells after cerebral ischemia. *J Cereb Blood Flow Metab* **29(2)**:398-410.

Cuadrado-Godia, E., Dwivedi, P., Sharma, S., Ois Santiago, A., Roquer Gonzalez, J., Balcells, M., Laird, J., Turk, M., Suri, H. S., Nicolaides, A., Saba, L., Khanna, N. N. & Suri, J. S. (2018) Cerebral Small Vessel Disease: A Review Focusing on Pathophysiology, Biomarkers, and Machine Learning Strategies. *J Stroke* **20(3)**:302-20.

D'souza, M. M., Gorthi, S. P., Vadwala, K., Trivedi, R., Vijayakumar, C., Kaur, P. & Khushu, S. (2018) Diffusion tensor tractography in cerebral small vessel disease: correlation with cognitive function. *Neuroradiol J* **31(1)**:83-89.

Dawson, J. D., Uc, E. Y., Anderson, S. W., Johnson, A. M. & Rizzo, M. (2010) Neuropsychological predictors of driving errors in older adults. *J Am Geriatr Soc* **58(6)**:1090-6.

De Groot, J. C., De Leeuw, F. E., Oudkerk, M., Hofman, A., Jolles, J. & Breteler, M. M. (2000) Cerebral white matter lesions and depressive symptoms in elderly adults. *Arch Gen Psychiatry* **57(11)**:1071-6.

De Groot, M., Verhaaren, B. F., De Boer, R., Klein, S., Hofman, A., Van Der Lugt, A., Ikram, M. A., Niessen, W. J. & Vernooij, M. W. (2013) Changes in normal-appearing white matter precede development of white matter lesions. *Stroke* **44(4)**:1037-42.

De Guio, F., Mangin, J. F., Duering, M., Ropele, S., Chabriat, H. & Jouvent, E. (2015) White matter edema at the early stage of cerebral autosomal-dominant arteriopathy with subcortical infarcts and leukoencephalopathy. *Stroke* **46(1)**:258-61.

De Laat, K. F., Van Norden, A. G., Gons, R. A., Van Oudheusden, L. J., Van Uden, I. W., Bloem, B. R., Zwiers, M. P. & De Leeuw, F. E. (2010) Gait in elderly with cerebral small vessel disease. *Stroke* **41(8)**:1652-8.

De Leeuw, F. E., De Kleine, M., Frijns, C. J., Fijnheer, R., Van Gijn, J. & Kappelle, L. J. (2002) Endothelial cell activation is associated with cerebral white matter lesions in patients with cerebrovascular disease. *Ann N Y Acad Sci* **977**:306-14.

De Vis, J. B., Zwanenburg, J. J., Van Der Kleij, L. A., Spijkerman, J. M., Biessels, G. J., Hendrikse, J. & Petersen, E. T. (2016) Cerebrospinal fluid volumetric MRI mapping as a simple measurement for evaluating brain atrophy. *Eur Radiol* **26**:1254-62.

Debruyne, J. C., Versijpt, J., Van Laere, K. J., De Vos, F., Keppens, J., Strijckmans, K., Achten, E., Slegers, G., Dierckx, R. A., Korf, J. & De Reuck, J. L. (2003) PET visualization of microglia in multiple sclerosis patients using [11C]PK11195. *Eur J Neurol* **10(3)**:257-64.

Delgado, P., Riba-Llena, I., Tovar, J. L., Jarca, C. I., Mundet, X., Lopez-Rueda, A., Orfila, F., Llussa, J., Manresa, J. M., Alvarez-Sabin, J., Nafria, C., Fernandez, J. L., Maisterra, O. & Montaner, J. (2014) Prevalence and associated factors of silent brain infarcts in a Mediterranean cohort of hypertensives. *Hypertension* **64(3)**:658-63.

Delis, D. C., Kaplan, E. & Kramer, J. H. (2001) *Delis-Kaplan Executive Function Scale (D-KEFS)*. San Antonio, TX: The Psychological Corporation.

Della Nave, R., Foresti, S., Pratesi, A., Ginestroni, A., Inzitari, M., Salvadori, E., Giannelli, M., Diciotti, S., Inzitari, D. & Mascalchi, M. (2007) Whole-brain histogram and voxel-based analyses of diffusion tensor imaging in patients with leukoaraiosis: correlation with motor and cognitive impairment. *AJNR Am J Neuroradiol* **28(7)**:1313-9.

Deplanque, D., Lavallee, P. C., Labreuche, J., Gongora-Rivera, F., Jaramillo, A., Brenner, D., Abboud, H., Klein, I. F., Touboul, P. J., Vicaut, E. & Amarenco, P. (2013) Cerebral and extracerebral vasoreactivity in symptomatic lacunar stroke patients: a case-control study. *Int J Stroke* **8(6)**:413-21.

Di Donato, I., Bianchi, S., De Stefano, N., Dichgans, M., Dotti, M. T., Duering, M., Jouvent, E., Korczyn, A. D., Lesnik-Oberstein, S. A. J., Malandrini, A., Markus, H. S., Pantoni, L., Penco, S., Rufa, A., Sinanović, O., Stojanov, D. & Federico, A. (2017) Cerebral Autosomal Dominant Arteriopathy with Subcortical Infarcts and Leukoencephalopathy (CADASIL) as a model of small vessel disease: update on clinical, diagnostic, and management aspects. *BMC Med* **15**.

Di Rosa, M. & Malaguarnera, L. (2016) Chitinase 3 Like-1: An Emerging Molecule Involved in Diabetes and Diabetic Complications. *Pathobiology* **83(5)**:228-42.

Dichgans, M., Mayer, M., Uttner, I., Bruning, R., Muller-Hocker, J., Rungger, G., Ebke, M., Klockgether, T. & Gasser, T. (1998) The phenotypic spectrum of CADASIL: clinical findings in 102 cases. *Ann Neurol* **44(5)**:731-9.

Dichgans, M., Wick, M. & Gasser, T. (1999) Cerebrospinal fluid findings in CADASIL. *Neurology* **53(1)**:233.

Ding, J., Sigurethsson, S., Jonsson, P. V., Eiriksdottir, G., Charidimou, A., Lopez, O. L., Van Buchem, M. A., Guethnason, V. & Launer, L. J. (2017) Large Perivascular Spaces Visible on Magnetic Resonance Imaging, Cerebral Small Vessel Disease Progression, and Risk of Dementia: The Age, Gene/Environment Susceptibility-Reykjavik Study. *JAMA Neurol* **74(9)**:1105-1112.

Doll, D. N., Barr, T. L. & Simpkins, J. W. (2014) Cytokines: Their Role in Stroke and Potential Use as Biomarkers and Therapeutic Targets. *Aging Dis* **5(5)**:294-306.

Donato, A. J., Morgan, R. G., Walker, A. E. & Lesniewski, L. A. (2015) Cellular and Molecular Biology of Aging Endothelial Cells. *J Mol Cell Cardiol* **89(0 0)**:122-35.

Doubal, F. N., Maclullich, A. M., Ferguson, K. J., Dennis, M. S. & Wardlaw, J. M. (2010) Enlarged perivascular spaces on MRI are a feature of cerebral small vessel disease. *Stroke* **41(3)**:450-4.

Drazyk, A. M., Tan, R. Y. Y., Tay, J., Traylor, M., Das, T. & Markus, H. S. (2019) Encephalopathy in a Large Cohort of British Cerebral Autosomal Dominant Arteriopathy With Subcortical Infarcts and Leukoencephalopathy Patients. *Stroke* **50(2)**:283-290.

Duering, M., Csanadi, E., Gesierich, B., Jouvent, E., Herve, D., Seiler, S., Belaroussi, B., Ropele, S., Schmidt, R., Chabriat, H. & Dichgans, M. (2013) Incident lacunes preferentially localize to the edge of white matter hyperintensities: insights into the pathophysiology of cerebral small vessel disease. *Brain* **136(Pt 9)**:2717-26.

Duering, M., Finsterwalder, S., Baykara, E., Tuladhar, A. M., Gesierich, B., Konieczny, M. J., Malik, R., Franzmeier, N., Ewers, M., Jouvent, E., Biessels, G. J., Schmidt, R., De Leeuw, F. E., Pasternak, O. & Dichgans, M. (2018) Free water determines diffusion alterations and clinical status in cerebral small vessel disease. *Alzheimers Dement* **14(6)**:764-774.

Dufouil, C., Chalmers, J., Coskun, O., Besancon, V., Bousser, M. G., Guillon, P., Macmahon, S., Mazoyer, B., Neal, B., Woodward, M., Tzourio-Mazoyer, N. & Tzourio, C. (2005) Effects of blood pressure lowering on cerebral white matter hyperintensities in patients with stroke: the PROGRESS (Perindopril Protection Against Recurrent Stroke Study) Magnetic Resonance Imaging Substudy. *Circulation* **112(11)**:1644-50.

Durand-Birchenall, J., Leclercq, C., Daouk, J., Monet, P., Godefroy, O. & Bugnicourt, J. M. (2012) Attenuation of Brain White Matter Lesions After Lacunar Stroke. *Int J Prev Med* **3(2)**:134-8.

Dziewulska, D. & Lewandowska, E. (2012) Pericytes as a new target for pathological processes in CADASIL. *Neuropathology* **32(5)**:515-21.

Dziewulska, D., Nycz, E. & Rajczewska-Oleszkiewicz, C. (2017) Changes in the Vascular Extracellular Matrix as a Potential Cause of Myocyte Loss via

Anoikis in Cerebral Autosomal Dominant Arteriopathy with Subcortical Infarcts and Leukoencephalopathy. *Journal of Clinical & Experimental Pathology* **7(6)**:1-5.

Edison, P., Archer, H. A., Gerhard, A., Hinz, R., Pavese, N., Turkheimer, F. E., Hammers, A., Tai, Y. F., Fox, N., Kennedy, A., Rossor, M. & Brooks, D. J. (2008) Microglia, amyloid, and cognition in Alzheimer's disease: An [11C](R)PK11195-PET and [11C]PIB-PET study. *Neurobiol Dis* **32(3)**:412-9.

Eggink, E., Moll Van Charante, E. P., Van Gool, W. A. & Richard, E. (2019) A Population Perspective on Prevention of Dementia. *J Clin Med* **8(6)**.

Elahy, M., Jackaman, C., Mamo, J. C., Lam, V., Dhaliwal, S. S., Giles, C., Nelson, D. & Takechi, R. (2015) Blood-brain barrier dysfunction developed during normal aging is associated with inflammation and loss of tight junctions but not with leukocyte recruitment. *Immun Ageing* **12**:2.

Erdő, F., Denes, L. & De Lange, E. (2017) Age-associated physiological and pathological changes at the blood–brain barrier: A review. *J Cereb Blood Flow Metab* **37(1)**:4-24.

Erta, M., Quintana, A. & Hidalgo, J. (2012) Interleukin-6, a Major Cytokine in the Central Nervous System. *Int J Biol Sci* **8(9)**:1254-66.

Eskildsen, S. F., Gyldensted, L., Nagenthiraja, K., Nielsen, R. B., Hansen, M. B., Dalby, R. B., Frandsen, J., Rodell, A., Gyldensted, C., Jespersen, S. N., Lund, T. E., Mouridsen, K., Braendgaard, H. & Ostergaard, L. (2017) Increased cortical capillary transit time heterogeneity in Alzheimer's disease: a DSC-MRI perfusion study. *Neurobiol Aging* **50**:107-118.

Esposito, K., Pontillo, A., Ciotola, M., Di Palo, C., Grella, E., Nicoletti, G. & Giugliano, D. (2002) Weight loss reduces interleukin-18 levels in obese women. *J Clin Endocrinol Metab* **87(8)**:3864-6.

Faraco, G. & Iadecola, C. (2013) Hypertension: a harbinger of stroke and dementia. *Hypertension* **62(5)**:810-7.

Farrall, A. J. & Wardlaw, J. M. (2009) Blood-brain barrier: ageing and microvascular disease--systematic review and meta-analysis. *Neurobiol Aging* **30(3)**:337-52.

Farrall, A. W., Joanna. (2009) Blood–brain barrier: Ageing and microvascular disease – systematic review and meta-analysis **30(3)**:337–352.

Fassbender, K., Bertsch, T., Mielke, O., Muhlhauser, F. & Hennerici, M. (1999) Adhesion molecules in cerebrovascular diseases. Evidence for an inflammatory endothelial activation in cerebral large- and small-vessel disease. *Stroke* **30(8)**:1647-50.

Faustman, D. & Davis, M. (2010) TNF receptor 2 pathway: drug target for autoimmune diseases. *Nat Rev Drug Discov* **9(6)**:482-93.

Fazekas, F., Chawluk, J. B., Alavi, A., Hurtig, H. I. & Zimmerman, R. A. (1987) MR signal abnormalities at 1.5 T in Alzheimer's dementia and normal aging. *AJR Am J Roentgenol* **149(2)**:351-6.

Fazekas, F., Schmidt, R. & Scheltens, P. (1998) Pathophysiologic mechanisms in the development of age-related white matter changes of the brain. *Dement Geriatr Cogn Disord* **9 Suppl 1**:2-5.

Felderhoff-Mueser, U., Sifringer, M., Polley, O., Dzietko, M., Leineweber, B., Mahler, L., Baier, M., Bittigau, P., Obladen, M., Ikonomidou, C. & Buhrer, C. (2005) Caspase-1-processed interleukins in hyperoxia-induced cell death in the developing brain. *Ann Neurol* **57(1)**:50-9.

Ferrand, J. (1902) Essai sur l'hémiplégie des vieillards. Les lacunes de desintegration cérébrale. Avec 8 planches. *Jules Rousset; Paris*.

Fisher, C. M. (1968) The arterial lesions underlying lacunes. *Acta Neuropathol* **12(1)**:1-15.

Fisher, C. M. (1982) Lacunar strokes and infarcts: a review. *Neurology* **32(8)**:871-6.

Fisher, M. (2012) Thrombomodulin and the brain: past, present, and future. In *Neurology*.), United States, vol. 78, pp. 157-8.

Fjell, A. M., Walhovd, K. B., Fennema-Notestine, C., Mcevoy, L. K., Hagler, D. J., Holland, D., Brewer, J. B. & Dale, A. M. (2009) One-Year Brain Atrophy Evident in Healthy Aging. *J Neurosci* **29(48)**:15223-31.

Fornage, M., Chiang, Y. A., O'meara, E. S., Psaty, B. M., Reiner, A. P., Siscovick, D. S., Tracy, R. P. & Longstreth, W. T. (2008) Biomarkers of inflammation and MRI-defined small vessel disease of the brain: the Cardiovascular Health Study. *Stroke* **39(7)**:1952-9.

Forsberg, K. M. E., Zhang, Y., Reiners, J., Ander, M., Niedermayer, A., Fang, L., Neugebauer, H., Kassubek, J., Katona, I., Weis, J., Ludolph, A. C., Del Tredici, K., Braak, H. & Yilmazer-Hanke, D. (2018) Endothelial damage,

vascular bagging and remodeling of the microvascular bed in human microangiopathy with deep white matter lesions. *Acta Neuropathol Commun* **6**.

Fu, Y., Liu, Q., Anrather, J. & Shi, F. D. (2015) Immune interventions in stroke. *Nat Rev Neurol* **11(9)**:524-35.

Fu, Y. & Yan, Y. (2018) Emerging Role of Immunity in Cerebral Small Vessel Disease. *Front Immunol* **9**:67.

Gao, Z., Wang, W., Wang, Z., Zhao, X., Shang, Y., Guo, Y., Gong, M., Yang, L., Shi, X., Xu, X., An, N. & Wu, W. (2014) Cerebral Microbleeds Are Associated with Deep White Matter Hyperintensities, but Only in Hypertensive Patients. *PLoS One* **9(3)**.

Gary, D. S., Bruce-Keller, A. J., Kindy, M. S. & Mattson, M. P. (1998) Ischemic and excitotoxic brain injury is enhanced in mice lacking the p55 tumor necrosis factor receptor. *J Cereb Blood Flow Metab* **18(12)**:1283-7.

Gerhard, A., Schwarz, J., Myers, R., Wise, R. & Banati, R. B. (2005) Evolution of microglial activation in patients after ischemic stroke: a [11C](R)-PK11195 PET study. *Neuroimage* **24(2)**:591-5.

Ghosh, M., Balbi, M., Hellal, F., Dichgans, M., Lindauer, U. & Plesnila, N. (2015) Pericytes are involved in the pathogenesis of cerebral autosomal dominant arteriopathy with subcortical infarcts and leukoencephalopathy. *Ann Neurol* **78(6)**:887-900.

Giannetti, P., Politis, M., Su, P., Turkheimer, F. E., Malik, O., Keihaninejad, S., Wu, K., Waldman, A., Reynolds, R., Nicholas, R. & Piccini, P. (2015) Increased PK11195-PET binding in normal-appearing white matter in clinically isolated syndrome. *Brain* **138(Pt 1)**:110-9.

Giuliani, F., Hader, W. & Yong, V. W. (2005) Minocycline attenuates T cell and microglia activity to impair cytokine production in T cell-microglia interaction. *J Leukoc Biol* **78(1)**:135-43.

Godin, O., Maillard, P., Crivello, F., Alperovitch, A., Mazoyer, B., Tzourio, C. & Dufouil, C. (2009) Association of white-matter lesions with brain atrophy markers: the three-city Dijon MRI study. *Cerebrovasc Dis* **28(2)**:177-84.

Godin, O., Tzourio, C., Maillard, P., Mazoyer, B. & Dufouil, C. (2011) Antihypertensive treatment and change in blood pressure are associated with

the progression of white matter lesion volumes: the Three-City (3C)-Dijon Magnetic Resonance Imaging Study. *Circulation* **123(3)**:266-73.

Gomis, M., Sobrino, T., Ois, A., Millan, M., Rodriguez-Campello, A., Perez De La Ossa, N., Rodriguez-Gonzalez, R., Jimenez-Conde, J., Cuadrado-Godia, E., Roquer, J. & Davalos, A. (2009) Plasma beta-amyloid 1-40 is associated with the diffuse small vessel disease subtype. *Stroke* **40(10)**:3197-201.

Gons, R. A., De Laat, K. F., Van Norden, A. G., Van Oudheusden, L. J., Van Uden, I. W., Norris, D. G., Zwiers, M. P. & De Leeuw, F. E. (2010) Hypertension and cerebral diffusion tensor imaging in small vessel disease. *Stroke* **41(12)**:2801-6.

Goodall, E. F., Wang, C., Simpson, J. E., Baker, D. J., Drew, D. R., Heath, P. R., Saffrey, M. J., Romero, I. A. & Wharton, S. B. (2018) Age-associated changes in the blood-brain barrier: comparative studies in human and mouse. *Neuropathol Appl Neurobiol* **44(3)**:328-340.

Gorelick, P. B., Scuteri, A., Black, S. E., Decarli, C., Greenberg, S. M., Iadecola, C., Launer, L. J., Laurent, S., Lopez, O. L., Nyenhuis, D., Petersen, R. C., Schneider, J. A., Tzourio, C., Arnett, D. K., Bennett, D. A., Chui, H. C., Higashida, R. T., Lindquist, R., Nilsson, P. M., Roman, G. C., Sellke, F. W. & Seshadri, S. (2011) Vascular contributions to cognitive impairment and dementia: a statement for healthcare professionals from the american heart association/american stroke association. *Stroke* **42(9)**:2672-713.

Gottesman, R., Cummiskey, C., Chambless, L., Wu, K., Aleksic, N., Folsom, A. & Sharrett, A. (2009) Hemostatic Factors and Subclinical Brain Infarction in a Community-Based Sample: The ARIC Study. *Cerebrovasc Dis* **28(6)**:589-94.

Gottschall, P. E. & Deb, S. (1996) Regulation of matrix metalloproteinase expressions in astrocytes, microglia and neurons. *Neuroimmunomodulation* **3(2-3)**:69-75.

Gouw, A. A., Seewann, A., Van Der Flier, W. M., Barkhof, F., Rozemuller, A. M., Scheltens, P. & Geurts, J. J. (2011) Heterogeneity of small vessel disease: a systematic review of MRI and histopathology correlations. *J Neurol Neurosurg Psychiatry* **82(2)**:126-35.

Gouw, A. A., Seewann, A., Vrenken, H., Van Der Flier, W. M., Rozemuller, J. M., Barkhof, F., Scheltens, P. & Geurts, J. J. (2008) Heterogeneity of white matter

hyperintensities in Alzheimer's disease: post-mortem quantitative MRI and neuropathology. *Brain* **131(Pt 12)**:3286-98.

Graumann, U., Reynolds, R., Steck, A. J. & Schaeren-Wiemers, N. (2003) Molecular changes in normal appearing white matter in multiple sclerosis are characteristic of neuroprotective mechanisms against hypoxic insult. *Brain Pathol* **13(4)**:554-73.

Greenberg, S. M. (2006) Small vessels, big problems. *N Engl J Med* **354(14)**:1451-3.

Gregoire, S. M., Smith, K., Jager, H. R., Benjamin, M., Kallis, C., Brown, M. M., Cipolotti, L. & Werring, D. J. (2012) Cerebral microbleeds and long-term cognitive outcome: longitudinal cohort study of stroke clinic patients. *Cerebrovasc Dis* **33(5)**:430-5.

Griffanti, L., Jenkinson, M., Suri, S., Zsoldos, E., Mahmood, A., Filippini, N., Sexton, C. E., Topiwala, A., Allan, C., Kivimaki, M., Singh-Manoux, A., Ebmeier, K. P., Mackay, C. E. & Zamboni, G. (2018) Classification and characterization of periventricular and deep white matter hyperintensities on MRI: A study in older adults. *Neuroimage* **170**:174-181.

Groeschel, S., Chong, W. K., Surtees, R. & Hanefeld, F. (2006) Virchow-Robin spaces on magnetic resonance images: normative data, their dilatation, and a review of the literature. *Neuroradiology* **48(10)**:745-54.

Guerrini, U., Sironi, L., Tremoli, E., Cimino, M., Pollo, B., Calvio, A. M., Paoletti, R. & Asdente, M. (2002) New insights into brain damage in stroke-prone rats: a nuclear magnetic imaging study. *Stroke* **33(3)**:825-30.

Gulyas, B., Toth, M., Vas, A., Shchukin, E., Kostulas, K., Hillert, J. & Halldin, C. (2012) Visualising neuroinflammation in post-stroke patients: a comparative PET study with the TSPO molecular imaging biomarkers [11C]PK11195 and [11C]vinpocetine. *Curr Radiopharm* **5(1)**:19-28.

Gunn, R. N., Gunn, S. R. & Cunningham, V. J. (2001) Positron emission tomography compartmental models. *J Cereb Blood Flow Metab* **21(6)**:635-52.

Gunn, R. N., Lammertsma, A. A., Hume, S. P. & Cunningham, V. J. (1997) Parametric imaging of ligand-receptor binding in PET using a simplified reference region model. *Neuroimage* **6(4)**:279-87.

Gunstad, J., Bausserman, L., Paul, R. H., Tate, D. F., Hoth, K., Poppas, A., Jefferson, A. L. & Cohen, R. A. (2006) C-reactive protein, but not homocysteine, is

related to cognitive dysfunction in older adults with cardiovascular disease. *J Clin Neurosci* **13(5)**:540-6.

Guo, X., Pantoni, L., Simoni, M., Bengtsson, C., Bjorkelund, C., Lissner, L., Gustafson, D. & Skoog, I. (2009) Blood pressure components and changes in relation to white matter lesions: a 32-year prospective population study. *Hypertension* **54(1)**:57-62.

Gurol, M. E., Irizarry, M. C., Smith, E. E., Raju, S., Diaz-Arrastia, R., Bottiglieri, T., Rosand, J., Growdon, J. H. & Greenberg, S. M. (2006) Plasma beta-amyloid and white matter lesions in AD, MCI, and cerebral amyloid angiopathy. *Neurology* **66(1)**:23-9.

Haarmann, A., Deiß, A., Prochaska, J., Foerch, C., Weksler, B., Romero, I., Couraud, P. O., Stoll, G., Rieckmann, P. & Buttmann, M. (2010) Evaluation of Soluble Junctional Adhesion Molecule-A as a Biomarker of Human Brain Endothelial Barrier Breakdown. *PLoS One* **5(10)**.

Hachinski, V. (2008) World Stroke Day 2008: "little strokes, big trouble". In *Stroke*.), United States, vol. 39, pp. 2407-20.

Hainsworth, A. H., Brittain, J. F. & Khatun, H. (2012) Pre-clinical models of human cerebral small vessel disease: utility for clinical application. *J Neurol Sci* **322(1-2)**:237-40.

Hainsworth, A. H. & Markus, H. S. (2008) Do in vivo experimental models reflect human cerebral small vessel disease? A systematic review. *J Cereb Blood Flow Metab* **28(12)**:1877-91.

Hainsworth, A. H., Oommen, A. T. & Bridges, L. R. (2015) Endothelial cells and human cerebral small vessel disease. *Brain Pathol* **25(1)**:44-50.

Hall, C. N., Reynell, C., Gesslein, B., Hamilton, N. B., Mishra, A., Sutherland, B. A., O'farrell, F. M., Buchan, A. M., Lauritzen, M. & Attwell, D. (2014) Capillary pericytes regulate cerebral blood flow in health and disease. *Nature* **508(7494)**:55-60.

Han, J. H., Wong, K. S., Wang, Y. Y., Fu, J. H., Ding, D. & Hong, Z. (2009) Plasma level of sICAM-1 is associated with the extent of white matter lesion among asymptomatic elderly subjects. *Clin Neurol Neurosurg* **111(10)**:847-51.

Hanyu, H., Asano, T., Tanaka, Y., Iwamoto, T., Takasaki, M. & Abe, K. (2002) Increased blood-brain barrier permeability in white matter lesions of

Binswanger's disease evaluated by contrast-enhanced MRI. *Dement Geriatr Cogn Disord* **14(1)**:1-6.

Hardy, J. A. & Higgins, G. A. (1992) Alzheimer's disease: the amyloid cascade hypothesis. *Science* **256(5054)**:184-5.

Harutyunyan, M., Christiansen, M., Johansen, J. S., Kober, L., Torp-Petersen, C. & Kastrup, J. (2012) The inflammatory biomarker YKL-40 as a new prognostic marker for all-cause mortality in patients with heart failure. *Immunobiology* **217(6)**:652-6.

Hassan, A., Hunt, B. J., O'sullivan, M., Bell, R., D'souza, R., Jeffery, S., Bamford, J. M. & Markus, H. S. (2004) Homocysteine is a risk factor for cerebral small vessel disease, acting via endothelial dysfunction. *Brain* **127(Pt 1)**:212-9.

Hassan, A., Hunt, B. J., O'sullivan, M., Parmar, K., Bamford, J. M., Briley, D., Brown, M. M., Thomas, D. J. & Markus, H. S. (2003) Markers of endothelial dysfunction in lacunar infarction and ischaemic leukoaraiosis. *Brain* **126(Pt 2)**:424-32.

Hassan, M. I., Saxena, A. & Ahmad, F. (2012) Structure and function of von Willebrand factor. *Blood Coagul Fibrinolysis* **23(1)**:11-22.

Hazama, F., Ozaki, T. & Amano, S. (1979) Scanning electron microscopic study of endothelial cells of cerebral arteries from spontaneously hypertensive rats. *Stroke* **10(3)**:245-52.

Heppner, F. L., Greter, M., Marino, D., Falsig, J., Raivich, G., Hovelmeyer, N., Waisman, A., Rulicke, T., Prinz, M., Priller, J., Becher, B. & Aguzzi, A. (2005) Experimental autoimmune encephalomyelitis repressed by microglial paralysis. *Nat Med* **11(2)**:146-52.

Heye, A. K., Thrippleton, M. J., Armitage, P. A., Valdes Hernandez, M. D. C., Makin, S. D., Glatz, A., Sakka, E. & Wardlaw, J. M. (2016) Tracer kinetic modelling for DCE-MRI quantification of subtle blood-brain barrier permeability. *Neuroimage* **125**:446-455.

Hilal, S., Ikram, M. A., Verbeek, M. M., Franco, O. H., Stoops, E., Vanderstichele, H., Niessen, W. J. & Vernooij, M. W. (2018) C-Reactive Protein, Plasma Amyloid-beta Levels, and Their Interaction With Magnetic Resonance Imaging Markers. *Stroke* **49(11)**:2692-2698.

Hollocks, M. J., Lawrence, A. J., Brookes, R. L., Barrick, T. R., Morris, R. G., Husain, M. & Markus, H. S. (2015) Differential relationships between apathy and depression with white matter microstructural changes and functional outcomes. *Brain* **138(Pt 12)**:3803-15.

Holtmannspotter, M., Peters, N., Opherk, C., Martin, D., Herzog, J., Bruckmann, H., Samann, P., Gschwendtner, A. & Dichgans, M. (2005) Diffusion magnetic resonance histograms as a surrogate marker and predictor of disease progression in CADASIL: a two-year follow-up study. *Stroke* **36(12)**:2559-65.

Hopperton, K. E., Mohammad, D., Trepanier, M. O., Giuliano, V. & Bazinet, R. P. (2018) Markers of microglia in post-mortem brain samples from patients with Alzheimer's disease: a systematic review. *Mol Psychiatry* **23(2)**:177-198.

Hoshi, T., Kitagawa, K., Yamagami, H., Furukado, S., Hougaku, H. & Hori, M. (2005) Relations of serum high-sensitivity C-reactive protein and interleukin-6 levels with silent brain infarction. *Stroke* **36(4)**:768-72.

Hu, X., Leak, R. K., Shi, Y., Suenaga, J., Gao, Y., Zheng, P. & Chen, J. (2015) Microglial and macrophage polarization-new prospects for brain repair. *Nat Rev Neurol* **11(1)**:56-64.

Hudson, H. M. & Larkin, R. S. (1994) Accelerated image reconstruction using ordered subsets of projection data. *IEEE Trans Med Imaging* **13(4)**:601-9.

Huijts, M., Duits, A., Staals, J., Kroon, A. A., De Leeuw, P. W. & Van Oostenbrugge, R. J. (2014) Basal ganglia enlarged perivascular spaces are linked to cognitive function in patients with cerebral small vessel disease. *Curr Neurovasc Res* **11(2)**:136-41.

Huisa, B. N., Caprihan, A., Thompson, J., Prestopnik, J., Qualls, C. R. & Rosenberg, G. A. (2015) Long-Term Blood-Brain Barrier Permeability Changes in Binswanger Disease. *Stroke* **46(9)**:2413-8.

Iadecola, C. (2013) The pathobiology of vascular dementia. *Neuron* **80(4)**.

Ilhan, D., Ozbabalik, D., Gulcan, E., Ozdemir, O. & Gulbacs, Z. (2010) Evaluation of platelet activation, coagulation, and fibrinolytic activation in patients with symptomatic lacunar stroke. *Neurologist* **16(3)**:188-91.

Inzitari, D., Pracucci, G., Poggesi, A., Carlucci, G., Barkhof, F., Chabriat, H., Erkinjuntti, T., Fazekas, F., Ferro, J. M., Hennerici, M., Langhorne, P., O'brien, J., Scheltens, P., Visser, M. C., Wahlund, L. O., Waldemar, G.,

Wallin, A. & Pantoni, L. (2009) Changes in white matter as determinant of global functional decline in older independent outpatients: three year follow-up of LADIS (leukoaraiosis and disability) study cohort. *Bmj* **339**:b2477.

Ishikawa, M., Cooper, D., Arumugam, T. V., Zhang, J. H., Nanda, A. & Granger, D. N. (2004) Platelet-leukocyte-endothelial cell interactions after middle cerebral artery occlusion and reperfusion. *J Cereb Blood Flow Metab* **24(8)**:907-15.

Ishikawa, M., Cooper, D., Russell, J., Salter, J. W., Zhang, J. H., Nanda, A. & Granger, D. N. (2003) Molecular determinants of the prothrombogenic and inflammatory phenotype assumed by the postischemic cerebral microcirculation. *Stroke* **34(7)**:1777-82.

Issac, T. G., Chandra, S. R., Christopher, R., Rajeswaran, J. & Philip, M. (2015) Cerebral Small Vessel Disease Clinical, Neuropsychological, and Radiological Phenotypes, Histopathological Correlates, and Described Genotypes: A Review **2015**:11.

Jalal, F. Y., Yang, Y., Thompson, J., Lopez, A. C. & Rosenberg, G. A. (2012) Myelin loss associated with neuroinflammation in hypertensive rats. *Stroke* **43(4)**:1115-22.

Jalal, F. Y., Yang, Y., Thompson, J. F., Roitbak, T. & Rosenberg, G. A. (2015) Hypoxia-induced neuroinflammatory white-matter injury reduced by minocycline in SHR/SP. *J Cereb Blood Flow Metab* **35(7)**:1145-53.

Janssen, B., Vugts, D. J., Windhorst, A. D. & Mach, R. H. (2018) PET Imaging of Microglial Activation-Beyond Targeting TSPO. *Molecules* **23(3)**.

Jefferson, A. L., Massaro, J. M., Wolf, P. A., Seshadri, S., Au, R., Vasan, R. S., Larson, M. G., Meigs, J. B., Keaney, J. F., Jr., Lipinska, I., Kathiresan, S., Benjamin, E. J. & Decarli, C. (2007) Inflammatory biomarkers are associated with total brain volume: the Framingham Heart Study. *Neurology* **68(13)**:1032-8.

Jespersen, S. N. & Østergaard, L. (2012) The roles of cerebral blood flow, capillary transit time heterogeneity, and oxygen tension in brain oxygenation and metabolism. *J Cereb Blood Flow Metab* **32(2)**:264-77.

Jiang, Y. X., Zhang, G. H., Wang, Z. M. & Yang, H. (2014) Serum YKL-40 levels as a prognostic factor in patients with intracerebral hemorrhage. *Clin Biochem* **47(18)**:302-6.

Jimenez-Balado, J., Riba-Llena, I., Abril, O., Garde, E., Penalba, A., Ostos, E., Maisterra, O., Montaner, J., Noviembre, M., Mundet, X., Ventura, O., Pizarro, J. & Delgado, P. (2019) Cognitive Impact of Cerebral Small Vessel Disease Changes in Patients With Hypertension. *Hypertension* **73(2)**:342-349.

Jin, X., Liu, J., Liu, K. J., Rosenberg, G. A., Yang, Y. & Liu, W. (2013) Normobaric hyperoxia combined with minocycline provides greater neuroprotection than either alone in transient focal cerebral ischemia. *Exp Neurol* **240**:9-16.

Johnson, P. C., Brendel, K. & Meezan, E. (1982) Thickened cerebral cortical capillary basement membranes in diabetics. *Arch Pathol Lab Med* **106(5)**:214-7.

Jokinen, H., Lipsanen, J., Schmidt, R., Fazekas, F., Gouw, A. A., Van Der Flier, W. M., Barkhof, F., Madureira, S., Verdelho, A., Ferro, J. M., Wallin, A., Pantoni, L., Inzitari, D. & Erkinjuntti, T. (2012) Brain atrophy accelerates cognitive decline in cerebral small vessel disease: the LADIS study. *Neurology* **78(22)**:1785-92.

Jokinen, H., Schmidt, R., Ropele, S., Fazekas, F., Gouw, A. A., Barkhof, F., Scheltens, P., Madureira, S., Verdelho, A., Ferro, J. M., Wallin, A., Poggesi, A., Inzitari, D., Pantoni, L. & Erkinjuntti, T. (2013) Diffusion changes predict cognitive and functional outcome: the LADIS study. *Ann Neurol* **73(5)**:576-83.

Jones, D. K., Lythgoe, D., Horsfield, M. A., Simmons, A., Williams, S. C. & Markus, H. S. (1999) Characterization of white matter damage in ischemic leukoaraiosis with diffusion tensor MRI. *Stroke* **30(2)**:393-7.

Joutel, A., Corpechot, C., Ducros, A., Vahedi, K., Chabriat, H., Mouton, P., Alamowitch, S., Domenga, V., Cecillion, M., Marechal, E., Maciazek, J., Vayssiere, C., Cruaud, C., Cabanis, E. A., Ruchoux, M. M., Weissenbach, J., Bach, J. F., Bousser, M. G. & Tournier-Lasserve, E. (1996) Notch3 mutations in CADASIL, a hereditary adult-onset condition causing stroke and dementia. *Nature* **383(6602)**:707-10.

Joutel, A., Monet-Lepretre, M., Gosele, C., Baron-Menguy, C., Hammes, A., Schmidt, S., Lemaire-Carrette, B., Domenga, V., Schedl, A., Lacombe, P. & Hubner, N. (2010) Cerebrovascular dysfunction and microcirculation rarefaction precede white matter lesions in a mouse genetic model of cerebral ischemic small vessel disease. *J Clin Invest* **120(2)**:433-45.

Kaiser, D., Weise, G., Moller, K., Scheibe, J., Posel, C., Baasch, S., Gawlitza, M., Lobsien, D., Diederich, K., Minnerup, J., Kranz, A., Boltze, J. & Wagner, D. C. (2014) Spontaneous white matter damage, cognitive decline and neuroinflammation in middle-aged hypertensive rats: an animal model of early-stage cerebral small vessel disease. *Acta Neuropathol Commun* **2**:169.

Kalaria, R. N. (1996) Cerebral vessels in ageing and Alzheimer's disease. *Pharmacol Ther* **72(3)**:193-214.

Kalinowska, A. & Losy, J. (2006) PECAM-1, a key player in neuroinflammation. *Eur J Neurol* **13(12)**:1284-90.

Kamtchum-Tatuene, J. & Jickling, G. C. (2019) Blood Biomarkers for Stroke Diagnosis and Management. *Neuromolecular Med*.

Kario, K., Matsuo, T., Kobayashi, H., Asada, R. & Matsuo, M. (1996) 'Silent' cerebral infarction is associated with hypercoagulability, endothelial cell damage, and high Lp(a) levels in elderly Japanese. *Arterioscler Thromb Vasc Biol* **16(6)**:734-41.

Kawabori, M. & Yenari, M. A. (2015) Inflammatory Responses in Brain Ischemia. *Curr Med Chem* **22(10)**:1258-77.

Kazakova, M. H. & Sarafian, V. S. (2009) YKL-40--a novel biomarker in clinical practice? *Folia Med (Plovdiv)* **51(1)**:5-14.

Kearney-Schwartz, A., Rossignol, P., Bracard, S., Felblinger, J., Fay, R., Boivin, J. M., Lecompte, T., Lacolley, P., Benetos, A. & Zannad, F. (2009) Vascular structure and function is correlated to cognitive performance and white matter hyperintensities in older hypertensive patients with subjective memory complaints. *Stroke* **40(4)**:1229-36.

Khan, U., Porteous, L., Hassan, A. & Markus, H. S. (2007) Risk factor profile of cerebral small vessel disease and its subtypes. *J Neurol Neurosurg Psychiatry* **78(7)**:702-6.

Khatri, M., Wright, C. B., Nickolas, T. L., Yoshita, M., Paik, M. C., Kranwinkel, G., Sacco, R. L. & Decarli, C. (2007) Chronic Kidney Disease Is Associated With White Matter Hyperintensity Volume: The Northern Manhattan Study (NOMAS). *Stroke* **38(12)**:3121-6.

Kim, K. W., Macfall, J. R. & Payne, M. E. (2008) Classification of white matter lesions on magnetic resonance imaging in elderly persons. *Biol Psychiatry* **64(4)**:273-80.

Kim, Y., Kim, Y. K., Kim, N. K., Kim, S. H., Kim, O. J. & Oh, S. H. (2014) Circulating matrix metalloproteinase-9 level is associated with cerebral white matter hyperintensities in non-stroke individuals. *Eur Neurol* **72(3-4)**:234-40.

Kjaergaard, A. D., Johansen, J. S., Bojesen, S. E. & Nordestgaard, B. G. (2015) Elevated plasma YKL-40, lipids and lipoproteins, and ischemic vascular disease in the general population. *Stroke* **46(2)**:329-35.

Kloppenborg, R. P., Geerlings, M. I., Visseren, F. L., Mali, W. P., Vermeulen, M., Van Der Graaf, Y. & Nederkoorn, P. J. (2014) Homocysteine and progression of generalized small-vessel disease: the SMART-MR Study. *Neurology* **82(9)**:777-83.

Knopman, D. S., Mosley, T. H., Jr., Bailey, K. R., Jack, C. R., Jr., Schwartz, G. L. & Turner, S. T. (2008) Associations of microalbuminuria with brain atrophy and white matter hyperintensities in hypertensive sibships. *J Neurol Sci* **271(1-2)**:53-60.

Knottnerus, I. L., Govers-Riemslag, J. W., Hamulyak, K., Rouhl, R. P., Staals, J., Spronk, H. M., Van Oerle, R., Van Raak, E. P., Lodder, J., Ten Cate, H. & Van Oostenbrugge, R. J. (2010) Endothelial activation in lacunar stroke subtypes. *Stroke* **41(8)**:1617-22.

Knox, C. A., Yates, R. D., Chen, I. & Klara, P. M. (1980) Effects of aging on the structural and permeability characteristics of cerebrovasculature in normotensive and hypertensive strains of rats. *Acta Neuropathol* **51(1)**:1-13.

Koga, H., Sugiyama, S., Kugiyama, K., Watanabe, K., Fukushima, H., Tanaka, T., Sakamoto, T., Yoshimura, M., Jinnouchi, H. & Ogawa, H. (2005) Elevated levels of VE-cadherin-positive endothelial microparticles in patients with type 2 diabetes mellitus and coronary artery disease. *J Am Coll Cardiol* **45(10)**:1622-30.

Koh, S. H., Park, C. Y., Kim, M. K., Lee, K. Y., Kim, J., Chang, D. I., Kim, H. T. & Kim, S. H. (2011) Microbleeds and free active MMP-9 are independent risk factors for neurological deterioration in acute lacunar stroke. *Eur J Neurol* **18(1)**:158-64.

Korherr, C., Hofmeister, R., Wesche, H. & Falk, W. (1997) A critical role for interleukin-1 receptor accessory protein in interleukin-1 signaling. *Eur J Immunol* **27(1)**:262-7.

Kozuka, K., Kohriyama, T., Nomura, E., Ikeda, J., Kajikawa, H. & Nakamura, S. (2002) Endothelial markers and adhesion molecules in acute ischemic stroke--sequential change and differences in stroke subtype. *Atherosclerosis* **161(1)**:161-8.

Kreisl, W. C., Jenko, K. J., Hines, C. S., Lyoo, C. H., Corona, W., Morse, C. L., Zoghbi, S. S., Hyde, T., Kleinman, J. E., Pike, V. W., Mcmahon, F. J. & Innis, R. B. (2013) A genetic polymorphism for translocator protein 18 kDa affects both in vitro and in vivo radioligand binding in human brain to this putative biomarker of neuroinflammation. *J Cereb Blood Flow Metab* **33(1)**:53-8.

Krishnan, M. S., O'brien, J. T., Firbank, M. J., Pantoni, L., Carlucci, G., Erkinjuntti, T., Wallin, A., Wahlund, L. O., Scheltens, P., Van Straaten, E. C. & Inzitari, D. (2006) Relationship between periventricular and deep white matter lesions and depressive symptoms in older people. The LADIS Study. *Int J Geriatr Psychiatry* **21(10)**:983-9.

Kruyer, A., Soplop, N., Strickland, S. & Norris, E. H. (2015) Chronic Hypertension Leads to Neurodegeneration in the TgSwDI Mouse Model of Alzheimer's Disease. *Hypertension* **66(1)**:175-82.

Kuller, L. H. & Lopez, O. L. (2016) Cardiovascular disease and dementia risk: an ever growing problem in an aging population. *Expert Rev Cardiovasc Ther* **14(7)**:771-3.

Kumar, A., Muzik, O., Shandal, V., Chugani, D., Chakraborty, P. & Chugani, H. T. (2012) Evaluation of age-related changes in translocator protein (TSPO) in human brain using 11C-[R]-PK11195 PET. *J Neuroinflammation* **9**:232.

Kummer, D. & Ebnet, K. (2018) Junctional Adhesion Molecules (JAMs): The JAM-Integrin Connection. In *Cells*.), vol. 7.

Könnecke, H. & Bechmann, I. (2013) The Role of Microglia and Matrix Metalloproteinases Involvement in Neuroinflammation and Gliomas. *Clin Dev Immunol* **2013**.

Lambert, C., Benjamin, P., Zeestraten, E., Lawrence, A. J., Barrick, T. R. & Markus, H. S. (2016) Longitudinal patterns of leukoaraiosis and brain atrophy in symptomatic small vessel disease. *Brain* **139(Pt 4)**:1136-51.

Lambert, C., Sam Narean, J., Benjamin, P., Zeestraten, E., Barrick, T. R. & Markus, H. S. (2015) Characterising the grey matter correlates of leukoaraiosis in cerebral small vessel disease. *Neuroimage Clin* **9**:194-205.

Lammertsma, A. A. & Hume, S. P. (1996) Simplified reference tissue model for PET receptor studies. *Neuroimage* **4(3 Pt 1)**:153-8.

Lammie, G. A. (2000) Pathology of small vessel stroke. *Br Med Bull* **56(2)**:296-306.

Lammie, G. A. (2002) Hypertensive cerebral small vessel disease and stroke. *Brain Pathol* **12(3)**:358-70.

Largeau, B., Dupont, A. C., Guilloteau, D., Santiago-Ribeiro, M. J. & Arlicot, N. (2017) TSPO PET Imaging: From Microglial Activation to Peripheral Sterile Inflammatory Diseases? *Contrast Media Mol Imaging* **2017**.

Lavisse, S., Guillermier, M., Herard, A. S., Petit, F., Delahaye, M., Van Camp, N., Ben Haim, L., Lebon, V., Remy, P., Dolle, F., Delzescaux, T., Bonvento, G., Hantraye, P. & Escartin, C. (2012) Reactive astrocytes overexpress TSPO and are detected by TSPO positron emission tomography imaging. *J Neurosci* **32(32)**:10809-18.

Lawrence, A. J., Brookes, R. L., Zeestraten, E. A., Barrick, T. R., Morris, R. G. & Markus, H. S. (2015) Pattern and Rate of Cognitive Decline in Cerebral Small Vessel Disease: A Prospective Study. *PLoS One* **10(8)**:e0135523.

Lawrence, A. J., Chung, A. W., Morris, R. G., Markus, H. S. & Barrick, T. R. (2014) Structural network efficiency is associated with cognitive impairment in small-vessel disease. *Neurology* **83(4)**:304-11.

Lawrence, A. J., Patel, B., Morris, R. G., Mackinnon, A. D., Rich, P. M., Barrick, T. R. & Markus, H. S. (2013) Mechanisms of cognitive impairment in cerebral small vessel disease: multimodal MRI results from the St George's cognition and neuroimaging in stroke (SCANS) study. *PLoS One* **8(4)**:e61014.

Leco, K. J., Apte, S. S., Taniguchi, G. T., Hawkes, S. P., Khokha, R., Schultz, G. A. & Edwards, D. R. (1997) Murine tissue inhibitor of metalloproteinases-4 (Timp-4): cDNA isolation and expression in adult mouse tissues. *FEBS Lett* **401(2-3)**:213-7.

Lee, D. Y., Fletcher, E., Martinez, O., Ortega, M., Zozulya, N., Kim, J., Tran, J., Buonocore, M., Carmichael, O. & Decarli, C. (2009) Regional pattern of white matter microstructural changes in normal aging, MCI, and AD. *Neurology* **73(21)**:1722-8.

Lee, J. M., Zhai, G., Liu, Q., Gonzales, E. R., Yin, K., Yan, P., Hsu, C. Y., Vo, K. D. & Lin, W. (2007) Vascular permeability precedes spontaneous intracerebral hemorrhage in stroke-prone spontaneously hypertensive rats. *Stroke* **38(12)**:3289-91.

Lehmberg, J., Beck, J., Baethmann, A. & Uhl, E. (2006) Effect of P-selectin inhibition on leukocyte-endothelium interaction and survival after global cerebral ischemia. *J Neurol* **253(3)**:357-63.

Lewerenz, J. & Maher, P. (2015) Chronic Glutamate Toxicity in Neurodegenerative Diseases-What is the Evidence? *Front Neurosci* **9**:469.

Li, M., Meng, Y., Wang, M., Yang, S., Wu, H., Zhao, B. & Wang, G. (2017a) Cerebral gray matter volume reduction in subcortical vascular mild cognitive impairment patients and subcortical vascular dementia patients, and its relation with cognitive deficits. *Brain Behav* **7(8)**.

Li, P. & Qin, C. (2015) Elevated circulating VE-cadherin+CD144+endothelial microparticles in ischemic cerebrovascular disease. *Thromb Res* **135(2)**:375-81.

Li, Q., Yang, Y., Reis, C., Tao, T., Li, W., Li, X. & Zhang, J. H. (2018a) Cerebral Small Vessel Disease. In *Cell Transplant*.), vol. 27, pp. 1711-22.

Li, X., Yuan, J., Yang, L., Qin, W., Yang, S., Li, Y., Fan, H. & Hu, W. (2017b) The significant effects of cerebral microbleeds on cognitive dysfunction: An updated meta-analysis. In *PLoS One*.), vol. 12.

Li, Y., Li, M., Zhang, X., Shi, Q., Yang, S., Fan, H., Qin, W., Yang, L., Yuan, J., Jiang, T. & Hu, W. (2017c) Higher blood-brain barrier permeability is associated with higher white matter hyperintensities burden. *J Neurol* **264(7)**:1474-1481.

Li, Y., Li, M., Zuo, L., Shi, Q., Qin, W., Yang, L., Jiang, T. & Hu, W. (2018b) Compromised Blood-Brain Barrier Integrity Is Associated With Total Magnetic Resonance Imaging Burden of Cerebral Small Vessel Disease. *Front Neurol* **9**:221.

Liao, D., Cooper, L., Cai, J., Toole, J. F., Bryan, N. R., Hutchinson, R. G. & Tyroler, H. A. (1996) Presence and severity of cerebral white matter lesions and hypertension, its treatment, and its control. The ARIC Study. Atherosclerosis Risk in Communities Study. *Stroke* **27(12)**:2262-70.

Liem, M. K., Lesnik Oberstein, S. A., Haan, J., Van Der Neut, I. L., Ferrari, M. D., Van Buchem, M. A., Middelkoop, H. A. & Van Der Grond, J. (2009) MRI correlates of cognitive decline in CADASIL: a 7-year follow-up study. *Neurology* **72(2)**:143-8.

Lin, J. X., Tomimoto, H., Akiguchi, I., Wakita, H., Shibasaki, H. & Horie, R. (2001) White matter lesions and alteration of vascular cell composition in the brain of spontaneously hypertensive rats. *Neuroreport* **12(9)**:1835-9.

Lin, Z., Li, Y., Su, P., Mao, D., Wei, Z., Pillai, J. J., Moghekar, A., Van Osch, M., Ge, Y. & Lu, H. (2018) Non-contrast MR imaging of blood-brain barrier permeability to water. *Magn Reson Med* **80(4)**:1507-1520.

Liu, C., Li, C., Gui, L., Zhao, L., Evans, A. C., Xie, B., Zhang, J., Wei, L., Zhou, D., Wang, J. & Yin, X. (2014a) The pattern of brain gray matter impairments in patients with subcortical vascular dementia. *J Neurol Sci* **341(1-2)**:110-8.

Liu, C., Yan, S., Zhang, R., Chen, Z., Shi, F., Zhou, Y., Zhang, M. & Lou, M. (2018a) Increased blood-brain barrier permeability in contralateral hemisphere predicts worse outcome in acute ischemic stroke after reperfusion therapy. *J Neurointerv Surg* **10(10)**:937-941.

Liu, G. J., Middleton, R. J., Hatty, C. R., Kam, W. W., Chan, R., Pham, T., Harrison-Brown, M., Dodson, E., Veale, K. & Banati, R. B. (2014b) The 18 kDa translocator protein, microglia and neuroinflammation. *Brain Pathol* **24(6)**:631-53.

Liu, L. & Kubes, P. (2003) Molecular mechanisms of leukocyte recruitment: organ-specific mechanisms of action. *Thromb Haemost* **89(2)**:213-20.

Liu, Y., Braidy, N., Poljak, A., Chan, D. K. Y. & Sachdev, P. (2018b) Cerebral small vessel disease and the risk of Alzheimer's disease: A systematic review. *Ageing Res Rev* **47**:41-48.

Liu, Z. G., Hsu, H., Goeddel, D. V. & Karin, M. (1996) Dissection of TNF receptor 1 effector functions: JNK activation is not linked to apoptosis while NF-kappaB activation prevents cell death. *Cell* **87(3)**:565-76.

Lockhart, A., Davis, B., Matthews, J. C., Rahmoune, H., Hong, G., Gee, A., Earnshaw, D. & Brown, J. (2003) The peripheral benzodiazepine receptor ligand PK11195 binds with high affinity to the acute phase reactant alpha1-acid glycoprotein: implications for the use of the ligand as a CNS inflammatory marker. *Nucl Med Biol* **30(2)**:199-206.

Logan, J., Fowler, J. S., Volkow, N. D., Wang, G. J., Ding, Y. S. & Alexoff, D. L. (1996) Distribution volume ratios without blood sampling from graphical analysis of PET data. *J Cereb Blood Flow Metab* **16(5)**:834-40.

Loggia, M. L., Chonde, D. B., Akeju, O., Arabasz, G., Catana, C., Edwards, R. R., Hill, E., Hsu, S., Izquierdo-Garcia, D., Ji, R. R., Riley, M., Wasan, A. D., Zurcher, N. R., Albrecht, D. S., Vangel, M. G., Rosen, B. R., Napadow, V. & Hooker, J. M. (2015) Evidence for brain glial activation in chronic pain patients. *Brain* **138(Pt 3)**:604-15.

Lohner, V., Brookes, R. L., Hollocks, M. J., Morris, R. G. & Markus, H. S. (2017) Apathy, but not depression, is associated with executive dysfunction in cerebral small vessel disease. *PLoS One* **12(5)**:e0176943.

Loos, C. M., Klarenbeek, P., Van Oostenbrugge, R. J. & Staals, J. (2015) Association between Perivascular Spaces and Progression of White Matter Hyperintensities in Lacunar Stroke Patients. *PLoS One* **10(9)**:e0137323.

Loos, C. M., Staals, J., Wardlaw, J. M. & Van Oostenbrugge, R. J. (2012) Cavitation of deep lacunar infarcts in patients with first-ever lacunar stroke: a 2-year follow-up study with MR. *Stroke* **43(8)**:2245-7.

Low, A., Mak, E., Rowe, J. B., Markus, H. S. & O'brien, J. T. (2019) Inflammation and cerebral small vessel disease: A systematic review. *Ageing Res Rev* **53**:100916.

Lu, Q.-L., Li, C., Song, Y., Wang, L. & Jia, Z.-R. (2017) Relationship of cerebral microbleeds to inflammatory marker levels. *Neuroimmunol Neuroinflammation 2017* **4**:145-51.

Luissint, A. C., Artus, C., Glacial, F., Ganeshamoorthy, K. & Couraud, P. O. (2012) Tight junctions at the blood brain barrier: physiological architecture and disease-associated dysregulation. *Fluids Barriers CNS* **9**:23.

Lund, R. W. (2014) Lacunar infarction, mortality over time and mortality relative to other ischemic strokes. *J Insur Med* **44(1)**:32-7.

Lundberg, M., Eriksson, A., Tran, B., Assarsson, E. & Fredriksson, S. (2011) Homogeneous antibody-based proximity extension assays provide sensitive and specific detection of low-abundant proteins in human blood. *Nucleic Acids Res* **39(15)**:e102.

Lyoo, C. H., Ikawa, M., Liow, J. S., Zoghbi, S. S., Morse, C. L., Pike, V. W., Fujita, M., Innis, R. B. & Kreisl, W. C. (2015) Cerebellum Can Serve As a Pseudo-Reference Region in Alzheimer Disease to Detect Neuroinflammation Measured with PET Radioligand Binding to Translocator Protein. *J Nucl Med* **56(5)**:701-6.

Machado, L. S., Kozak, A., Ergul, A., Hess, D. C., Borlongan, C. V. & Fagan, S. C. (2006) Delayed minocycline inhibits ischemia-activated matrix metalloproteinases 2 and 9 after experimental stroke. *BMC Neurosci* **7**:56.

Maclullich, A. M., Wardlaw, J. M., Ferguson, K. J., Starr, J. M., Seckl, J. R. & Deary, I. J. (2004) Enlarged perivascular spaces are associated with cognitive function in healthy elderly men. *J Neurol Neurosurg Psychiatry* **75(11)**:1519-23.

Maillard, P., Carmichael, O., Fletcher, E., Reed, B., Mungas, D. & Decarli, C. (2012) Coevolution of white matter hyperintensities and cognition in the elderly. *Neurology* **79(5)**:442-8.

Maillard, P., Fletcher, E., Harvey, D., Carmichael, O., Reed, B., Mungas, D. & Decarli, C. (2011) White matter hyperintensity penumbra. *Stroke* **42(7)**:1917-22.

Maiuolo, J., Gliozzi, M., Musolino, V., Scicchitano, M., Carresi, C., Scarano, F., Bosco, F., Nucera, S., Ruga, S., Zito, M. C., Mollace, R., Palma, E., Fini, M., Muscoli, C. & Mollace, V. (2018) The "Frail" Brain Blood Barrier in Neurodegenerative Diseases: Role of Early Disruption of Endothelial Cell-to-Cell Connections. *Int J Mol Sci* **19(9)**.

Majid, A. (2014) Neuroprotection in Stroke: Past, Present, and Future. *ISRN Neurol* **2014**.

Malko, J. A., Hoffman, J. C., Jr. & Green, R. C. (1991) MR measurement of intracranial CSF volume in 41 elderly normal volunteers. *AJNR Am J Neuroradiol* **12(2)**:371-4.

Marchetti, L., Klein, M., Schlett, K., Pfizenmaier, K. & Eisel, U. L. (2004) Tumor necrosis factor (TNF)-mediated neuroprotection against glutamate-induced excitotoxicity is enhanced by N-methyl-D-aspartate receptor activation. Essential role of a TNF receptor 2-mediated phosphatidylinositol 3-kinase-dependent NF-kappa B pathway. *J Biol Chem* **279(31)**:32869-81.

Markus, H. S., Hunt, B., Palmer, K., Enzinger, C., Schmidt, H. & Schmidt, R. (2005) Markers of endothelial and hemostatic activation and progression of cerebral white matter hyperintensities: longitudinal results of the Austrian Stroke Prevention Study. *Stroke* **36(7)**:1410-4.

Marstrand, J. R., Garde, E., Rostrup, E., Ring, P., Rosenbaum, S., Mortensen, E. L. & Larsson, H. B. (2002) Cerebral perfusion and cerebrovascular reactivity are reduced in white matter hyperintensities. *Stroke* **33(4)**:972-6.

Martinez Sosa, S. & Smith, K. J. (2017) Understanding a role for hypoxia in lesion formation and location in the deep and periventricular white matter in small vessel disease and multiple sclerosis. *Clin Sci (Lond)* **131(20)**:2503-2524.

Marz, P., Gadient, R. A. & Otten, U. (1996) Expression of interleukin-6 receptor (IL-6R) and gp130 mRNA in PC12 cells and sympathetic neurons: modulation by tumor necrosis factor alpha (TNF-alpha). *Brain Res* **706(1)**:71-9.

Mcaleese, K. E., Alafuzoff, I., Charidimou, A., De Reuck, J., Grinberg, L. T., Hainsworth, A. H., Hortobagyi, T., Ince, P., Jellinger, K., Gao, J., Kalaria, R. N., Kovacs, G. G., Kovari, E., Love, S., Popovic, M., Skrobot, O., Taipa, R., Thal, D. R., Werring, D., Wharton, S. B. & Attems, J. (2016) Post-mortem assessment in vascular dementia: advances and aspirations. *BMC Med* **14(1)**:129.

Mcpherson, S. E. & Cummings, J. L. (1996) Neuropsychological aspects of vascular dementia. *Brain Cogn* **31(2)**:269-82.

Meier, I. B., Gu, Y., Guzaman, V. A., Wiegman, A. F., Schupf, N., Manly, J. J., Luchsinger, J. A., Viswanathan, A., Martinez-Ramirez, S., Greenberg, S. M., Mayeux, R. & Brickman, A. M. (2014) Lobar microbleeds are associated with a decline in executive functioning in older adults. *Cerebrovasc Dis* **38(5)**:377-83.

Mhatre, M., Nguyen, A., Kashani, S., Pham, T., Adesina, A. & Grammas, P. (2004) Thrombin, a mediator of neurotoxicity and memory impairment. *Neurobiol Aging* **25(6)**:783-93.

Miners, J. S., Schulz, I. & Love, S. (2018) Differing associations between Abeta accumulation, hypoperfusion, blood-brain barrier dysfunction and loss of PDGFRB pericyte marker in the precuneus and parietal white matter in Alzheimer's disease. *J Cereb Blood Flow Metab* **38(1)**:103-115.

Minguez, B., Rovira, A., Alonso, J. & Cordoba, J. (2007) Decrease in the volume of white matter lesions with improvement of hepatic encephalopathy. *AJNR Am J Neuroradiol* **28(8)**:1499-500.

Mitaki, S., Nagai, A., Oguro, H. & Yamaguchi, S. (2016) C-reactive protein levels are associated with cerebral small vessel-related lesions. *Acta Neurol Scand* **133(1)**:68-74.

Mitrushina, M., Boone, K. B., Razani, J. & D'elia, L. F. (2005) *Handbook of Normative Data for Neuropsychological Assessment.* USA, Oxford University Press, second edition.

Miwa, K., Tanaka, M., Okazaki, S., Furukado, S., Sakaguchi, M. & Kitagawa, K. (2011) Relations of blood inflammatory marker levels with cerebral microbleeds. *Stroke* **42(11)**:3202-6.

Miyao, S., Takano, A., Teramoto, J. & Takahashi, A. (1992) Leukoaraiosis in relation to prognosis for patients with lacunar infarction. *Stroke* **23(10)**:1434-8.

Mizrahi, R., Rusjan, P. M., Kennedy, J., Pollock, B., Mulsant, B., Suridjan, I., De Luca, V., Wilson, A. A. & Houle, S. (2012) Translocator protein (18 kDa) polymorphism (rs6971) explains in-vivo brain binding affinity of the PET radioligand [18F]-FEPPA. *J Cereb Blood Flow Metab* **32(6)**:968-72.

Mok, V. C., Lam, W. W., Fan, Y. H., Wong, A., Ng, P. W., Tsoi, T. H., Yeung, V. & Wong, K. S. (2009) Effects of statins on the progression of cerebral white matter lesion: Post hoc analysis of the ROCAS (Regression of Cerebral Artery Stenosis) study. *J Neurol* **256(5)**:750-7.

Molko, N., Pappata, S., Mangin, J. F., Poupon, F., Lebihan, D., Bousser, M. G. & Chabriat, H. (2002) Monitoring disease progression in CADASIL with diffusion magnetic resonance imaging: a study with whole brain histogram analysis. *Stroke* **33(12)**:2902-8.

Montagne, A., Barnes, S. R., Sweeney, M. D., Halliday, M. R., Sagare, A. P., Zhao, Z., Toga, A. W., Jacobs, R. E., Liu, C. Y., Amezcua, L., Harrington, M. G., Chui, H. C., Law, M. & Zlokovic, B. V. (2015) Blood-Brain Barrier Breakdown in the Aging Human Hippocampus. *Neuron* **85(2)**:296-302.

Montagne, A., Nikolakopoulou, A. M., Zhao, Z., Sagare, A. P., Si, G., Lazic, D., Barnes, S. R., Daianu, M., Ramanathan, A., Go, A., Lawson, E. J., Wang, Y., Mack, W. J., Thompson, P. M., Schneider, J. A., Varkey, J., Langen, R., Mullins, E., Jacobs, R. E. & Zlokovic, B. V. (2018) Pericyte degeneration causes white matter dysfunction in the mouse central nervous system. *Nat Med* **24(3)**:326-337.

Mooradian, A. D. (1988) Effect of aging on the blood-brain barrier. *Neurobiol Aging* **9(1)**:31-9.

Mooradian, A. D. & Mccuskey, R. S. (1992) In vivo microscopic studies of age-related changes in the structure and the reactivity of cerebral microvessels. *Mech Ageing Dev* **64(3)**:247-54.

Moriya, Y., Kozaki, K., Nagai, K. & Toba, K. (2009) Attenuation of brain white matter hyperintensities after cerebral infarction. *AJNR Am J Neuroradiol* **30(3)**:E43.

Morris, R. S., Simon Jones, P., Alawneh, J. A., Hong, Y. T., Fryer, T. D., Aigbirhio, F. I., Warburton, E. A. & Baron, J. C. (2018) Relationships between selective neuronal loss and microglial activation after ischaemic stroke in man. *Brain* **141(7)**:2098-2111.

Moses, W. W. (2011) Fundamental Limits of Spatial Resolution in PET. *Nucl Instrum Methods Phys Res A* **648 Supplement 1**:S236-40.

Muller, W. A., Weigl, S. A., Deng, X. & Phillips, D. M. (1993) PECAM-1 is required for transendothelial migration of leukocytes. *J Exp Med* **178(2)**:449-60.

Munoz Maniega, S., Chappell, F. M., Valdes Hernandez, M. C., Armitage, P. A., Makin, S. D., Heye, A. K., Thrippleton, M. J., Sakka, E., Shuler, K., Dennis, M. S. & Wardlaw, J. M. (2017) Integrity of normal-appearing white matter: Influence of age, visible lesion burden and hypertension in patients with small-vessel disease. *J Cereb Blood Flow Metab* **37(2)**:644-656.

Nagahama, Y., Okina, T., Suzuki, N., Matsuzaki, S., Yamauchi, H., Nabatame, H. & Matsuda, M. (2003) Factor structure of a modified version of the wisconsin

card sorting test: an analysis of executive deficit in Alzheimer's disease and mild cognitive impairment. *Dement Geriatr Cogn Disord* **16(2)**:103-12.

Nam, K. W., Kwon, H. M., Jeong, H. Y., Park, J. H., Kwon, H. & Jeong, S. M. (2019) Serum homocysteine level is related to cerebral small vessel disease in a healthy population. *Neurology* **92(4)**:e317-e325.

Nawashiro, H., Tasaki, K., Ruetzler, C. A. & Hallenbeck, J. M. (1997) TNF-alpha pretreatment induces protective effects against focal cerebral ischemia in mice. *J Cereb Blood Flow Metab* **17(5)**:483-90.

Ncdrf, C. (2016) Trends in adult body-mass index in 200 countries from 1975 to 2014: a pooled analysis of 1698 population-based measurement studies with 19.2 million participants. *Lancet* **387(10026)**:1377-1396.

Nelson, H. & Willison, J. R. (1991) *National Adult Reading Test (NART): Test Manual. NFER-Nelson, second edition.*

Nimse, S. B., Sonawane, M. D., Song, K. S. & Kim, T. (2016) Biomarker detection technologies and future directions. *Analyst* **141(3)**:740-55.

Nitkunan, A., Barrick, T. R., Charlton, R. A., Clark, C. A. & Markus, H. S. (2008) Multimodal MRI in cerebral small vessel disease: its relationship with cognition and sensitivity to change over time. *Stroke* **39(7)**:1999-2005.

Nitkunan, A., Lanfranconi, S., Charlton, R. A., Barrick, T. R. & Markus, H. S. (2011) Brain atrophy and cerebral small vessel disease: a prospective follow-up study. *Stroke* **42(1)**:133-8.

Norrving, B. (2003) Long-term prognosis after lacunar infarction. *Lancet Neurol* **2(4)**:238-45.

Nylander, R., Kilander, L., Ahlstrom, H., Lind, L. & Larsson, E. M. (2018) Small Vessel Disease on Neuroimaging in a 75-Year-Old Cohort (PIVUS): Comparison With Cognitive and Executive Tests. *Front Aging Neurosci* **10**:217.

Nylander, R., Lind, L., Wikstrom, J., Lindahl, B., Venge, P., Larsson, A., Arnlov, J., Berglund, L., Ahlstrom, H., Johansson, L. & Larsson, E. M. (2015) Relation between cardiovascular disease risk markers and brain infarcts detected by magnetic resonance imaging in an elderly population. *J Stroke Cerebrovasc Dis* **24(2)**:312-8.

O'brien, J. T., Paling, S., Barber, R., Williams, E. D., Ballard, C., Mckeith, I. G., Gholkar, A., Crum, W. R., Rossor, M. N. & Fox, N. C. (2001) Progressive brain atrophy on serial MRI in dementia with Lewy bodies, AD, and vascular dementia. *Neurology* **56(10)**:1386-8.

O'brien, J. T. & Thomas, A. (2015) Vascular dementia. *Lancet* **386(10004)**:1698-706.

O'sullivan, M., Lythgoe, D. J., Pereira, A. C., Summers, P. E., Jarosz, J. M., Williams, S. C. & Markus, H. S. (2002) Patterns of cerebral blood flow reduction in patients with ischemic leukoaraiosis. *Neurology* **59(3)**:321-6.

Ojala, J., Alafuzoff, I., Herukka, S. K., Van Groen, T., Tanila, H. & Pirttila, T. (2009) Expression of interleukin-18 is increased in the brains of Alzheimer's disease patients. *Neurobiol Aging* **30(2)**:198-209.

Okazaki, S., Hornberger, E., Griebe, M., Gass, A., Hennerici, M. G. & Szabo, K. (2015) MRI Characteristics of the Evolution of Supratentorial Recent Small Subcortical Infarcts. *Frontiers in Neurology* **6**:118.

Okello, A., Edison, P., Archer, H. A., Turkheimer, F. E., Kennedy, J., Bullock, R., Walker, Z., Kennedy, A., Fox, N., Rossor, M. & Brooks, D. J. (2009) Microglial activation and amyloid deposition in mild cognitive impairment: a PET study. *Neurology* **72(1)**:56-62.

Ong, K. L., Leung, R. Y., Babinska, A., Salifu, M. O., Ehrlich, Y. H., Kornecki, E., Wong, L. Y., Tso, A. W., Cherny, S. S., Sham, P. C., Lam, T. H., Lam, K. S. & Cheung, B. M. (2009) Elevated plasma level of soluble F11 receptor/junctional adhesion molecule-A (F11R/JAM-A) in hypertension. *Am J Hypertens* **22(5)**:500-5.

Opherk, C., Peters, N., Herzog, J., Luedtke, R. & Dichgans, M. (2004) Long-term prognosis and causes of death in CADASIL: a retrospective study in 411 patients. *Brain* **127(Pt 11)**:2533-9.

Owen, D. R., Howell, O. W., Tang, S. P., Wells, L. A., Bennacef, I., Bergstrom, M., Gunn, R. N., Rabiner, E. A., Wilkins, M. R., Reynolds, R., Matthews, P. M. & Parker, C. A. (2010) Two binding sites for [3H]PBR28 in human brain: implications for TSPO PET imaging of neuroinflammation. *J Cereb Blood Flow Metab* **30(9)**:1608-18.

Owen, D. R., Yeo, A. J., Gunn, R. N., Song, K., Wadsworth, G., Lewis, A., Rhodes, C., Pulford, D. J., Bennacef, I., Parker, C. A., Stjean, P. L., Cardon, L. R.,

Mooser, V. E., Matthews, P. M., Rabiner, E. A. & Rubio, J. P. (2012) An 18-kDa translocator protein (TSPO) polymorphism explains differences in binding affinity of the PET radioligand PBR28. *J Cereb Blood Flow Metab* **32(1)**:1-5.

Paciaroni, M., Caso, V. & Agnelli, G. (2009) The concept of ischemic penumbra in acute stroke and therapeutic opportunities. *Eur Neurol* **61(6)**:321-30.

Pan, W. & Kastin, A. J. (2002) TNFalpha transport across the blood-brain barrier is abolished in receptor knockout mice. *Exp Neurol* **174(2)**:193-200.

Pantoni, L. (2008) Leukoaraiosis: from an ancient term to an actual marker of poor prognosis. *Stroke* **39(5)**:1401-3.

Pantoni, L. (2010) Cerebral small vessel disease: from pathogenesis and clinical characteristics to therapeutic challenges. *Lancet Neurol* **9(7)**:689-701.

Pantoni, L. & Garcia, J. H. (1995) The significance of cerebral white matter abnormalities 100 years after Binswanger's report. A review. *Stroke* **26(7)**:1293-301.

Pantoni, L. & Garcia, J. H. (1997) Pathogenesis of Leukoaraiosis.

Pantoni, L., Poggesi, A. & Inzitari, D. (2007) The relation between white-matter lesions and cognition. *Curr Opin Neurol* **20(4)**:390-7.

Panés, J., Perry, M. & Granger, D. N. (1999) Leukocyte-endothelial cell adhesion: avenues for therapeutic intervention. *Br J Pharmacol* **126(3)**:537-50.

Papakonstantinou, E., Bacopoulou, F., Brouzas, D., Megalooikonomou, V., D'elia, D., Bongcam-Rudloff, E. & Vlachakis, D. (2019) NOTCH3 and CADASIL syndrome: a genetic and structural overview. *EMBnet J* **24**.

Pappata, S., Levasseur, M., Gunn, R. N., Myers, R., Crouzel, C., Syrota, A., Jones, T., Kreutzberg, G. W. & Banati, R. B. (2000) Thalamic microglial activation in ischemic stroke detected in vivo by PET and [11C]PK1195. *Neurology* **55(7)**:1052-4.

Passamonti, L., Rodríguez, P. V., Hong, Y. T., Allinson, K. S., Bevan-Jones, W. R., Williamson, D., Jones, P. S., Arnold, R., Borchert, R. J., Surendranathan, A., Mak, E., Su, L., Fryer, T. D., Aigbirhio, F. I., O'brien, J. T. & Rowe, J. B. (2018) [11C]PK11195 binding in Alzheimer disease and progressive supranuclear palsy. *Neurology* **90(22)**:e1989-96.

Passamonti, L., Tsvetanov, K. A., Jones, P. S., Bevan-Jones, W. R., Arnold, R., Borchert, R. J., Mak, E., Su, L., O'brien, J. T. & Rowe, J. B. (2019) Neuroinflammation and Functional Connectivity in Alzheimer's Disease: Interactive Influences on Cognitive Performance. *J Neurosci* **39(36)**:7218-7226.

Passiak, B. S., Liu, D., Kresge, H. A., Cambronero, F. E., Pechman, K. R., Osborn, K. E., Gifford, K. A., Hohman, T. J., Schrag, M. S., Davis, L. T. & Jefferson, A. L. (2019) Perivascular spaces contribute to cognition beyond other small vessel disease markers. *Neurology* **92(12)**:e1309-e1321.

Pasternak, O., Sochen, N., Gur, Y., Intrator, N. & Assaf, Y. (2009) Free water elimination and mapping from diffusion MRI. *Magn Reson Med* **62(3)**:717-30.

Patel, B., Lawrence, A. J., Chung, A. W., Rich, P., Mackinnon, A. D., Morris, R. G., Barrick, T. R. & Markus, H. S. (2013) Cerebral microbleeds and cognition in patients with symptomatic small vessel disease. *Stroke* **44(2)**:356-61.

Patlak, C. S. & Blasberg, R. G. (1985) Graphical evaluation of blood-to-brain transfer constants from multiple-time uptake data. Generalizations. *J Cereb Blood Flow Metab* **5(4)**:584-90.

Paul, J., Strickland, S. & Melchor, J. P. (2007) Fibrin deposition accelerates neurovascular damage and neuroinflammation in mouse models of Alzheimer's disease. *J Exp Med* **204(8)**:1999-2008.

Pavlovic, A. M., Pekmezovic, T., Obrenovic, R., Novakovic, I., Tomic, G., Mijajlovic, M. & Sternic, N. (2011) Increased total homocysteine level is associated with clinical status and severity of white matter changes in symptomatic patients with subcortical small vessel disease. *Clin Neurol Neurosurg* **113(9)**:711-5.

Peppiatt, C. M., Howarth, C., Mobbs, P. & Attwell, D. (2006) Bidirectional control of CNS capillary diameter by pericytes. *Nature* **443(7112)**:700-4.

Pescini, F., Donnini, I., Cesari, F., Nannucci, S., Valenti, R., Rinnoci, V., Poggesi, A., Gori, A. M., Giusti, B., Rogolino, A., Carluccio, A., Bianchi, S., Dotti, M. T., Federico, A., Balestrino, M., Adriano, E., Abbate, R., Inzitari, D. & Pantoni, L. (2017) Circulating Biomarkers in Cerebral Autosomal Dominant Arteriopathy with Subcortical Infarcts and Leukoencephalopathy Patients. *J Stroke Cerebrovasc Dis* **26(4)**:823-833.

Peters, R. (2006) Ageing and the brain. *Postgrad Med J* **82(964)**:84-8.

Pierpaoli, C., Jezzard, P., Basser, P. J., Barnett, A. & Di Chiro, G. (1996) Diffusion tensor MR imaging of the human brain. *Radiology* **201(3)**:637-48.

Pippucci, T., Maresca, A., Magini, P., Cenacchi, G., Donadio, V., Palombo, F., Papa, V., Incensi, A., Gasparre, G., Valentino, M. L., Preziuso, C., Pisano, A., Ragno, M., Liguori, R., Giordano, C., Tonon, C., Lodi, R., Parmeggiani, A., Carelli, V. & Seri, M. (2015) Homozygous NOTCH3 null mutation and impaired NOTCH3 signaling in recessive early-onset arteriopathy and cavitating leukoencephalopathy. *EMBO Mol Med* **7(6)**:848-58.

Pobezinskaya, Y. L. & Liu, Z. (2012) The role of TRADD in death receptor signaling. *Cell Cycle* **11(5)**:871-6.

Poels, M. M., Ikram, M. A., Van Der Lugt, A., Hofman, A., Krestin, G. P., Breteler, M. M. & Vernooij, M. W. (2011) Incidence of cerebral microbleeds in the general population: the Rotterdam Scan Study. *Stroke* **42(3)**:656-61.

Poggesi, A., Pantoni, L., Inzitari, D., Fazekas, F., Ferro, J., O'brien, J., Hennerici, M., Scheltens, P., Erkinjuntti, T., Visser, M., Langhorne, P., Chabriat, H., Waldemar, G., Wallin, A. & Wahlund, A. (2011) 2001-2011: A Decade of the LADIS (Leukoaraiosis And DISability) Study: What Have We Learned about White Matter Changes and Small-Vessel Disease? *Cerebrovasc Dis* **32(6)**:577-588.

Poggesi, A., Pasi, M., Pescini, F., Pantoni, L. & Inzitari, D. (2016) Circulating biologic markers of endothelial dysfunction in cerebral small vessel disease: A review. *J Cereb Blood Flow Metab* **36(1)**:72-94.

Politis, M., Giannetti, P., Su, P., Turkheimer, F., Keihaninejad, S., Wu, K., Waldman, A., Malik, O., Matthews, P. M., Reynolds, R., Nicholas, R. & Piccini, P. (2012) Increased PK11195 PET binding in the cortex of patients with MS correlates with disability. *Neurology* **79(6)**:523-30.

Polivka, J., Krakorova, K., Peterka, M. & Topolcan, O. (2016) Current status of biomarker research in neurology. *EPMA J* **7(1)**.

Pradhan, A. D., Manson, J. E., Rifai, N., Buring, J. E. & Ridker, P. M. (2001) C-reactive protein, interleukin 6, and risk of developing type 2 diabetes mellitus. *Jama* **286(3)**:327-34.

Pretnar-Oblak, J., Sabovic, M., Pogacnik, T., Sebestjen, M. & Zaletel, M. (2017) Flow-mediated dilatation and intima-media thickness in patients with lacunar infarctions. *Acta Neurologica Scandinavica* **113(4)**:273-277.

Price, C. J., Wang, D., Menon, D. K., Guadagno, J. V., Cleij, M., Fryer, T., Aigbirhio, F., Baron, J. C. & Warburton, E. A. (2006) Intrinsic activated microglia map to the peri-infarct zone in the subacute phase of ischemic stroke. *Stroke* **37(7)**:1749-53.

Radlinska, B. A., Ghinani, S. A., Lyon, P., Jolly, D., Soucy, J. P., Minuk, J., Schirrmacher, R. & Thiel, A. (2009) Multimodal microglia imaging of fiber tracts in acute subcortical stroke. *Ann Neurol* **66(6)**:825-32.

Rajani, R. M., Quick, S., Ruigrok, S. R., Graham, D., Harris, S. E., Verhaaren, B. F. J., Fornage, M., Seshadri, S., Atanur, S. S., Dominiczak, A. F., Smith, C., Wardlaw, J. M. & Williams, A. (2018) Reversal of endothelial dysfunction reduces white matter vulnerability in cerebral small vessel disease in rats. *Sci Transl Med* **10(448)**.

Ramirez, J., Mcneely, A. A., Berezuk, C., Gao, F. & Black, S. E. (2016) Dynamic Progression of White Matter Hyperintensities in Alzheimer's Disease and Normal Aging: Results from the Sunnybrook Dementia Study. *Front Aging Neurosci* **8**.

Ramsay, S. C., Weiller, C., Myers, R., Cremer, J. E., Luthra, S. K., Lammertsma, A. A. & Frackowiak, R. S. (1992) Monitoring by PET of macrophage accumulation in brain after ischaemic stroke. *Lancet* **339(8800)**:1054-5.

Rannikmae, K., Sivakumaran, V., Millar, H., Malik, R., Anderson, C. D., Chong, M., Dave, T., Falcone, G. J., Fernandez-Cadenas, I., Jimenez-Conde, J., Lindgren, A., Montaner, J., O'donnell, M., Pare, G., Radmanesh, F., Rost, N. S., Slowik, A., Soderholm, M., Traylor, M., Pulit, S. L., Seshadri, S., Worrall, B. B., Woo, D., Markus, H. S., Mitchell, B. D., Dichgans, M., Rosand, J. & Sudlow, C. L. M. (2017) COL4A2 is associated with lacunar ischemic stroke and deep ICH: Meta-analyses among 21,500 cases and 40,600 controls. *Neurology* **89(17)**:1829-1839.

Rathcke, C. N., Thomsen, S. B., Linneberg, A. & Vestergaard, H. (2012) Variations of CHI3L1, levels of the encoded glycoprotein YKL-40 and prediction of fatal and non-fatal ischemic stroke. *PLoS One* **7(8)**:e43498.

Rathcke, C. N. & Vestergaard, H. (2009) YKL-40--an emerging biomarker in cardiovascular disease and diabetes. *Cardiovasc Diabetol* **8**:61.

Raz, L., Yang, Y., Thompson, J., Hobson, S., Pesko, J., Mobashery, S., Chang, M. & Rosenberg, G. (2018) MMP-9 inhibitors impair learning in spontaneously hypertensive rats. *PLoS One* **13(12)**.

Raz, N., Yang, Y., Dahle, C. L. & Land, S. (2012) Volume of white matter hyperintensities in healthy adults: contribution of age, vascular risk factors, and inflammation-related genetic variants. *Biochim Biophys Acta* **1822(3)**:361-9.

Rehli, M., Krause, S. W. & Andreesen, R. (1997) Molecular characterization of the gene for human cartilage gp-39 (CHI3L1), a member of the chitinase protein family and marker for late stages of macrophage differentiation. *Genomics* **43(2)**:221-5.

Rehli, M., Niller, H. H., Ammon, C., Langmann, S., Schwarzfischer, L., Andreesen, R. & Krause, S. W. (2003) Transcriptional regulation of CHI3L1, a marker gene for late stages of macrophage differentiation. *J Biol Chem* **278(45)**:44058-67.

Renkema, G. H., Boot, R. G., Au, F. L., Donker-Koopman, W. E., Strijland, A., Muijsers, A. O., Hrebicek, M. & Aerts, J. M. (1998) Chitotriosidase, a chitinase, and the 39-kDa human cartilage glycoprotein, a chitin-binding lectin, are homologues of family 18 glycosyl hydrolases secreted by human macrophages. *Eur J Biochem* **251(1-2)**:504-9.

Reske-Nielsen, E., Lundbaek, K. & Rafaelsen, O. J. (1966) Pathological changes in the central and peripheral nervous system of young long-term diabetics : I. Diabetic encephalopathy. *Diabetologia* **1(3-4)**:233-41.

Reus, G. Z., Fries, G. R., Stertz, L., Badawy, M., Passos, I. C., Barichello, T., Kapczinski, F. & Quevedo, J. (2015) The role of inflammation and microglial activation in the pathophysiology of psychiatric disorders. *Neuroscience* **300**:141-54.

Riba-Llena, I., Nafria, C., Mundet, X., Lopez-Rueda, A., Fernandez-Cortinas, I., Jarca, C. I., Jimenez-Balado, J., Domingo, M., Tovar, J. L., Orfila, F., Pujadas, F., Alvarez-Sabin, J., Maisterra, O., Montaner, J. & Delgado, P. (2016) Assessment of enlarged perivascular spaces and their relation to target organ

damage and mild cognitive impairment in patients with hypertension. *Eur J Neurol* **23(6)**:1044-50.

Rissanen, E., Tuisku, J., Rokka, J., Paavilainen, T., Parkkola, R., Rinne, J. O. & Airas, L. (2014) In Vivo Detection of Diffuse Inflammation in Secondary Progressive Multiple Sclerosis Using PET Imaging and the Radioligand (1)(1)C-PK11195. *J Nucl Med* **55(6)**:939-44.

Rissanen, E., Tuisku, J., Vahlberg, T., Sucksdorff, M., Paavilainen, T., Parkkola, R., Rokka, J., Gerhard, A., Hinz, R., Talbot, P. S., Rinne, J. O. & Airas, L. (2018) Microglial activation, white matter tract damage, and disability in MS. *Neurol Neuroimmunol Neuroinflamm* **5(3)**.

Rizzi, L., Marques, F. C., Rosset, I., Moriguchi, E. H., Picon, P. D., Chaves, M. L. & Roriz-Cruz, M. (2014) C-reactive protein and cognition are unrelated to leukoaraiosis. *ScientificWorldJournal* **2014**:121679.

Rodriguez-Arellano, J. J., Parpura, V., Zorec, R. & Verkhratsky, A. (2016) Astrocytes in physiological aging and Alzheimer's disease. *Neuroscience* **323**:170-82.

Romero, J. R., Vasan, R. S., Beiser, A. S., Au, R., Benjamin, E. J., Decarli, C., Wolf, P. A. & Seshadri, S. (2010) Association of matrix metalloproteinases with MRI indices of brain ischemia and aging. *Neurobiol Aging* **31(12)**:2128-35.

Rosano, C., Perera, S., Inzitari, M., Newman, A. B., Longstreth, W. T. & Studenski, S. (2016) Digit Symbol Substitution test and future clinical and subclinical disorders of cognition, mobility and mood in older adults. *Age Ageing* **45(5)**:688-95.

Rosenberg, G. A. (2012) Neurological diseases in relation to the blood–brain barrier. *J Cereb Blood Flow Metab* **32(7)**:1139-51.

Rosenberg, G. A. (2016) Matrix Metalloproteinase-Mediated Neuroinflammation in Vascular Cognitive Impairment of the Binswanger Type. *Cell Mol Neurobiol* **36(2)**:195-202.

Rosenberg, G. A. (2018) Binswanger's disease: biomarkers in the inflammatory form of vascular cognitive impairment and dementia. *J Neurochem* **144(5)**:634-643.

Rosenberg, G. A., Bjerke, M. & Wallin, A. (2014) Multimodal markers of inflammation in the subcortical ischemic vascular disease type of vascular cognitive impairment. *Stroke* **45(5)**:1531-8.

Rosenberg, G. A., Cunningham, L. A., Wallace, J., Alexander, S., Estrada, E. Y., Grossetete, M., Razhagi, A., Miller, K. & Gearing, A. (2001a) Immunohistochemistry of matrix metalloproteinases in reperfusion injury to rat brain: activation of MMP-9 linked to stromelysin-1 and microglia in cell cultures. *Brain Res* **893(1-2)**:104-12.

Rosenberg, G. A., Sullivan, N. & Esiri, M. M. (2001b) White matter damage is associated with matrix metalloproteinases in vascular dementia. *Stroke* **32(5)**:1162-8.

Rossi Espagnet, M. C., Romano, A., Carducci, F., Calabria, L. F., Fiorillo, M., Orzi, F. & Bozzao, A. (2012) Grey matter volume alterations in CADASIL: a voxel-based morphometry study. *J Headache Pain* **13(3)**:231-8.

Rothaug, M., Becker-Pauly, C. & Rose-John, S. (2016) The role of interleukin-6 signaling in nervous tissue. *Biochim Biophys Acta* **1863(6 Pt A)**:1218-27.

Rothe, M., Sarma, V., Dixit, V. M. & Goeddel, D. V. (1995) TRAF2-mediated activation of NF-kappa B by TNF receptor 2 and CD40. *Science* **269(5229)**:1424-7.

Rouhl, R. P., Damoiseaux, J. G., Lodder, J., Theunissen, R. O., Knottnerus, I. L., Staals, J., Henskens, L. H., Kroon, A. A., De Leeuw, P. W., Tervaert, J. W. & Van Oostenbrugge, R. J. (2012) Vascular inflammation in cerebral small vessel disease. *Neurobiol Aging* **33(8)**:1800-6.

Rovira, A., Minguez, B., Aymerich, F. X., Jacas, C., Huerga, E., Cordoba, J. & Alonso, J. (2007) Decreased white matter lesion volume and improved cognitive function after liver transplantation. *Hepatology* **46(5)**:1485-90.

Rufa, A., Blardi, P., De Lalla, A., Cevenini, G., De Stefano, N., Zicari, E., Auteri, A., Federico, A. & Dotti, M. T. (2008) Plasma levels of asymmetric dimethylarginine in cerebral autosomal dominant arteriopathy with subcortical infarct and leukoencephalopathy. *Cerebrovasc Dis* **26(6)**:636-40.

Rupprecht, R., Papadopoulos, V., Rammes, G., Baghai, T. C., Fan, J., Akula, N., Groyer, G., Adams, D. & Schumacher, M. (2010) Translocator protein (18 kDa) (TSPO) as a therapeutic target for neurological and psychiatric disorders. *Nat Rev Drug Discov* **9(12)**:971-88.

Russo, M. V. & Mcgavern, D. B. (2015) Immune Surveillance of the CNS following Infection and Injury. *Trends Immunol* **36(10)**:637-650.

Rutten-Jacobs, L. C. A., Tozer, D. J., Duering, M., Malik, R., Dichgans, M., Markus, H. S. & Traylor, M. (2018) Genetic Study of White Matter Integrity in UK Biobank (N=8448) and the Overlap With Stroke, Depression, and Dementia. *Stroke* **49(6)**:1340-1347.

Sachdev, P., Wen, W., Chen, X. & Brodaty, H. (2007) Progression of white matter hyperintensities in elderly individuals over 3 years. *Neurology* **68(3)**:214-22.

Sadoshima, S. & Heistad, D. (1982) Sympathetic nerves protect the blood-brain barrier in stroke-prone spontaneously hypertensive rats. *Hypertension* **4(6)**:904-7.

Salifu, M. O., Kolff, Q., Murty, P., Haria, D. M., Zimpa, M., Shakeel, M., Lee, H., Kornecki, E. & Babinska, A. (2007) Relationship between the soluble F11 receptor and markers of inflammation in hemodialysis patients. *J Investig Med* **55(3)**:115-9.

Samuelsson, M., Soderfeldt, B. & Olsson, G. B. (1996) Functional outcome in patients with lacunar infarction. *Stroke* **27(5)**:842-6.

Santos, C. Y., Snyder, P. J., Wu, W. C., Zhang, M., Echeverria, A. & Alber, J. (2017) Pathophysiologic relationship between Alzheimer's disease, cerebrovascular disease, and cardiovascular risk: A review and synthesis. In *Alzheimers Dement (Amst).*), vol. 7, pp. 69-87.

Sarchielli, P., Nardi, K., Chiasserini, D., Eusebi, P., Tantucci, M., Di Piero, V., Altieri, M., Marini, C., Russo, T., Silvestrini, M., Paolino, I., Calabresi, P. & Parnetti, L. (2013) Immunological profile of silent brain infarction and lacunar stroke. *PLoS One* **8(7)**:e68428.

Satizabal, C. L., Zhu, Y. C., Mazoyer, B., Dufouil, C. & Tzourio, C. (2012) Circulating IL-6 and CRP are associated with MRI findings in the elderly: the 3C-Dijon Study. *Neurology* **78(10)**:720-7.

Schmidt, R., Enzinger, C., Ropele, S., Schmidt, H. & Fazekas, F. (2003) Progression of cerebral white matter lesions: 6-year results of the Austrian Stroke Prevention Study. *Lancet* **361(9374)**:2046-8.

Schmidt, R., Schmidt, H., Haybaeck, J., Loitfelder, M., Weis, S., Cavalieri, M., Seiler, S., Enzinger, C., Ropele, S., Erkinjuntti, T., Pantoni, L., Scheltens, P., Fazekas, F. & Jellinger, K. (2011) Heterogeneity in age-related white matter changes. *Acta Neuropathol* **122(2)**:171-85.

Schmidt, R., Schmidt, H., Pichler, M., Enzinger, C., Petrovic, K., Niederkorn, K., Horner, S., Ropele, S., Watzinger, N., Schumacher, M., Berghold, A., Kostner, G. M. & Fazekas, F. (2006) C-reactive protein, carotid atherosclerosis, and cerebral small-vessel disease: results of the Austrian Stroke Prevention Study. *Stroke* **37(12)**:2910-6.

Schmidt, R., Seiler, S. & Loitfelder, M. (2016) Longitudinal change of small-vessel disease-related brain abnormalities. *J Cereb Blood Flow Metab* **36(1)**:26-39.

Schneider, J. A., Arvanitakis, Z., Bang, W. & Bennett, D. A. (2007) Mixed brain pathologies account for most dementia cases in community-dwelling older persons. *Neurology* **69(24)**:2197-204.

Schuitemaker, A., Kropholler, M. A., Boellaard, R., Van Der Flier, W. M., Kloet, R. W., Van Der Doef, T. F., Knol, D. L., Windhorst, A. D., Luurtsema, G., Barkhof, F., Jonker, C., Lammertsma, A. A., Scheltens, P. & Van Berckel, B. N. (2013) Microglial activation in Alzheimer's disease: an (R)-[(1)(1)C]PK11195 positron emission tomography study. *Neurobiol Aging* **34(1)**:128-36.

Schultz, N. A. & Johansen, J. S. (2010) YKL-40—A Protein in the Field of Translational Medicine: A Role as a Biomarker in Cancer Patients? *Cancers (Basel)* **2(3)**:1453-91.

Scott, G., Mahmud, M., Owen, D. R. & Johnson, M. R. (2017) Microglial positron emission tomography (PET) imaging in epilepsy: Applications, opportunities and pitfalls. *Seizure* **44**:42-47.

Sedimbi, S. K., Hagglof, T. & Karlsson, M. C. (2013) IL-18 in inflammatory and autoimmune disease. *Cell Mol Life Sci* **70(24)**:4795-808.

Seo, S. W., Hwa Lee, B., Kim, E. J., Chin, J., Sun Cho, Y., Yoon, U. & Na, D. L. (2007) Clinical significance of microbleeds in subcortical vascular dementia. *Stroke* **38(6)**:1949-51.

Seshadri, S., Wolf, P. A., Beiser, A. S., Selhub, J., Au, R., Jacques, P. F., Yoshita, M., Rosenberg, I. H., D'agostino, R. B. & Decarli, C. (2008) Association of plasma total homocysteine levels with subclinical brain injury: cerebral volumes, white matter hyperintensity, and silent brain infarcts at volumetric magnetic resonance imaging in the Framingham Offspring Study. *Arch Neurol* **65(5)**:642-9.

Sesso, H. D., Buring, J. E., Rifai, N., Blake, G. J., Gaziano, J. M. & Ridker, P. M. (2003) C-reactive protein and the risk of developing hypertension. *Jama* **290(22)**:2945-51.

Shao, R. (2013) YKL-40 acts as an angiogenic factor to promote tumor angiogenesis. *Front Physiol* **4**:122.

Shereen, A., Nemkul, N., Yang, D., Adhami, F., Dunn, R. S., Hazen, M. L., Nakafuku, M., Ning, G., Lindquist, D. M. & Kuan, C. Y. (2011) Ex vivo diffusion tensor imaging and neuropathological correlation in a murine model of hypoxia-ischemia-induced thrombotic stroke. *J Cereb Blood Flow Metab* **31(4)**:1155-69.

Shi, K., Tian, D. C., Li, Z. G., Ducruet, A. F., Lawton, M. T. & Shi, F. D. (2019) Global brain inflammation in stroke. *Lancet Neurol*.

Shi, Y., Thrippleton, M. J., Makin, S. D., Marshall, I., Geerlings, M. I., De Craen, A. J., Van Buchem, M. A. & Wardlaw, J. M. (2016) Cerebral blood flow in small vessel disease: A systematic review and meta-analysis. In *J Cereb Blood Flow Metab*.), vol. 36, pp. 1653-67.

Shi, Y. & Wardlaw, J. M. (2016) Update on cerebral small vessel disease: a dynamic whole-brain disease.

Shoamanesh, A., Preis, S. R., Beiser, A. S., Vasan, R. S., Benjamin, E. J., Kase, C. S., Wolf, P. A., Decarli, C., Romero, J. R. & Seshadri, S. (2015) Inflammatory biomarkers, cerebral microbleeds, and small vessel disease: Framingham Heart Study. In *Neurology*.), vol. 84, pp. 825-32.

Simpson, J. E., Fernando, M. S., Clark, L., Ince, P. G., Matthews, F., Forster, G., O'brien, J. T., Barber, R., Kalaria, R. N., Brayne, C., Shaw, P. J., Lewis, C. E. & Wharton, S. B. (2007a) White matter lesions in an unselected cohort of the elderly: astrocytic, microglial and oligodendrocyte precursor cell responses. *Neuropathol Appl Neurobiol* **33(4)**:410-9.

Simpson, J. E., Ince, P. G., Higham, C. E., Gelsthorpe, C. H., Fernando, M. S., Matthews, F., Forster, G., O'brien, J. T., Barber, R., Kalaria, R. N., Brayne, C., Shaw, P. J., Stoeber, K., Williams, G. H., Lewis, C. E. & Wharton, S. B. (2007b) Microglial activation in white matter lesions and nonlesional white matter of ageing brains. *Neuropathol Appl Neurobiol* **33(6)**:670-83.

Singh, T. & Newman, A. B. (2011) Inflammatory markers in population studies of aging. *Ageing Res Rev* **10(3)**:319-29.

Singhal, S., Bevan, S., Barrick, T., Rich, P. & Markus, H. S. (2004) The influence of genetic and cardiovascular risk factors on the CADASIL phenotype. *Brain* **127(Pt 9)**:2031-8.

Singhal, S., Rich, P. & Markus, H. S. (2005) The spatial distribution of MR imaging abnormalities in cerebral autosomal dominant arteriopathy with subcortical infarcts and leukoencephalopathy and their relationship to age and clinical features. *AJNR Am J Neuroradiol* **26(10)**:2481-7.

Sironi, L., Guerrini, U., Tremoli, E., Miller, I., Gelosa, P., Lascialfari, A., Zucca, I., Eberini, I., Gemeiner, M., Paoletti, R. & Gianazza, E. (2004) Analysis of pathological events at the onset of brain damage in stroke-prone rats: a proteomics and magnetic resonance imaging approach. *J Neurosci Res* **78(1)**:115-22.

Smedbakken, L., Jensen, J. K., Hallen, J., Atar, D., Januzzi, J. L., Halvorsen, B., Aukrust, P. & Ueland, T. (2011) Activated leukocyte cell adhesion molecule and prognosis in acute ischemic stroke. *Stroke* **42(9)**:2453-8.

Smith, E. E., Egorova, S., Blacker, D., Killiany, R. J., Muzikansky, A., Dickerson, B. C., Tanzi, R. E., Albert, M. S., Greenberg, S. M. & Guttmann, C. R. (2008) Magnetic resonance imaging white matter hyperintensities and brain volume in the prediction of mild cognitive impairment and dementia. *Arch Neurol* **65(1)**:94-100.

Smith, E. E., O'donnell, M., Dagenais, G., Lear, S. A., Wielgosz, A., Sharma, M., Poirier, P., Stotts, G., Black, S. E., Strother, S., Noseworthy, M. D., Benavente, O., Modi, J., Goyal, M., Batool, S., Sanchez, K., Hill, V., Mccreary, C. R., Frayne, R., Islam, S., Dejesus, J., Rangarajan, S., Teo, K. & Yusuf, S. (2015) Early Cerebral Small Vessel Disease and Brain Volume, Cognition, and Gait. *Ann Neurol* **77(2)**:251-61.

Snowdon, D. A., Greiner, L. H., Mortimer, J. A., Riley, K. P., Greiner, P. A. & Markesbery, W. R. (1997) Brain infarction and the clinical expression of Alzheimer disease. The Nun Study. *Jama* **277(10)**:813-7.

Soares, J. M., Marques, P., Alves, V. & Sousa, N. (2013) A hitchhiker's guide to diffusion tensor imaging. *Front Neurosci* **7**.

Sobowale, O. A., Parry-Jones, A. R., Smith, C. J., Tyrrell, P. J., Rothwell, N. J. & Allan, S. M. (2016) Interleukin-1 in Stroke: From Bench to Bedside. *Stroke* **47(8)**:2160-7.

Sohrabji, F. (2007) Guarding the blood-brain barrier: a role for estrogen in the etiology of neurodegenerative disease. *Gene Expr* **13(6)**:311-9.

Song, Y., Li, Q., Long, L., Zhang, N. & Liu, Y. (2015) Asn563Ser polymorphism of CD31/PECAM-1 is associated with atherosclerotic cerebral infarction in a southern Han population. *Neuropsychiatr Dis Treat* **11**:15-20.

Spangler, K. M., Challa, V. R., Moody, D. M. & Bell, M. A. (1994) Arteriolar tortuosity of the white matter in aging and hypertension. A microradiographic study. *J Neuropathol Exp Neurol* **53(1)**:22-6.

Staekenborg, S. S., Su, T., Van Straaten, E. C., Lane, R., Scheltens, P., Barkhof, F. & Van Der Flier, W. M. (2010) Behavioural and psychological symptoms in vascular dementia; differences between small- and large-vessel disease. *J Neurol Neurosurg Psychiatry* **81(5)**:547-51.

Staszewski, J., Piusińska-Macoch, R., Brodacki, B., Skrobowska, E. & Stępień, A. (2018) IL-6, PF-4, sCD40 L, and homocysteine are associated with the radiological progression of cerebral small-vessel disease: a 2-year follow-up study. *Clin Interv Aging* **13**:1135-41.

Staszewski, J., Skrobowska, E., Piusinska-Macoch, R., Brodacki, B. & Stepien, A. (2019) IL-1alpha and IL-6 predict vascular events or death in patients with cerebral small vessel disease-Data from the SHEF-CSVD study. *Adv Med Sci* **64(2)**:258-266.

Stewart, P. A., Magliocco, M., Hayakawa, K., Farrell, C. L., Del Maestro, R. F., Girvin, J., Kaufmann, J. C., Vinters, H. V. & Gilbert, J. (1987) A quantitative analysis of blood-brain barrier ultrastructure in the aging human. *Microvasc Res* **33(2)**:270-82.

Stojanov, D., Aracki-Trenkic, A., Vojinovic, S., Ljubisavljevic, S., Benedeto-Stojanov, D., Tasic, A. & Vujnovic, S. (2015) Imaging characteristics of cerebral autosomal dominant arteriopathy with subcortical infarcts and leucoencephalopathy (CADASIL). *Bosn J Basic Med Sci* **15(1)**:1-8.

Sugama, S. & Conti, B. (2008) Interleukin-18 and stress. *Brain Res Rev* **58(1)**:85-95.

Tagami, M., Nara, Y., Kubota, A., Fujino, H. & Yamori, Y. (1990) Ultrastructural changes in cerebral pericytes and astrocytes of stroke-prone spontaneously hypertensive rats. *Stroke* **21(7)**:1064-71.

Taheri, S., Gasparovic, C., Huisa, B. N., Adair, J. C., Edmonds, E., Prestopnik, J., Grossetete, M., Shah, N. J., Wills, J., Qualls, C. & Rosenberg, G. A. (2011a) Blood-brain barrier permeability abnormalities in vascular cognitive impairment. *Stroke* **42(8)**:2158-63.

Taheri, S., Gasparovic, C., Shah, N. J. & Rosenberg, G. A. (2011b) Quantitative measurement of blood-brain barrier permeability in human using dynamic contrast-enhanced MRI with fast T1 mapping. *Magn Reson Med* **65(4)**:1036-42.

Tailor, A., Cooper, D. & Granger, D. N. (2005) Platelet-vessel wall interactions in the microcirculation. *Microcirculation* **12(3)**:275-85.

Tan, R. Y. Y. & Markus, H. S. (2016) CADASIL: Migraine, Encephalopathy, Stroke and Their Inter-Relationships. *PLoS One* **11(6)**.

Tarkowski, E., Blennow, K., Wallin, A. & Tarkowski, A. (1999) Intracerebral production of tumor necrosis factor-alpha, a local neuroprotective agent, in Alzheimer disease and vascular dementia. *J Clin Immunol* **19(4)**:223-30.

Tay, J., Tuladhar, A. M., Hollocks, M. J., Brookes, R. L., Tozer, D. J., Barrick, T. R., Husain, M., De Leeuw, F. E. & Markus, H. S. (2019) Apathy is associated with large-scale white matter network disruption in small vessel disease. *Neurology* **92(11)**:e1157-e1167.

Tchalla, A. E., Wellenius, G. A., Sorond, F. A., Travison, T. G., Dantoine, T. & Lipsitz, L. A. (2015) Elevated circulating vascular cell Adhesion Molecule-1 (sVCAM-1) is associated with concurrent depressive symptoms and cerebral white matter Hyperintensities in older adults. *BMC Geriatr* **15**:62.

Ten Dam, V. H., Van Den Heuvel, D. M., De Craen, A. J., Bollen, E. L., Murray, H. M., Westendorp, R. G., Blauw, G. J. & Van Buchem, M. A. (2007) Decline in total cerebral blood flow is linked with increase in periventricular but not deep white matter hyperintensities. *Radiology* **243(1)**:198-203.

Ter Telgte, A., Van Leijsen, E. M. C., Wiegertjes, K., Klijn, C. J. M., Tuladhar, A. M. & De Leeuw, F. E. (2018) Cerebral small vessel disease: from a focal to a global perspective. *Nat Rev Neurol* **14(7)**:387-398.

Terasaki, Y., Liu, Y., Hayakawa, K., Pham, L., Lo, E., Ji, X. & Arai, K. (2014) Mechanisms of Neurovascular Dysfunction in Acute Ischemic Brain. *Curr Med Chem* **21(18)**:2035-42.

Thiel, A., Cechetto, D. F., Heiss, W. D., Hachinski, V. & Whitehead, S. N. (2014) Amyloid burden, neuroinflammation, and links to cognitive decline after ischemic stroke. *Stroke* **45(9)**:2825-9.

Thompson, C. S. & Hakim, A. M. (2009) Living beyond our physiological means: small vessel disease of the brain is an expression of a systemic failure in arteriolar function: a unifying hypothesis. *Stroke* **40(5)**:e322-30.

Thornberry, N. A., Bull, H. G., Calaycay, J. R., Chapman, K. T., Howard, A. D., Kostura, M. J., Miller, D. K., Molineaux, S. M., Weidner, J. R., Aunins, J. & Et Al. (1992) A novel heterodimeric cysteine protease is required for interleukin-1 beta processing in monocytes. *Nature* **356(6372)**:768-74.

Thrippleton, M. J., Backes, W. H., Sourbron, S., Ingrisch, M., Van Osch, M. J. P., Dichgans, M., Fazekas, F., Ropele, S., Frayne, R., Van Oostenbrugge, R. J., Smith, E. E. & Wardlaw, J. M. (2019) Quantifying blood-brain barrier leakage in small vessel disease: Review and consensus recommendations. *Alzheimers Dement* **15(6)**:840-858.

Tibbling, G., Link, H. & Ohman, S. (1977) Principles of albumin and IgG analyses in neurological disorders. I. Establishment of reference values. *Scand J Clin Lab Invest* **37(5)**:385-90.

Toledo, J. B., Arnold, S. E., Raible, K., Brettschneider, J., Xie, S. X., Grossman, M., Monsell, S. E., Kukull, W. A. & Trojanowski, J. Q. (2013) Contribution of cerebrovascular disease in autopsy confirmed neurodegenerative disease cases in the National Alzheimer's Coordinating Centre. *Brain* **136(Pt 9)**:2697-706.

Tomimoto, H., Akiguchi, I., Suenaga, T., Nishimura, M., Wakita, H., Nakamura, S. & Kimura, J. (1996) Alterations of the blood-brain barrier and glial cells in white-matter lesions in cerebrovascular and Alzheimer's disease patients. *Stroke* **27(11)**:2069-74.

Topakian, R., Barrick, T. R., Howe, F. A. & Markus, H. S. (2010) Blood-brain barrier permeability is increased in normal-appearing white matter in patients with lacunar stroke and leucoaraiosis. *J Neurol Neurosurg Psychiatry* **81(2)**:192-7.

Touyz, R. M. (2004) Reactive oxygen species, vascular oxidative stress, and redox signaling in hypertension: what is the clinical significance? *Hypertension* **44(3)**:248-52.

Traylor, M., Tozer, D. J., Croall, I. D., Lisiecka Ford, D. M., Olorunda, A. O., Boncoraglio, G., Dichgans, M., Lemmens, R., Rosand, J., Rost, N. S., Rothwell, P. M., Sudlow, C. L. M., Thijs, V., Rutten-Jacobs, L. & Markus, H. S. (2019) Genetic variation in PLEKHG1 is associated with white matter hyperintensities (n = 11,226). *Neurology* **92(8)**:e749-e757.

Traystman, R. J. (2003) Animal models of focal and global cerebral ischemia. *Ilar j* **44(2)**:85-95.

Turkheimer, F. E., Edison, P., Pavese, N., Roncaroli, F., Anderson, A. N., Hammers, A., Gerhard, A., Hinz, R., Tai, Y. F. & Brooks, D. J. (2007) Reference and target region modeling of [11C]-(R)-PK11195 brain studies. *J Nucl Med* **48(1)**:158-67.

Tuttolomondo, A., Di Sciacca, R., Di Raimondo, D., Serio, A., D'aguanno, G., La Placa, S., Pecoraro, R., Arnao, V., Marino, L., Monaco, S., Natale, E., Licata, G. & Pinto, A. (2009a) Plasma levels of inflammatory and thrombotic/fibrinolytic markers in acute ischemic strokes: relationship with TOAST subtype, outcome and infarct site. *J Neuroimmunol* **215(1-2)**:84-9.

Tuttolomondo, A., Pinto, A., Corrao, S., Di Raimondo, D., Fernandez, P., Di Sciacca, R., Arnao, V. & Licata, G. (2009b) Immuno-inflammatory and thrombotic/fibrinolytic variables associated with acute ischemic stroke diagnosis. *Atherosclerosis* **203(2)**:503-8.

Umemura, T., Kawamura, T., Sakakibara, T., Kanai, A., Sano, T., Hotta, N. & Sobue, G. (2008) Association of soluble adhesion molecule and C-reactive protein levels with silent brain infarction in patients with and without type 2 diabetes. *Curr Neurovasc Res* **5(2)**:106-11.

Valenti, R., Poggesi, A., Pescini, F., Inzitari, D. & Pantoni, L. (2008) Psychiatric disturbances in CADASIL: a brief review. *Acta Neurol Scand* **118(5)**:291-5.

Van Der Doef, T. F., Doorduin, J., Van Berckel, B. N. M. & Cervenka, S. (2015) Assessing brain immune activation in psychiatric disorders: clinical and preclinical PET imaging studies of the 18-kDa translocator protein. *Clin Transl Imaging* **3(6)**:449-460.

Van Der Flier, W. M., Van Straaten, E. C., Barkhof, F., Verdelho, A., Madureira, S., Pantoni, L., Inzitari, D., Erkinjuntti, T., Crisby, M., Waldemar, G., Schmidt, R., Fazekas, F. & Scheltens, P. (2005) Small vessel disease and general cognitive function in nondisabled elderly: the LADIS study. *Stroke* **36(10)**:2116-20.

Van Der Veen, P. H., Muller, M., Vincken, K. L., Hendrikse, J., Mali, W. P., Van Der Graaf, Y. & Geerlings, M. I. (2015) Longitudinal relationship between cerebral small-vessel disease and cerebral blood flow: the second manifestations of arterial disease-magnetic resonance study. *Stroke* **46(5)**:1233-8.

Van Dijk, E. J., Breteler, M. M., Schmidt, R., Berger, K., Nilsson, L. G., Oudkerk, M., Pajak, A., Sans, S., De Ridder, M., Dufouil, C., Fuhrer, R., Giampaoli, S., Launer, L. J. & Hofman, A. (2004) The association between blood pressure, hypertension, and cerebral white matter lesions: cardiovascular determinants of dementia study. *Hypertension* **44(5)**:625-30.

Van Dijk, E. J., Prins, N. D., Vermeer, S. E., Vrooman, H. A., Hofman, A., Koudstaal, P. J. & Breteler, M. M. (2005) C-reactive protein and cerebral small-vessel disease: the Rotterdam Scan Study. *Circulation* **112(6)**:900-5.

Van Dijk, E. J., Prins, N. D., Vrooman, H. A., Hofman, A., Koudstaal, P. J. & Breteler, M. M. (2008) Progression of cerebral small vessel disease in relation to risk factors and cognitive consequences: Rotterdam Scan study. *Stroke* **39(10)**:2712-9.

Van Horssen, J., Singh, S., Van Der Pol, S., Kipp, M., Lim, J. L., Peferoen, L., Gerritsen, W., Kooi, E. J., Witte, M. E., Geurts, J. J., De Vries, H. E., Peferoen-Baert, R., Van Den Elsen, P. J., Van Der Valk, P. & Amor, S. (2012) Clusters of activated microglia in normal-appearing white matter show signs of innate immune activation. *J Neuroinflammation* **9**:156.

Van Leijsen, E. M., Bergkamp, M. I., Van Uden, I. W., Cooijmans, S., Ghafoorian, M., Van Der Holst, H. M., Norris, D. G., Kessels, R. P., Platel, B., Tuladhar, A. M. & De Leeuw, F. E. (2019) Cognitive consequences of regression of cerebral small vessel disease. *Eur Stroke J* **4(1)**:85-9.

Van Leijsen, E. M., Van Uden, I. W., Ghafoorian, M., Bergkamp, M. I., Lohner, V., Kooijmans, E. C., Van Der Holst, H. M., Tuladhar, A. M., Norris, D. G., Van

Dijk, E. J., Rutten-Jacobs, L. C., Platel, B., Klijn, C. J. & De Leeuw, F. E. (2017) Nonlinear temporal dynamics of cerebral small vessel disease: The RUN DMC study. *Neurology* **89(15)**:1569-77.

Van Norden, A. G., De Laat, K. F., Van Dijk, E. J., Van Uden, I. W., Van Oudheusden, L. J., Gons, R. A., Norris, D. G., Zwiers, M. P. & De Leeuw, F. E. (2012) Diffusion tensor imaging and cognition in cerebral small vessel disease: the RUN DMC study. *Biochim Biophys Acta* **1822(3)**:401-7.

Venneti, S., Lopresti, B. J. & Wiley, C. A. (2006) The peripheral benzodiazepine receptor (Translocator protein 18kDa) in microglia: from pathology to imaging. *Prog Neurobiol* **80(6)**:308-22.

Vermeer, S. E., Longstreth, W. T., Jr. & Koudstaal, P. J. (2007) Silent brain infarcts: a systematic review. *Lancet Neurol* **6(7)**:611-9.

Vermeer, S. E., Prins, N. D., Den Heijer, T., Hofman, A., Koudstaal, P. J. & Breteler, M. M. (2003) Silent brain infarcts and the risk of dementia and cognitive decline. *N Engl J Med* **348(13)**:1215-22.

Vernooij, M. W., Van Der Lugt, A., Ikram, M. A., Wielopolski, P. A., Niessen, W. J., Hofman, A., Krestin, G. P. & Breteler, M. M. (2008) Prevalence and risk factors of cerebral microbleeds: the Rotterdam Scan Study. *Neurology* **70(14)**:1208-14.

Vilar-Bergua, A., Riba-Llena, I., Nafría, C., Bustamante, A., Llombart, V., Delgado, P. & Montaner, J. (2016) Blood and CSF biomarkers in brain subcortical ischemic vascular disease: Involved pathways and clinical applicability. *J Cereb Blood Flow Metab* **36(1)**:55-71.

Wada, H. (1998) Blood-brain barrier permeability of the demented elderly as studied by cerebrospinal fluid-serum albumin ratio. *Intern Med* **37(6)**:509-13.

Wada, M., Nagasawa, H., Kurita, K., Koyama, S., Arawaka, S., Kawanami, T., Tajima, K., Daimon, M. & Kato, T. (2007) Microalbuminuria is a risk factor for cerebral small vessel disease in community-based elderly subjects. *J Neurol Sci* **255(1-2)**:27-34.

Wada, M., Nagasawa, H., Kurita, K., Koyama, S., Arawaka, S., Kawanami, T., Tajima, K., Daimon, M. & Kato, T. (2008) Cerebral small vessel disease and C-reactive protein: results of a cross-sectional study in community-based Japanese elderly. *J Neurol Sci* **264(1-2)**:43-9.

Wada, M., Takahashi, Y., Iseki, C., Kawanami, T., Daimon, M. & Kato, T. (2011) Plasma fibrinogen, global cognitive function, and cerebral small vessel disease: results of a cross-sectional study in community-dwelling Japanese elderly. *Intern Med* **50(9)**:999-1007.

Waller, R., Baxter, L., Fillingham, D. J., Coelho, S., Pozo, J. M., Mozumder, M., Frangi, A. F., Ince, P. G., Simpson, J. E. & Highley, J. R. (2019) Iba-1-/CD68+ microglia are a prominent feature of age-associated deep subcortical white matter lesions. *PLoS One* **14(1)**:e0210888.

Wallin, A., Roman, G. C., Esiri, M., Kettunen, P., Svensson, J., Paraskevas, G. P. & Kapaki, E. (2018) Update on Vascular Cognitive Impairment Associated with Subcortical Small-Vessel Disease. *J Alzheimers Dis* **62(3)**:1417-1441.

Wang, W., Prince, C. Z., Mou, Y. & Pollman, M. J. (2002) Notch3 signaling in vascular smooth muscle cells induces c-FLIP expression via ERK/MAPK activation. Resistance to Fas ligand-induced apoptosis. *J Biol Chem* **277(24)**:21723-9.

Wang, X., Barone, F. C., Aiyar, N. V. & Feuerstein, G. Z. (1997) Interleukin-1 receptor and receptor antagonist gene expression after focal stroke in rats. *Stroke* **28(1)**:155-61; discussion 161-2.

Wang, X., Chappell, F. M., Valdes Hernandez, M., Lowe, G., Rumley, A., Shuler, K., Doubal, F. & Wardlaw, J. M. (2016) Endothelial Function, Inflammation, Thrombosis, and Basal Ganglia Perivascular Spaces in Patients with Stroke. *J Stroke Cerebrovasc Dis* **25(12)**:2925-31.

Wardlaw, J., Smith, C. & Dichgans, M. (2013a) Mechanisms underlying sporadic cerebral small vessel disease: insights from neuroimaging. *Lancet Neurol* **12(5)**.

Wardlaw, J. M. (2005) What causes lacunar stroke? *J Neurol Neurosurg Psychiatry* **75**:617-9.

Wardlaw, J. M. (2010) Blood-brain barrier and cerebral small vessel disease. *J Neurol Sci* **299(1-2)**:66-71.

Wardlaw, J. M., Doubal, F., Armitage, P., Chappell, F., Carpenter, T., Munoz Maniega, S., Farrall, A., Sudlow, C., Dennis, M. & Dhillon, B. (2009) Lacunar stroke is associated with diffuse blood-brain barrier dysfunction. *Ann Neurol* **65(2)**:194-202.

Wardlaw, J. M., Doubal, F. N., Valdes-Hernandez, M., Wang, X., Chappell, F. M., Shuler, K., Armitage, P. A., Carpenter, T. C. & Dennis, M. S. (2013b) Blood-brain barrier permeability and long-term clinical and imaging outcomes in cerebral small vessel disease. *Stroke* **44(2)**:525-7.

Wardlaw, J. M., Farrall, A., Armitage, P. A., Carpenter, T., Chappell, F., Doubal, F., Chowdhury, D., Cvoro, V. & Dennis, M. S. (2008) Changes in background blood-brain barrier integrity between lacunar and cortical ischemic stroke subtypes. *Stroke* **39(4)**:1327-32.

Wardlaw, J. M., Lewis, S. C., Keir, S. L., Dennis, M. S. & Shenkin, S. (2006) Cerebral microbleeds are associated with lacunar stroke defined clinically and radiologically, independently of white matter lesions. *Stroke* **37(10)**:2633-6.

Wardlaw, J. M., Makin, S. J., Valdés Hernández, M. C., Armitage, P. A., Heye, A. K., Chappell, F. M., Muñoz-Maniega, S., Sakka, E., Shuler, K., Dennis, M. S. & Thrippleton, M. J. (2017) Blood-brain barrier failure as a core mechanism in cerebral small vessel disease and dementia: evidence from a cohort study. *Alzheimers Dement* **13(6)**:634-43.

Wardlaw, J. M., Sandercock, P. A., Dennis, M. S. & Starr, J. (2003) Is breakdown of the blood-brain barrier responsible for lacunar stroke, leukoaraiosis, and dementia? *Stroke* **34(3)**:806-12.

Wardlaw, J. M., Smith, E. E., Biessels, G. J., Cordonnier, C., Fazekas, F., Frayne, R., Lindley, R. I., O'brien, J. T., Barkhof, F., Benavente, O. R., Black, S. E., Brayne, C., Breteler, M., Chabriat, H., Decarli, C., De Leeuw, F. E., Doubal, F., Duering, M., Fox, N. C., Greenberg, S., Hachinski, V., Kilimann, I., Mok, V., Oostenbrugge, R., Pantoni, L., Speck, O., Stephan, B. C. M., Teipel, S., Viswanathan, A., Werring, D., Chen, C., Smith, C., Van Buchem, M., Norrving, B., Gorelick, P. B. & Dichgans, M. (2013c) Neuroimaging standards for research into small vessel disease and its contribution to ageing and neurodegeneration. *Lancet Neurol* **12(8)**:822-38.

Wechsler, D. (1997a) *Wechsler Adult Intelligence Scale-Third edition (WAIS-III).* San Antonio, TX, The Psychological Corporation.

Wechsler, D. (1997b) *Wechsler Memory Scale - Third Edition (WMS-III UK) Administration and Scoring Manual.* San Antonio, TX, The Psychological Corporation.

Wersching, H., Duning, T., Lohmann, H., Mohammadi, S., Stehling, C., Fobker, M., Conty, M., Minnerup, J., Ringelstein, E. B., Berger, K., Deppe, M. & Knecht, S. (2010) Serum C-reactive protein is linked to cerebral microstructural integrity and cognitive function. *Neurology* **74(13)**:1022-9.

Wetzel, M., Li, L., Harms, K. M., Roitbak, T., Ventura, P. B., Rosenberg, G. A., Khokha, R. & Cunningham, L. A. (2008) Tissue inhibitor of metalloproteinases-3 facilitates Fas-mediated neuronal cell death following mild ischemia. *Cell Death Differ* **15(1)**:143-51.

Whitwell, J. L., Crum, W. R., Watt, H. C. & Fox, N. C. (2001) Normalization of cerebral volumes by use of intracranial volume: implications for longitudinal quantitative MR imaging. *AJNR Am J Neuroradiol* **22(8)**:1483-9.

Wimmer, I., Tietz, S., Nishihara, H., Deutsch, U., Sallusto, F., Gosselet, F., Lyck, R., Muller, W. A., Lassmann, H. & Engelhardt, B. (2019) PECAM-1 Stabilizes Blood-Brain Barrier Integrity and Favors Paracellular T-Cell Diapedesis Across the Blood-Brain Barrier During Neuroinflammation. *Front Immunol* **10**:711.

Wiseman, S., Marlborough, F., Doubal, F., Webb, D. J. & Wardlaw, J. (2014) Blood markers of coagulation, fibrinolysis, endothelial dysfunction and inflammation in lacunar stroke versus non-lacunar stroke and non-stroke: systematic review and meta-analysis. *Cerebrovasc Dis* **37(1)**:64-75.

Wong, S. M., Jansen, J. F. A., Zhang, C. E., Hoff, E. I., Staals, J., Van Oostenbrugge, R. J. & Backes, W. H. (2019) Blood-brain barrier impairment and hypoperfusion are linked in cerebral small vessel disease. *Neurology* **92(15)**:e1669-e1677.

Wong, T. Y., Klein, R., Sharrett, A. R., Couper, D. J., Klein, B. E., Liao, D. P., Hubbard, L. D. & Mosley, T. H. (2002) Cerebral white matter lesions, retinopathy, and incident clinical stroke. *Jama* **288(1)**:67-74.

Wright, C. B., Moon, Y., Paik, M. C., Brown, T. R., Rabbani, L., Yoshita, M., Decarli, C., Sacco, R. & Elkind, M. S. (2009) Inflammatory biomarkers of vascular risk as correlates of leukoariosis. *Stroke* **40(11)**:3466-71.

Yamada, K., Sakai, K., Owada, K., Mineura, K. & Nishimura, T. (2010) Cerebral white matter lesions may be partially reversible in patients with carotid artery stenosis. *AJNR Am J Neuroradiol* **31(7)**:1350-2.

Yamamoto, Y., Craggs, L., Baumann, M., Kalimo, H. & Kalaria, R. N. (2011) Review: molecular genetics and pathology of hereditary small vessel diseases of the brain. *Neuropathol Appl Neurobiol* **37(1)**:94-113.

Yamamoto, Y., Craggs, L. J., Watanabe, A., Booth, T., Attems, J., Low, R. W., Oakley, A. E. & Kalaria, R. N. (2013) Brain microvascular accumulation and distribution of the NOTCH3 ectodomain and granular osmiophilic material in CADASIL. *J Neuropathol Exp Neurol* **72(5)**:416-31.

Yamawaki, M., Wada-Isoe, K., Yamamoto, M., Nakashita, S., Uemura, Y., Takahashi, Y., Nakayama, T. & Nakashima, K. (2015) Association of cerebral white matter lesions with cognitive function and mood in Japanese elderly people: a population-based study. *Brain Behav* **5(3)**.

Yang, Y., Candelario-Jalil, E., Thompson, J. F., Cuadrado, E., Estrada, E. Y., Rosell, A., Montaner, J. & Rosenberg, G. A. (2010) Increased intranuclear matrix metalloproteinase activity in neurons interferes with oxidative DNA repair in focal cerebral ischemia. *J Neurochem* **112(1)**:134-49.

Yang, Y., Estrada, E. Y., Thompson, J. F., Liu, W. & Rosenberg, G. A. (2007) Matrix metalloproteinase-mediated disruption of tight junction proteins in cerebral vessels is reversed by synthetic matrix metalloproteinase inhibitor in focal ischemia in rat. *J Cereb Blood Flow Metab* **27(4)**:697-709.

Yang, Y., Kimura-Ohba, S., Thompson, J. F., Salayandia, V. M., Cosse, M., Raz, L., Jalal, F. Y. & Rosenberg, G. A. (2018) Vascular tight junction disruption and angiogenesis in spontaneously hypertensive rat with neuroinflammatory white matter injury. *Neurobiol Dis* **114**:95-110.

Yang, Y. & Rosenberg, G. A. (2011) Blood-Brain Barrier Breakdown in Acute and Chronic Cerebrovascular Disease. *Stroke* **42(11)**:3323-8.

Yang, Y. & Rosenberg, G. A. (2015) Matrix metalloproteinases as therapeutic targets for stroke. *Brain Res* **1623**:30-8.

Yao, M., Zhu, Y. C., Soumare, A., Dufouil, C., Mazoyer, B., Tzourio, C. & Chabriat, H. (2014) Hippocampal perivascular spaces are related to aging and blood pressure but not to cognition. *Neurobiol Aging* **35(9)**:2118-25.

Yaqub, M., Van Berckel, B. N., Schuitemaker, A., Hinz, R., Turkheimer, F. E., Tomasi, G., Lammertsma, A. A. & Boellaard, R. (2012) Optimization of

supervised cluster analysis for extracting reference tissue input curves in (R)-[11C]PK11195 brain PET studies. *J Cereb Blood Flow Metab* **32(8)**:1600-8.

Yatsiv, I., Morganti-Kossmann, M. C., Perez, D., Dinarello, C. A., Novick, D., Rubinstein, M., Otto, V. I., Rancan, M., Kossmann, T., Redaelli, C. A., Trentz, O., Shohami, E. & Stahel, P. F. (2002) Elevated intracranial IL-18 in humans and mice after traumatic brain injury and evidence of neuroprotective effects of IL-18-binding protein after experimental closed head injury. *J Cereb Blood Flow Metab* **22(8)**:971-8.

Yilmaz, G. & Granger, D. N. (2008) Cell adhesion molecules and ischemic stroke. *Neurol Res* **30(8)**:783-93.

Ylikoski, A., Erkinjuntti, T., Raininko, R., Sarna, S., Sulkava, R. & Tilvis, R. (1995) White matter hyperintensities on MRI in the neurologically nondiseased elderly. Analysis of cohorts of consecutive subjects aged 55 to 85 years living at home. *Stroke* **26(7)**:1171-7.

Yokokura, M., Mori, N., Yagi, S., Yoshikawa, E., Kikuchi, M., Yoshihara, Y., Wakuda, T., Sugihara, G., Takebayashi, K., Suda, S., Iwata, Y., Ueki, T., Tsuchiya, K. J., Suzuki, K., Nakamura, K. & Ouchi, Y. (2011) In vivo changes in microglial activation and amyloid deposits in brain regions with hypometabolism in Alzheimer's disease. *Eur J Nucl Med Mol Imaging* **38(2)**:343-51.

Yong, V. W. (2005) Metalloproteinases: mediators of pathology and regeneration in the CNS. *Nat Rev Neurosci* **6(12)**:931-44.

Yong, V. W., Power, C., Forsyth, P. & Edwards, D. R. (2001) Metalloproteinases in biology and pathology of the nervous system. *Nat Rev Neurosci* **2(7)**:502-11.

Yoshida, M., Tomitori, H., Machi, Y., Katagiri, D., Ueda, S., Horiguchi, K., Kobayashi, E., Saeki, N., Nishimura, K., Ishii, I., Kashiwagi, K. & Igarashi, K. (2009) Acrolein, IL-6 and CRP as markers of silent brain infarction. *Atherosclerosis* **203(2)**:557-62.

Young, V. G., Halliday, G. M. & Kril, J. J. (2008) Neuropathologic correlates of white matter hyperintensities. *Neurology* **71(11)**:804-11.

Yu, Q., Tao, H., Wang, X. & Li, M. (2015) Targeting brain microvascular endothelial cells: a therapeutic approach to neuroprotection against stroke. *Neural Regen Res* **10(11)**:1882-91.

Yuen, C. M., Chiu, C. A., Chang, L. T., Liou, C. W., Lu, C. H., Youssef, A. A. & Yip, H. K. (2007) Level and value of interleukin-18 after acute ischemic stroke. *Circ J* **71(11)**:1691-6.

Zeestraten, E. A., Benjamin, P., Lambert, C., Lawrence, A. J., Williams, O. A., Morris, R. G., Barrick, T. R. & Markus, H. S. (2016) Application of Diffusion Tensor Imaging Parameters to Detect Change in Longitudinal Studies in Cerebral Small Vessel Disease. *PLoS One* **11(1)**:e0147836.

Zhang, C. E., Wong, S. M., Uiterwijk, R., Backes, W. H., Jansen, J. F. A., Jeukens, C., Van Oostenbrugge, R. J. & Staals, J. (2019) Blood–brain barrier leakage in relation to white matter hyperintensity volume and cognition in small vessel disease and normal aging. *Brain Imaging Behav* **13(2)**:389-95.

Zhang, C. E., Wong, S. M., Van De Haar, H. J., Staals, J., Jansen, J. F., Jeukens, C. R., Hofman, P. A., Van Oostenbrugge, R. J. & Backes, W. H. (2017) Blood-brain barrier leakage is more widespread in patients with cerebral small vessel disease. *Neurology* **88(5)**:426-432.

Zhang, J., Liu, L., Sun, H., Li, M., Li, Y., Zhao, J., Li, J., Liu, X., Cong, Y., Li, F. & Li, Z. (2018) Cerebral Microbleeds Are Associated With Mild Cognitive Impairment in Patients With Hypertension. *J Am Heart Assoc* **7(11)**.

Zhang, R., Chopp, M., Zhang, Z., Jiang, N. & Powers, C. (1998) The expression of P- and E-selectins in three models of middle cerebral artery occlusion. *Brain Res* **785(2)**:207-14.

Zhang, X., Meng, H., Blaivas, M., Rushing, E. J., Moore, B. E., Schwartz, J., Lopes, M. B. S., Worrall, B. B. & Wang, M. M. (2012) Von Willebrand Factor permeates small vessels in CADASIL and inhibits smooth muscle gene expression. *Transl Stroke Res* **3(1)**:138-45.

Zhong, Z., Deane, R., Ali, Z., Parisi, M., Shapovalov, Y., O'banion, M. K., Stojanovic, K., Sagare, A., Boillee, S., Cleveland, D. W. & Zlokovic, B. V. (2008) ALS-causing SOD1 mutants generate vascular changes prior to motor neuron degeneration. *Nat Neurosci* **11(4)**:420-2.

Zhou, A. & Jia, J. (2009) Different cognitive profiles between mild cognitive impairment due to cerebral small vessel disease and mild cognitive impairment of Alzheimer's disease origin. *J Int Neuropsychol Soc* **15(6)**:898-905.

Zupan, M., Šabović, M., Zaletel, M., Popovič, K. & Žvan, B. (2015) The presence of cerebral and/or systemic endothelial dysfunction in patients with leukoaraiosis - a case control pilot study. *BMC Neurol* **15**.

Zurcher, N. R., Loggia, M. L., Lawson, R., Chonde, D. B., Izquierdo-Garcia, D., Yasek, J. E., Akeju, O., Catana, C., Rosen, B. R., Cudkowicz, M. E., Hooker, J. M. & Atassi, N. (2015) Increased in vivo glial activation in patients with amyotrophic lateral sclerosis: assessed with [(11)C]-PBR28. *Neuroimage Clin* **7**:409-14.

Østergaard, L., Engedal, T. S., Moreton, F., Hansen, M. B., Wardlaw, J. M., Dalkara, T., Markus, H. S. & Muir, K. W. (2016) Cerebral small vessel disease: Capillary pathways to stroke and cognitive decline. *J Cereb Blood Flow Metab* **36(2)**:302-25.